SPLASH ON LEAVES AND THE DISPERSAL OF SPORE CARRYING DROPLETS

by

OLIVER CHARLES MACDONALD

Thesis submitted to the University of London in partial fulfilment of the requirement for the degree of Doctor of Philosophy

October 1988

Physiology and Environmental Physics Dept.
Rothamsted Experimental Station
Harpenden
Herts
AL5 2JQ

ABSTRACT

The thesis reviews previous work carried out to investigate splash dispersed diseases and briefly describes their importance in crop production. It also reviews the relevant literature concerning investigations into rain splash and discusses the limitations of our present knowledge with respect to the prediction of the dispersal of splash borne disease propagules within plant canopies.

A mathematical model is described that calculates the trajectories of particles in a fluid, and the application of this model to predic-ting the paths followed by splash droplets is described. The conduct and results of several different experiments carried out to ascertain the accuracy of the model when applied to splash droplets are then discussed. The conclusion is drawn that the model accurately predicts the trajectories of splash droplets.

The design of equipment to measure, photographically, the size and velocity of droplets produced by the splash of simulated rain drops on leaves is described. The results of experiments using this equipment to investigate splash on leaves under different conditions are presented. The results are discussed with the view of describing statistically the size and velocity distri-

butions of splash droplets, and also the effect on distributions of varying the size and velocity of impacting drops. The use of the measurements in determining the length scales likely to be involved in the dispersal of splash borne disease is also discussed.

AKNOWLEDGEMENTS

I would like to thank Dr. H. A. McCartney, my supervisor, for his advice, encouragement and helpful criticism during the course of my reseach and the preperation of this thesis.

Also:-

Dr Malcolm Potts, my father, for the funding of the work.

Dera and Louis Bodo, my parents, for their additional financial support and encouragement.

Dr Peter Walklate, PEP, Rothamsted, for many helpful discussions and his preperation of figure 6.7.

Dr Bruce Fitt, Plant Pathology Department, Rothamsted, for his advise on plant diseases

The Staff of the photographic department at Rothamsted for their preperation of figures 3.1 - 3.7 and 7.1 - 7.4.

Janet Why, Computing Department, Rothamsted, for preparing the final text.

Mrs Maureen Lacey and Corinne Quayle for their assistance with experiments.

LIST OF CONTENTS

Title		i
Abstract		ii
Acknowledgements		iv
List of Contents		v
List of Tables		ix
List of Figures		xi
List of Plates		xiv
1.	Introduction	1
	1.1 Objectives	
	1.2 Disease dispersal by water splash	2
	1.2.1 Evidence for splash dispersal	3
	1.2.2 Patterns of splash dispersal	5
	1.2.3 Potential for dispersal by splash	6
	1.2.4 Droplet trajectories	8
	1.3 Physics of splashing	9
	1.3.1 Previous studies	
	1.3.2 Number and size of splash droplets	11
	1.3.3 Theoretical models of splash	13
2	Modelling the dispersal of splash droplets	14
	2.1 Introduction	
	2.2 The model	15
	2.2.1 Forces acting on a particle	

2.2.2 The equation of motion for a splash droplet 17

2.2.3 Estimating drag on a droplet 20

2.3 Uncertainty and accuracy of model 22

2.3.1 Effect of air temperature and pressure on particle range

2.3.2 Evaporation 24

3 Verification of the trajectory model 27

3.1 Comparison of measured and predicted terminal velocities

3.2 Comparison of predicted and observed droplet trajectories in still air 29

3.2.1 Vibrating needle experiments

(a) Methods 30

(b) Results 39

3.2.2 Spinning disc experiments 40

(a) Methods

(b) Results 43

3.3 Conclusions 47

4 Investigation of splash on leaves: Experimental technique. 49

4.1 Photographic experiments

4.1.1 Equipment 51

4.1.2 Analysis of photographs 59

4.1.3 Experimental methods 62

5 Results and discussion. Size, speed and angle of ejection of splash droplets 67

5.1 Impact speed of incident droplets

5.2 General observations of splash 72

5.3 Splash droplet size distributions 78

5.3.1 Collection results 79

5.3.2 Photographic results 81

5.4.1 Initial velocity of splash droplets 85

5.4.2 Angles of ejection 89

5.5 Relationships between size, speed and angle 92

5.5.1 Droplet size and initial droplet speed

5.5.2 Speed and angle of ejection 104

5.5.3 Size and angle of ejection 126

6 Dispersal of splash droplets 133

6.1 Horizontal distribution

6.1.1 Measurements

(a) Numbers of drops per splash

(b) Distances splashed 138

6.1.2 Calculated horizontal distances 145

6.2 Vertical droplet range 158

6.3 Radial distribution 164

7 169

7.1 Applications

7.2 Horizontal ranges

7.3 Effect of splash height on droplet dispersal 174

7.4 Effect of wind 180

7.5 Turbulence

7.6 Spore dispersal 186

7.7 Deposition 188

8 Conclusions 195

8.1 Modelling droplet trajectories

8.2 Experimental techniques

8.3 Splash on leaves 196

8.4 Significance of results 198

References 201

Appendix 1 208

Appendix 2 210

Publications 218

LIST OF TABLES

		Page
2.1	Calculation of Cd	21
2.2	Effect of atmospheric changes on droplet range	23
2.3	Evaporation of droplets	25
3.1	Diameters of droplets collected in vibrating needle experiments	34
3.2	Comparison of observed and calculated droplet range	38
4.1	Experimental parameters	63
5.1	Impact velocity of drops	67
5.2	Mean diameter, speed and angle of ejection of droplets	76
5.3	Geometric mean diameter, speed and angle of ejection	77
5.4	Geometric mean of collected droplet diameters	79
5.5	Mean and SD of square root of droplet velocity	87
5.6a	Regression coeficients, distributions of log. initial velocity	109
b	square root initial velocity	110
5.7	Proportion of horizontally ejected droplets with velocity greater then median	117
5.8	Regression coefficients, root velocity distributions by angle of ejection	122
5.9	Regression coefficients, log velocity distributions by angle of ejection	124

5.10 Regression coefficients, distributions of ejection angles by droplet size 124

6.1 Number of droplets/splash 138

6.2 Number of droplets with distance from splash, by size 139+

6.3 Number of droplets with distance from splash 143

6.4 Mean range of droplets by size

6.5 Radial distribution of droplets from barley leaf 166

7.1 Stopping distances 175

7.2-7.6 Mean calculated range of droplets 176+

7.6 Effect of height on droplet range 178

7.7 Effect of wind on droplet range 181

7.8 Effect of turbulence on droplet range 184

7.9 Relationship between droplet size and spores carried 187

LIST OF FIGURES

		Page
3.1	Sedimentation velocities	28
3.2	Vibrating needle droplet generators	31
3.3	Comparison of observed and calculated droplet ranges	39
3.4	Spinning disc atomiser	41
3.5	Droplet production from spinning disc	42
3.6	Relationship between droplet size and range (spinning disc experiments)	44-46
4.1	Photographic setup	50
4.2	Droplet detector	52
4.3	Timing sequence	55
4.4	Oscilloscope trace, illustrating timing	57
4.5	Radial positions of droplet samplers	65
5.1	Size distributions of collected droplets	80
5.2	Size distributions of photographed droplets	82
5.3	Angles of droplet ejection	90
5.4	Relationship between droplet size and speed	93
5.5	Relationship between droplet speed and angle of ejection	94
5.6	Relationship between droplet size and angle of ejection	95

5.7 Relationship between mean droplet velocity and size, droplets <1 mm 97

5.8 Relationship between mean droplet velocity and size, all droplets 98

5.9 Mean velocity of different sized droplets

a 7.6 mg drop falling 2.8 m onto a bean leaf 102

b 34 mg drop falling 5.1 m onto a bean leaf 103

5.10-5.13 Distributions of logarithms of droplet velocities 105+

5.14-5.17 Distributions of sqr-root droplet velocities 111+

5.18 Mean initial velocity vs angle of droplet ejection 115

5.19-5.22 Effect of angle of ejection on velocity distibution 118+

5.23 Regression coefficients; root velocity distribuion vs angle of ejection 123

5.24 Mean droplet diamter vs angle of ejection 125

5.25 Regression coefficients; angle of ejection frequency vs droplet diameter 127

6.1 Droplet number, size and distance from splash 134+

6.2 Mean droplet diameter with distance from splash 144

6.3 Percentage of droplets with distance from splash 145+

6.4 Droplet volume with distance from splash 150+

6.5 Mean observed range of droplets with size 155

6.6 Mean calculated range of droplets with size 156

6.7 Droplet diameter, vertical component of velocity and heights reached by droplets 159+

6.8 Radial distribution of droplets from barley leaf 167

7.1 Calculated horizontal range of 200 micron droplets 170
7.2 Calculated horizontal range of 1 mm droplets 171
7.3 Calculated vertical range of 200 micron droplets 172
7.4 Calculated vertical range of 1 mm droplets 173
7.5 Effect of height on droplet range 179
7.6 Droplet range in moving air 185
7.7 Calculated spore dispersal gradient 189

LIST OF PLATES

1	Droplet stream from hollow needle	32
2	Droplet stream from solid needle	36
3a	Splash on bean leaf	69
b	Splash on barley leaf	70
4	Splash on smooth surface	71
5a-b	Splash on leaves	73
c-d		74
6	Drops flung off leaf by impact	100
7	Vertical view of splash on barley leaf	165

CHAPTER 1

Introduction

1.1 Objectives

The aim of this work is to investigate the nature of water splash on leaf surfaces and to develop a simple model capable of predicting the trajectories of water droplets through the air. It is hoped that in this way we may expand our knowledge of the dissemination of plant pathogens by splash. Until now most investigations into splash have concentrated on splashes either from flat solid surfaces or from thin liquid films above such. However plant surfaces are rarely flat or rigid, suggesting that it is unwise to assume that the findings from such investigations have any great relevance to the problems of disease dispersal in plants.

By modelling the trajectories of droplets it may be possible to make predictions of the movement of disease propagules. This can be achieved in the laboratory, if the parameters describing air movements in the crop canopy can be determined. This may lead to a greater understanding of the effects of weather and crop structure on the dispersal of several important diseases. This may in turn help in the development of techniques to control these diseases.

The dispersal of disease propagules can be divided into three phases; their removal from the site of infection, their movement through the air and their deposition onto a new site. This thesis describes a series of experiments investigating the first two of these phases and goes on to discuss all three.

Following convention (Gregory 1973), incident or impacting water drops will always be referred to as drops, while water ejected from splashes will be referred to as droplets.

1.2 Disease dispersal by water splash

Plant diseases caused by fungi and bacteria are dispersed by a wide variety of mechanisms. Many are dispersed by wind, the disease propagules being released directly into the air under dry conditions. Others, as noted by Stepanov (1935), produce propagules that are embedded in mucilage which effectively prevents their removal by wind or by movement of the leaves caused by any other mechanisms. Some of these may be spread by insects which pick up spores when they walk over the mucilage. Most however are probably spread by the combined action of wind and rain.

Water splash is probably second only to wind in its importance as a mechanism for the dispersal of fungal and bacterial plant pathogens (Fitt and McCartney, 1986), particularly amongst those diseases that affect foliage and soft fruit. Splash has been suggested as being the principle mechanism for the dispersal of many plant diseases; for example, Black pod disease (*Phytophthora palmivora*) of cocoa, (Thorold 1955), Halo blight (*Phaseolus vulgaris*) of beans, (Walker and Patel 1963), Grey mold of Raspberries caused by *Botrytis cinerea*, (Jarvis 1962); Gregory (1973) lists many other examples.

Typical of splash dispersed pathogens are some of the saprophytic and parasitic slime-spored fungi (Gregory 1973). These include species belonging to various genera within the Ascomycetes, including the *Fungi imperfecti* (Deuteromycetes), those Ascomycetes for which the ascigenous stage has never been found. Examples are found amongst the genera *Fusarium*, *Colletotrichum* and *Gliocladium* (Ingold 1971).

Dispersal of the spores takes place when the mucilage mat is wetted, as may happen during rain, a heavy dew-fall, or when sprinkler irrigation systems are used. The mat absorbs water and swells releasing the spores that are then free to move into the

surrounding film of water. Dispersal can then take place when either the liquid containing the spores drips off the original surface, possibly breaking up on impact and further scattering spores, or when a large enough rain drop or a drip from a higher leaf lands in the spore suspension causing a splash, and thus dispersing spores in the resulting droplets.

Splash dispersal is not restricted to slime spored pathogens. Ramalingam and Rati (1979) demonstrated the dispersal of the non-wettable spores of *Aspergillus flavus* in splash droplets, the dissemination of which had previously been linked with the occurence of rain (Sreeramulu and Ramalingam 1963). Hirst and Stedman (1963) suggested that rain drops could cause the liberation of dry spores by a 'tap and puff' mechanism. Impacting rain drops 'tap' the leaf shaking off spores. A local high speed pressure wave caused by the radial flow of liquid then blows spores off the leaf. It has also been suggested that the very small water droplets in mist can pick up spores when blown across a leaf (Dowding, 1969).

1.2.1 *Evidence for splash dispersal*

Spore dispersal in splash droplets was first studied by Faulwetter (1917a) who obtained data suggesting that wind-blown rain was probably responsible for the dispersal of the angular leaf spot of cotton (*Gossypium* spp.).

In his pioneering experiments investigating splash dispersal Faulwetter (1917b) showed that in a moderate wind (10 miles per hour) considerable numbers of potentially spore carrying water droplets could be splashed to distances of up to 8 feet, and that a few were carried as far as 16 feet from the site of infection. Stepanov (1935) was the first to definitely establish that fungal spores are carried in splash droplets, when he allowed water drops to fall on to

sporulating cultures of various fungi. The resulting droplets were collected on glass slides 200-250 mm from the point of impact and in several cases 'contained so many spores as to be impossible to count'.

Guthrie (1957) and Gregory *et al.* (1959) carried out a more detailed investigation in which they allowed large water drops to fall, under various conditions, into suspensions of several different fungal spores in water. In one experiment drops 5 mm in diameter were allowed to fall 7.4 m into a 0.1 mm thick film of water containing $5x10^6$ macroconidia of *Fusarium solani* per ml. Of an estimated 5200 splash droplets produced, over 2000 contained spores. Over the whole series of experiments, between 14 and 47% of splash droplets contained spores under any given set of conditions. Most spores were collected from large droplets (>200 µm diameter), with larger droplets carrying greater numbers of spores. Fitt and Lysandrou (1983) found that in splash from a suspension of spores of *Pseudocercosporella herpotrichoides*, most spore carrying droplets were 200-400 µm in diameter and that the numbers of spores carried in droplets increased linearly with the square of droplet diameter. This suggests that there may be a link between the surface area of droplets and the number of spores carried. Droplets with diameters greater than 1000 µm carried the most spores.

Similarly, Fitt and Nijman (1983) found that 60% of spores of *P. herpotrichoides* were carried in droplets with diameters greater than 1000 µm but less than 2% were in droplets smaller than 100 µm. Very few droplets smaller than 30 µm carried any spores at all. Spores were present in droplets, regardless of whether spores originated in the target liquid or in the incident drop.

As a more natural target Gregory and his co-workers (1959) used a twig of sycamore (*Acer pseudoplatanus*) bearing conidial

fructifications of the coral-spot fungus *Nectria cinnabarina*. Size spectra were similar to those produced by the same size drops hitting a thin film of water on a glass plate. Unlike the artificial surfaces however, all the droplets carried spores. However, more recent experiments suggest that splashes on natural surfaces disperse fewer spores. Fitt and Nijman (1983) estimated that only about 25 spores of *P. herpotrichoides* were distributed by each splash when artificial rain fell onto infected straw.

1.2.2 *Patterns of splash dispersal*

Using a fluorescent tracer the patterns of dispersal of splash droplets have been investigated under natural conditions over mown grass (Stedman, 1979), in field beans (Stedman, 1980a) and in a wheat crop (Stedman, 1980b). The experiments showed that for drops falling near their terminal velocity, larger drops (4.2 mm diameter) splashed greater volumes of water than did smaller ones (3.1 mm diameter). The volume of water ejected by a splash was shown to be relatively insensitive to substantial changes in drop impact velocity. It was only when drops fell less than 4 m (equivalent to a 30% reduction in impact velocity from a terminal velocity of about 10.5 m s^{-1}), that height of fall was found to have an effect on the volume of water splashed. Also, greater volumes were splashed from a rigid perspex surface than from a non-rigid leaf or perspex sheet. In winds of up to 6 m s^{-1} splash droplets were detected at distances of up to 16 m downwind when the splash was at crop height. However, when splashes took place within the canopy very few splash products were detected beyond 3 m in any of the wind conditions investigated. The dispersal gradients were steeper for splashed spores than for spores dispersed in dry air under similar conditions (Stedman, 1979 and 1980b).

Brennan and his co-workers studied the dissemination of spores of

Septoria nodorum by simulated rain in both still (Brennan *et al.*, 1985a) and moving air (Brennan *et al.*, 1985b). Droplets were allowed to fall onto both spore suspensions and infected straw in a wind tunnel/rain tower complex, described by Fitt *et al.* (1986). Droplets were collected on vertical and horizontal surfaces and several different suction samplers were used to test for the presence of airborne spores. In still air there was a steep dispersal gradient and spores were collected up to 1 m away from and up to 50 cm above the splash. The number of spore carrying droplets and the total number of spores decreased exponentially with distance from the splash. In moving air (wind speed 3 m s^{-1}) there was a shallower gradient of deposition. In this case the gradient was only exponential up to 2 m from the target, beyond which there was long tail of spore carrying droplets deposited up to 4 m downwind. Small numbers of spores were also found to be airborne at that distance.

1.2.3 *Potential for dispersal by splash*

The potential for transporting spores by rain splash is considerable. Hirst (1959) points out that during an inch of rain about 150,000 drops fall per square inch of ground. The rain drops vary in size from 0.2 mm up to a limit of about 5 mm. Above this size the drops become unstable and break up before they reach their terminal velocity. The majority of rain drops have diameters of less than 1 mm although the proportion of larger drops is greater in the rain from convective clouds (Best, 1950). As a general rule, for drops larger than 1.5 mm, and with sufficient averaging over time and space, the number of drops within a given size class can be estimated using the equation described by Marshall and Palmer (1948);

$$N_D = N_0 e^{-D}$$

Where D is droplet diameter, N_D is the number of droplets between D and D+ΔD in unit volume space, N_0 is the theoretical value of N_D for D=0 and is equal to 8×10^4 m^{-3} cm^{-1} for all intensities, and $e^{-D} = 41.R^{-0.21}$ where R is the rainfall intensity in mm hr^{-1}. For greater accuracy, the distributions described by the more generalised gamma function can be used (Ulbrich, 1983);

$$N_D = N_0 \, D^{\mu} \, e^{-D}$$

In this case N_0 has the units m^{-3} $cm^{-1-\mu}$ where the exponent μ has any positive or negative value.

Only those drops with diameters greater than about 0.4 mm are likely to cause splashes (Harlow and Shannon, 1967). Smaller droplets tend to bounce off surfaces (Spillman, 1984). However, all drops of water that settle will add to the surface film of water that forms on leaf surfaces and thus enhance splashing or cause run off which may result in drip splash.

Droplets from one splash do not tend to travel very far. Collisions between rain drops and splash droplets and the interception of splash droplets by leaves may further reduce the distance that they travel. However, there is also the potential for secondary splash, spores being carried by a succession of droplets resulting from a sequence of splashes. This may substantially increase the potential distance to which spores may be carried.

Small spore carrying droplets may also evaporate leaving dry spores suspended in the air. Calculations show that even in 90% humidity a droplet of 80 μm diameter will evaporate in less than one minute (Hirst, 1959), possibly leaving a dry spore suspended in the air. If not washed out by the rain, spores carried in such droplets may stay airborne for very long periods, and thus result in the spread of

pathogens over great distances.

The importance of airborne spores is largely unknown. Most splash dispersed spores are not well protected against such environmental hazards as desiccation or ultra-violet radiation, and so may not survive long periods suspended in the atmosphere. Of course, the threat from such hazards will be less during rain. Airborne spores of splash dispersed diseases have been implicated in the spread of cocoa black pod (*Phytophthora* spp.) up into the tree canopy (Gregory *et al.*, 1984). However the spores are probably dispersed over relatively short distances, several metres at most. Also the dispersal takes place under a tree canopy where the humidity is likely to be high and spores are shaded from harmful radiation.

1.2.4. *Droplet trajectories*

The trajectory of a droplet, and consequently the distance that it travels, depends upon the initial velocity of the droplet and on the local wind speed and turbulence.

For convenience spore carrying droplets can be divided into two groups: ballistic droplets that are only slightly affected by local air currents; and airborne droplets that may be carried long distances by turbulent airstreams. Only when the terminal velocity of a droplet is less than about three times the wind friction velocity will the turbulent eddies have the dominant effect on the trajectory of the drop (Elliot and Wilson, 1979). However, the mean air flow still affects the trajectories of all particles.

Wind speeds within crop canopies are generally small, for example, Shaw and McCartney (1985) found that at mid canopy within a mature barley crop wind speeds were less than 0.3 m s^{-1} for 90% of the time. Winds of this magnitude will have little effect on most spore carrying droplets. Turbulent intensity levels within canopies

can be large, however (Perrier *et al.*, 1972) and occasional strong gusts are found (Shaw *et al.*, 1979; Shaw and McCartney, 1985). These occasional strong gusts have been shown to be important in the dispersal of some wind dispersed pathogens, with spores being more likely to be dislodged from the fruiting bodies. Consequently, the average distances travelled by spores may be greater than the mean wind speeds suggest. Small spore carrying droplets are likely to be affected in the same way.

The structure of the canopy will also affect dispersal. In the case of short plants such as seedling crops or the stubble remaining after harvest, the wind will be less attenuated by the canopy and consequently have a greater effect on the dispersal of splash droplets. Nevertheless, although the potential for long range spore transport exists, splash is primarily a short range process.

1.3 Physics of splashing

1.3.1 *Previous studies*

The first photographic investigations of splash were those by Worthington (1877a & b) which examined the impact of drops on solid surfaces and later on liquid films (Worthington, 1882 and Worthington and Cole, 1897). It was noted that on striking a surface a drop formed a crown of liquid with radial ribs and which became thickened at the circumference. The radial ribs formed a number of jets of liquid which were ejected from the crown and broke up to form droplets. The number of jets was observed to increase with both drop size and impact velocity. When the splash occurred in a film of water a relatively large column of water, known as the Rayleigh jet, rose from the surface near the point of impact when the crown finally collapsed. It was also noted that very small disturbances in the target surface, or disturbances on the surface of a body falling into

a liquid, could cause large changes in the form of the splash.

Some of these findings were confirmed by Engel (1955). Impacts on several different surfaces were compared and it was suggested that the amount of spray produced, i.e. the amount of liquid thrown into the air as opposed to flowing across the surface, was a function of the roughness of the target surface and that spray formation probably occurs when the pressure of liquid on the surface is at a maximum.

Impacts on a hard, smooth, surface such as a buffed iron plate and dry clean glass, produced fewer droplets with more horizontal trajectories than did impacts on a slightly rough surface (an unpolished iron plate) which gave considerable upward splash. Splashes on flexible surfaces such as natural and synthetic rubber were similar, but the harder more resilient, natural rubber produced splash with a greater vertical component. A drop impinging on a particulate surface, fine moist sand, produced an upward moving splash crown containing water together with sand particles and left a crater in the surface. Al-Durrah and Bradford (1982), working on splashing on soils, showed that the angle at which droplets were ejected was related to the soil shear strength. This was due to the greater cavitation that occurred on soils of lower strength.

Levin and Hobbs (1971) gave a more detailed description of a splash. Irregularities on a solid rough surface initiate disturbances in the fluid that forms the crown causing it to become unstable. A relatively thick cylinder of water occurs at the rim of the crown which breaks up into a series of jets moving out from the perimeter of the corona. The formation of these jets is affected by a complex two-dimensional mesh of waves that exist in the crown running both parrallel and perpendicular to the surface. A crown is not produced when water drops impact on a very smooth surface, the drop simply spreads out radially across the surface. Allen (1976)

showed that there was a linear relationship between the surface Reynolds number ($Re_s = e\ u_0/\nu$ where u_0 is the impact velocity and e the height of the roughness elements) and the formation of a crown, and that the surface roughness only affects crown breakup when $Re_s > 64$.

Splashes in very thin liquid layers also produce a crown but the lack of surface irregularities reduces the disturbances that occur. This has the result that droplets are produced over a period about five times as long as when the impact occurs on a solid surface. The crown produced by splashes into liquid is almost vertical. Splashes in deep water usually produce a bubble beneath the surface (Blanchard and Woodcock, 1957). It is the collapse of this sub-surface cavity, combined with the subsidence of the crown that causes the formation of the Rayleigh jet.

1.3.2 *Number and size of splash droplets*

Levin and Hobbs (1971) estimated that about 110 droplets greater than 50 μm in diameter were produced when a 2.5 mm drop, falling 1.5 m, impacted on to a roughened copper hemisphere. The droplet size distribution was log-normal. Only droplets with diameters greater than 50 μm were counted. However, large numbers of droplets smaller than this were noted as being present. An estimate of the numbers of these small droplets based on the number of jets produced by the crown suggested that they followed the same size distribution as the larger droplets. Mutcheler (1971) found that the distribution of droplet sizes closely approximated a normal distribution when described on a volume basis.

Gregory, Guthrie and Bunce (1959), in their investigation of the dispersal of fungal spores by splash (see section 1.2.1), measured the size and number of droplets collected at various distances from

the target. An estimated maximum of 5200 droplets were produced by a single 5 mm drop falling 7.4 m into a horizontal spore suspension 0.1 mm thick on a glass surface. It was suggested that this number was probably an underestimate. Droplets were collected at distances of up to 1 m from the splash. Most droplets travelled between 80 and 180 mm. This distance varied little in different conditions although droplets of different sizes had different maximum ranges. Droplets of intermediate size, 150 to 325 μm diameter, reached the greatest distances, and vertical heights. The total number of droplets produced by a splash increased with drop size, impact velocity and decreasing film thickness. Hobbs and Kezweeny (1967) also reported that the number of droplets produced by 3 mm diameter drops splashing in water was greater for those impacting at higher velocities. The maximum impact velocity investigated was only about 25% of the drop sedimentation velocity. Droplets were collected with diameters between 5 and 2400 μm with the smallest droplets being the most numerous.

Ghadiri-Khorzoojhi (1978) measured the velocities of droplets splashed from a variety of soil and artificial surfaces using high speed cine photography. The angle at which splash droplets were ejected from the splash corona was found to be slightly different from the angle of the corona itself. It was suggested that this was due to a rotational flow of water within the splash corona. Droplets were not all produced at the same stage during the splash. Large numbers were thrown off between 0.2 and 0.7 ms after impact but a few droplets were still being ejected after 8 ms. Faster droplets were produced earlier in the splash. Droplets were observed with velocities ranging from less than 0.5 to greater than 20 m s^{-1}.

It was concluded by Faulwetter (1917b) that droplets from splashes on liquid surfaces were formed almost entirely of water from

the surface film. However Gregory (1952) and Timmons *et al.* (1971) showed that droplets consisted of a mixture of liquid from both the film and the incident drop. Timmons and his co-workers found that the proportion of splashed liquid originating from the incident drop declined from 41% to a minimum of about 8% as the depth of a target film of water was increased from 0.5 mm to 18 mm.

1.3.3 *Theoretical models of splash*

While most investigations into splash have been principally experimental, some theoretical studies have been carried out. Harlow and Shannon (1967) used the marker and cell technique (Harlow and Welch, 1967) to solve the full Navier-Stokes equations and model the splash process in an incompressible fluid. Although they ignored the effects of surface tension, the technique showed the importance of even a very thin layer of surface water in forming an upward moving crown of liquid. More recently Ferreira *et al.* (1985) have used the same technique, validated by experiment (Ferreira and Singer 1985), to examine drop impact in relation to soil erosion. It was shown that as the depth of water above a surface decreased the number of droplets ejected increases. Also the number of droplets was reduced when the underlying surface was composed of fine sand and therefore deformable. This was due to the absorption of energy due to the cratering of the underlying surface.

CHAPTER 2

Modelling the dispersal of splash droplets

2.1 Introduction

Modelling of the splash process and the trajectories of splash droplets will lead to a better understanding of the spread of splash dispersed pathogens. Models based on empirical correlations between fungal disease development and rainfall intensity have been devised (eg. Rapilly and Jolivet, 1976), but there is little evidence to justify the relationships. In other cases the spread of certain diseases has been linked to particular conditions. For example, Royale *et al.* (1986) demonstrated a relationship between sudden outbreaks of *Septoria* and the occurence of short convective rain showers. However, rainfall intensity varies widely even within a given classification (Ulbrich, 1983), and rain-splash intensity has been shown to vary over an order of magnitude within a single rain classification (Walklate *et al.*, in preperation). Clearly we need to better define the conditions under which dispersal is likely. The potential for splash dispersal by rain will depend on rainfall intensity, rain drop size spectra and the relative efficiency of drops of different sizes to cause splash. Thus, knowledge of the effect of rain drop size and impact velocity on splash may help us to identify the rainfall conditions under which disease dispersal is most likely. The rate of spread of disease depends on the distances travelled by spores. An understanding of the splash process will allow the prediction of dispersal distances under different conditions of rainfall and so lead to better estimates of the rates of disease spread. An ability to predict dispersal by splash will also be important if irrigation methods are suspected as an agent responsible for disease dispersal, and in cases of drip splash caused

by heavy dew deposit on leaves.

The movement of small drops out of the canopy may be important in the long range dispersal of disease. Modelling the movement of smaller droplets that can escape the canopy will help us to determine how likely or important long distance dispersal is, and in all cases how different conditions will affect the processes involved.

Sampling for splash dispersed spores is very difficult, no currently available sampler is capable of isometrically sampling all the different sizes of spore carrying droplets. Better understanding of the movement of spore carrying droplets may help us to devise better sampling regimes. By expanding our understanding of the effect of different conditions on splash disease dispersal we will also be able to devise systems appropriate for sensing the conditions under which dispersal is likely, and if we understand the relationships between the weather, the crop and dispersal we may be able to further develop simple models for forecasting disease outbreaks.

This chapter describes a model for calculating the trajectories of splash droplets. Further chapters describe the verification of the model by the comparison of its predictions with the results of experiments.

2.2 The model

The trajectory of a spherical projectile through a fluid can be computed using numerical integration. Within certain limits the trajectory of a splash droplet can be calculated using the same method.

2.2.1 *Forces acting on a particle*

In a vacuum a moving particle is only acted upon by the force of gravity and so its path describes a parabola; however a droplet

moving through the air is acted upon by several forces:

1. The force due to gravity or the weight of the body, $\hat{F}g=m.\hat{g}$ where m is the mass of the particle and $\hat{g}$ is the acceleration due to gravity, (9.8 m s^{-2}) and is directed downwards. (n.b. $\hat{}$ symbol denotes a vector quantity).

2. Drag on the droplet, $\hat{F}_D$, caused by the viscosity of the surrounding medium. The drag is a result of two factors, shear stress due to a gradient of velocities at the surface of the droplet, and form drag caused by a reduction in pressure at the rear of the droplet in comparison to the front. The drag force acts in a direction opposite to that of the motion of the particle:

$$\hat{F}_D = -\tfrac{1}{2}\,\rho_f\,\hat{v}_r\,v_r\,\frac{\Pi}{4}\,d^2\,Cd \qquad - 1 -$$

where d is the particle diameter, $\hat{v}_r$ is the particle velocity, v_r the particle speed, both are relative to the surrrounding fluid, ρ_f is the density of the fluid and Cd is a dimensionless parameter known as the drag coefficient. Cd is a function of the shape of the particle and its Reynolds number (Re) which can be defined as $v_r.d/\nu$; where ν is the Kinematic viscosity of the surrounding medium, (for air, at 1 atm, 20°C, ν=1.49x10^{-5} m s^{-1}). Calculation of the value of Cd is discussed in section 2.2.3.

3. Archimedean buoyant force, $\hat{F}_A$, is a force equal to the weight of fluid displaced by the particle acting in the opposite direction to gravity. In the case of a water droplet in air this force is very small. This force is equal to 1/6 $\pi d^3 \rho_f g$ where ρ_f is the density of

the surrounding air and d is the particle diameter. This force can also be written in the form $\hat{F}_A=-m_f.\hat{g}$ where m_f is the mass of liquid displaced.

4. The force on an accelerating body. This is the energy needed to induce a field of flow within the surrounding fluid and is given by;

$$\hat{F}_A=-\tfrac{1}{2}.m_f.\frac{d\hat{v}_r}{dt} \qquad - 2 -$$

If the fluid is not accelerating then $\frac{d\hat{v}_r}{dt} \equiv \frac{d\hat{v}}{dt}$; where v is the absolute velocity of the particle.

Drag along with gravity are the two most important forces, the archimedean buoyant force and the force on an accelerating body are generally negligible for a droplet moving through the air.

2.2.2 *The equation of motion for a splash droplet*

If all the forces acting on a droplet are included the equation of motion in vector form can be written as;

$$m.\frac{d\hat{v}}{dt} = \hat{F}_g + \hat{F}_A + \hat{F}_D + \hat{F}_a \qquad - 3 -$$

thus for a non-accelerating fluid

$$(m+\tfrac{1}{2}m_f)\ \frac{d\hat{v}}{dt} = (m-m_f)\ g - \frac{\Pi}{8}\ \rho_f\ \hat{v}_r|v_r|d^{\,2}Cd \qquad - 4 -$$

Expressing masses m and m_f in terms of density ($m = \frac{\Pi}{6}\ d^3\ \rho_p$ and $m_f = \frac{\Pi}{6}\ d^3\ \rho_f$; where ρ_p is the density of the particle.) rearranging equation 4 becomes (Chow, 1979);

$$\frac{d\hat{v}}{dt} = \frac{1}{A}\,[-B\hat{y}+C\hat{v}_r|v_r|Cd(v_r)] \qquad - 5 -$$

where $\hat{y}$ is the unit vector in the vertical direction.

where A, B and C are constants. $A = 1+\frac{1}{2}\rho$, $B = (1-\rho)g$ and $C = 3\rho/4d$; ρ is the density ratio of the surrounding fluid and particle $(=\rho_f/\rho_p)$ and v_r is the particle velocity relative to the surrounding medium. In the case of a water droplet moving through the air A = 1.00061, B = 9.788 m s^{-2}, C = 0.000915/d and ρ = 0.00122.

If we consider the movement of a droplet through the air in two dimensions we can resolve the forces acting on the drop into horizontal (x direction) and vertical (y direction) components.

$$F_x = |\hat{F}|\ \text{Cos}\ \theta \qquad - 6a -$$

and

$$F_y = |\hat{F}|\ \text{Sin}\ \theta \qquad - 6b -$$

where θ is the direction of the force measured relative to the horizontal. If w_r is the speed of the drop relative to the fluid, u and v the horizontal and vertical components of the particles velocity and u_f and v_f the components of the fluid velocity then $\text{Cos}\ \theta = \frac{u-u_f}{w_r}$ and $\text{Sin}\ \theta = \frac{v-v_f}{w_r}$.

The horizontal component of the equation of motion of the particle is thus;

$$m\frac{d^2x}{dt^2} = \frac{1}{8}\,\Pi\,\rho_f\,d^2\,w_r\,(u_f-u)\,Cd - \tfrac{1}{2}m_f\frac{dw}{dt}\cdot\frac{u-u_f}{w_r} \qquad - 7 -$$

Substituting density for mass as before and rearranging this becomes;

$$\frac{d^2x}{dt^2} = \frac{C}{A}\,w_r(u_f-u)Cd \qquad - 8 -$$

and the vertical component;

$$m \frac{d^2y}{dt^2} = m_f\, g - m.g + \frac{1}{8} \Pi\, \rho_f\, d^2\, w_r\, (v_f - v)\, Cd - \tfrac{1}{2} m_f \frac{dw}{dt} \cdot \left(\frac{v - v_f}{w_r} \right) \qquad - 9 -$$

and rearranging;

$$\frac{d^2y}{dt^2} = \frac{1}{A} [C\, w_r\, (v_f - v)\, Cd - B] \qquad - 10 -$$

The components A, B and C are defined as before.

Because of the complicated derivatives involved it is impractical to apply the commonly used Taylor's series expansion to solve the equation analytically. The equations were solved numerically using a Runge-Kutta method to carry out the integration (Chow 1979).

A fourth order Runge-Kutta formula was chosen, this has the general form

$$Z_{i+1} = Z_i + \frac{1}{6} (\Delta_1 Z_i + 2\Delta_2 Z_i - 2\Delta_3 Z_i + \Delta_4 Z_i) \qquad - 11 -$$

the increments being calculated as follows

$$\Delta_1 Z_i = hf\ (Z_i, t_i) \qquad - 12a -$$

$$\Delta_2 Z_i = hf\ (Z_i + \tfrac{1}{2}\Delta_1 Z_i, t_i + \tfrac{1}{2}h) \qquad - 12b -$$

$$\Delta_3 Z_i = hf\ (Z_i + \tfrac{1}{2}\Delta_2 Z_i, t_i + \tfrac{1}{2}h) \qquad - 12c -$$

$$\Delta_4 Z_i = hf\ (Z_i + \Delta_3 Z_i, t_i + h) \qquad - 12d -$$

h is the interval between iterations. With the normal level of numeric accuracy available on the HP1000 minicomputer that was used for most of the work a time step of 2 ms was found to be best.

Using this method we can compute the position and velocity at time t_{i+1} based on the values at time t_i. The complete set of equations to do this in two dimensions are presented by Chow (1979).

2.2.3 *Estimating drag on a droplet*

For spheres the relationship between Re and Cd is well known, for example see Clift *et al.* (1978). Although difficult to determine analytically, several empirical functions can be used to determine the value of Cd for a given value of Re with reasonable accuracy. For water drops however there are two factors that complicate the relationship. Firstly, the flow of air over the surface of the drop can induce a flow of liquid within the drop resulting in a reduction in the skin friction component of the drag. Secondly, the pressure on the drop may cause it to deform from a spherical shape so that calculating the drag coefficient on the basis of a sphere is no longer a reliable method (Pruppacher and Beard, 1970).

Fortunately, these factors do not become important until quite large Reynolds numbers. Only drops larger than about 1 mm are significantly nonspherical (Plesset and Prosperetti 1977), which approximates to a Reynolds number of about 300 when travelling at terminal velocity. The effect of internal circulation on the trajectory of a droplet will also be small. LeClair *et al.* (1972) developed a model for water drop circulation and calculated that for Reynolds numbers less than 300 the reduction in drag of a liquid water drop compared with that of a rigid sphere was less than 1%. At higher Reynolds numbers where the drop deforms significantly from a spherical shape and starts to oscillate the internal circulation becomes unsteady changing between zero and a maximum very rapidly, on a time scale observed to be less than a second. This makes the effect

TABLE 2.1

Reynolds number range	Drag coefficient
$Re < 0.01$	$Cd = 3/16 + 24/Re$
$0.01 < Re < 20$	$Cd = 24/Re\ [1 + 0.1315\ Re^{(0.82 - 0.05\ w)}]$
$20 < Re < 260$	$Cd = 24/Re\ [\ 1+ 0.1935\ Re^{\ 0.6305}\ ]$
$260 < Re < 1500$	$\log_{10} Cd = 1.6435 - 1.1242w + 0.1558w^2$
$1500 < Re < 12000$	$\log_{10} Cd = -2.4571 + 2.558w - 0.9295w^2 + 0.1049w^3$

$w = \log_{10} Re$

Equations used to calculate Cd for different ranges of Re, after Clift *et al.* (1978)

of internal circulation difficult to calculate. However for most splash droplets Re is expected to be less than 300 during flight and so the effects will be negligable.

To calculate the values of Cd the equations presented by Clift *et al.* (1978, p112) were chosen as they gave good coverage of the region of low Reynolds number which corresponds to most splash droplets (Table 2.1).

2.3 Uncertainty and accuracy of model

2.3.1 *Effect of air temperature and pressure on particle range*

Temperature and pressure can affect the movement of particles through their effect on the viscosity and density of the air. All calculations were made assuming an air temperature of 20°C and 1 atm pressure (1013.15 mb). To assess the likely error caused by variation in these values a number of droplet trajectories were calculated using different values for the viscosity and densities of air and water to correspond to different temperatures and pressures. The effect of changing the air pressure was negligible. The effect of isolated changes in air density and kinematic viscosity due to a 20°C change in temperature are illustrated in Table 2.2.

Even under the extreme conditions illustrated in Table 2.2 the effect on droplet range was in all cases less than 10%, the degree of change decreasing with increasing droplet size. As the viscosity of the air increases with rising temperature so the density decreases. If both factors are included they tended therefore to cancel one another out so that the overall error caused by ignoring natural variations in the atmosphere is very small.

TABLE 2.2

a) Changes in the kinematic viscosity (υ) and density (ρ_a).

Temperature (°C)	$\upsilon(m^2s^{-1})$	ρ_a (g cm^{-3})
0	1.32×10^{-5}	1.2740
20	1.49×10^{-5}	1.2200
40	1.69×10^{-5}	1.1189

b) Effect on droplet range of changing υ.

Droplet ranges are in cm.
All droplets are ejected horizontally.

Droplet diameter	Initial velocity	Height of fall	Kinematic viscosity ($\times 10^{-5}$ $m^2 s^{-1}$) 1.32	1.49	1.69
1000 μm	3 m s^{-1}	70 cm	88.1	86.9	85.4
500 μm	4 m s^{-1}	60 cm	71.0	68.4	65.5
250 μm	5 m s^{-1}	50 cm	35.7	33.4	31.0
125 μm	6 m s^{-1}	20 cm	13.9	12.8	11.8

c) Effect on droplet range of changing ρ_a.

Initial velocities and heights of fall as in table b.

	ρa		
Droplet diameter (μm)	1.2740	1.2200	1.1189
1000	85.9	86.9	88.9
500	66.5	68.4	72.0
250	32.1	33.4	36.2
125	12.3	12.8	14.0

2.3.2 *Evaporation*

The evaporation of droplets is probably the single most important factor likely to cause errors in trajectory calculations, particularly for small droplets. The time that a small droplet takes to evaporate to dryness may be short in comparison to the time that a droplet is airborne. Amsden (1962) calculated the approximate lifetime of a droplet of water, in seconds, to be $\frac{d^2}{80}\Delta t$; where d is the droplet diameter in microns and Δt the difference between wet and dry bulb temperatures. Some examples of droplet lifetimes listed by Matthews (1982) are given in Table 2.3.

The rate of change in the diameter of a water droplet in dry air dD/dt has been described by the following equation;

$$\frac{dD}{dt} = \frac{-4.M_L.D_V}{D.\rho_L.R.T_f} \cdot \Delta P_L \cdot \frac{Sh}{2} \qquad - 13 -$$

Where M_L is the molecular weight of water, D_V is the diffusivity of water vapour in air (0.24 $cm^2\ s^{-1}$ at 20°C), D is the droplet diameter, ρ the density of water, R the universal gas constant (8.314 $J\ K^{-1}\ mol^{-1}$), T_f the film temperature which equals 1/2 x (temperature of droplet surface - temperature of air), ΔP_L is the difference in partial preassure of water vapour between the droplet surface and the surrounding air and Sh is the Sherwood number which is a function of dimensionless time and mass transfer due to convection that arises as a result of motion of the droplet relative to the air and can be defined, for water droplets, as;

$$Sh = 1.755 + 0.535\ Re^{1/2}\ Sc^{1/3} \qquad - 14 -$$

Re being the Reynolds number and Sc the Schmidt number or ratio of

TABLE 2•3

Lifetime and fall distance of water droplets before evaporation to dryness in various conditions.
(after Matthews 1979)

Temp °C 20 ΔT °C 2.2 RH% 80			Temp °C 30 ΔT °C 7.7 RH% 50		
Initial droplet diameter (μm)	Lifetime to extinction	Fall distance	Initial droplet diameter (μm)	Lifetime to extinction	Fall distance
50	14s	0.5m	50	4s	0.15m
100	57s	8.5m	100	16s	2.4m
200	227s	136.4m	200	65s	39m

the kinetmatic viscosity of the air to the diffusivity of water vapour, ν_a/D_V, Goering *et al.* (1972), Williamson and Threadgill (1974) and Wedding *et al.* (1986).

Due to the increased surface area to volume ratio the effects of evaporation are most apparent with small droplets. A 200 μm droplet will take about 16 times as long to completely evaporate as a 50 μm one. This somewhat mitigates the importance of evaporation from the point of view of disease dispersal, where large droplets appear to be more important (see Chapter 1). Also, in crop canopies, particularly under conditions when dispersal of spores in splash droplets is likely to occur, i.e. during rain, the relative humidity approaches 100% (H.A. McCartney pers. comm.), and thus the effects of evaporation will be small. Under laboratory conditions the humidity may be less and so evaporation may be more important. However in the experiments described here droplets were photographed within a fraction of a second of being produced and so will not have had time to evaporate significantly.

The model is verified for accuracy and illustrated in use in the following chapters. In particular Chapter 7 details some of the applications of the model.

CHAPTER 3

Verification of the Trajectory Model

The model calculates particle or droplet trajectories given their initial velocities. Thus the accuracy of the model was assessed by comparison of the actual distances travelled by droplets with distances predicted from droplet trajectories calculated from measured values of droplet velocity.

3.1 Comparison of measured and predicted terminal velocities

The terminal velocities of droplets as calculated by the model were compared with measurements of terminal velocity taken from the literature. This was also done by Chow (1979) who showed that equation 5 could be used to accurately predict the sedimentation velocity of water droplets up to 2000 μm in diameter. The model used in these experiments differs only in the formulae for determining Cd and so would be expected to give similar results. Fig. 3.1 shows the terminal velocities of water drops, V_t, calculated by the model and values taken from the literature (Edmonds, 1979; Fuchs, 1964; Matthews, 1984) as a function of particle diameter.

The figure shows there to be excellent agreement between the calculated and reported values of V_t for droplets with diameters up to about 1500 μm, a range which covers the vast majority of splash droplets. The terminal velocities of larger droplets are overestimated. This is because of the increased drag caused by drop deformation which is not allowed for in the calculations. Very small discontinuities do occur because the equations for estimating Cd change for different size ranges, however the errors caused by these are less than 1%.

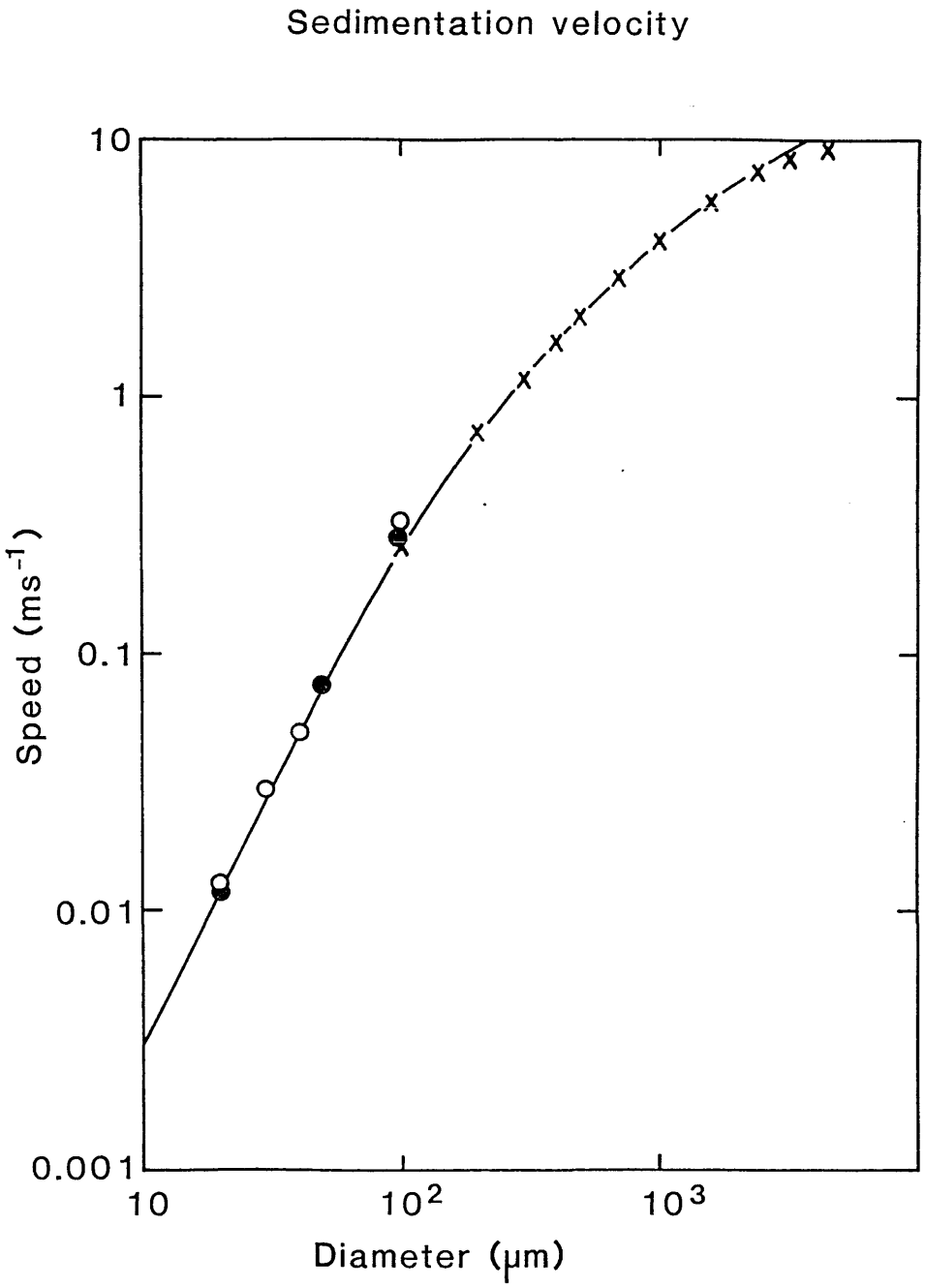


Fig 3•1. Comparison of calculated droplet sedimentation velocity with reported measured values.

——— Model calculations
● Matthews (1982)
O Edmonds (1979)
× Fuchs (1964)

3.2 Comparison of predicted and observed droplet trajectories in still air

The next stage was to compare calculated and observed trajectories of droplets in two dimensions.

Two sets of experiments were carried out to measure droplet trajectories in still air, one used a vibrating needle to produce streams of monosized droplets, between about 200 and 1000 μm in diameter. The other used a spinning disc atomiser which produced droplets with diameters ranging from less than 50 to over 500 μm. In the vibrating needle experiments it was possible to measure the trajectories of a stream of almost identical droplets. However the droplets produced by this method had only a limited range of velocities, between 0.6 and 2.0 m s^{-1}. Ghadiri-Khorzoojhi (1978) showed that splash droplets produced from drop impacts with solid surfaces can have velocities of greater than 20 m s^{-1}. Proper verification of the model therefore, also required comparisons with faster moving droplets. This was done using a spinning disc atomiser, which produced much faster moving droplets but had the disadvantage of producing droplets with a wide spectrum of different velocities and sizes and therefore precluded the possibility of looking at individual trajectories.

3.2.1 *Vibrating needle experiments*

The experiments set out to measure the initial velocity and size of droplets and to determine the distance travelled by those droplets. Droplets were produced using a vibrating needle. A sample of the droplets generated were collected for sizing and the stream of droplets produced by the apparatus was photographed to determine their initial velocity and the distance that they travelled.

(a) Methods

A needle, vibrating at a constant frequency and with sufficient amplitude can be made to produce a stream of monosized droplets either by dipping the tip of the needle into a body of liquid (Wolf 1961) or by pumping liquid through a hollow needle (Mason *et al.*, 1963). Both techniques were used in the experiments. In both cases the needle was attached to the core of a loudspeaker from which the paper cone had been removed. The needle was then vibrated by connecting the speaker to a waveform generator (Radio Spares 610-629 or Hewlett Packard 8015A) and a simple amplifier. When the needle was vibrated at or near its resonance frequency the tip moved through an arc of 5-10 mm or more, this was sufficient to throw off a stream of droplets with velocities of around 1 m s^{-1}.

The solid needles used were no.0 insect mounting pins, 38 mm long and with a diameter of 0.4 mm, these were soldered onto a small zinc plate glued to the loudspeaker core (Fig. 3.2a). The apparatus was adjusted so that, when still, the tip of the needle just broke the surface of a small reservoir of water and when vibrated, a constant stream of droplets was thrown from the water. The level of water in the reservoir was kept constant by connecting it to a much larger supply (Plate 1).

The hollow needles used were blunt ended hypodermic needles, 250 mm long and of various external diameters, 0.5 to 1.0 mm (The Stainless Tube and Needle Co. Ltd. Warwickshire). These were held in a groove between two zinc plates glued to the speaker core so that a length of 20-50 mm was free to vibrate. The other end of the needle was clamped and connected to an infusion pump (Braun, Perfusor VI) set to supply water at a rate of about 30 $ml.hr^{-1}$. Figure 3.2b shows the apparatus in diagrammatic form.

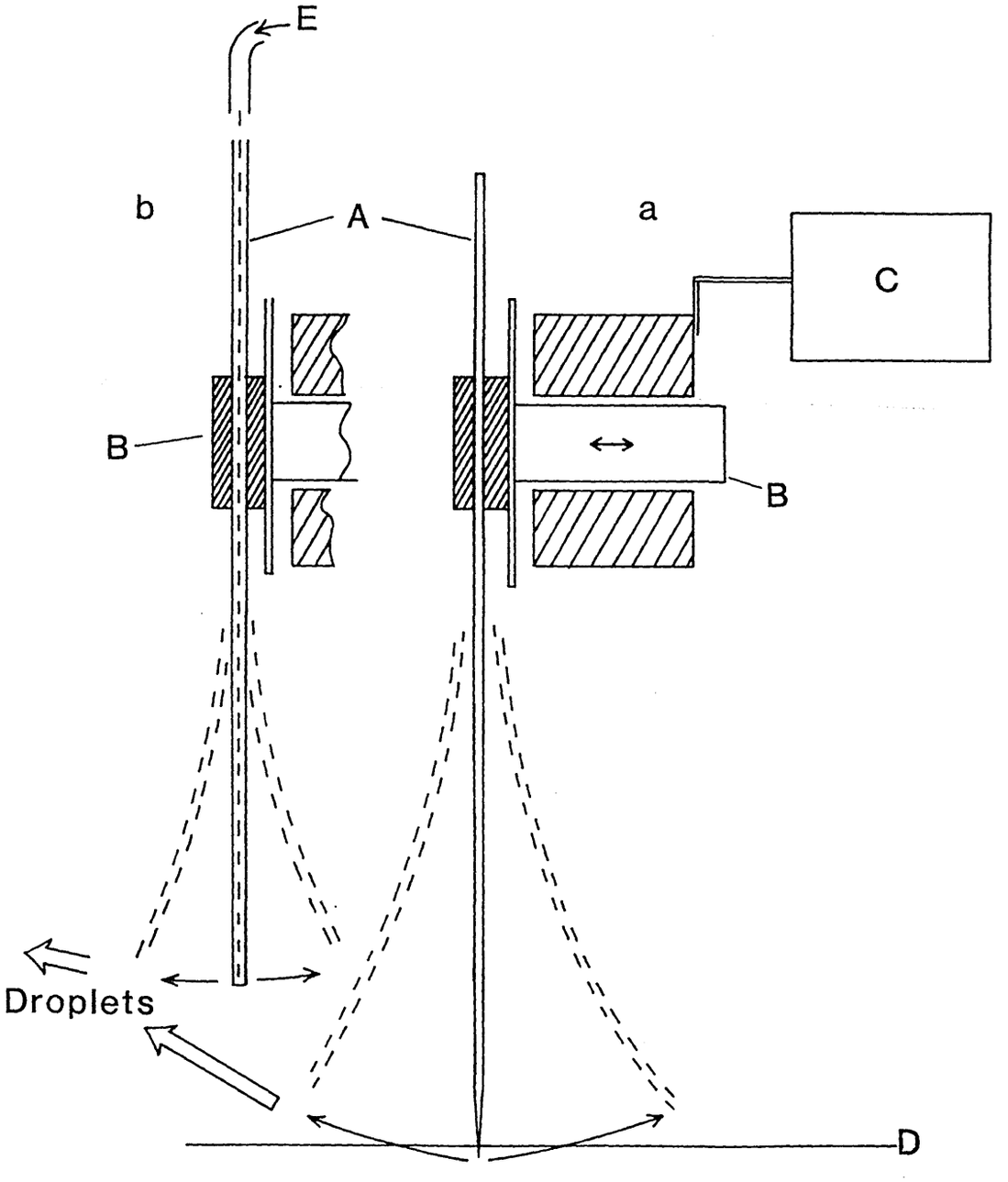


Fig 3·2. Schematic diagram of the vibrating needle droplet generators (a) Solid needle generator. (b) Hollow needle generator. A, needle; B, loudspeaker core; C, signal generator and amplifier; D, water surface; E, water feed from a syringe pump. Arrows indicate the direction of droplet movement.

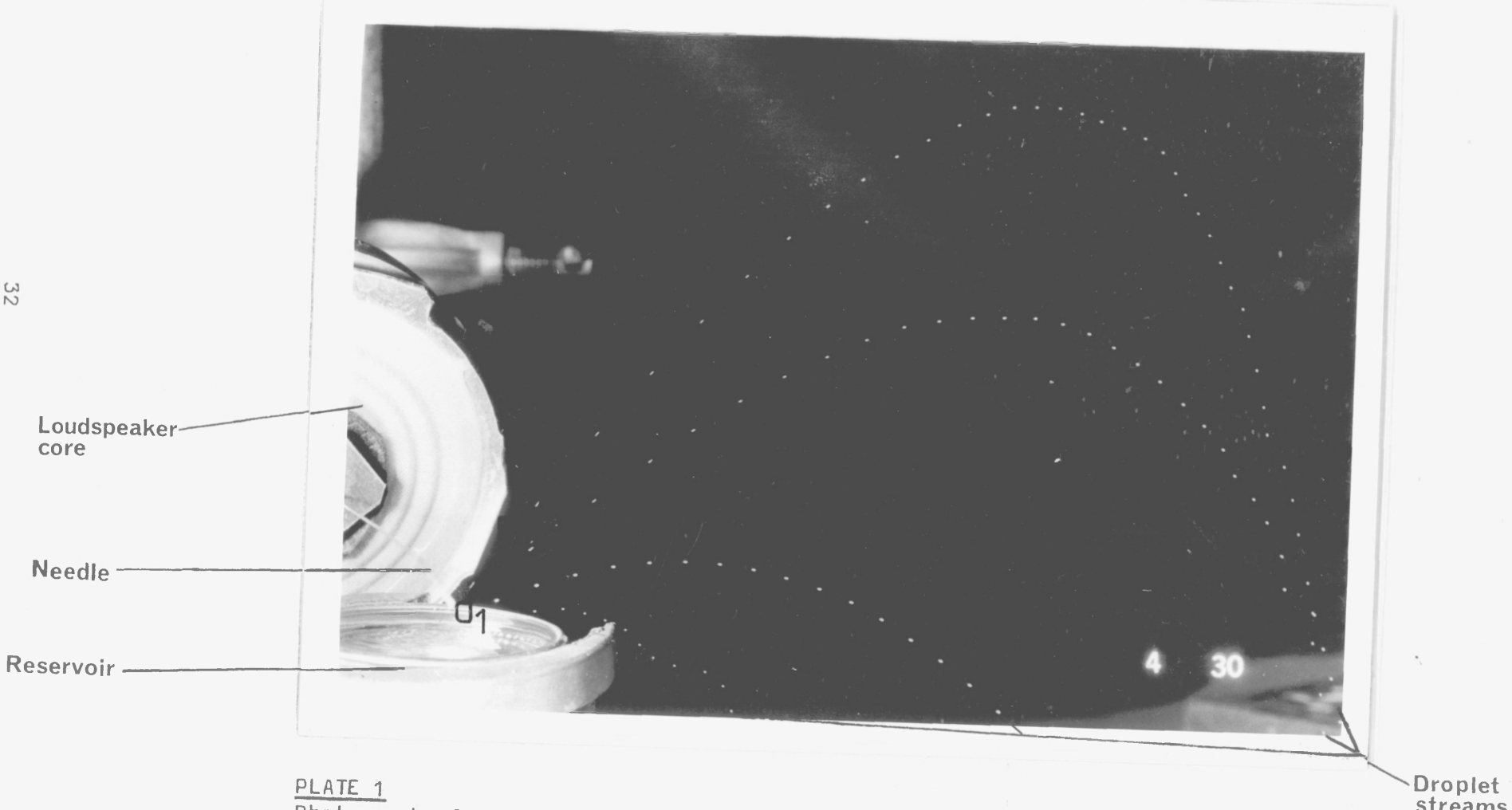


PLATE 1
Photograph of droplet streams produced by a solid needle.
See text for explanation.

Droplets were sized using the technique described by Fitt *et al.* (1982). A sample of droplets was collected on fixed photographic film before and after each trial. The mean droplet diameter was then determined by measuring the diameter of the resultant craters left in the gelatine layer. If a significant difference was found in the size of droplets collected before and after the trial then the results were discarded.

In both types of experiment streams of monosized droplets each with the same velocity were produced. The diameters of droplets were in the range from 200 to 1000 μm with velocities between 0.6 and 2.0 m s^{-1}. The size and velocity of the droplets remained remarkably constant if the conditions were left unchanged. Within any single stream the standard deviation of both values was typically only 2-3% of the mean. Table 3.1 shows the sizes of droplets measured in two sample trials.

In many cases, particularly when using the hollow needles, several streams of droplets were produced simultaneously. Although the separate streams differed from one another in the sizes and velocities of droplets, each individual stream still consisted of monosized droplets with identical trajectories and each could therefore be used for the experiments.

The velocities and distances travelled by the droplets were determined by photographing the droplet streams using an Olympus OM2, 35 mm camera. An electronic flash unit (Olympus Quick Auto 310) set to deliver a flash of about 1/40,000 second duration was used to freeze the motion of the droplets. The flash gun was mounted beside the camera and white pieces of card were placed around the experimental area but outside the field of view to act as reflectors and give even illumination of the droplets. A 50 mm Zuiko macro lens with various extension tubes was used to obtain the desired

TABLE 3•1

Example of droplet diameters measured during vibrating needle experiments.

a) Crater diameter (microns)

230	230	240	240	
250	230	250	240	mean = 237
250	230	230	210	Standard deviation = 1.078×10
230	240	250	240	

Mean droplet diameter	156 μm
Standard deviation of diameter	7•1 μm

b) Crater diameter (microns)

950	940	970	950	
950	950	960	940	mean = 938
880	820	930	960	Standard deviation = 4.10×10
950	980			

Mean droplet diameter	604 μm
Standard deviation of diameter	26 μm

magnification. The exact magnification was varied depending on the distance travelled by droplets in the stream, the aim being to just include the whole trajectory in the photograph. The camera was mounted on an adjustable stand so that it could be placed in such a position that the droplets were travelling parallel with the film plane. A calibrated scale was included in the field of view and used to determine the magnification for each photograph. Black and white Ilford HP-5 film, rated at 400 ASA, was used. This was developed and printed in the laboratory. The camera was set for automatic exposure with the lens stopped down to either f8 or f11. This gave a sufficient depth of field, making focussing less critical, while still permitting the use of the very short duration flash neccesary to freeze the image.

The speed of the droplets, v, was calculated from the vibration frequency of the needle, f, and the distance, D, measured between consecutive droplets in the stream, thus: $v=D.f$. It was verified that one droplet was produced for each oscillation of the needle by observing the apparatus with a stroboscopic lamp. In a number of cases where the flow rate of liquid through the hollow needle was very low, it was found that droplets were produced at only half the vibration frequency of the needle, in such cases the calculation of v was adjusted accordingly. Plates 1 and 2 show an example of the photographs taken. Measurements of velocity were made from the pair of droplets nearest the needle (d1 and d2) and assumed to apply at the mid point between the two droplets, the height of this point was taken to be zero. The distance travelled by the droplets was measured between the two points at which the droplet stream crossed the zero height plane.



PLATE 2
Photograph of droplet stream produced by a vibrating hollow needle.
See text for explanation.

(b) Results

The initial velocities and sizes of droplets were used to calculate the trajectories and thus the distances travelled by the droplets.

The measured ranges compared well with those predicted by the model (Table 3.2). Figure 3.3 shows graphically the predicted and measured distances that droplets travelled in the vibrating needle experiments. The error bars in the figure indicate the uncertainties in the calculated distances due to the errors in measurements of droplet size and velocity. The predicted distance travelled by droplets is generally within 10% of the measured values of range. The points plotted in the figure represent droplets in the size range 200-1000 μm with initial speeds in the range 0.6-2 m s^{-1}. The plotted points fall close to a 1:1 relationship and the slope of best fit line (shown as a broken line in the figure) is not significantly different from one.

There is a slight, but not significant, tendency for the model to underestimate the distance travelled by droplets. This may be an experimental artifact caused by the entrainment of air in the droplet stream. Because each droplet is moving in the wake of the previous one its drag may be reduced slightly, causing it to move further than expected. Yalin (1977), quoting from Loo (1967), reports that for sediments settling in water, there is no significant effect on the drag coefficient of particles unless they are within two diameters of one another. In these cases droplets were several tens of diameters apart. However, because there was a steady stream of droplets, all following the same path it is possible that air could be entrained along the path of droplet travel.

TABLE 3•2

Droplet diameter (um)	Initial Speed ($m\ s^{-1}$)	Initial angle	Observed range (O)	Calculated range (E)	E/O
322	0.82	57	34	40	1.16
322	0.615	61	20	23	1.17
228	1.185	19	57	52	0.79
190	1.19	17	46	44	0.96
228	1.165	13	47	41	0.87
230	1.66	44	98	81	0.83
230	1.61	45	105	84	0.80
230	1.425	49	76	70	0.92
257	1.35	29	111	79	0.70
257	1.425	40	85	85	1.00
221	1.99	52	90	90	1.00
227	1.0	30	41	48	1.16
755	0.76	80	17	18	1.03
577	0.56	52	37	28	0.75
727	0.64	61	40	32	0.81
578	0.79	78	26	21	0.82
744	0.97	75	44	42	0.96
1019	1.06	52	88	100	1.14
1049	1.36	31	152	151	0.99
1001	0.63	38	38	38	0.99
545	0.99	72	46	45	0.97
604	0.95	73	42	41	0.97
604	0.97	74	46	40	0.89

Comparison of observed range and ranges calculated from the measured diameters and initial velocities of droplets. Angles are relative to thehorizontal, all distances are in mm. Measurements are averages from several photographs.

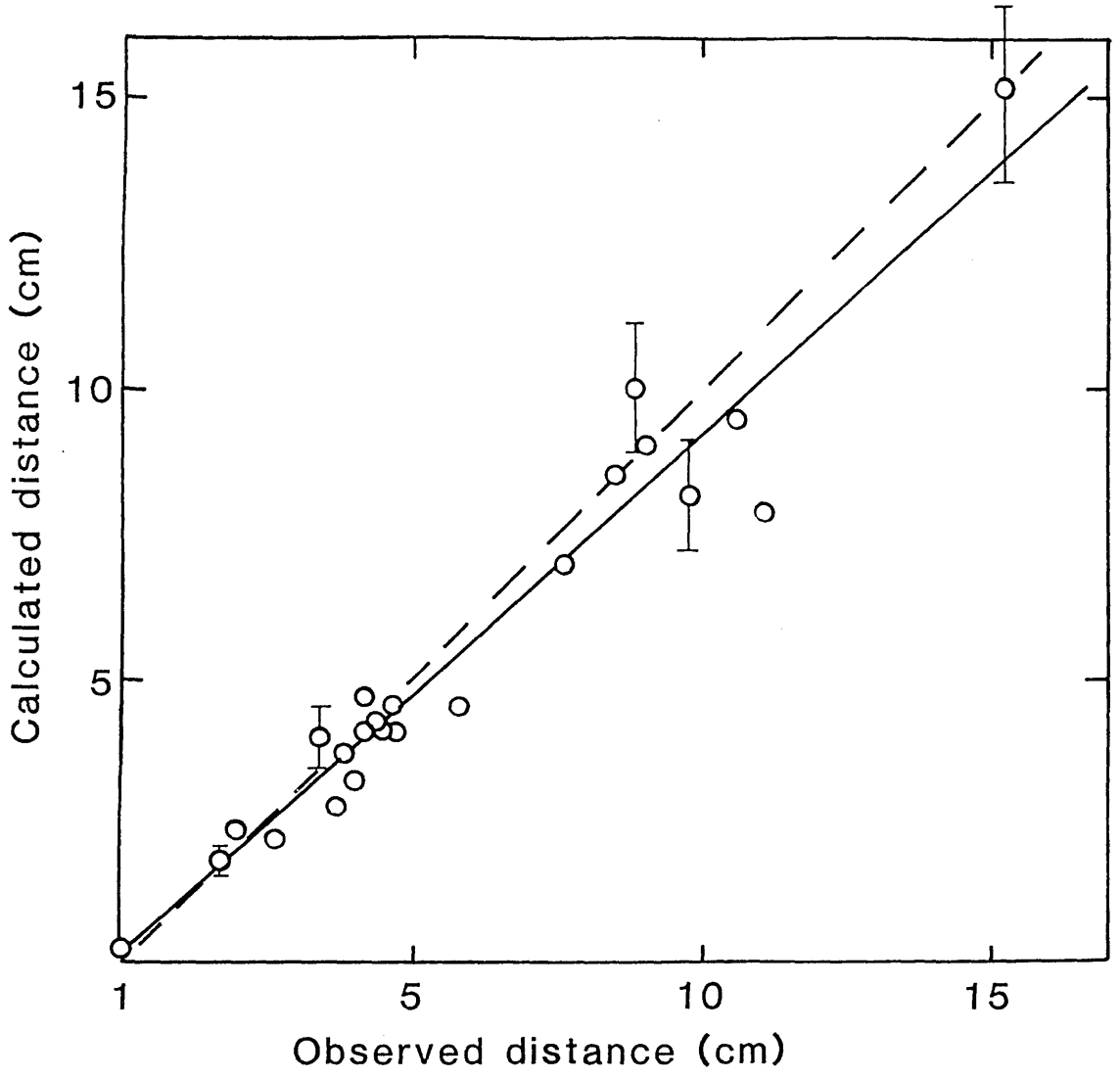


Fig 3·3. Observed and calculated distances travelled by drops in the vibrating needle experiments. Sample error bars show the typical levels of uncertainty in the calculated ranges.
——— Regression line (calculated vs observed)
- - - 1:1 line.

3.2.2 *Spinning disc experiments*

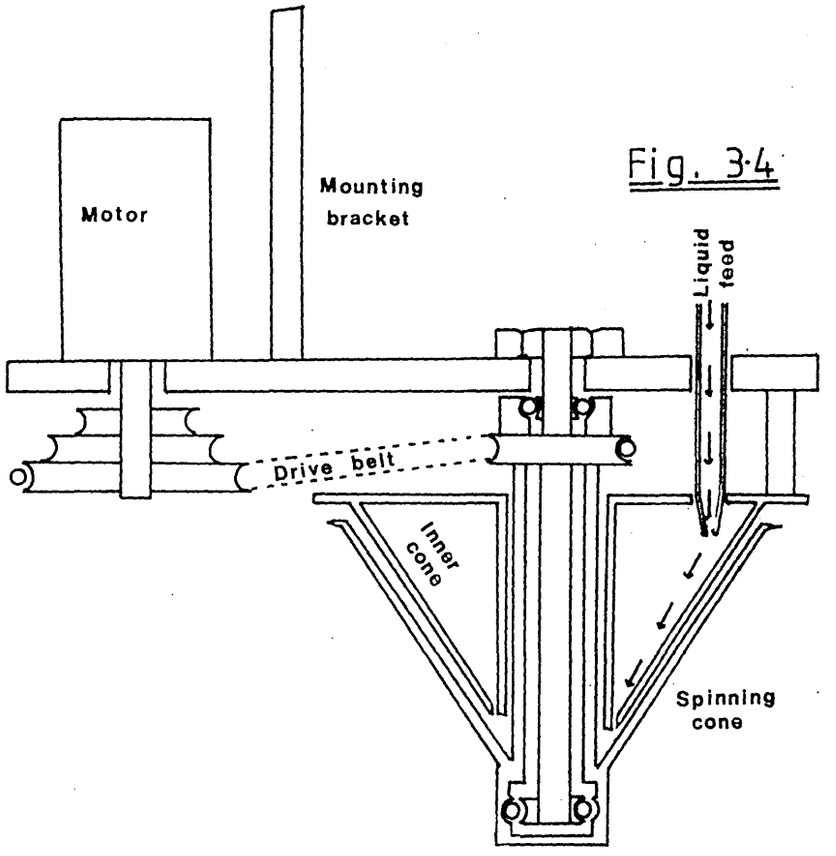
(a) Methods

Droplets were produced using a Micromax (Micron Sprayers Limited) spinning disc atomiser (Fig. 3.4). This consists of a hollow spinning cone mounted with the apex pointing downwards and rotated, through a belt drive, by an electric motor at a speed ranging between 1000 and 5000 rpm. Liquid is fed into the centre of the cone through two flow restricting nozzles. As the cone rotates the liquid flows up the inside of the cone forming a film. Droplets are formed as the film is thrown from the edge. To help produce an even flow of liquid the inside of the cone is grooved. At the upper edge of the cone the grooves are extended to form teeth. These encourage the formation of ligaments in the liquid which reduces the variation in the size of droplets produced. The atomiser produces droplets with a spectrum of sizes between 100 and 700 μm and with initial velocities of several metres per second. This is much faster than those attainable in the vibrating needle experiments.

The atomiser was mounted within an enclosure which had a thin vertical slot cut in one side of it to allow only a narrow stream of droplets to escape (Fig. 3.5). The flow of liquid to the sprayer was maintained at a constant rate to ensure that the size spectrum of droplets produced remained constant.

The same camera and lens as used in the vibrating needle experiments was positioned close to the slot and used to photograph the emerging stream of droplets. Double exposure photographs were taken by firing two flash guns (an Olympus Quick Auto 310 and an Olympus T32), with a known time delay between them, while the camera shutter was open (see Section 4.1). Photographs were taken in dim light in the laboratory. The lens was stopped down to f11 with the

Fig. 3·4



Simplified diagram of Micromax spinning disc atomiser

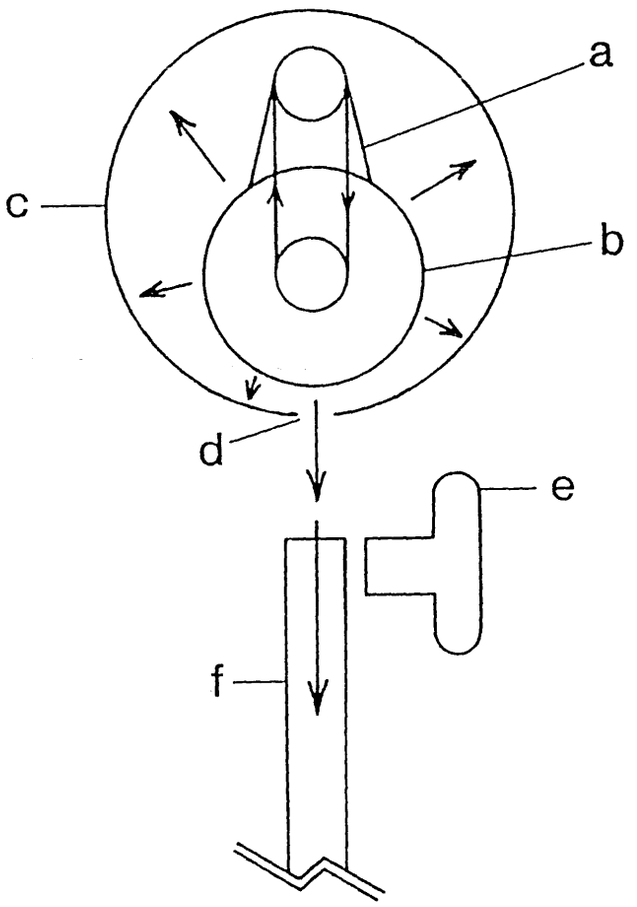


Fig. 3·5. Schematic diagram (plan) of droplet production using a spinning disc.
a, spinning disc droplet generator
b, disc
c, enclosure containing generator
d, vertical slot allowing droplets to escape
e, camera
f, droplet collecting film
Arrows indicate droplet movement.

camera set for manual operation with a shutter speed of 1/30 second. Ilford HP-5 black and white film was used.

The photographs were analysed by projecting the negatives directly onto a screen. The speed of the droplets was determined by measuring the distance between the two images of a single droplet and relating this to the time delay between the two flashes. The size of droplets and the direction in which they were travelling could be determined directly from the photographs.

Droplets were collected on fixed photographic film at a known height below and at various distances beyond the point at which the photographs were taken. Droplets were sized and the mean diameter of droplets collected at each distance from the sprayer was calculated.

In each test the initial velocity and size of a representative sample of droplets was measured from the photographs. These values were then used to calculate the distance travelled by each droplet.

Comparison of the predicted and observed trajectories of these experiments was less straightforward than for the vibrating needle experiments. Both the sizes and the distances travelled by droplets were measured but because of the greater distances travelled by droplets and the lack of similarity in the trajectories it was not possible to determine the trajectories of individual droplets. A representative sample of droplets was chosen from the photographs and the theoretical distance travelled was calculated from the measured size and velocity of each droplet. The calculated ranges were then compared with the mean size of droplets collected on the photographic film at each distance from the sprayer.

(b) Results

Figure 3.6a-c show the calculated range (distance travelled between the camera and impact onto a surface 385 mm below) for each

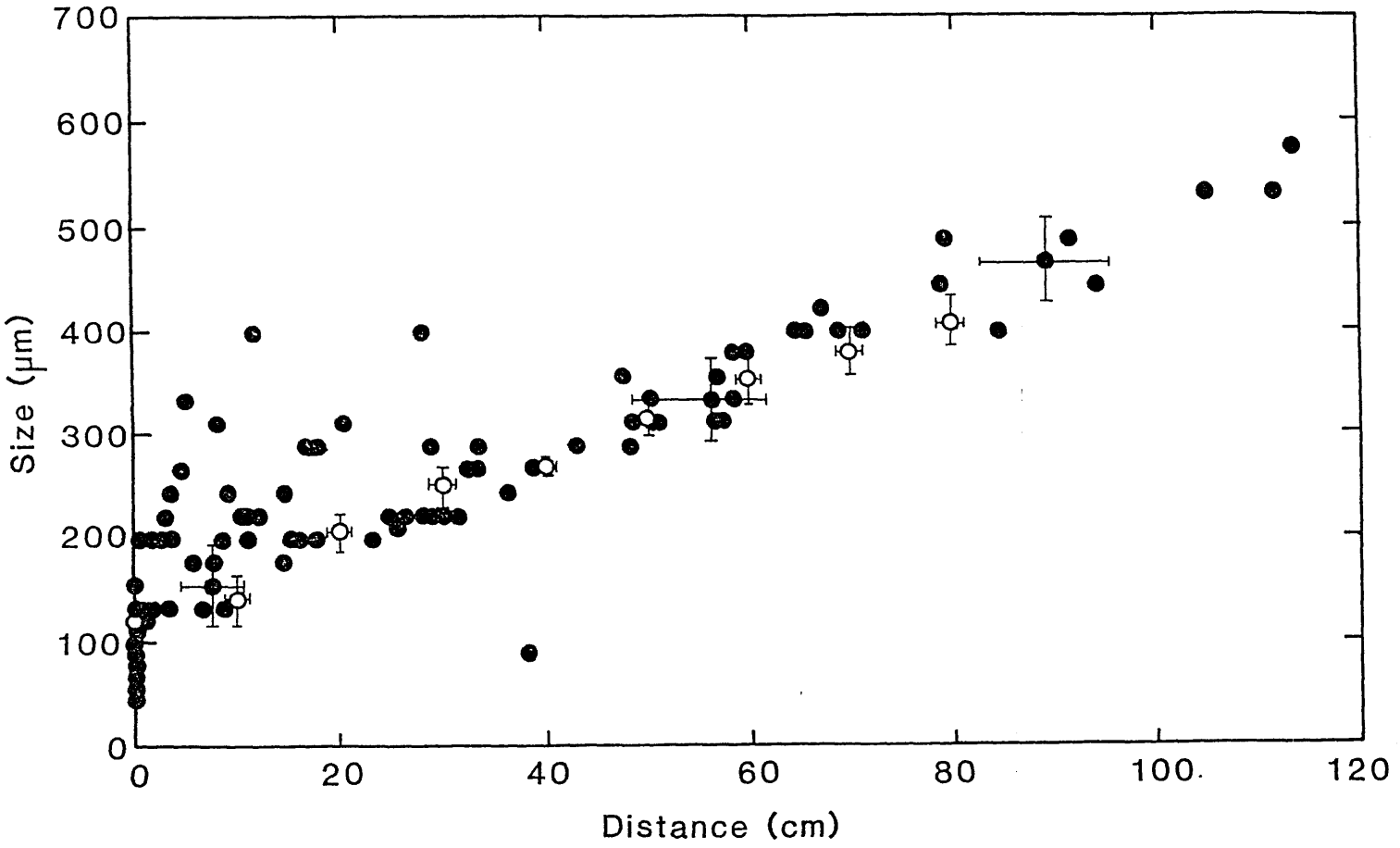


Fig 3.6(a) Relationship between droplet size and distance travelled by droplets in the first spinning disc experiment. O, observed; vertical error bars represent standard deviation of droplet sizes, horizontal bars are the distance over which droplets were collected. ●, Distances calculated from the measured velocities of individual drops. Points with error bars indicated the typical level of uncertainty due to errors in the size and velocity measurements.

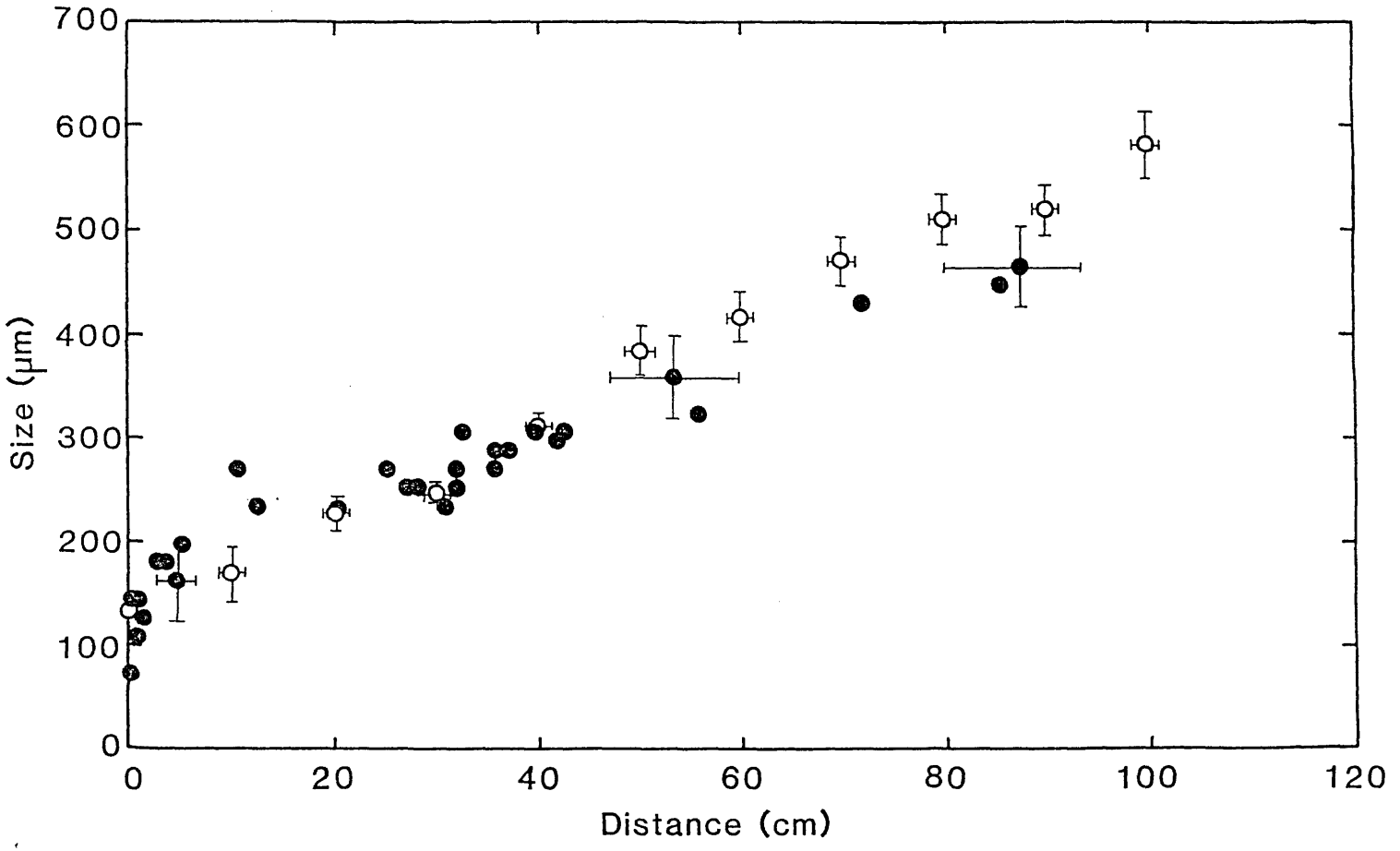


Fig 3.6(b) For legend see Fig 3.6(a)

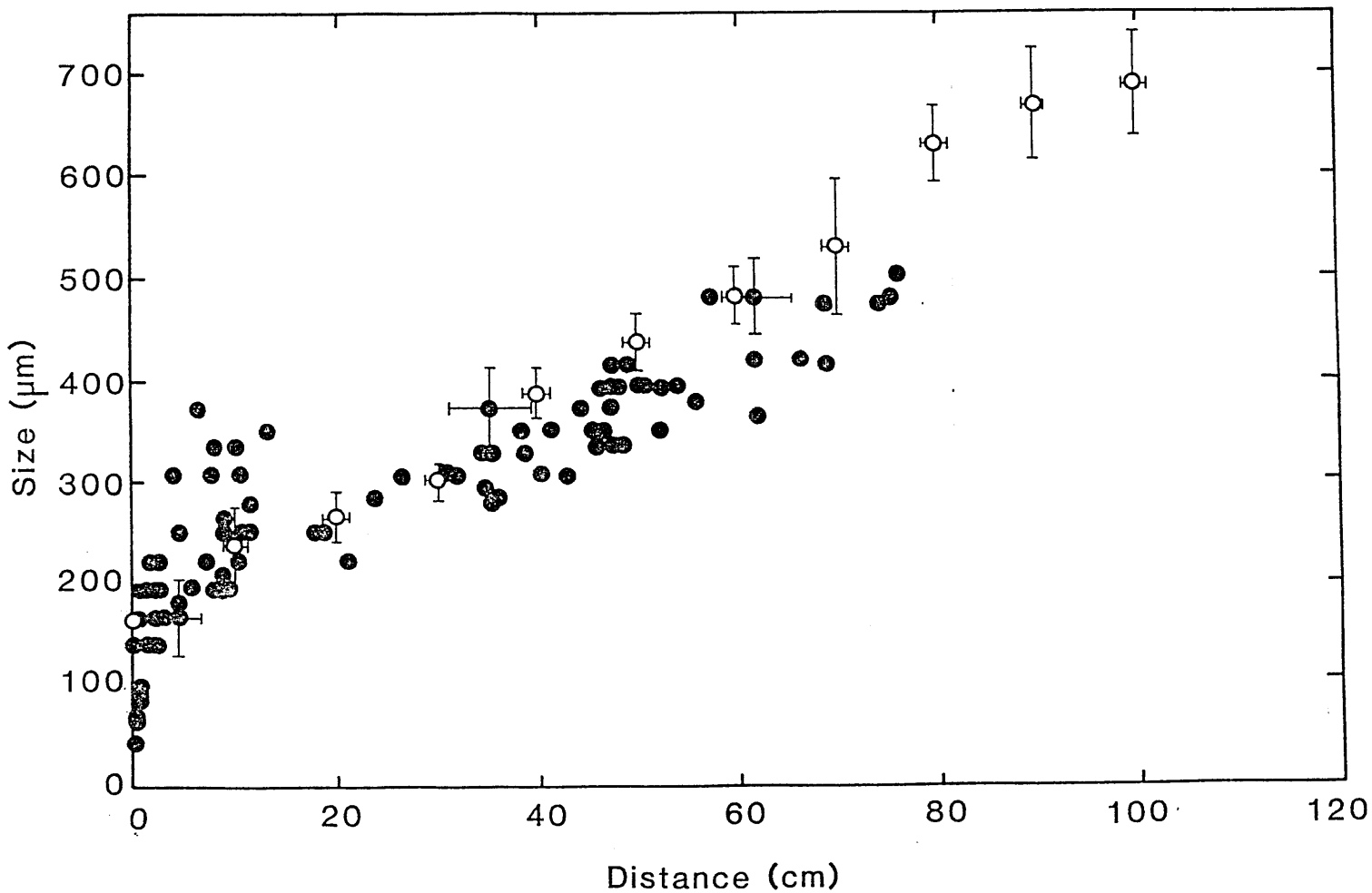


Fig 3.6(c) For legend see Fig 3.6(a)

droplet, shown by solid circles, plotted against measured diameter. Also shown in the figure is the measured distance travelled, plotted against mean and standard deviation in diameter of the droplets collected at each distance from the camera, shown by open circles with error bars. An indication of the uncertainties in estimating the size and velocity of droplets from photographs is shown by the error bars around some of the solid circles. The resolution of the film and magnification available only allowed measurements of droplet diameter to be made with an accuracy of about 40 μm, and those for speed to be made with an accuracy of about 0.1 m s^{-1}.

The predicted and measured relationships between droplet size and distance travelled are similar in each of the three experimental trials. For any droplet size the predicted distance is usually within 15% of the measured values, this is within the limits of accuracy available due to errors in the size and velocity measurements. Since the relationship between the distances travelled by droplets and the size of the droplets was approximately linear, regression lines were fitted through both the predicted and measured ranges. There was no significant difference between predicted and measured regression lines for two of the trials (Figs 3.6a and c). In the second of the three trials (Fig. 3.6b) a significant difference was found. In this case differences in the mean distance travelled were still less than 15% in the majority of cases and rarely more than 25%.

3.3 Conclusions

Both of these experiments have shown that the model is capable of predicting the trajectory of a water droplet in still air with an accuracy generally better than 15%. The Reynolds numbers of droplets used in the trials were in the range from 100 to >1000. The model should be applicable up to Reynolds numbers of about 1500; beyond

this point the value of Cd for a water drop begins to differ significantly from that for a solid sphere due to deformation of the drop and to internal circulation within the drop (Clift et al., 1978).

A Reynolds number of 1500 corresponds to a 3500 μm droplet moving at about 6 m s^{-1}, or a 100 μm droplet moving at 225 m s^{-1}, these values are well outside the limits that would be expected during splash formation. The results therefore show that the model can usefully describe the travel of the majority of droplets produced by rain splash.

It must be noted that measurements were only made in still air. Experiments to measure the trajectories of droplets in moving air in a wind tunnel were attempted but it proved impossible to isometrically sample or accurately size droplets under those conditions. A suggested alternative approach would be to use solid particles, such as glass spheres which have a similar density to water, as droplet analogues. These would be easier to sample as the problems of having to collect them on surfaces on which they can subsequently be sized would not arise.

Since the model calculates droplet trajectories relative to the surrounding air there is no reason to believe that it would not be applicable to conditions where there is a smooth, steady airflow. However turbulent airflows may not be adequately coped with.

CHAPTER 4

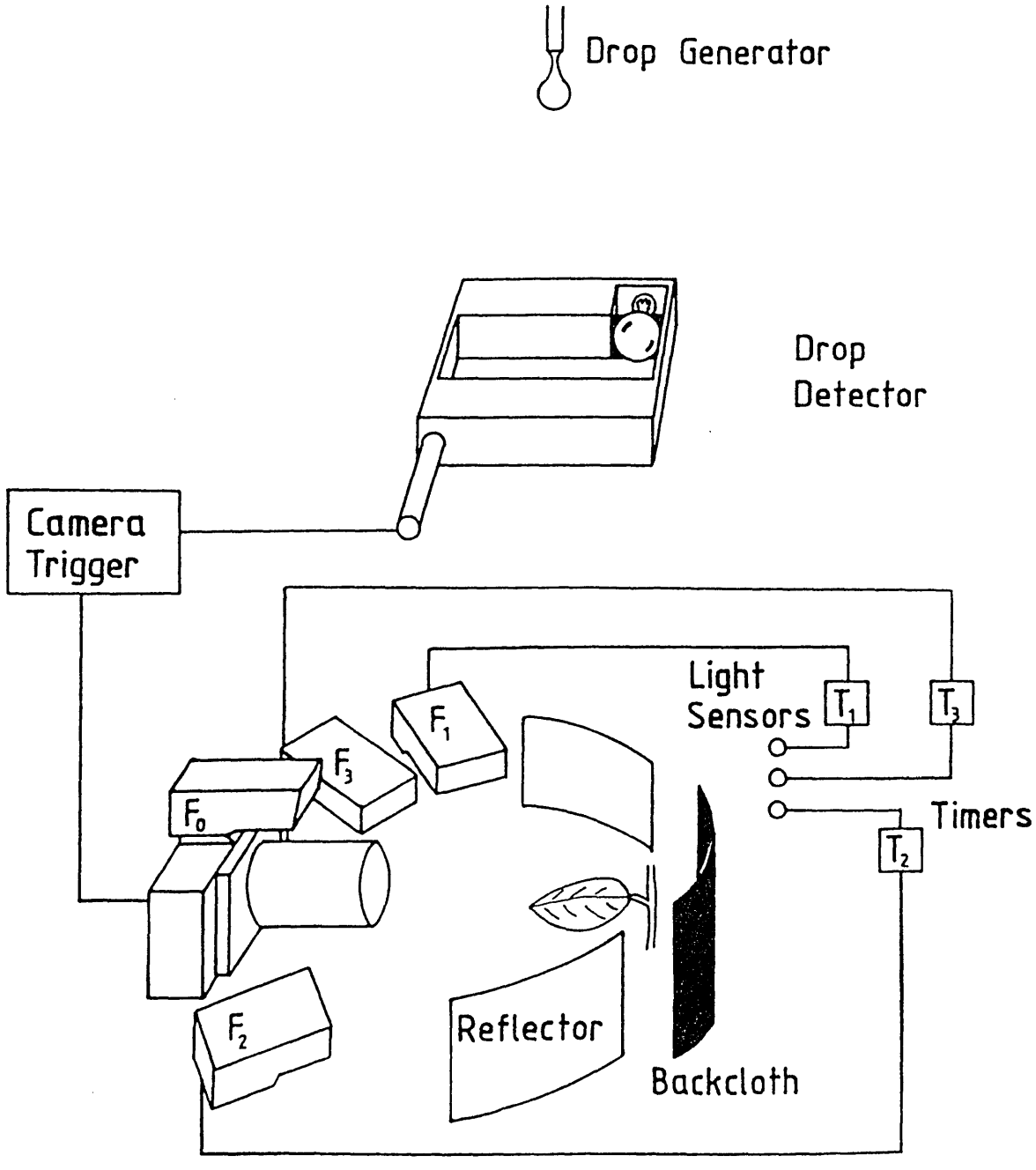
Investigation of Splash on Leaves: Experimental Technique

The droplet trajectory model described in Chapter 2 can be used to investigate splash dispersal by calculating the potential distances and heights to which spore carrying droplets may travel. To do this, knowledge of the distribution of the initial sizes and velocities of the droplets produced by a splash is needed. Although such values have been previously measured for certain cases, such as splashes on liquid films and solid surfaces, no information that is directly relevant to splash on plant surfaces has been published. A series of experiments was therefore carried out to investigate the value of these parameters for splashes on leaf surfaces. The experiments took two forms. The first set was a photographic investigation of splash on leaves to measure the initial speed, angle of ejection and size of droplets. The second set of experiments measured the size spectrum of droplets collected at different distances from the splash. The second set of experiments served as a check on the validity of the first set (see Section 4.2) by enabling the results of the first set of experiments to be compared with those gathered using a totally different technique.

4.1 Photographic experiments

The formation of splash droplets can be studied photographically with high speed cinematography or by multiple exposure still photography (see Chapter 1). The use of high speed cinematography, although well suited for this type of investigation, was prohibitively expensive. A multiple exposure still photographic technique was developed that was suitable for investigating the splash of drops on leaves. In this technique successive,

Fig 4.1 Schematic diagram of layout for taking multiple image photographs. Droplets fall through the drop detector triggering a light activated switch and activating the camera trigger. Flash gun F_0 is fired by the camera when the shutter opens. Light sensors detect this flash, starting timers T_1 - T_3 which after preset delays trigger flash guns F_1 - F_3.



superimposed images of the splash process were recorded on the same piece of photographic film. The speed and direction of movement of individual droplets can be found by measurement of the distance and time delay between consecutive images of the droplet. Because the splash process is completed in only a few milliseconds, it is impractical to use a conventional mechanical shutter to achieve a multiple exposure image. Thus a method was developed where the splash was illuminated by successive short duration flashes while the camera shutter was held open.

The apparatus used to take the multiple image photographs is illustrated schematically in Fig. 4.1. Falling drops were detected by a sensor before they struck the target leaf (B). A signal from the sensor opened the shutter of the camera (C) and triggered up to four flash guns (F_0-F_3) in a predetermined sequence while the shutter remained open.

4.1.1

The camera and first flash gun were triggered when the drop passed through a light beam before impacting on the target. The incident drop detector consisted of a 6 V torch bulb placed behind a lens. This was to give a collimated beam, that was then directed between two plane parallel mirrors, each about 5 x 2.5 cm, placed 5 cm apart (Fig. 4.2). The light was collected at the opposite ends of the mirrors by a light activated switch (Radio Spares stock no. 305-434) mounted in a long tube to shield it from ambient light. A drop passing between the two mirrors reduced the intensity of light entering the tube and activated the light sensitive switch. The signal from the switch operated a time delay circuit, the output from which switched a relay that triggered the camera motorwind and thus started the picture taking process.

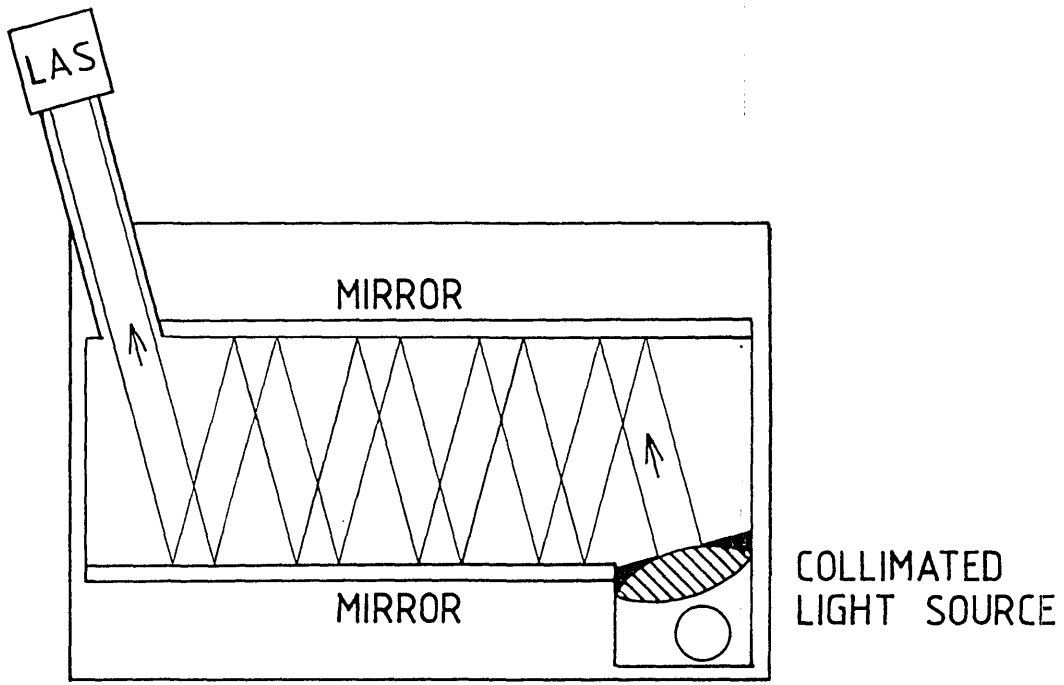


Fig 4•2. Schematic diagram of drop detector.
LAS is light activated switch.

By adjusting the time delay and/or height of the drop sensor above the leaf, it was possible to synchronise the camera operation and splash. Due to an inherent delay of around 100 ms between the closing of the relay and the opening of the shutter, the time delay was usually set to zero. For photographs of splash, it was found to be best to trigger the camera and first flash just before the drop impacted on the leaf. This allowed for small variations in the timing of the photograph in relation to the impact and provided a long enough time window between the first and last flashes to included the whole of the period over which droplets were produced.

Two methods of synchronising the drop impact and flash sequence were used. In the early experiments the drop impact was coordinated with the flash sequence by replacing the target leaf with a microphone attached to a dual trace oscilloscope. The trace produced by the sound of the drop hitting the microphone was compared with the simultaneously recorded trace from a light sensor detecting the light from the flash guns. The height of the drop sensor or the length of the time delay was then adjusted to give the correct timing for the flashes. In later experiments a video camera (Hitachi HV-730K) was substituted for the film camera and the splash recorded using a video tape recorder (JVC BR6400-TR). The recorded image was used to synchronise the splash and photography. This had the advantage that the leaf did not have to be moved and gave some idea of how the splash image would appear on film before the pictures were actually taken. This was useful in checking the position of the flash guns and ensured that there was no localised over or under exposure of the photographs due to either bright reflections or shading of part of the field of view by other elements of the plant. The amount of time and film wastage caused by poor photographs was therefore reduced.

Because of the relatively low resolution of the video image compared with 35 mm film, it was not possible to use the video camera and recorder for recording images and taking measurements, even with freeze frame and single frame advance facilities.

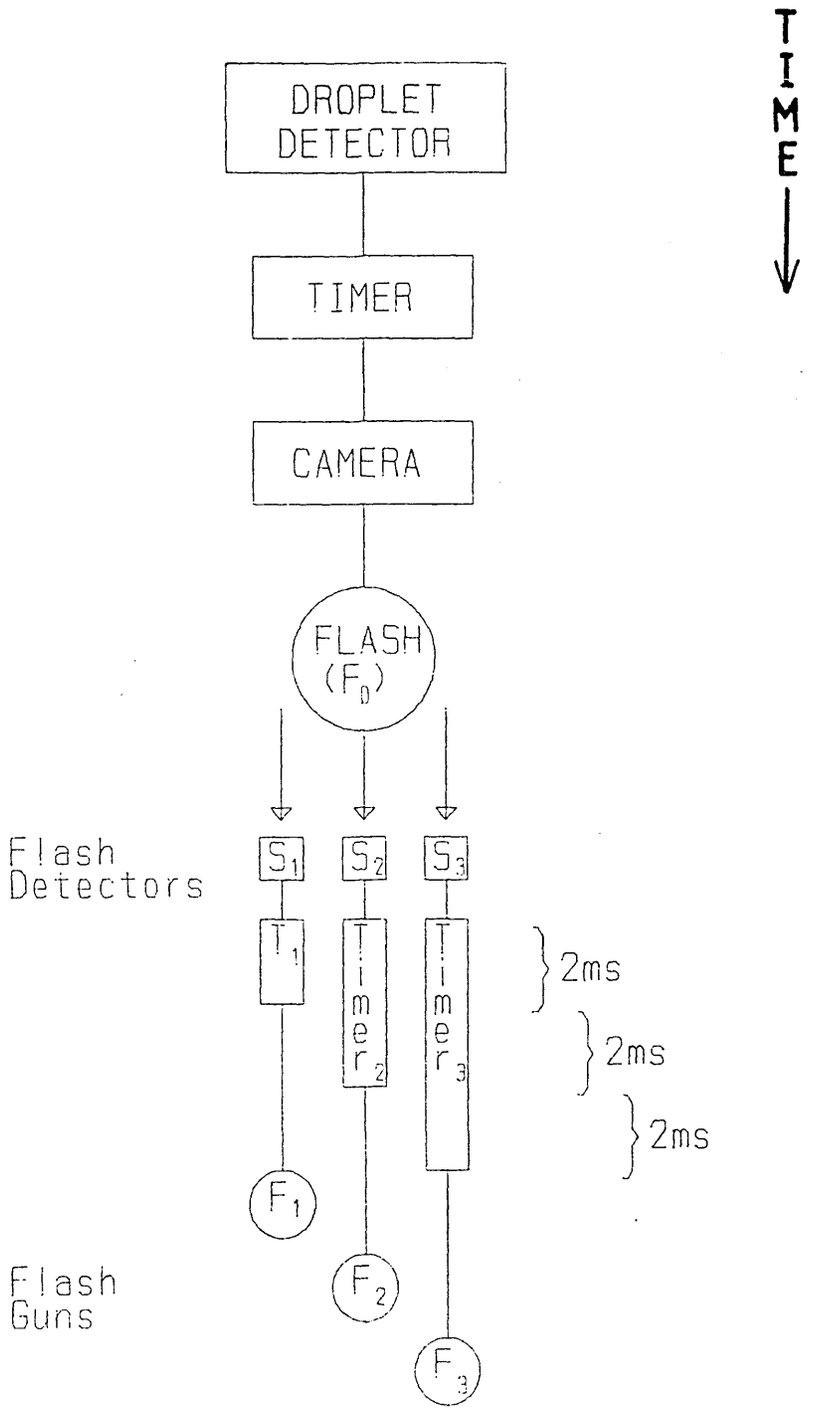
The photographs were taken using either an Olympus OM-2 or OM-2n, 35 mm single lens reflex camera. The sequence of events is shown diagrammatically in Fig. 4.3. The first flash lamp (F_0) was fired automatically by the camera's own synchronisation mechanism when the shutter was opened. The light from this first flash was detected by a set of three light sensitive switches (D_1-D_3) each connected to a seperate time delay circuit (T_1-T_3). Each circuit triggered another flash gun (F_1-F_3), after a predetermined adjustable delay. The details of the delay circuits are given in Appendix I.

The first flash gun (F_0) was mounted on the camera 'hot shoe'. The others (F_1-F_3) were placed to give oblique lighting across the field of view (Fig. 4.1). The individual light sources produced bright but uneven, localised, reflections from the droplets that left much of the droplet invisible on the resulting image, and could have resulted in droplet sizes being underestimated. To give more even illumination, pieces of white reflective card were placed around the experimental area, outside of the field of view of the camera, to act as reflectors. Droplets were then photographed against a dark background. A small amount of sodium fluorescein was added to the water (about 0.05 g l^{-1}). This caused the droplets to fluoresce slightly when illuminated and rendered them slightly opaque and so further enhanced the images produced on the film.

A concentration of fluorescein of 100 ppm changes the surface tension and viscosity of water by a value less than 25% of that caused by a change in temperature of $1^{o}F$ (Timmons *et al.*, 1971). The

Fig 4.3

Flow diagram illustrating the picture taking sequence.



amount of fluorescein used was therefore unlikely to have any effect on the splash process.

Bright field illumination, as used by Reynolds *et al.* (1987), in which the light sources shine directly into the camera lens may have given better quality photographs and made the droplets more easily visible. However, such a system is more difficult and costly to set up. Multiple exposure photography is especially difficult to arrange with bright field illumination because of the requirement to ensure that the film retains enough reactivity to record subsequent superimposed images (Chella *et al.*, 1986). The system used proved satisfactory and had the advantages of cheapness and simplicity.

Using black and white film it proved exceedingly difficult to separate the images produced by the four flash guns or to determine which images were produced by the same droplet. Separation of the multiple-images was therefore aided by placing coloured filters over the flash guns and using colour reversal film (Ilfochrome, Ilford Ltd, rated at 100 ASA or Agfa Chrome CT 200, Agfa-Gevaert Ltd, rated at 200 ASA). Each flash thus produced a different coloured image and consecutive droplet images followed a set coloured pattern.

The time delay between the flashes was measured using a light sensitive diode and oscilloscope, from which a sample trace is shown in Fig. 4.4. Measurements could be made with an accuracy of about 0.05 ms. Typically flashes were triggered 2, 4 and 6 ms after the first.

When the delay time between images was set at approximately 2 ms, some of the faster moving droplets traversed a significant proportion of the field of view between flashes, for example a droplet moving at 5 m s^{-1} would have travelled 10 mm in 2 ms. This made it difficult to relate images of the same droplet to one another and in some cases, especially with the higher magnification photographs, meant

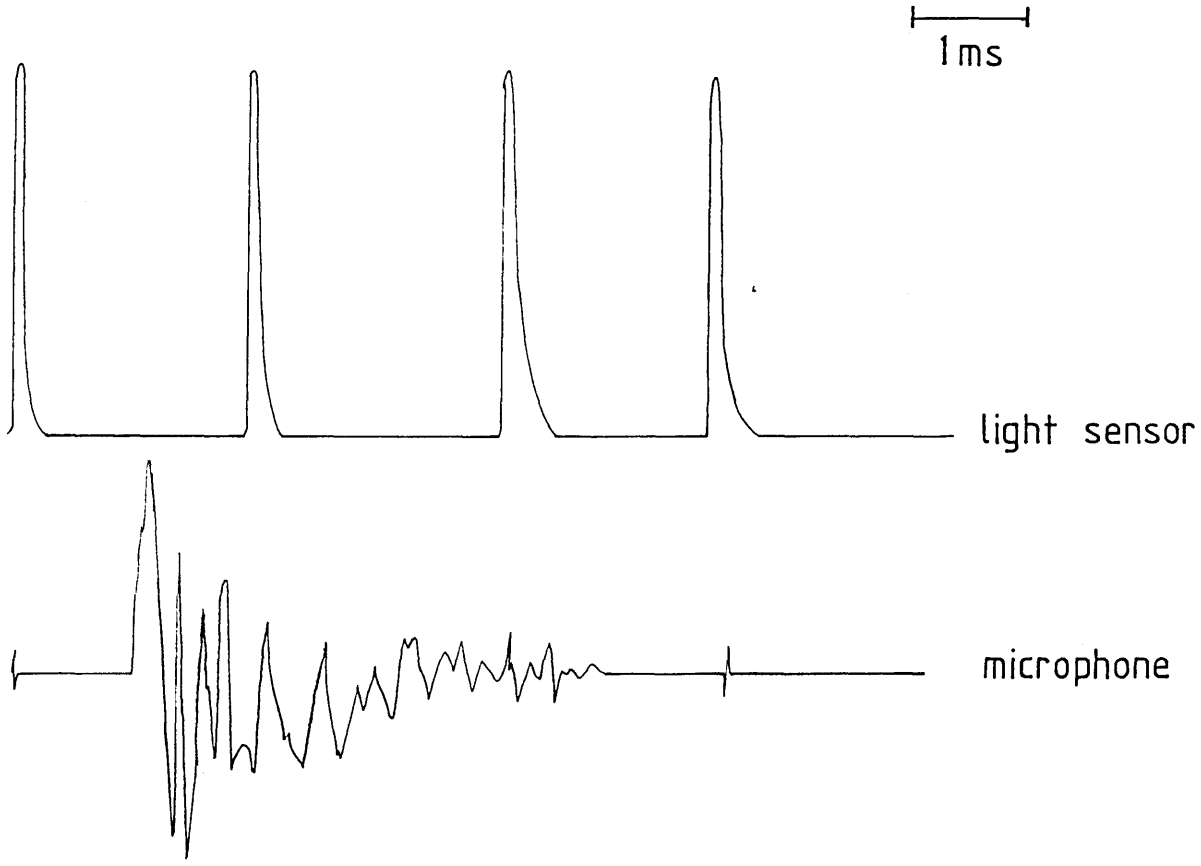


Fig 4•4. Tracing of oscilloscope screen showing the timing of drop impact and flash guns.

that some of the later images were lost from the photograph. This was partly overcome by taking photographs at different magnifications. To further aid in the analysis of fast moving droplets, one or more of the flashes could be extended so that the droplet left a streak rather than a distinct frozen image. Usually the flash guns were set to minimum power, which gave a flash of about 0.025 ms duration. To record a streak the flash guns were set to deliver a longer flash of about 0.5 ms. The velocity of the droplet could then be determined by measuring the length of the streak. The accuracy of this method of determining droplet velocities was not as good as that found when measuring the distance between images, typically +/- 0.4 m s^{-1} compared with +/- 0.1 m s^{-1}. This was because the distance over which measurements were taken was smaller and the exact ends of the streak were difficult to precisely define, because there was a gradual trailing off of the light output from the flash guns when used at the higher power settings. Interference between images also occurred with the streaks intersecting. Therefore, the measurements of velocity were made using the multiple image technique whenever possible.

The camera was used with several different combinations of lenses and extension tubes to give a magnification of between about 1:2 and 1:4 on the film. Thus when using 35mm film the field of view was between about 70 x 50 mm and 140 x 100 mm. The resolution of the film used was about 100 lines per mm. This allowed measurements of droplet diameter to be made with an accuracy of 50 μm or better, and measurements of droplet speed to be measured within 0.1 m s^{-1}.

A camera lens aperture of f11 was found to give the best exposure. The camera shutter speed was set at 1/15 second in most experiments. This was long enough to ensure that all the flash guns fired while the shutter was fully open. At the same time it was

short enough to allow photographs to be taken under normal lighting conditions in the laboratory obviating the need for experiments to be carried out in a dark room.

Photographs were processed in the laboratory as soon as possible after they were taken. Processing was carried out using either the Barfen Flex-E6 or Photocolor Chrome Six development process. This allowed immediate adjustments to be made to the apparatus if the photographs proved unsuitable in any way.

4.1.2 *Analysis of photographs*

The developed photographic slides were projected onto a screen for analysis. The size and direction in which individual droplets had been moving was measured directly and the position of each droplet, relative to the centre of the splash was recorded.

To determine the speed of droplets, measurements were taken of the distances between successive images of the same droplet. When a flash of long duration was used, the resulting image streak aided in the identification of the series of images corresponding to individual droplets by indicating the direction in which a droplet was travelling. With four images a maximum of three such measurements could be made. As many measurements as possible were made for each droplet and the corresponding speeds calculated and averaged. The resulting speed was taken as being that of the droplet at the mid point between the first and last images. This averaged out not only the errors in the measurements but also most of the effects of droplet acceleration. Remaining errors due to changing droplet velocity were negligible.

Measurements were only made for those droplets that were sharply in focus. Since the depth of field was very narrow, less than one centimeter, any variations in scale, with distance from the camera,

were avoided. Furthermore, to ensure that droplets were moving parallel with the plane of the film, and therefore that the distance measured was the true distance travelled by the droplet, measurements were only made of those droplets for which all of the images were in focus. It was critical therefore to ensure that the impacting drops were accurately targeted and fell within the focal plane. There was still some uncertainty in the measurements of velocity because of the finite size of the depth of field (<10 mm). Thus droplets with a small velocity component perpendicular to the plane of the film would have remained in focus. The percentage error can be calculated from the equation:

$$100 \times \left(1 - \frac{D_i}{\sqrt{D_i^2 \times D_f^2}} \right)$$

where D_i is the distance between the first and last images of a droplet and D_f is the depth of the focal plane. Thus the uncertainty for fast moving droplets, where D_i is large, was smaller than for slow moving droplets with smaller separations between the images. Given a depth of field of 5 mm and a time delay of 8 ms between the first and last flashes the error in speed measurements for a droplet moving at 5 m s^{-1} was less than 1% while for a droplet moving at 1 m s^{-1} the uncertainty was about 15%.

Measurements of droplet velocity could not be made at the point of droplet release, i.e. at the point of corona breakup, but were made at distances of up to 100 mm from centre of the splash. All the droplets would therefore have lost a proportion of their initial speed and may also have changed their direction due to the effects of gravity by the time they were photographed. In many cases this

change in velocity was negligible but in some cases, particularly for smaller droplets, quite large changes occurred and an estimate of initial velocity had to be made. Droplets were not all ejected from the same point but were formed at the edge of the corona. Since the exact point of droplet formation varies and is difficult to determine it was decided to estimate the initial velocities of droplets as if they were ejected from the point of drop impact.

The estimation of initial droplet velocities was carried out as follows: the model described in Chapter 2 was modified to work in reverse so that droplet trajectories could be calculated back in time. The resulting program enabled the initial velocities of most droplets to be calculated. In some cases however, back calculating the trajectories was not a reliable method of estimating the initial velocity of a droplet. When either the horizontal component of velocity approached zero or the vertical component of acceleration approached zero (i.e. the droplet reached its stopping distance or was falling at terminal velocity) the back trajectory method had no unique solution.

In those cases where a reliable and unique solution could not be found by back calculation of the trajectory, the initial droplet velocity was estimated from the calculated droplet trajectory which passed through both the point of impact and the point of droplet measurement and had the same velocity as the droplet at that point. This trajectory was found by comparing the measured position and velocity of the droplet with the positions and velocities of a table of trajectories, which passed through the point of impact, that had previously been calculated for a range of droplet sizes and velocities.

4.1.3 *Experimental method*

The plants used as targets were greenhouse grown barley, (*Hordeum vulgare*), cv IPEX, and field beans, (*Vicia faba*), cv Minden. For all trials only plants with fully extended, non-senescent, healthy leaves were used. Most trials were carried out on the leaves of young plants before flowering had occurred and with the leaves still attached to the plant. In some of the early experiments with barley leaves, sections of stem bearing a single leaf were cut from the plant. These were placed in water with the stem supported in a clamp and used as the target.

Drops were produced in a steady stream from a hypodermic needle fed with water at a constant rate by a syringe pump (Braun, Perfusor VI). The size of drop was determined by the diameter of the needle used. The size of impacting drops was measured from photographs and by collecting a sample in a petri dish and weighing them. In the following discussion drops are referred to by their weight, rather than their diameter as many drops were not spherical but tended to be flattened at the leading edge. Determining the size of drops on the basis of their diameter could therefore have been misleading. Tap water with about 0.05 g/l fluorescein, to enhance the photographic image (Section 4.1.1), was used for the experiments. The constant stream of drops that was produced meant that splashes occurred on wet leaves. No attempt was made to remove water that settled on the leaves.

Target leaves were positioned in the path of the falling drops. On barley leaves drops were targeted on the horizontal sections of the adaxial surface of the leaf. On bean leaves drops were allowed to fall on any part of the upper surface of roughly horizontal leaves, if neccessary leaves higher up the plant were removed to provide the falling drop with an unobstructed path. Other leaves on

the same level may also have been removed to ensure that neither the camera lens nor any of the light sources were obstructed, and that the photographs were taken against a dark background.

So that the photographs could be properly scaled each series of photographs included one of a millimetre grid placed at the target position. As measurements were only made for those droplets that were travelling in a direction parallel to the film plane, photographs were taken from various directions around the target to average out any orientational tendency of the splashes.

Four sets of experiments were carried out with different combinations of incident drop size and velocity and target leaf, as described in Table 4.1. Around 400 photographs were taken for each set of conditions.

TABLE 4.1

-1-	Splash of 34 mg drops	falling 2.8m	onto barley leaves
-2-	--------- 34 mg	---------- 2.8m	---- bean ------
-3-	--------- 34 mg	---------- 5.1m	----------
-4-	--------- 7.6mg	---------- 2.8m	----------

4.2 Droplet collection experiments

In a parallel series of experiments carried out under identical conditions, samples of droplets from the splashes were collected so that the distribution of droplet sizes, both overall and with distance from the splash, could be determined. These distributions were also estimated by calculating the trajectories and thus the deposition patterns of droplets using the data gathered from the photographs of initial velocities and droplet sizes. Comparison of the two sets of data served as a check for any bias in the sample of

droplets chosen from the photographs and gave an indication of the accuracy of the velocity estimates.

A known number of drops were allowed to impact onto leaves under the same four sets of conditions as for the photographic investigations (Table 4.1). Droplets produced by the resulting splashes were collected for sizing on photographic film fixed to remove the silver halide (Fitt *et al.*, 1982; Koenig and Spyers-Duran, 1961). Droplets that are deposited on the film dissolve the gelatine layer, producing a crater which has a diameter directly proportional to the size of the droplet and can be measured using a microscope.

For each test, strips of the film were placed along several radii around the leaf and extending up to 1 m from it (Fig. 4.5). By placing the strips along different radii any non-random distribution of droplets in the horizontal plane was taken into account. Preliminary investigations showed that many droplets were projected close to or below the horizontal. So that these droplets would also be caught, the collecting film was therefore placed 100 mm below the leaf.

Because of the increasing radial dispersal of droplets with distance, it was found necessary to expose the collecting surfaces at greater distances to a larger number of splashes than those near to the target. If this was not done, either the surfaces closest to the splashes were overloaded with liquid or virtually no droplets were collected at the greater distances. Individual pieces of film were exposed to between one and nearly 500 splashes. Close to the leaf, where individual strips were exposed to very few splashes, several separate surfaces were exposed and the droplet numbers totalled to minimise the effect of random variation.

The collecting film was examined under the microscope and the sizes of droplets collected at different distances recorded. In some

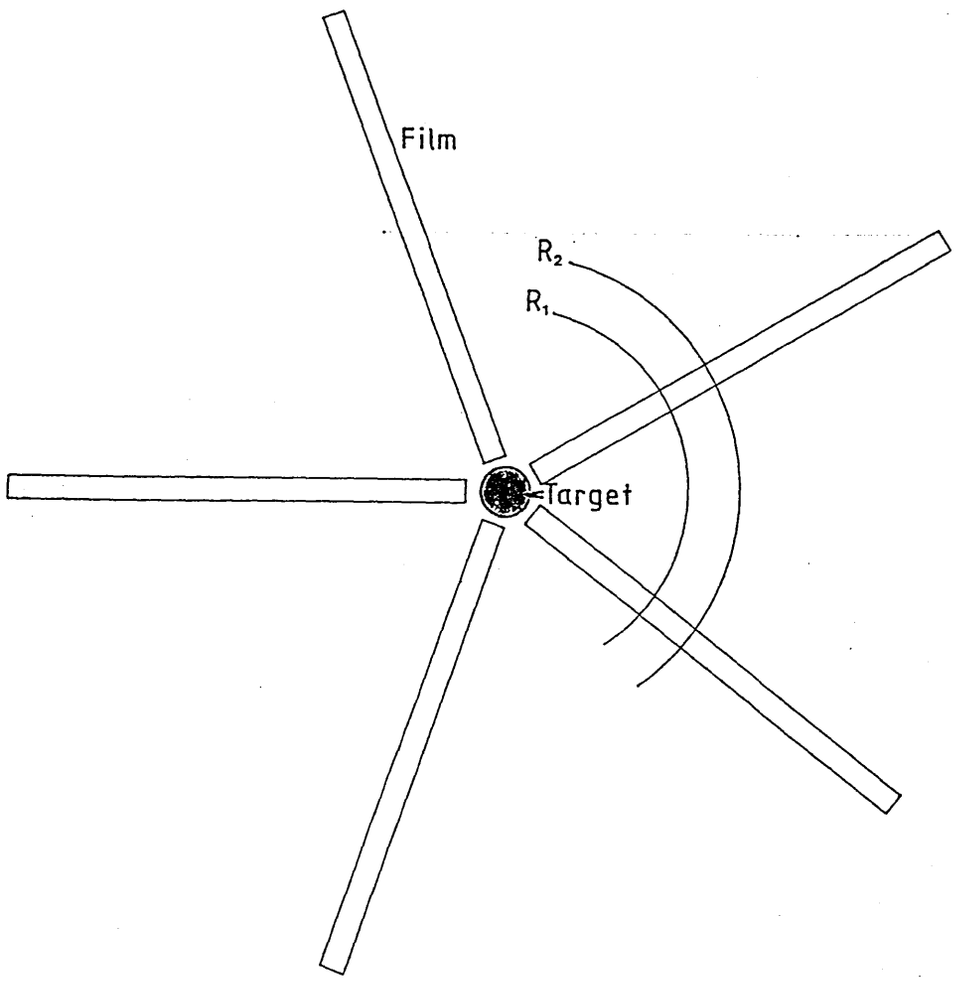


Fig 4.5
Vertical view (diagrammatic) of the arrangement of sampling film in the droplet collection experiments.

of the later experiments measurements were made with the aid of a seven bit digital frame store (Sight Systems, Newbury) attached to a microscope mounted video camera and a BBC microcomputer. This enabled readings to be made and recorded in a semi-automated fashion.

The total number of droplets of any given size, n_t, deposited by the splash of one incident drop on an anulus centered on the splash and with inner and outer radii, R_1 and R_2, was then calculated from the equation;

$$n_t = \frac{n_o}{A_s} \times \frac{\pi (R_1^2 - R_2^2)}{N_i}$$

Where n_o is the number of droplets counted, A_s is the area of the film examined between radii R_1 and R_2, and N_i is the total number of drops impacting on the target. The total number of droplets produced by one splash was estimated by integrating from 0 to x, where x is the greatest distance of splash. The distribution of drop size with distance, the distribution of distances travelled by a given drop size and the overall size distribution of splash droplets were also calculated.

CHAPTER 5

RESULTS and DISCUSSION: *Size, speed and angle of ejection of splash droplets*

In this chapter the results of the photographic investigation of droplet size and initial velocities and the overall droplet size distributions as determined by the collection experiments are presented. The droplet size distributions as determined by the two different techniques are also compared.

5.1 Impact speed of incident drops

A spherical 34 mg droplet has a diameter of about 4 mm and one of 7.6 mg a diameter of 2.4 mm at standard temperature and pressure (15°C, 1013.2 mb). The observed values for drop diameter, measured from photographs, compared well with the values calculated on the basis of drop weight and density. Measured diameters for the large drops ranged from 3.5 to 4.8 mm and for the smaller drops from 2.25 to 3 mm. These ranges although large are not unreasonable given that droplets are known to oscillate in flight and will therefore vary in their instantaneous observed diameter (Pruppacher and Beard, 1970).

The calculated impact velocities of drops of the sizes used in the experiments are given in Table 5.1.

TABLE 5.1

Drop mass (mg)	Fall height (m)	Impact velocity (m s^{-1})
34	2.8	6.50
7.6	2.8	5.83
34	5.1	7.95

Mutchler (1967) however observed that, at terminal velocity, droplets larger than 3 mm are significantly non-spherical tending to be

flattened at the leading edge. This was also observed in some of the photographs. This flattening causes an increase in frontal area and therefore an increase in the form drag which tends to reduce the velocity of the drop. This was not taken into account when the impact velocities were calculated so the values above may be slightly over-estimated.

The impact velocities of both 34 mg and 7.6 mg drops falling 2.8 m were measured. The same series of photographs used to determine splash droplet velocities was used for these measurements by selecting those frames in which two or more images of the impacting drop were visible. The velocities of the drops were then calculated using the same technique as for droplets. Using the same series of photographs obviated the need for a seperate series of experiments and ensured that the conditions under which the velocities of both the impacting drops and the splash droplets were recorded were identical, this reduced the likelyhood of any errors being introduced into the data.

The observed impact velocity of 7.6 mg drops after a fall of 2.8 m was 6.2 m s^{-1} and for 34 mg drops falling the same distance was 6.4 m s^{-1}. In the case of 34 mg drops falling 5.1 m no images were found that were suitable for measuring the impact velocity and so the calculated value (7.95 m s^{-1}) was assumed. The observed impact velocity of the larger drops falling 2.8 m did not appear to differ significantly from the velocity predicted by the model on the basis of the spherical diameter, although as expected they were slightly slower. However there was a signifiant difference between the observed and calculated impact velocity of the smaller drops. The mean diameter of the small drops was measured at 2.87 mm. This is somewhat larger than the value for spherical diameter calculated on the basis of drop mass (2.4 mm). The velocity of a spherical droplet

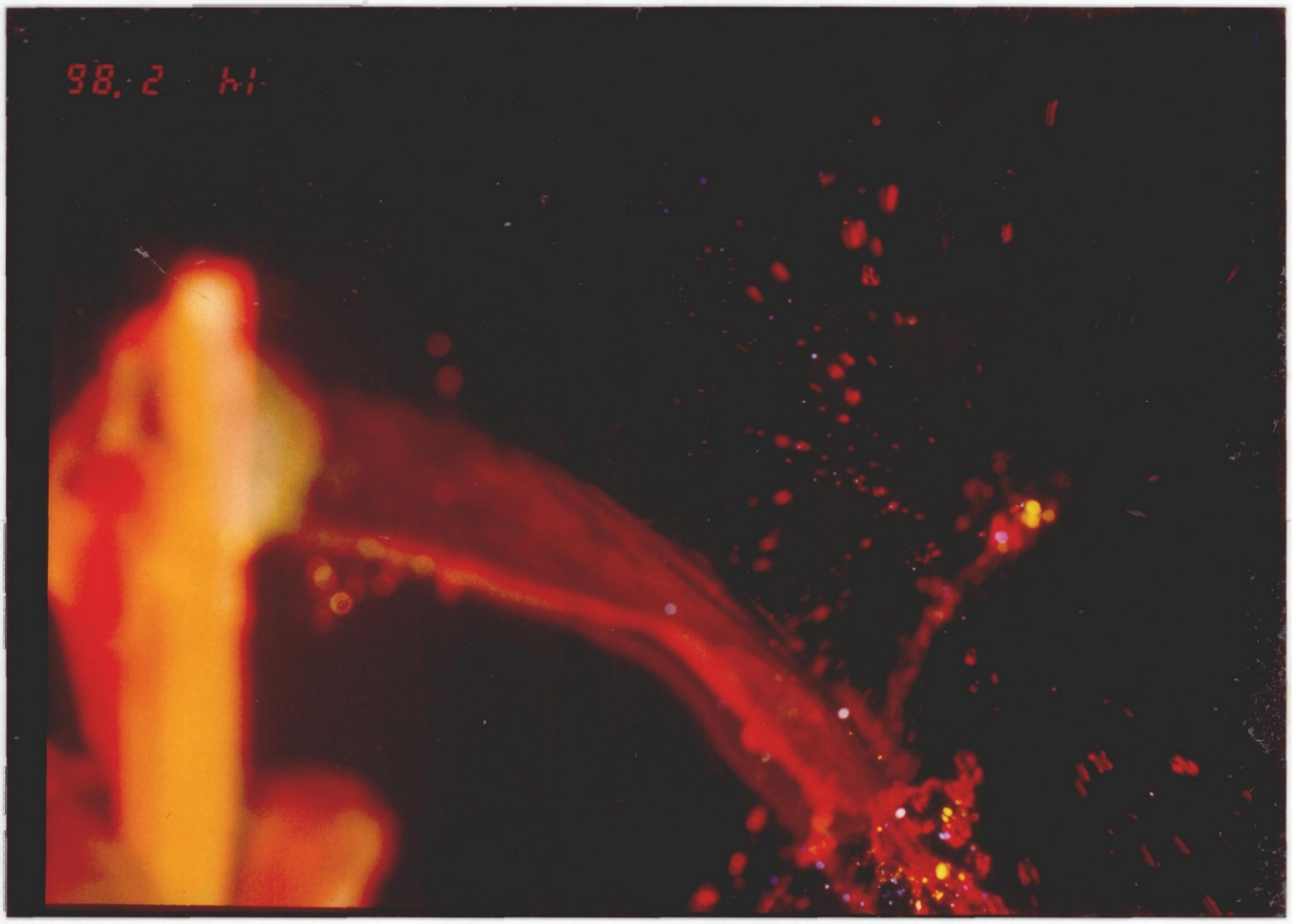


PLATE 4 a

Splash of a 34 mg drop falling 2.8 m onto a bean leaf.

Colour sequence:

	White	Red	Yellow	Blue	
Time	0	0.45	4.5	6.0	ms

The dates were printed upside-down because the camera had to be mounted inverted.

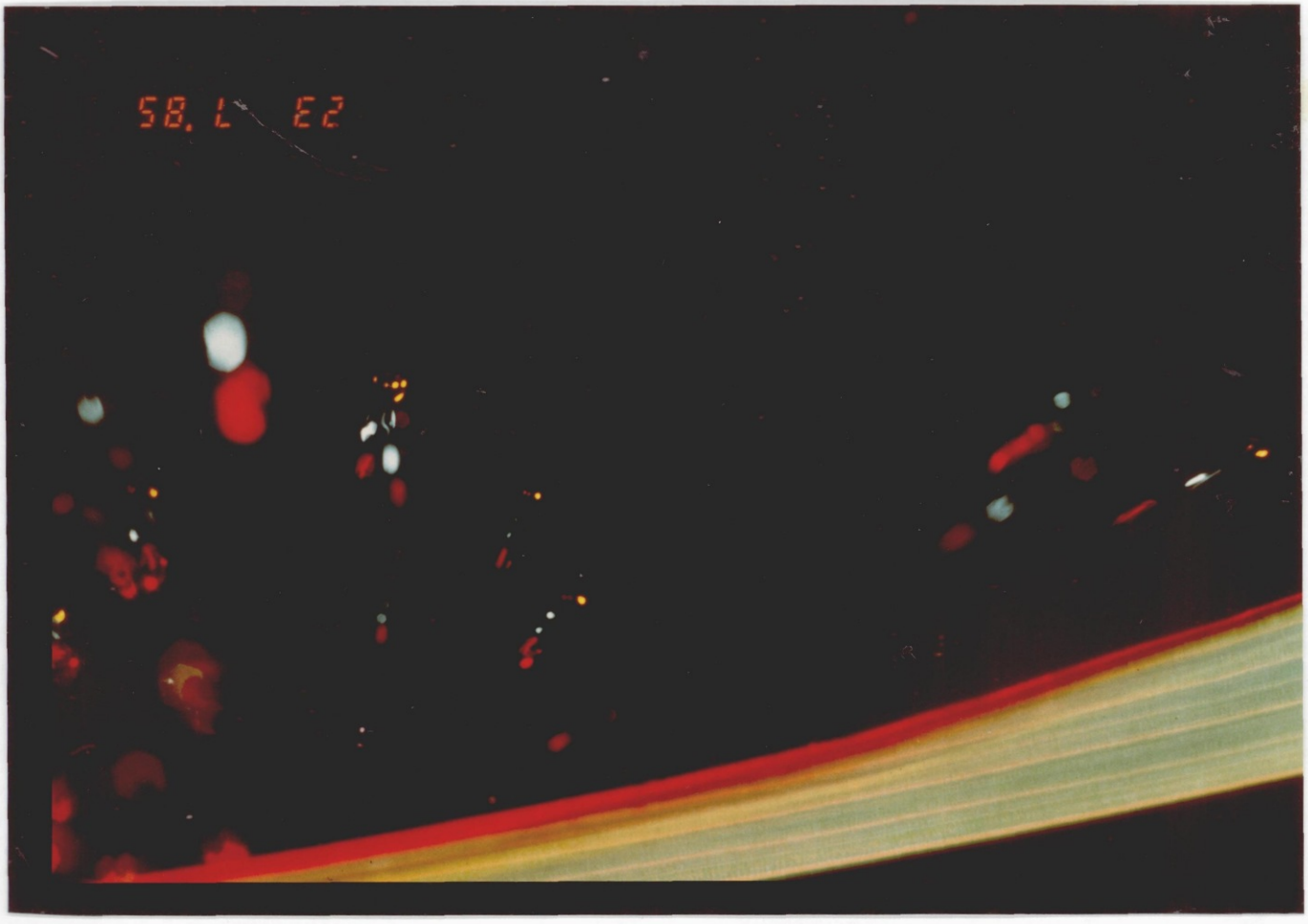


PLATE 4b

Splash of a 34 mg drop falling 2.8 m onto a barley leaf.

Colour sequence:

	Clear	Red	Green	Yellow	
Time	0	2.3	4.2	5.75	ms

Red and green flashes were 0.7 ms in duration.

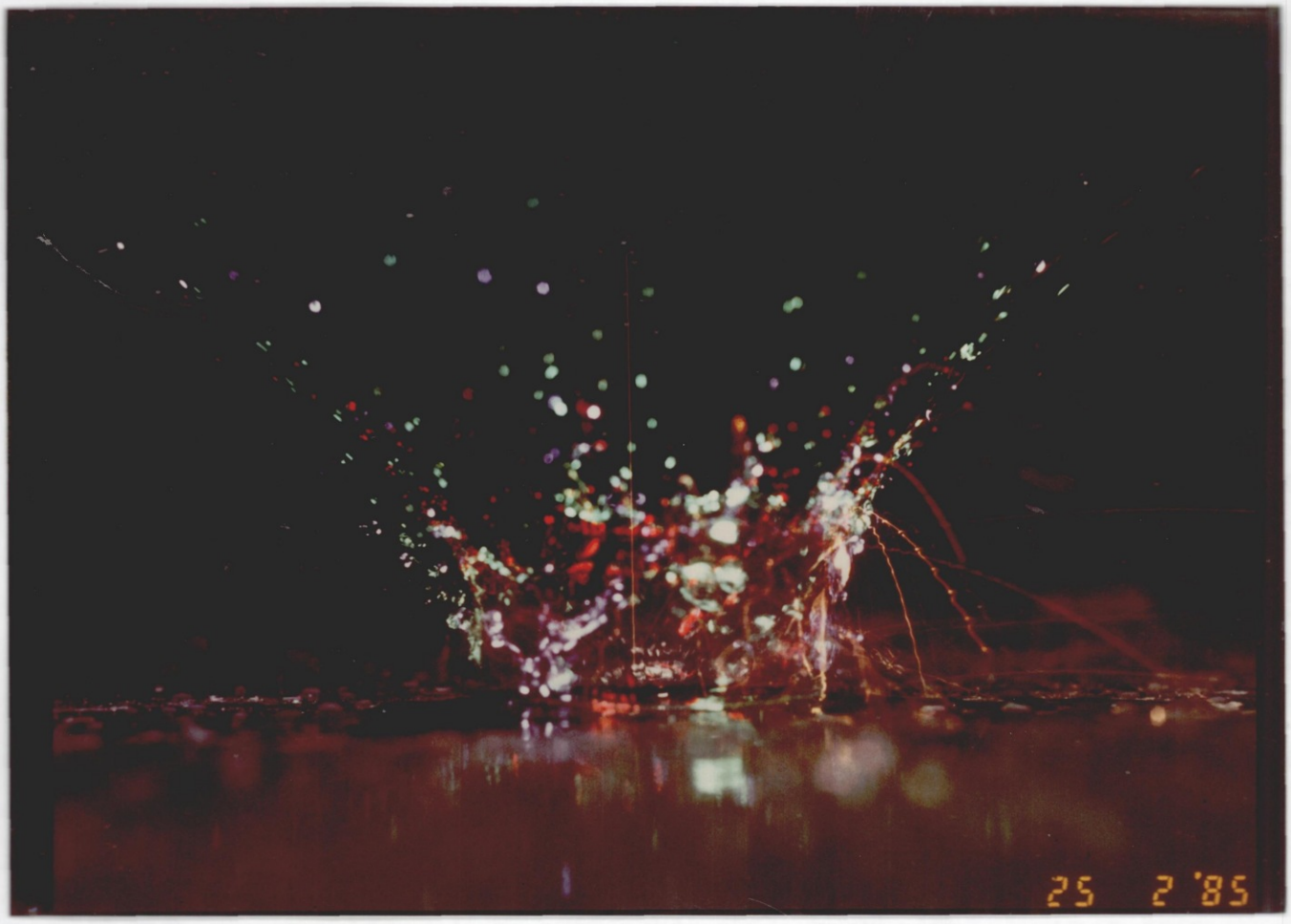


PLATE 3

Impact of a 34 mg drop falling 2.8 m onto a smooth, flat, surface (a piece of photographic paper)

Colour sequence:

White-Red-Green-Blue

The streaks left by some of the droplets were generated by shining a bright light through the field of view.

of 2.87 mm, after a fall of 2.8 m was calculated as being 6.05 m s^{-1}, this was not significantly different from the observed velocity.

Overall therefore the size and velocity of the 34 mg impacting drops appears to have been as predicted. It would appear that the smaller drops, originally weighed at 7.6 mg, may have been slightly larger than was intended. The measured diameter of 2.87 mm corresponds to a spherical drop having a mass of about 12 mg.

The size of drops produced by letting water fall from the end of a hollow needle is very sensitive to any changes in conditions. The drops that were weighed were not produced at the same time that the experiments were carried out and the difference in the two measurements of the size of the small drops could have been caused by any one of several factors. Previously published work (Ghadiri-Khorzhoojhi, 1978; Gregory *et al.*, 1959) suggests that a change in the drop mass of this magnitude, 7.6 to 12 mg, may not have a significant effect on the resulting splash.

5.2 General observations of splash

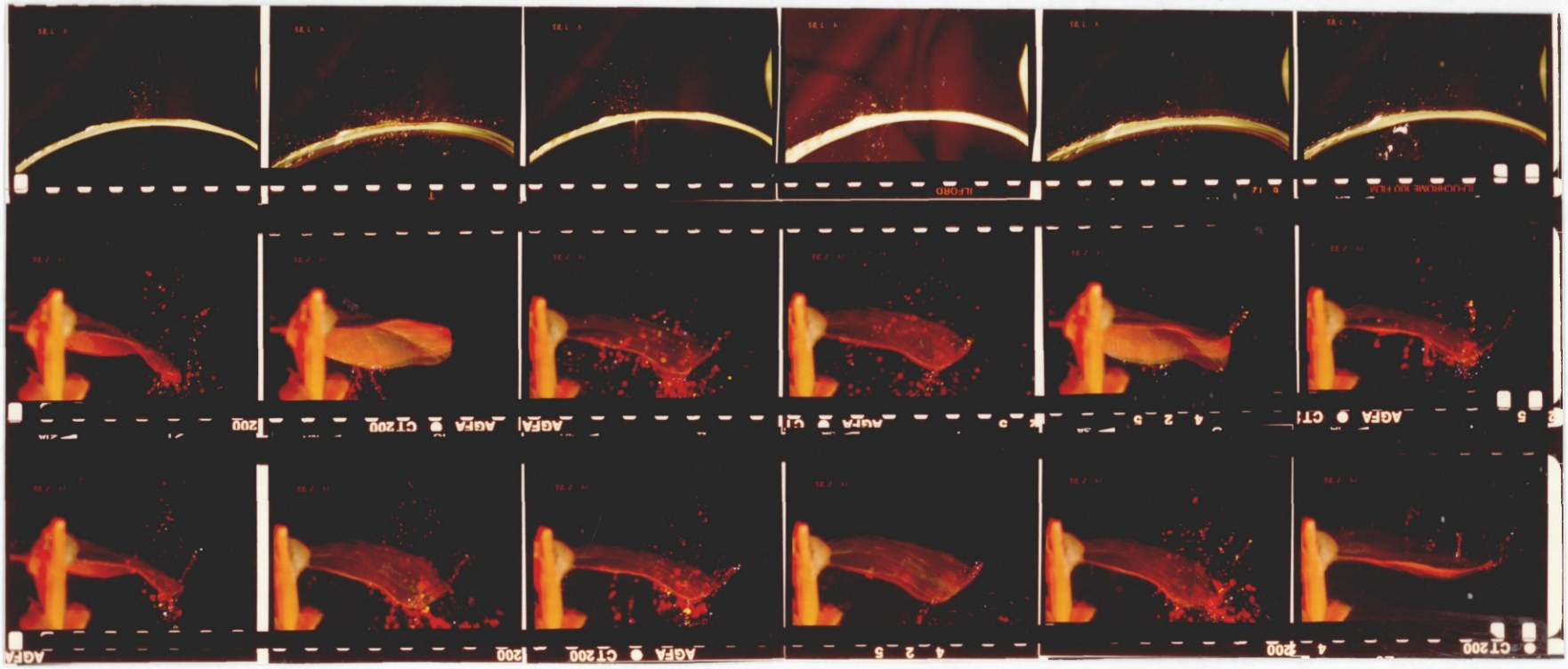
Plate 3 shows a splash caused by a 34 mg drop impacting onto a smooth surface, a sheet of photographic paper, Plate 4a shows a similar drop impacting onto a bean leaf and Plate 4b onto a barley leaf. It can clearly be seen that the impacts onto leaves and smooth solid surfaces cause splashes that are qualitatively very different. The impact onto a smooth surface produces a radially symmetrical corona which breaks up into a spray of droplets with angles of ejection that are oriented mainly between 15^{o} and 40^{o} above the horizontal. Furthermore, on a clean dry surface, there is a high degree of consistency in the dispersal pattern observed between splashes. The drop impacting onto a leaf surface however produces a more chaotic, and variable, spray of droplets. Droplets are observed

34 mg drops falling 2.8 m
onto barley leaves.

Colour sequence: White Red Green Yellow
Time: 0 1.1 3.1 4.4 ms

PLATE
5a

PLATE
5b



34 mg drops falling 2.8 m
onto bean leaves

Colour sequence: White Red Yellow Blue
Time: 0 0.45 4.5 6.0

34 mg drops falling 5.1 m
onto bean leaves

Colour sequence: White Red Green Yellow
Time: 0 2.3 4.5 6.0

PLATE 5c

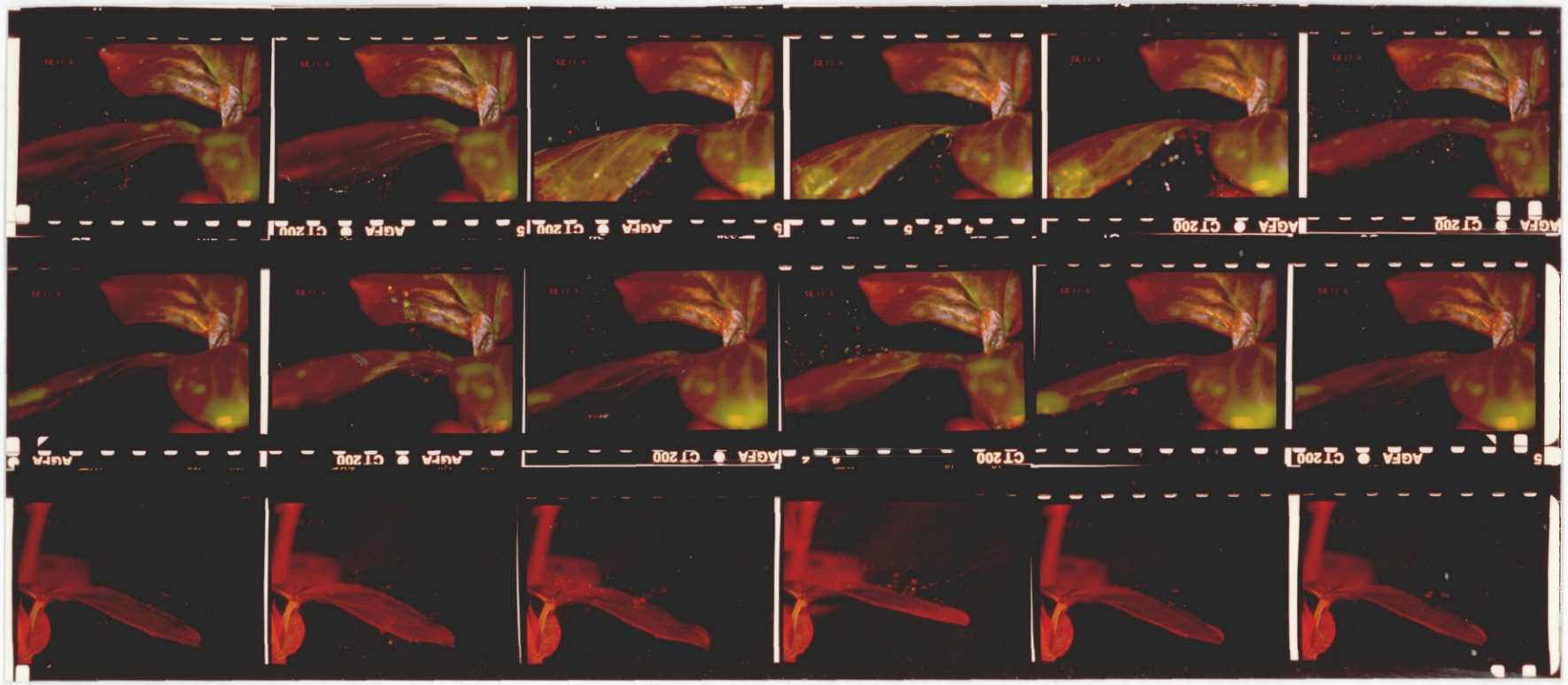


PLATE 5d

7.6 mg drops falling 2.8 m

Colour sequence: White Red Green Yellow
Time: 0 2.3 4.5 6.0

to have angles of ejection throughout virtually the whole vertical plane, with often no obviously favoured direction. There is no clearly defined corona, although in some cases sheets of water are produced. These have a fan-like structure and in this way appear to be like a partial corona, however they tend to move downwards at a shallow angle to the leaf surface. There is also a great deal of variation between splashes. Two droplets of the same size and velocity impacting on the same leaf often produce two totally different dispersal patterns. Plate 5 shows a selected series of photographs that demonstrate the variability in splash form. Another obvious difference is that the target moves on impact. In Plate 4b particularly, at least two images of the leaf can be distinguished demonstrating how it flexes under the force of the impact.

The experiments attempted to measure the size and initial velocities of droplets produced by the splashes of drops of a known size and impact velocity on leaves having two different and distinct structures. The main aim of these experiments being to characterise splash so that probabilities could be assigned to the likelyhood of a droplet of a given size following a given trajectory. The results of this study are presented below.

Measurements were made from the photographs of three parameters, the size, initial speed and direction of splash droplets. The mean values and the distributions around the mean are discussed below.

Table 5.2 shows, for all four of the experiments, the mean and median together with the standard deviation of the mean and coefficient of skewness for each of the three measured parameters: diameter, speed and angle of ejection, from each of the four experiments. The velocity and size distributions were significantly skewed in most cases. Attempts were therefore made to normalise the

TABLE 5.2

A) Droplet diameter(μm)

Expt	Mean	S.D.	Median	$\sqrt{b_1}$	b_2
A	337	258.31	277	1.44	5.84
B	322	262.47	222	1.30	4.99
C	320	256.87	240	1.59	6.08
D	212	211.61	162	2.35	10.81

B) Initial droplet speed (m s^{-1})

Expt	Mean	S.D.	Median	$\sqrt{b_1}$	b_2
A	1.74	1.286	1.40	2.49	13.72
B	3.44	2.473	3.00	0.85	3.06
C	2.41	1.535	2.00	1.16	4.54
D	3.01	1.967	2.75	0.86	3.86

C) Angle of droplet ejection (degrees from horizontal)

Expt	Mean	S.D.	Median	$\sqrt{b_1}$	b_2
A	+22	43.34	+30	0.78	3.03
B	+4	47.18	0	-0.01	2.06
C	+5	56.23	+3	0.09	1.70
D	+12	30.49	+8.5	0.05	3.64

Experimental details

Expt	Drop size (μm)	Fall height (m)	Target	Number of droplets observed
A	34	2.8	Barley	459
B	34	2.8	Bean	389
C	34	5.1	Bean	418
D	7.6	2.8	Bean	373

Mean and median values, together with standard deviations of the mean and coefficients of skewness and levels of kurtosis for the distributions of each of the measured parameters.

TABLE 5.3

A) Droplet diameter(μm)

Expt	Mean	S.D.	$\sqrt{b_1}$	b_2
A	251	0.349	0.28	-2.30
B	235	0.353	0.05	1.92
C	240	0.332	0.14	2.27
D	171	0.330	0.34	2.53

B) Initial droplet speed (m s^{-1})

Expt	Mean	S.D.	$\sqrt{b_1}$	b_2
A	1.40	0.293	0.13	1.61
B	2.53	0.512	-0.39	2.14
C	1.98	0.689	0.01	4.54
D	2.29	0.873	-0.19	3.86

C) Angle of droplet ejection (degrees from horizontal)

Expt	Mean	S.D.	$\sqrt{b_1}$	b_2
A	+39	0.418	-1.26	4.86
B	+25	0.441	-1.75	6.30
C	+33	0.500	-1.30	4.01
D	+20	0.252	-2.12	9.96

Experimental details

Expt	Drop size (μm)	Fall height (m)	Target	Number of droplets observed
A	34	2.8	Barley	459
B	34	2.8	Bean	389
C	34	5.1	Bean	418
D	7.6	2.8	Bean	373

Geometric means and standard deviations, with coefficients of skewness and levels of kurtosis for each of the measured parameters.

data. The corresponding data for the geometric means are shown in Table 5.3.

The cumulative frequency distributions of the parameters were plotted on probability axis and linear regression lines calculated. From these it is possible to estimate the probability of a given parameter being within a given range. For computational purposes the data were transformed to probits, defined as:

$$Y = 5 - \frac{1}{\sigma} (X - \mu) = a + bX$$

where, μ is the mean of X and σ is the standard deviation of X. The values of probits were calculated, using a computer, by interpolation from a table of 13 known values using an akima spline routine (Ruckdeschel, 1981, pp. 305-311).

Following Finney (1971) probit regression lines were calculated using an iterative process from empirically fitted regressions and the goodness of fit for the lines calculated using a chi squared test. The slope of the regression line, b, is an estimate of $1/\sigma$, where σ is the standard deviation. The y-axis intercept, a, is in itself fairly meaningless beyond its necessity for calculating the placement of the line. If the x-axis is plotted as probits then the median value is given by a+5.b.

5.3 Splash droplet size distributions

The size distributions of splash droplets were determined in two ways, from the measurements of splash droplets collected on fixed photographic film placed around the splash (Section 4.2) and by measurement of the sizes of droplets photographed. The splash droplet collection experiments sampled all droplets except those that travelled less than about 2 cm from the splash. As those droplets comprised only a very small fraction of the splashed droplets and as

all droplets on each film strip were counted and measured so that there was no bias in the sampling technique, the results of the collection experiments were assumed to represent the actual distribution of splash droplet sizes.

5.3.1 *Collection Results*

Droplets ranging in diameter from less than 30 μm to greater than 2.5 mm in diameter were collected up to 0.55 m from the splash. Using photographic film to sample the droplets it was possible to determine the size of splash droplets with an accuracy of about 10 μm. Droplets smaller than 30 μm did not appear to leave any trace on the collecting film.

The distribution of droplet sizes was heavily skewed with more small droplets than large ones in all cases. Plotting the logarithm of droplet sizes on a probability scale showed the overall size distribution to be approximately log-normal (Fig. 5.1). A similar distribution of droplet sizes was described by Leven and Hobbs (1971) for splashes on a solid surface. The geometric mean and standard deviation of droplet sizes for each experiment is shown in Table 5.4.

TABLE 5.4

Target	Drop size (mg)	Fall height (m)	Mean diameter (μm)	SD
Barley	34	2.8	262	0.385
Bean	34	2.8	228	0.384
Bean	34	5.1	204	0.369
Bean	7.6	2.8	105	0.360

The average size of droplets from splashes on barley leaves was larger than that for splashes on bean leaves. Larger impacting drops produced bigger droplets on average than did smaller ones while

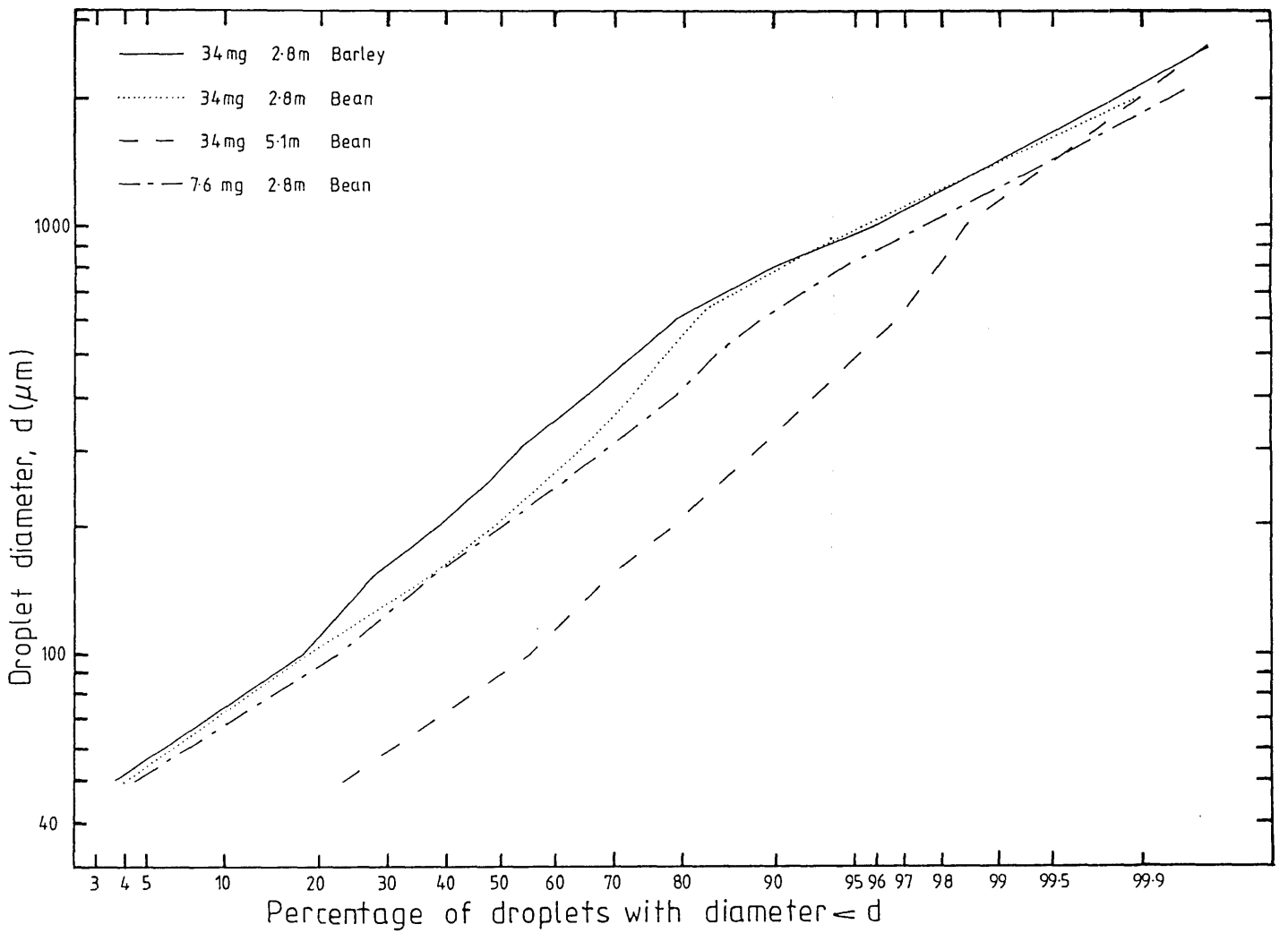


Fig 5•1. Size distributions of droplets collected from splashes on leaves.

faster drops produced smaller droplets than did slower ones. These results differ somewhat from the results of the photographic investigations, Tables 5.2 and 5.3. There is little difference between the two experiments in the mean diameter of droplets from the splash on bean or barley leaves of either 7.6 or 34 mg drops falling 2.8 m. However the photographic investigation suggests that the mean size of droplets produced by a 34 mg drop falling 5.1 m onto a bean leaf was much larger (319 μm) than did these collection experiments.

5.3.2 *Photographic results*

The size of droplets observed in the photographs ranged from less than 50 μm to over 1600 μm in diameter. Measurements were made with an accuracy of about 30 μm, the precise level of accuracy depending on the magnification of individual photographs. Droplets smaller than about 50 μm, although doubtless produced, may have escaped detection.

As with the size distributions measured from the droplet collection experiments, in none of the four cases were the sizes of splash droplets normally distributed. The droplet size distributions showed a significant degree of positive skewness (Table 5.2) for all of the experiments. Calculating the geometric mean and plotting the cumulative size distributions onto log-probability paper (Fig. 5.2) showed that the distributions were approximately log-normal. The mean diameter of splash droplets produced by 34 mg drops was not significantly different for splashes on bean and barley leaves, or for splashes produced by drops falling 5.1 or 2.8 m onto bean leaves. However the larger drops produced significantly larger splash droplets on average than did the smaller ones.

The distribution of droplet sizes observed for all four cases in the collection experiments is shown in Figure 5.1 and the

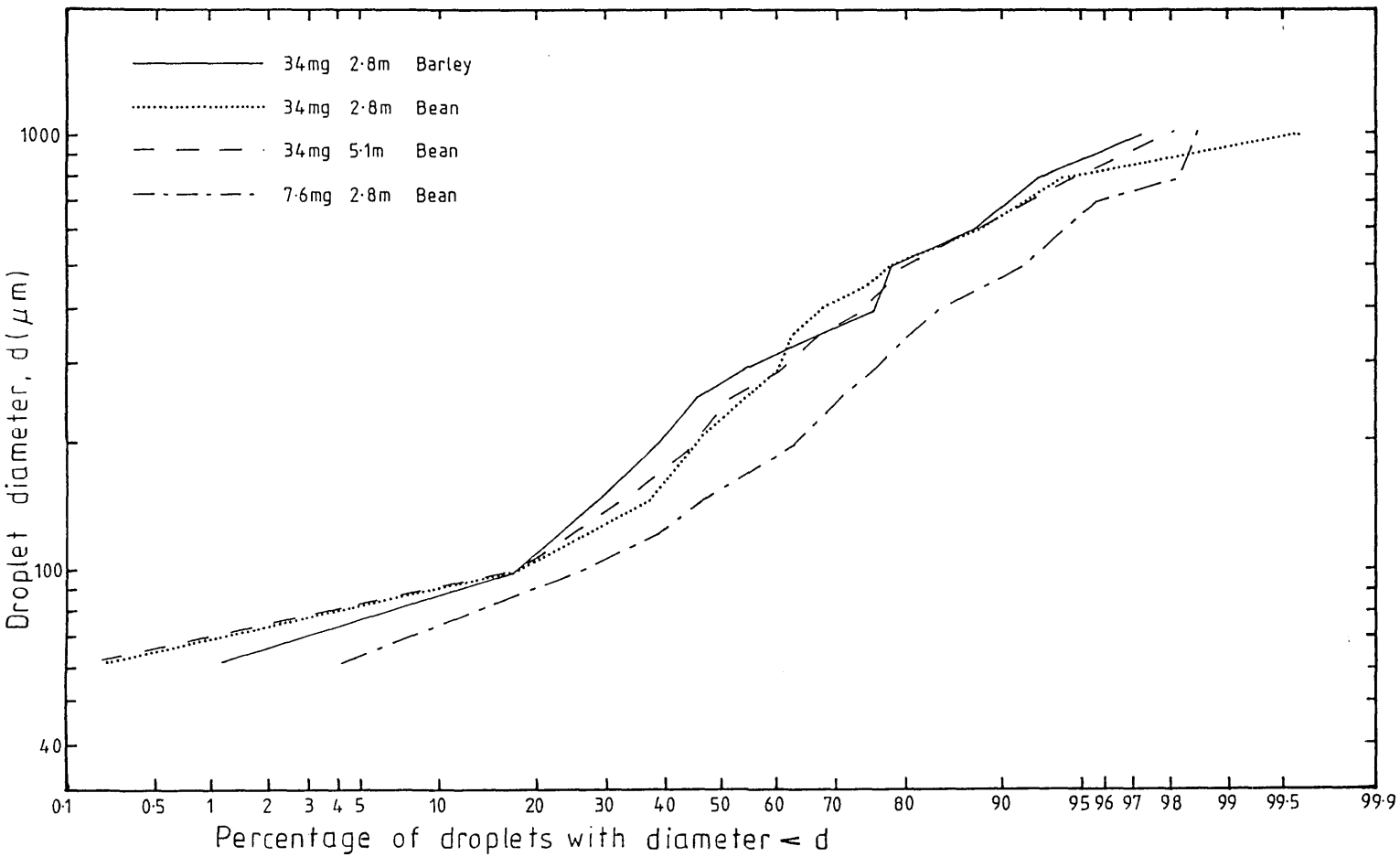


Fig 5•2. Size distributions of photographed droplets.

distributions derived from the photographic observations in Figure 5.1. For 36 mg drops falling 2.8 m onto both bean and barley leaves and 7.6 mg drops falling 5.1 m onto bean leaves the drop size distributions determined in the two seperate types of experiment were broadly similar. The mean size of droplets for each of the experiments was also similar and there was no significant difference between the means calculated from the photographs and the means of the collected samples for any of these three cases.

There was a large difference between the two estimates of droplet size distribution for the splash of a 34 mg droplet falling 5.1 m onto a bean leaf. The distribution estimated from the photographs is almost identical to that for the splash of a drop of the same size falling 2.8 m measured in the same way. The droplets collected on fixed photographic film however gave a distribution with a very much higher proportion of very small droplets, and correspondingly smaller mean. As is discussed in Section 5.4.2 the sample derived from the photographs may have been biased towards droplets following relatively unusual trajectories because of the interference between images. Plate 5 shows photographs of several splashes taken for each of the four conditions. In several of the frames showing the splash of a 34 mg drop falling 5.1 m (Plates 5b and 5c) sheets of water can be seen being ejected from the side of the leaf. These sheets later break up into clouds of droplets all having similar trajectories and so it is difficult to relate sequential images of the same droplet. Thus a sampling bias may be more marked in these cases. However, if a splash produces a large number of droplets all moving in the same direction a surface collecting these drops may become swamped, because many droplets land in the same place they coalesce and the larger droplets may obscure smaller ones. Thus accurately determining the droplet size spectra is difficult. In this way a

sampling bias may also affect the results gathered by collecting the droplets.

The drop size distributions measured from the photographs showed a smaller proportion of droplets in the 50-100 µm class than were observed when droplets were collected on film. The shape of the curve together with the findings of Ghadiri-Khorzoojhi (1978) and Levin and Hobbs (1971) both of whom found a high proportion of very small droplets ejected by splashes, suggests that the numbers of very small droplets was underestimated in the photographic study. This was probably because the photographic technique is relatively insensitive to smaller droplets.

The smallest droplets that could be observed had diameters of around 50 µm. No information on the initial velocities of droplets smaller than 50 µm could therefore be obtained. According to some reports as many as 50% of the droplets produced by a splash may be below 50 µm (Ghadiri-Korzoojhi, 1978; Gregory *et al.*, 1959; Levin and Hobbs, 1971). However droplets less than 50 µm in diameter carry few disease propagules and account for only a very small fraction of the total volume of liquid splashed. They are thus probably not important in the dispersal of splash-borne diseases (Fatemi and Fitt, 1983; Fitt and Bainbridge, 1983; Fitt and Lysandrou, 1984), though they may be responsible for the introduction of air-borne spores into the atmosphere (Brennan *et al.*, 1985b; Fitt and McCartney, 1986).

Furthermore the stopping distance of small particles is short; for example a 50 µm droplet has a terminal velocity of only 72 mm s^{-1} and even when projected straight upwards with a velocity of 10 m s^{-1} will reach a height of less than 4 mm. The initial velocity of small droplets thus has little influence on their dispersal, their transport being dominated by turbulence. The life time of such droplets before they completely evaporate is also short, typically of

the order of only a few seconds. For example, at 20°C with a relative humidity of 80% a free falling 50 μm water drop will evaporate to dryness after only 14 seconds (Matthews, 1979 p61), under dryer or hotter conditions its lifetime will be reduced even further (see Chapter 2).

It would appear that the photographic technique underestimated the numbers of very small droplets (<50 μm) produced by a splash. However, these small droplets may be of little importance in the local spread of disease. In any case as their lifetimes are so short and their trajectories dominated by turbulence there is little to be gained by modelling their movement using the methods described in this work.

Measuring the droplet size distribution by either of the techniques described is clearly subject to error in some cases. The photographic technique was only used to measure the diameters of droplets for which the velocities could also be determined, if the only measurement required was that of droplet diameter then the problem of relating the sequential images of many droplets with similar trajectories would not arise. Photographic measurement of droplet sizes may therefore be useful. However, determining the size of droplets by collection is faster, and it would be relatively easy to avoid the problems of swamping the sampling surface by placing it far enough below the target that the falling droplets had spread out sufficiently not to coalesce on impact.

5.4 Initial velocity of splash droplets

The range of initial droplet speeds measured varied from 0.1 to 11.8 m s^{-1}. Speeds could be measured with an accuracy of about 0.1 m s^{-1} at best. However additional inaccuracies may have been incorporated into the estimates of speed through the procedure used

for assessing the initial speed of a droplet from that actually measured.

Droplet speeds were not normally distributed but as with the size distributions showed significant postive skewness. The frequency of droplet speeds appeared to be log-normally distributed for the cases of 34 mg drops falling 2.8 m onto barley leaves and for 34 mg drops falling 5.1 m onto bean leaves. However for both 7.6 mg and 34 mg drops falling onto bean leaves the distributions of the logarithms of droplet speed were also significantly skewed. These two distributions were better fitted by a square-root normal distribution, i.e. the square roots of the speeds were normally distributed. Table 5.3 shows the values of the means together with coefficients of skewness $\sqrt{b_1}$ and the levels of kurtosis, b_2 for each of the four cases investigated. Splashes on bean leaves produced droplets with higher average initial speeds than did splashes on barley leaves (Table 5.5). Smaller incident drops resulted in droplets with slightly, but not significantly lower mean speeds than did the same size drops falling the same distance.

The variance of the mean of the square roots of velocity was significantly smaller for splashes on barley leaves than it was for any of those on bean leaves. Compared with 34 mg drops falling 2.8 m, both smaller and faster impacting drops produced splashes with significantly greater variances in droplet speeds. No reference to the degree of variation found by other workers could be found in the literature so no comparisons could be made with splashes in other situations.

Why the mean initial speed of droplets from splashes on barley leaves were lower than those from bean leaves is not readily apparent. The greater positive skewness of the distribution shows that it is, at least partly, due to an increase in the proportion of

TABLE 5•5

Mean and Standard deviation of the square roots of droplet velocity together with the coefficients of skewness and levels of kurtosis.

Expt	$\bar{x}$	S.D.	$\sqrt{b}_1$	b_2
A	1.56	0.424	1.01	5.27
B	2.99	1.583	0.24	2.21
C	2.19	2.312	0.50	2.65
D	2.67	2.966	0.03	2.56

Experimental details as table 5•2

slower droplets, while the maximum speed was similar. It may be that because barley leaves are more flexible than bean leaves they absorb more of the energy of impact reducing the amount returned to the droplets as speed. The lower variance in the speeds of droplets from barley leaves in comparison to bean leaves is also due to there being fewer fast droplets resulting in a more even spread of speeds.

The lower speed of droplets from the splash of smaller drops agrees with the findings of previous workers. Ghadiri and Payne (1979) measured a mean speed of 7.25 m s^{-1} for droplets between 200 and 400 μm produced by the splash of a 126 mg drop compared with only 4.6 m s^{-1} for the same sized droplets produced by a 22.5 mg drop impacting on the same surface at approximately the same speed. Unfortunately they gave no indication of the variance of droplet speeds observed making a more detailed comparison of the results presented here with their data impossible.

In the experiments described here most of the difference in the mean ejection speed of droplets produced by the splash of large and small drops on a bean leaf appear to be accounted for by a reduction in the speed of the very smallest droplets, <100 μm. The mean initial speed of droplets less than 100 μm in diameter produced by the impact of a 34 mg drop on a bean leaf was 4.12 m s^{-1} compared with only 2.39 m s^{-1} for a 7.6 mg impacting drop. For larger drops, between 100 and 1000 μm in diameter, the difference is much less, 3.36 m s^{-1} in the case of 34 mg impacting drops and 2.25 m s^{-1} for a 7.6 mg drop.

Tables 5.2, 5.3 and 5.5 shows that the mean speed of droplets from the splash of a 34 mg drop with an impact speed of 7.9 m s^{-1} is less than that from a similar sized drop striking the same target at a lower speed, 6.5 m s^{-1}. Why this should be is difficult to explain. It may be linked to the different distributions of initial

angles of ejection for droplets from these splashes. This is looked at later when the relationships between the three parameters are discussed (Section 5.5).

5.4.2 *Angles of ejection*

Droplets were observed to be ejected from leaves at all angles. Angles of droplet ejection were measured with an accuracy of about 5^{o}. As with the droplet velocity measurements the procedure used for estimating the initial angle of ejection from that observed may have introduced further errors into the final values.

In all cases the mean angle of droplet ejection was just above the horizontal. However the distributions of initial angles of velocity cannot be described simply.

Figure 5.3 shows the number of droplets of all sizes with initial angles of trajectory divided into 10^{o} classes. Splashes on barley leaves appear to produce a greater proportion of droplets with trajectories above the horizontal than do bean leaves. This is probably because barley leaves have a 'vee' shaped cross-section that tends to deflect droplets upwards. By comparison bean leaves are relatively flat and tend to lie at an angle to the horizontal, drooping towards the tip. This allows droplets to be ejected in any direction, except possibly straight down, though even that might be possible when a leaf is pushed aside by the impact of a fast or heavy drop. As the impacting drop increases in momentum the amount of flexing experienced by a leaf in response to an impact will increase. This is likely to result in an increasing number of droplets being ejected at angles approaching -90^{o}, i.e. vertically downwards, as drop size and velocity increases.

There is also some suggestion of an increase in the number of droplets projected almost vertically upwards from bean leaves as the

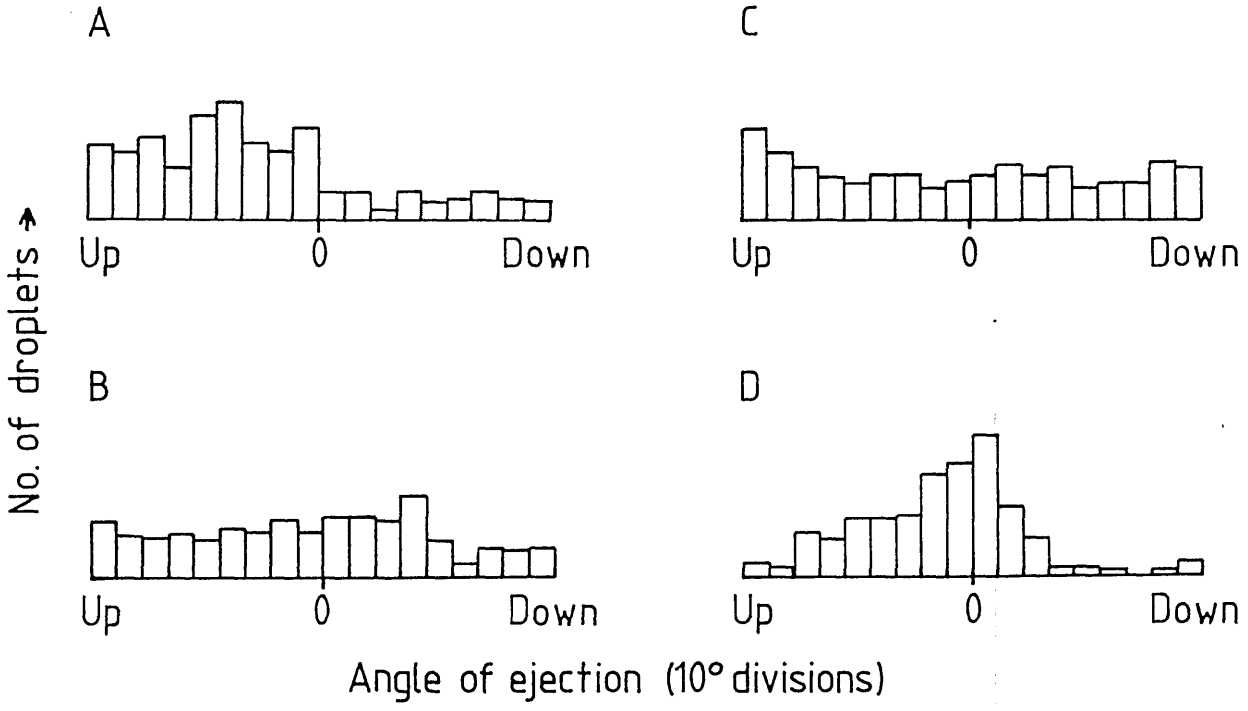


Fig 5.3. Numbers of droplets ejected at different angles.

A) Barley, 34 mg drop falling 2.8 m
B) Bean, 34 mg drop falling 2.8 m
C) Bean, 34 mg drop falling 5.1 m
D) Bean, 7.6 mg drop falling 2.8 m

size and velocity of the impacting drop increases. Only 8.8% of droplets splashed by drops with the lowest impact momentum, 7.6 mg falling 2.8 m, had initial trajectories within 30^{o} of the vertical. Increasing the impacting drop size to 34 mg increased this to 17.3%. Further increasing the impact momentum by increasing the height of fall, to 5.1 m, and therefore the impact velocity from 6.5 to 7.95 m s^{-1}, increased the proportion of droplets with initial trajectories within 30^{o} of the vertical to 25.2%.

Plate 5 shows several photographs of splashes from each of the cases investigated. It can be seen that the fastest moving drops deflected bean leaves to a greater extent than slower ones of the same size and that much of the liquid was simply deflected to one side thus producing a mass of droplets projected downwards. If this were the case for a large number of splashes, as seems to have been the case, then it would be expected that the mean angle of splash from the impact of faster drops would be directed more vertically downwards than from slower drops. However this was not the case, the distribution of initial trajectory angles shows the situation to be rather more complicated than a simple mean would indicate (Fig. 5.3). The faster impacts produced more droplets with initial angles that were directed steeply downwards (betweem -45^{o} and -90^{o}). However more droplets with almost vertically upward trajectories were also produced.

It should be noted that there may also be the possibility of a sampling bias affecting the distribution of measured trajectory angles. It was only possible to measure all of the three parameters investigated: speed, direction and size, for those droplets that could easilly be distinguished from others. This means that it was easier to take measurements for isolated droplets than it was for those moving amongst a cloud of others. As a consequence it is

possible that a greater proportion of droplets following relatively unusual trajectories were recorded than were actually present. This sort of sampling bias would have particularly affected those cases where large numbers of droplets are ejected with very similar trajectories, such as was the case for some of the splashes of large fast drops on bean leaves. Thus errors introduced in this way may have been sufficient to account for the apparently lower velocity of splash droplets produced by the impact of faster drops.

5.5 Relationships between size, speed and angle

It is not sufficient to only look at the three parameters in isolation, the relationships between them must also be investigated. Figures 5.4a to 5.4d show the relationship between the initial speed of splash droplets and their diameter, Figs 5.5a to 5.5d show the relationship between droplet diameter and the angle of droplet ejection and Figs 5.6a to 5.6d the relationship between initial speed and angle of ejection for each of the four cases investigated.

5.5.1 *Droplet size and initial droplet speed*

In all four cases there is a clear relationship apparent between droplet size and initial speed, the droplets with the highest velocities tended to be small and, in general, small droplets were ejected at higher speeds than were larger ones. However there is a great deal of scatter, in the case of the splash from the highest momentum drop (Fig. 5.4c) any relationship between size and velocity is almost totally obscured. The trend towards decreasing droplet velocity with increasing droplet size is most clearly apparent for droplets up to around 1000 μm in diameter. In some cases the larger droplets >1000 μm, which were only detected in very small numbers, had speeds higher than those of droplets less than 1000 μm in

Fig 5.4. Relationship between droplet size and initial speed.

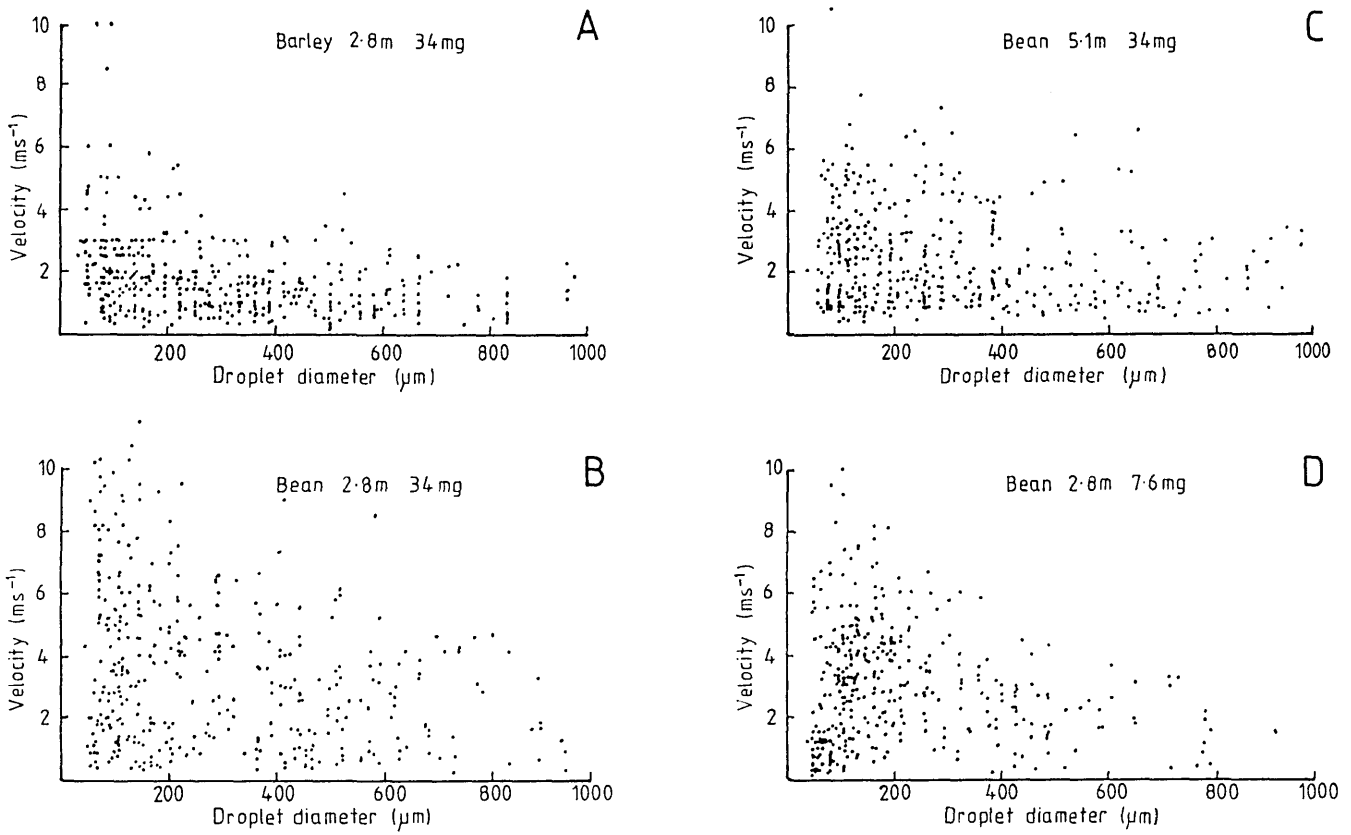


Fig 5.5. Relationship between initial speed and angle of ejection of droplets.

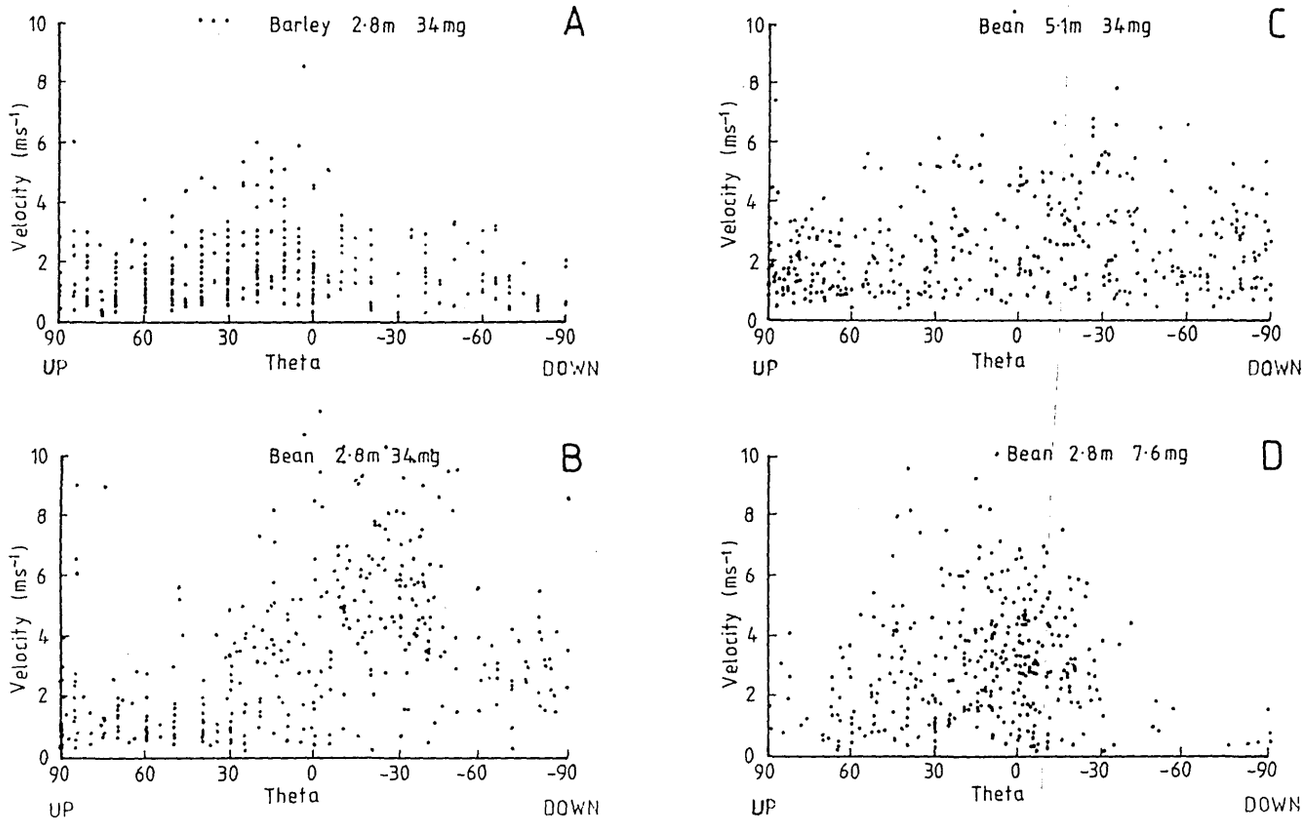
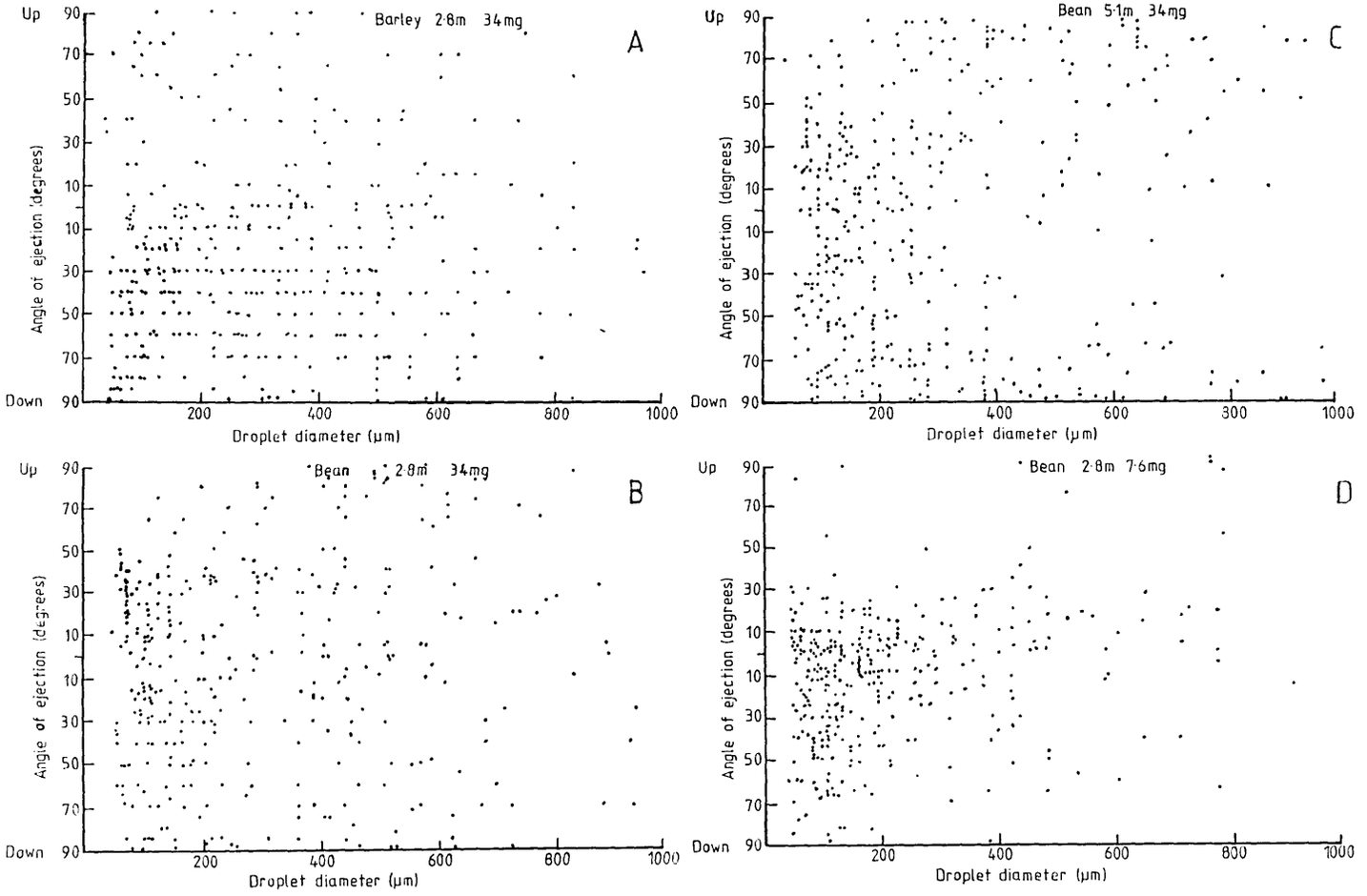


Fig 5.6 Relationship between droplet size and angle of ejection.



diameter. For example Fig. 5.7 shows the mean velocity of droplets ejected in splashes from barley leaves in ten equal size groups between 0 and 1000 μm. 98% of the droplets measured fell into this range and the decrease in speed with increasing droplet size can be clearly seen. Fig. 5.8 shows the mean velocity of droplets in ten equal size groups between 0 and 1555 μm, the largest detected in this trial, (i.e. for the complete set of data). The trend for decreasing velocity with increasing size appears to break down for diameters greater than about 900 μm. This is because of a relatively small number of large droplets with higher than expected velocities. A similar situation was observed for the splash of 34 mg drops falling 2.8 m onto bean leaves.

Out of over 1500 inidividual droplets examined the fastest measured was moving at 11.8 m s^{-1}. This is substantially slower than the maximum speed, of about 20 m s^{-1} that was reported by Ghadiri and Payne (1981) for splashes on saturated soil of 22.5 mg incident drops falling at 5.5 m s^{-1}. However, in their experiments very fast droplets were generally very small, in the 15 to 50 μm range. Droplets in this size range were largely beyond the resolving power of the equipment used in the experiments described here.

Further comparison shows that the smaller droplets from splashes on soil paste did have higher initial velocities than did those produced by the splash of drops of similar momentum on leaves. The mean velocity of droplets with diameters in the range from 200 to 400 μm was 4.60 m s^{-1} for splashes on soil but only 3.70 m s^{-1} for splash on a bean leaf and 1.69 m s^{-1} from a barley leaf. However, larger droplets from leaf splash had higher velocities than did similar sized droplets from splashes on soil. The average speed of droplets in the 800 to 1000 μm range was only 0.46 m s^{-1} from soil splash but 1.1 and 1.8 m s^{-1} respectively from splash on barley and bean leaves.

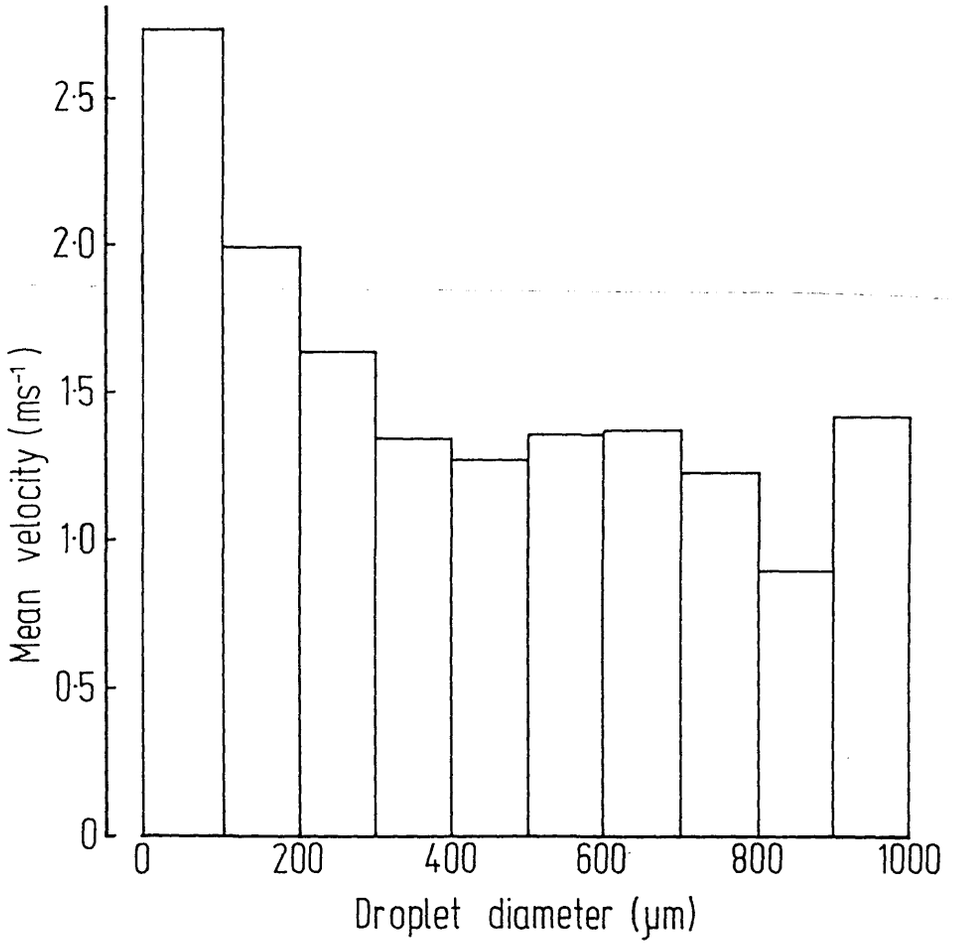


Fig 5.7
Mean velocity of different sized droplets up to 1 mm diameter from the splash of a 34 mg drop falling 2.8 m onto a bean leaf.

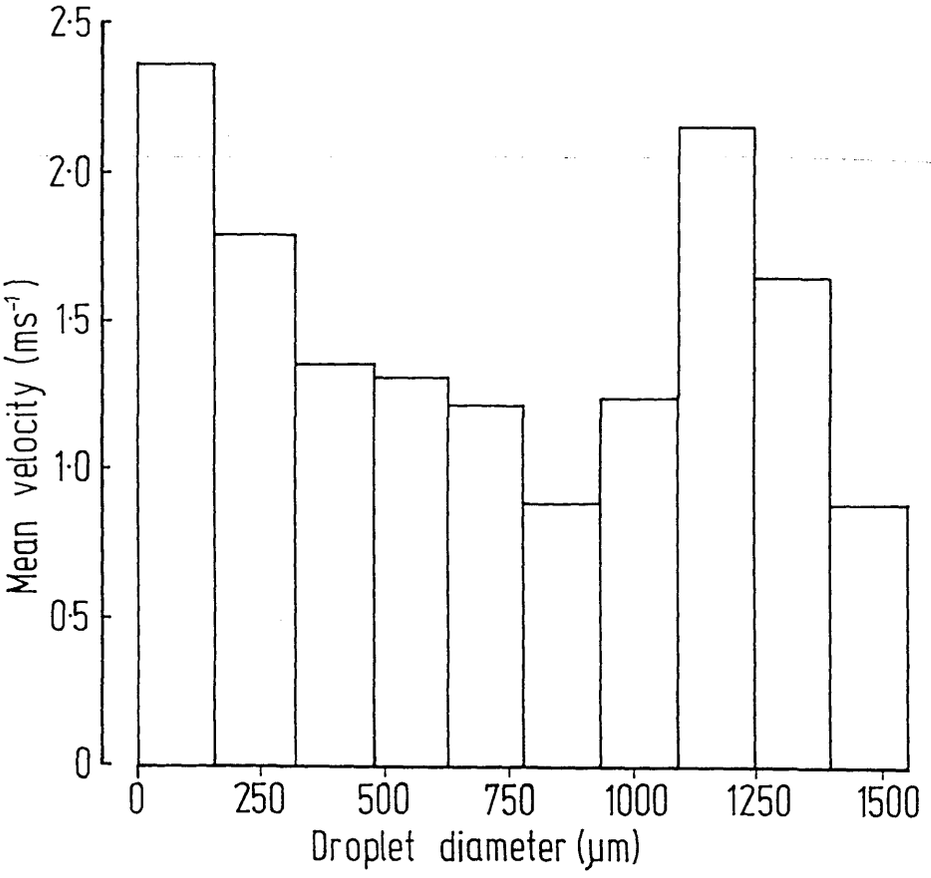


Fig 5.8
Mean velocity of all droplets, in 10 equal size classes, from the splash of a 34 mg drop falling 2.8 m onto a bean leaf.

The most likely explanation for the lower speed of the smaller splash droplets when compared to similar splashes on other surfaces is that some of the energy of the incident drop was absorbed by the leaf. In some cases the leaf tip was moved more than 10 mm by the impact of the simulated rain drops and may therefore have acted as a spring. Leaf movement can be seen in several of the photographs of splash. Plate 6 particularly, illustrates the magnitude of movement possible, on the right hand side of the photograph two clear images of the leaf can be distinguished at least a centimetre apart.

Ghadiri and Payne (1979) showed that the size of droplets ejected by a splash increased with time. If the leaf initially absorbed some of the impact energy of a drop then the smaller droplets, which are produced first, would be expected to have less momentum than droplets produced at the equivalent time by splashes on soil. As time passes and the flexing of the leaf increases it will offer greater resistance. Droplets that are produced later, and which are consequently larger, may therefore be less affected by the energy absorbed by the leaf and so would have velocities similar to those produced by soil splash.

The higher than expected velocity of the larger droplets produced by splashes on leaves may be due to two factors. Firstly, and probably most importantly, if a drop strikes the leaf near its edge, or in a region where the leaf is lying at an angle to the horizontal, then much of the liquid contained in the original drop forms a sheet that flows along the surface of the leaf and off its edge. This sheet then breaks up into relatively large droplets that retain much of the momentum of the original impacting drop and so have higher speeds than correspondingly sized droplets from splashes on solid surfaces.

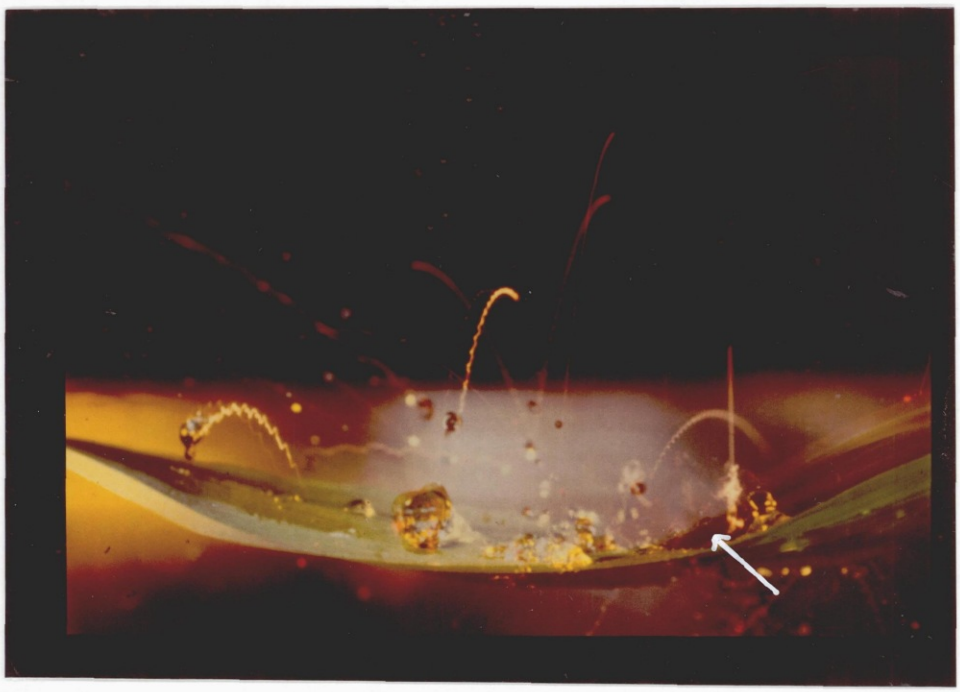


PLATE 6

Photograph of a splash on a barley leaf showing droplets present on the leaf surface before the impact being flung off by the force of the impact.

The arrow indicates the point of impact, streaks left by droplets as they move through a bright beam of light show that several of them do not originate from the splash.

The plate also clearly shows motion of the leaf due to the impact.

The suggestion that larger droplets are simply the deflected remnants of the impacting drop is supported by the observation that some very large droplets travel faster than expected. The numbers of these large and fast moving drops also increases as the momentum of the impacting drop increases. The situation may effectively be similar to that when a splash occurs on a rigid sloping surface. The greater the angle of slope the greater the downslope component of splash (Ghadiri-Khozoojhi, 1978). Drops with higher kinetic energy will of course cause greater deflection of the target leaf so that the effective slope of the target is increased. Evidence for this is seen in a comparison of the graphs for mean velocity against size for 34 mg drops striking bean leaves at 8 m s^{-1} (Fig. 5.9a) and 7.6 mg drops striking a bean leaf at 5.83 m s^{-1} (Fig. 5.9b). In the former case the average speed of droplets larger than 750 μm was 2.0 m s^{-1}. This is considerably faster than the velocities measured by Ghadiri-Khozoojhi (1978) for similar sized droplets from splashes on soils. In comparison the smaller incident drops ejected fewer than half as many droplets above 750 μm in diameter and with a mean velocity of only 1.2 m s^{-1}.

The second factor is that the rebounding leaf returns some of the energy of impact to the droplets. Large droplets being formed later in the splash process are most likely to be affected by the leaf rebounding. No direct evidence for this happening was found. However, the potential for the leaf motion to impart velocities on droplets was demonstrated. In many cases water drops present on the surface of the leaf were observed to be thrown of by the force of impact (Plate 6). The velocity of only a few of these droplets was measured but the indication was that they had velocities of the same order as droplets ejected from the splash, thus demonstrating the potential for the transfer of energy between leaf and droplet.

Fig 5.9 (b)

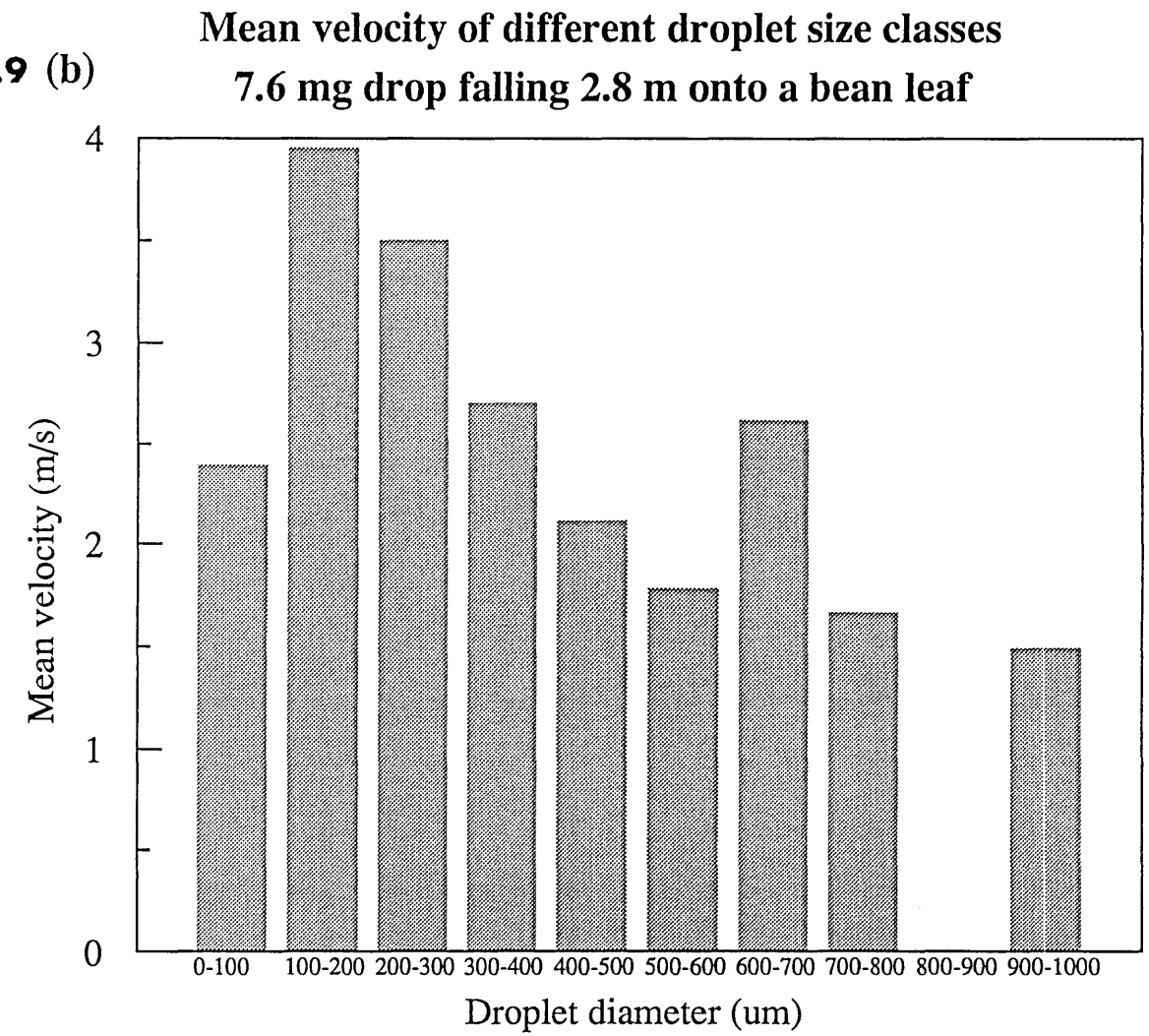
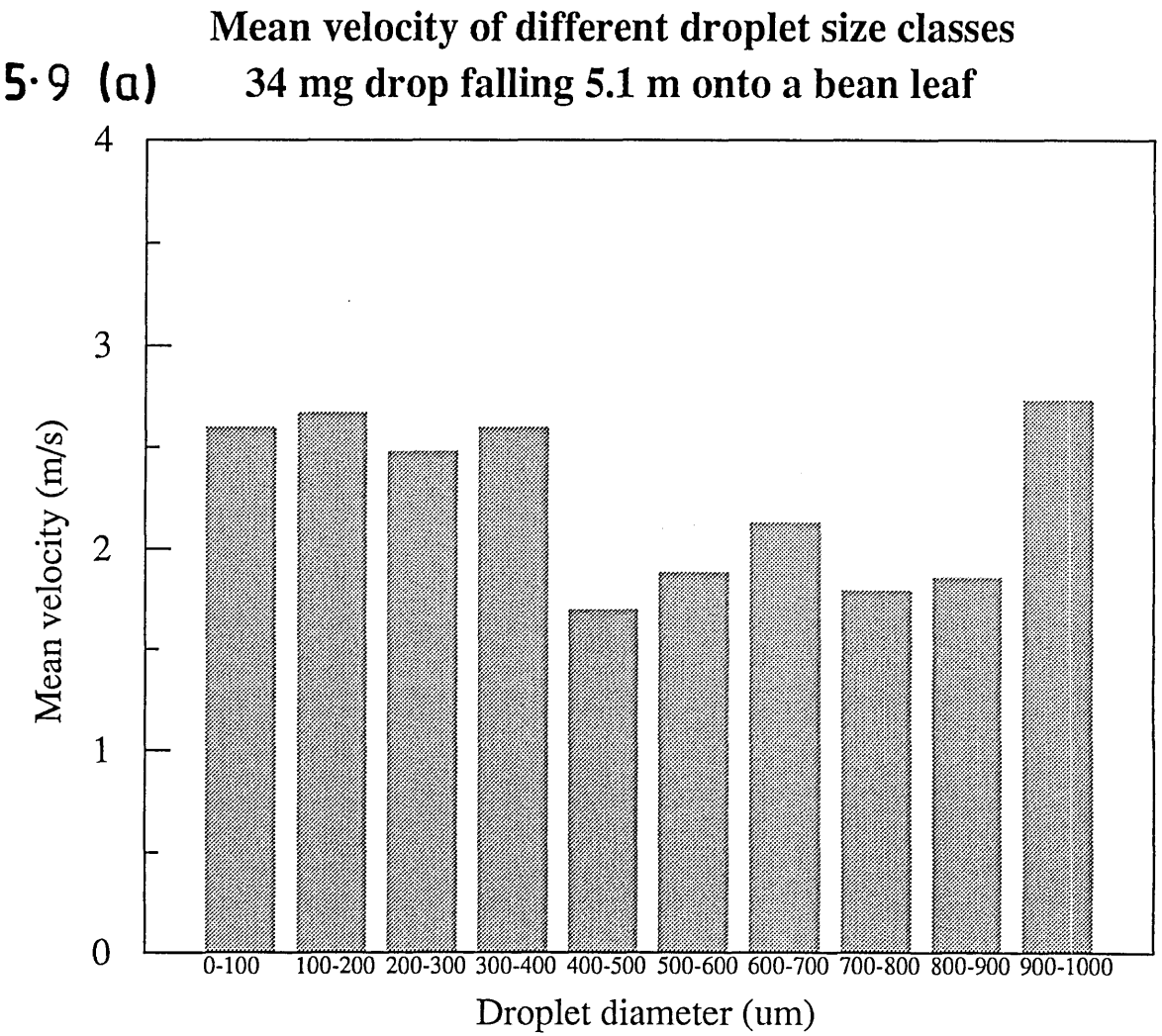

Mean velocity of different droplet size classes
7.6 mg drop falling 2.8 m onto a bean leaf
Mean velocity (m/s)
0
1
2
3
4
0-100
100-200
200-300
300-400
400-500
500-600
600-700
700-800
800-900
900-1000
Droplet diameter (um)

Fig 5·9 (a)


Mean velocity of different droplet size classes
34 mg drop falling 5.1 m onto a bean leaf
Mean velocity (m/s)
0
1
2
3
4
0-100
100-200
200-300
300-400
400-500
500-600
600-700
700-800
800-900
900-1000
Droplet diameter (um)

To examine and quantify the changes in the distributions of velocities with droplet size the frequency distributions of particle speed for different size classes were fitted to both log normal and square root normal distributions. This was done by plotting the cumulative distributions of the logarithm (Figs 5.10-5.13) or square root (Figs 5.14-5.17) of the speed for different sized droplets on probability scales. Regression coefficients and chi squared values for goodness of fit were calculated and are shown in Table 5.6.

The slope of the regression line, b, for the square root normal distribution increases with droplet size class indicating a decrease in the standard deviation of the diameter with increasing size. This increase in slope was apparent for all cases where a square-root transformation was carried out. This indicates a reduction in the variance of the speed with increasing droplet size and appears to be caused mainly by a reduction in the number of faster moving droplets as droplet size increases.

With the logarithmically transformed data this trend in the value of b is apparent in only two cases, a 34 mg drop falling onto a barley leaf and a 7.6 mg drop falling onto a bean leaf. In the other two cases no regular pattern in the value of b can be detected. However in these two cases the chi squared tests for the goodness of fit of the regression lines indicate that the square root transformation gave a better fit to the data than did the logarithmic one.

5.5.2 *Speed and angle of ejection*

Figures 5.5a-5.5d shows the relationship between the initial angles of droplet ejection and their speed. Figures 5.18a-d show the mean initial velocity of droplets ejected at different angles. The fastest droplets appear to be ejected close to the horizontal,

Fig 5.10 Change in velocity distribution with droplet diameter.

Barley
34 mg
2.8 m

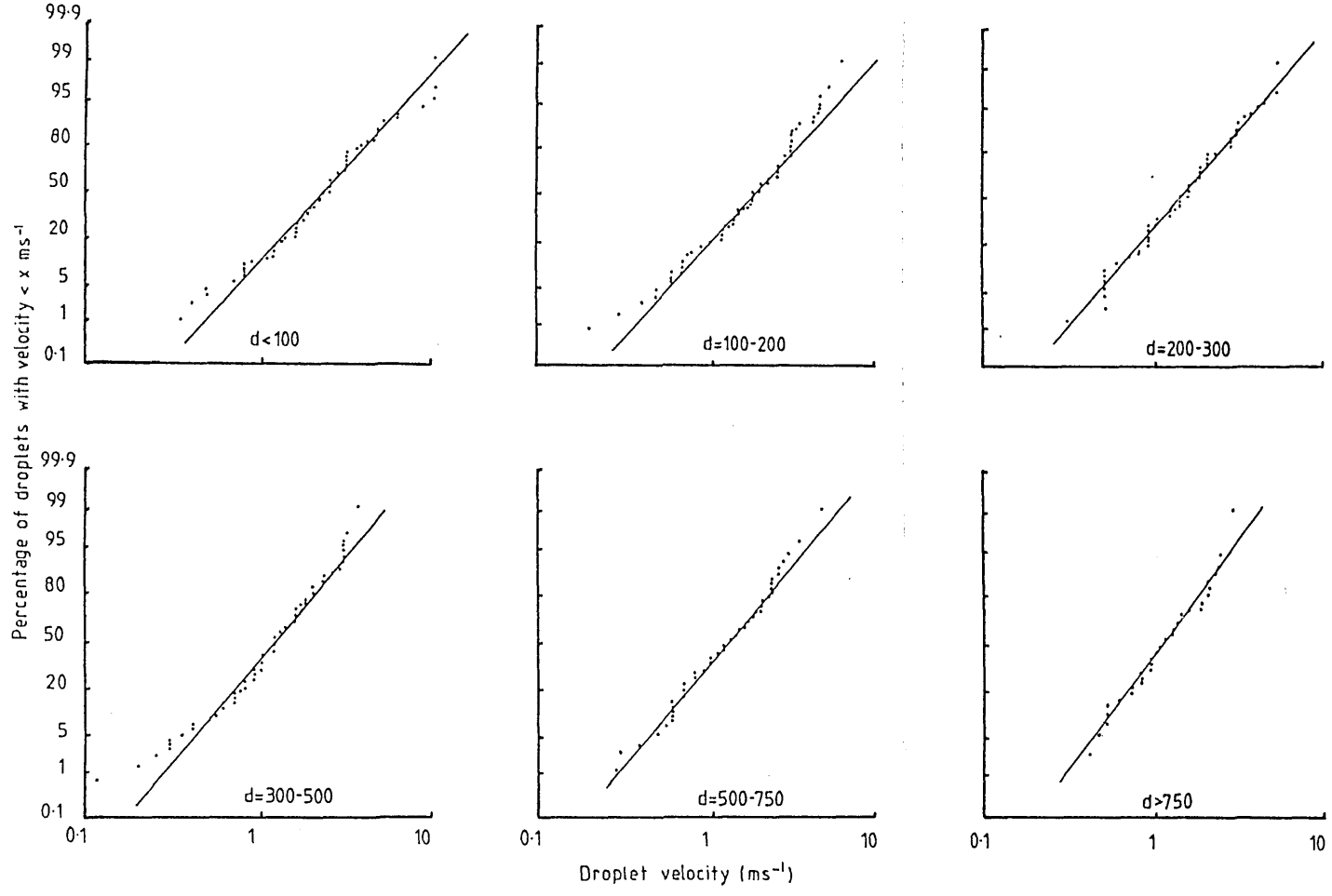


Fig 5.11. Change in velocity distribution with droplet diameter.

Bean
34 mg
2.8 m

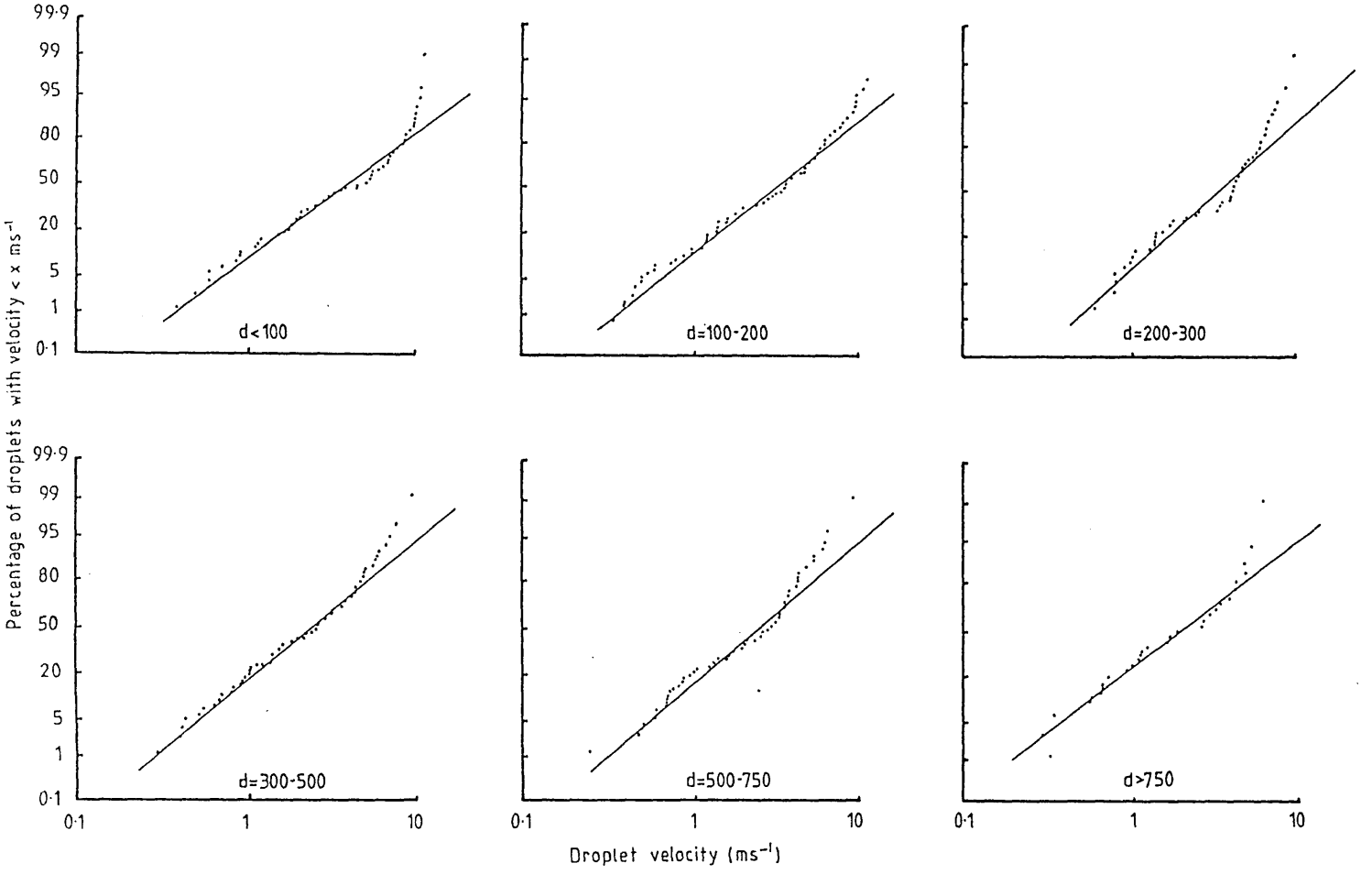


Fig 5.12. Change in velocity distribution with droplet diameter.

Bean
34 mg
5.1 m

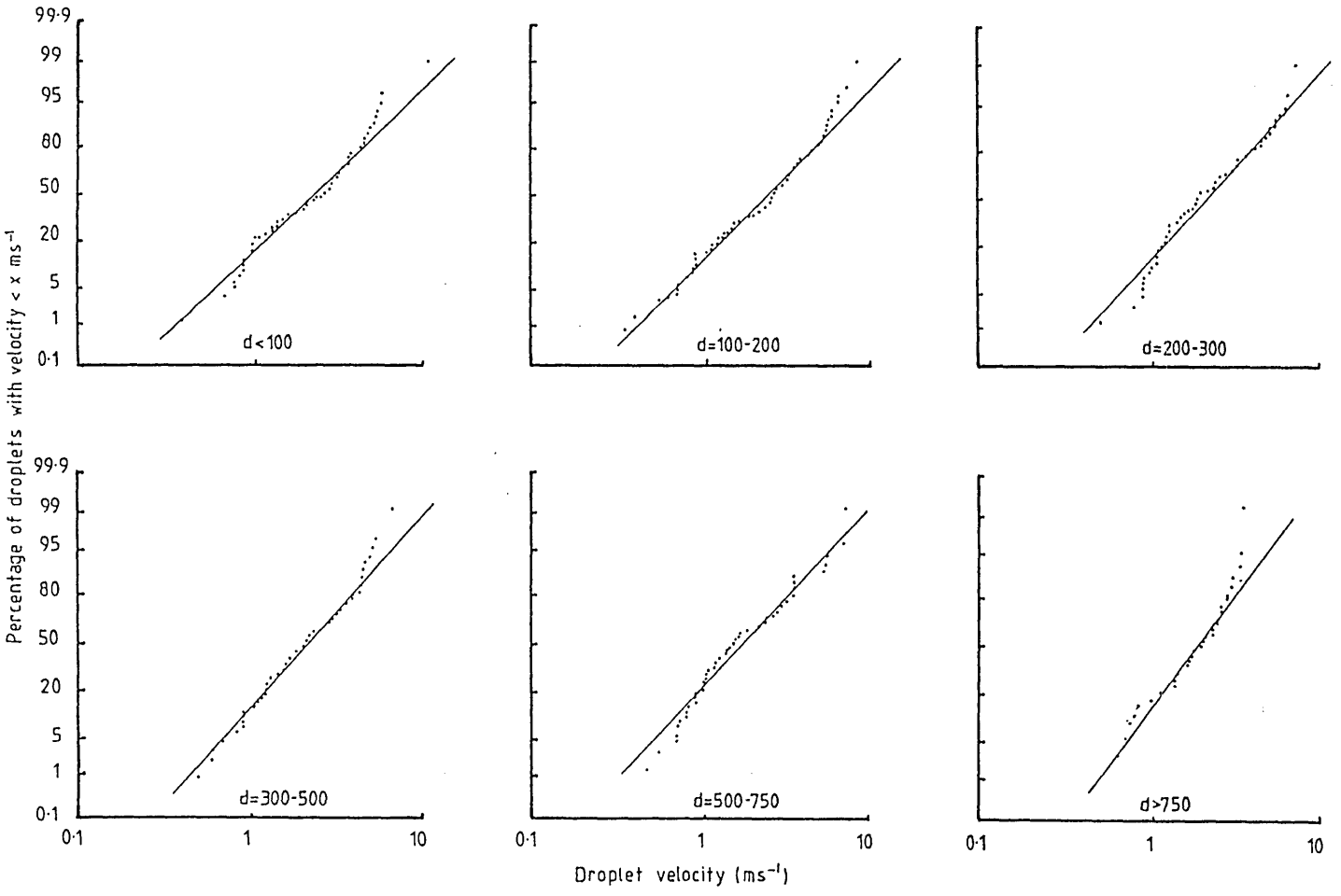
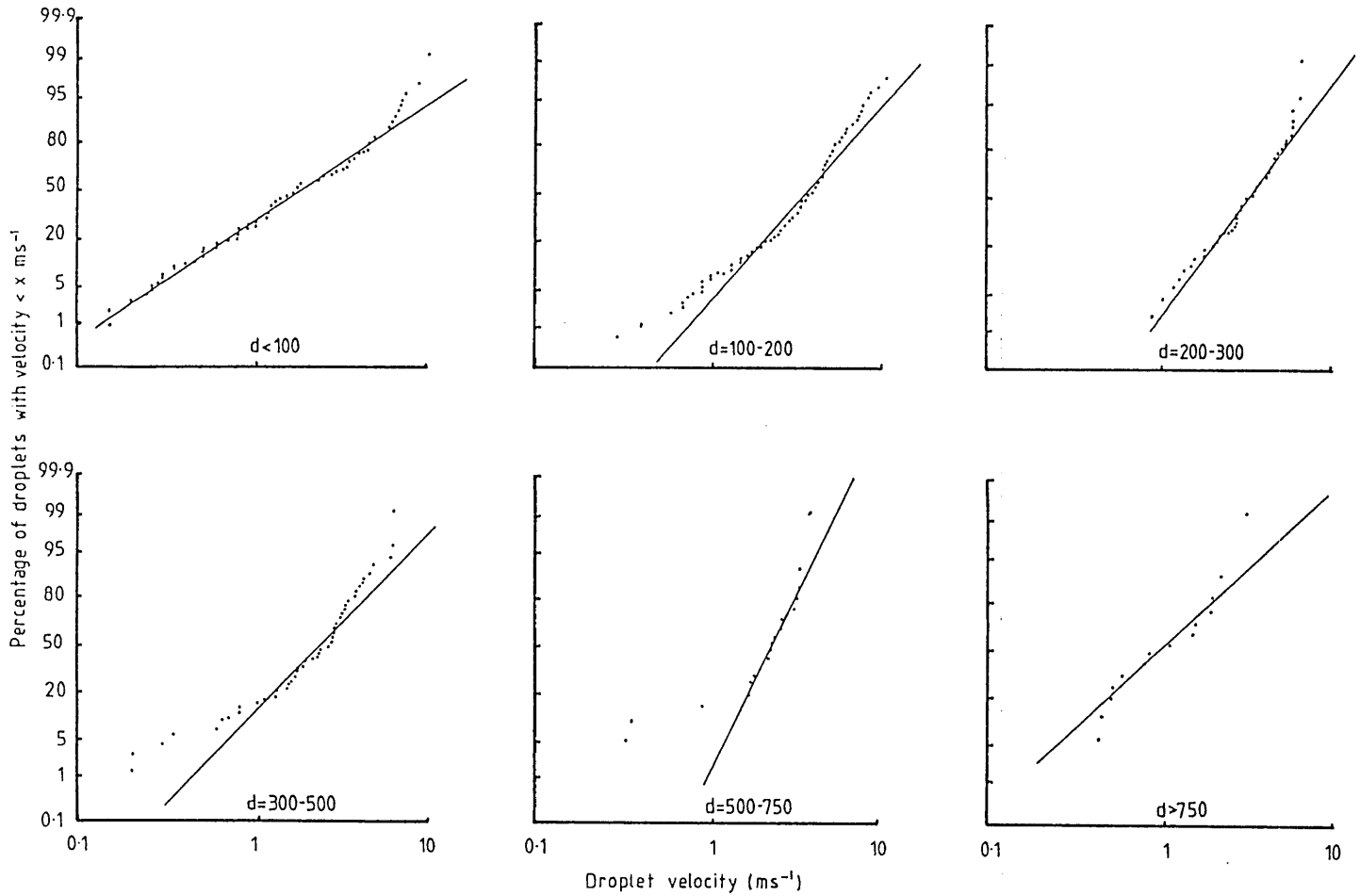


Fig 5.13. Change in velocity distribution with droplet diameter.

Bean
7.6 mg
2.8 m



Expts		DROPLET DIAMETER 0-100	100-200	200-300	300-500	500-750	>750
34 mg	a	3.84	4.19	4.55	4.81	4.79	4.99
2.8 m	b	3.49	3.47	3.58	3.74	3.65	4.17
Barley	χ^2	0.71	1.16	0.44	0.93	0.30	0.23
34 mg	a	3.76	3.85	3.58	4.19	4.14	4.50
2.8 m	b	2.37	2.50	2.83	2.64	2.74	2.38
Bean	χ^2	1.10	1.11	1.94	0.46	0.98	0.43
34 mg	a	4.00	3.89	3.97	3.92	4.42	3.96
5.1 m	b	3.10	3.23	3.49	3.51	3.25	4.18
Bean	χ^2	0.67	0.86	0.62	0.41	0.82	0.66
7.6 mg	a	4.60	3.22	3.12	3.95	3.59	5.16
2.8 m	b	2.12	3.50	4.34	3.33	4.79	2.90
Bean	χ^2	0.52	2.60	0.55	5.47	15.83	0.41

Table 5.6(a)

Regression coefficients and chi squared values for the goodness of fit for the distributions of the logarithms of initial velocities for different size classes.

Expts		DROPLET DIAMETER 0-100	100-200	200-300	300-500	500-750	>750
34 mg	a	1.92	1.71	1.89	1.60	1.86	1.44
2.8 m	b	2.05	2.44	2.61	3.13	2.86	3.47
Barley	χ^2	3.48	0.42	0.67	0.79	0.55	0.43
34 mg	a	2.75	2.62	2.19	2.58	2.37	2.84
2.8 m	b	1.15	1.32	1.50	1.61	1.74	1.59
Bean	χ^2	0.78	0.55	1.05	0.27	0.48	0.38
34 mg	a	2.43	2.21	2.19	2.09	2.55	1.14
5.1 m	b	1.71	1.80	1.94	2.02	1.94	2.84
Bean	χ^2	0.71	0.68	1.73	1.13	4.57	0.36
7.6 mg	a	3.28	1.44	1.20	1.87	1.39	2.45
2.8 m	b	1.28	1.91	2.11	2.12	2.54	2.55
Bean	χ^2	1.30	0.59	0.25	0.54	16.59	0.37

Table 5.6(b)

Regression coefficients and chi squared values for the goodness of fit for the distributions of the square roots of initial velocities for different size classes.

Fig 5.14. Change in velocity distribution with droplet diameter.

Barley
34 mg
2.8 m

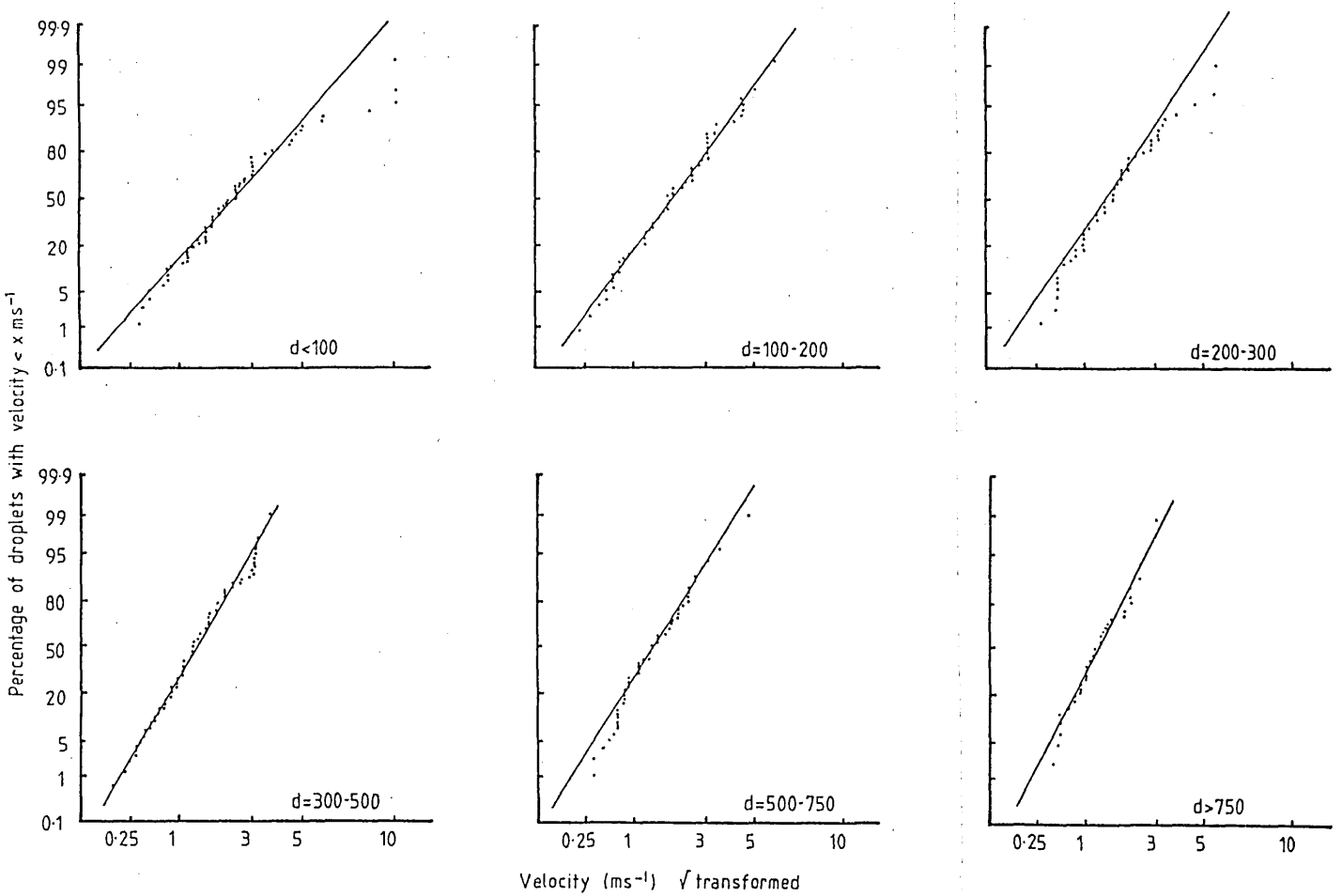


Fig 5.15. Change in velocity distribution with droplet diameter.

Bean
34 mg
2.8 m

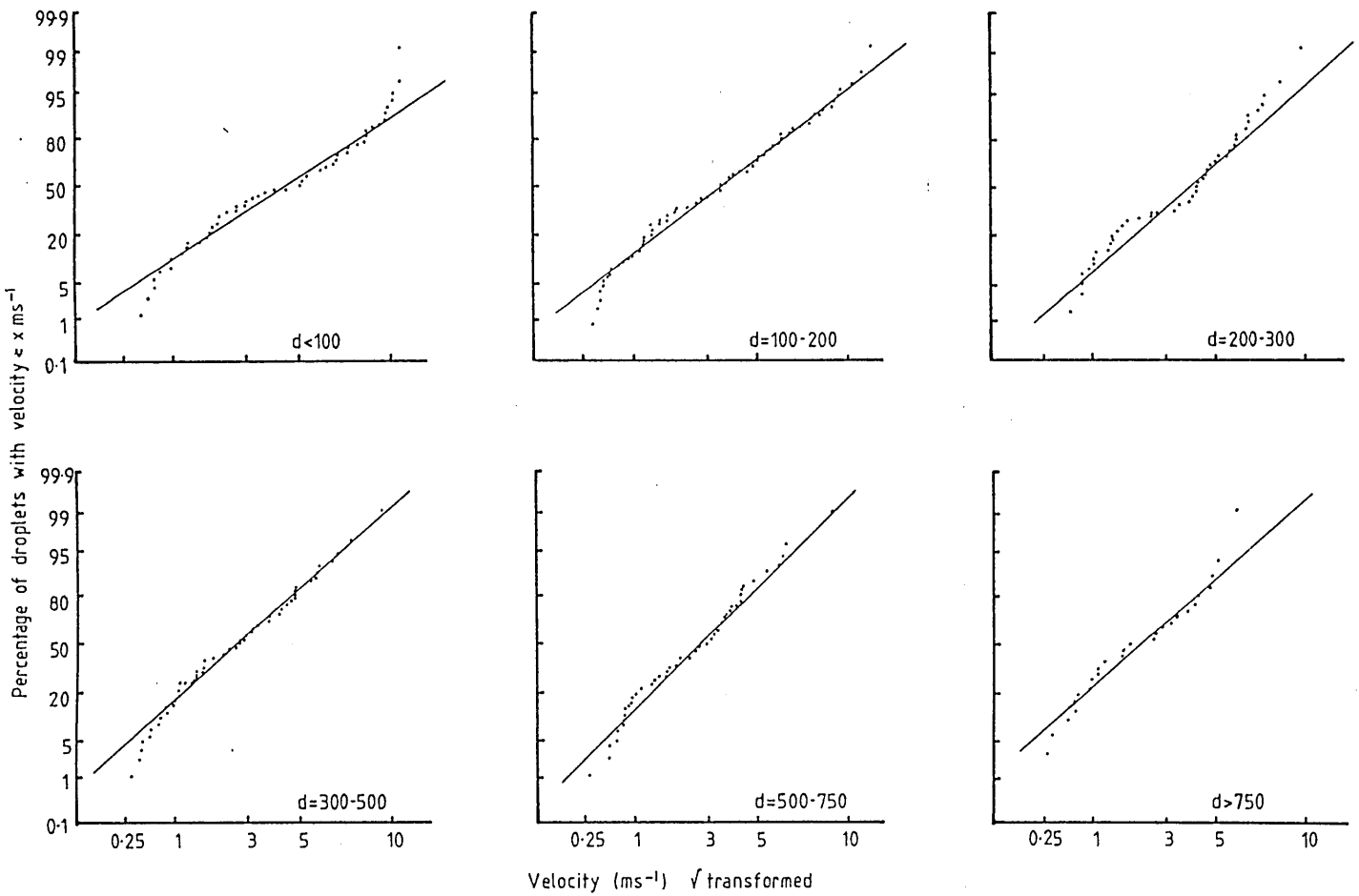


Fig 5.16. Change in velocity distribution with droplet diameter.

Bean
34 mg
5.1 m

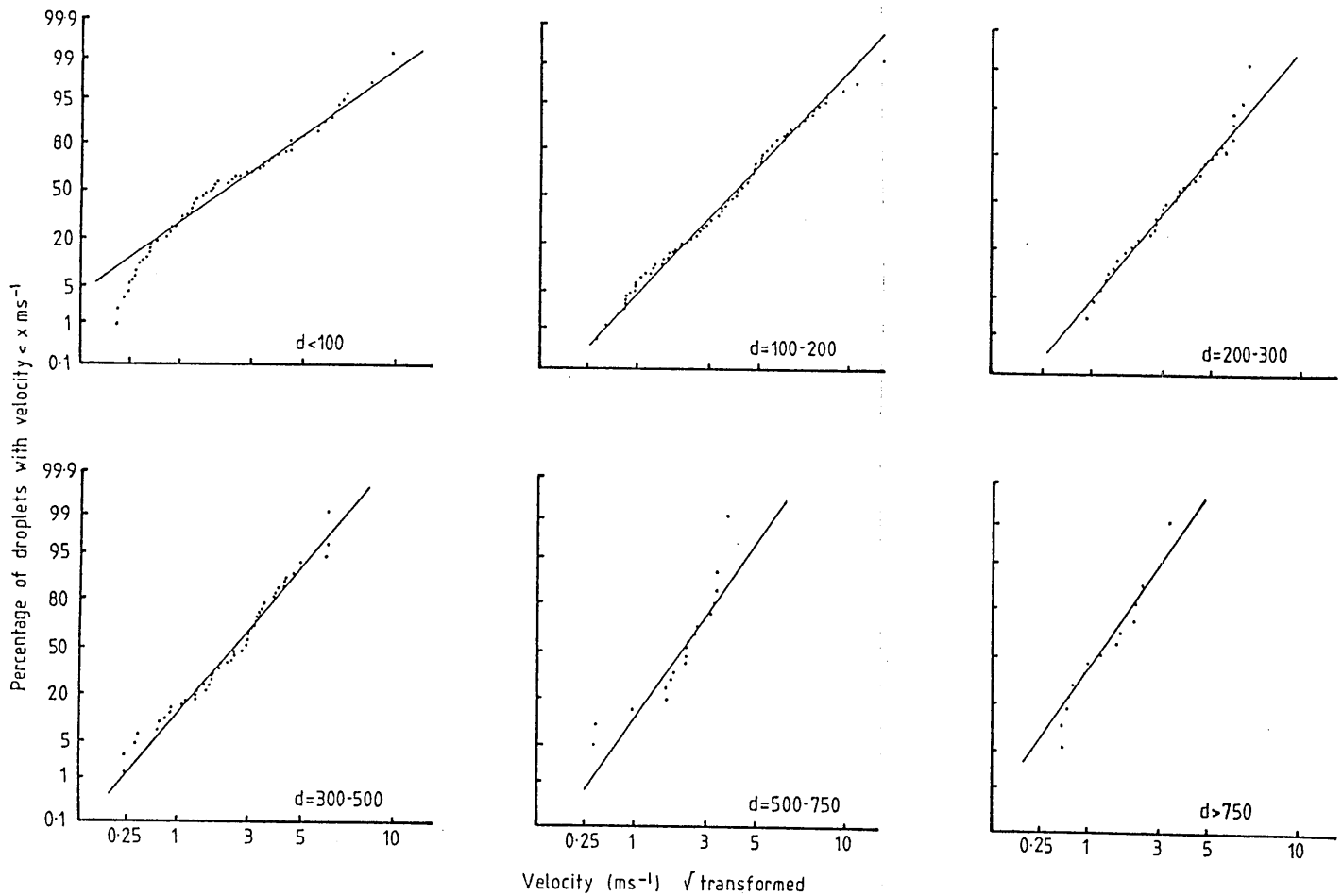
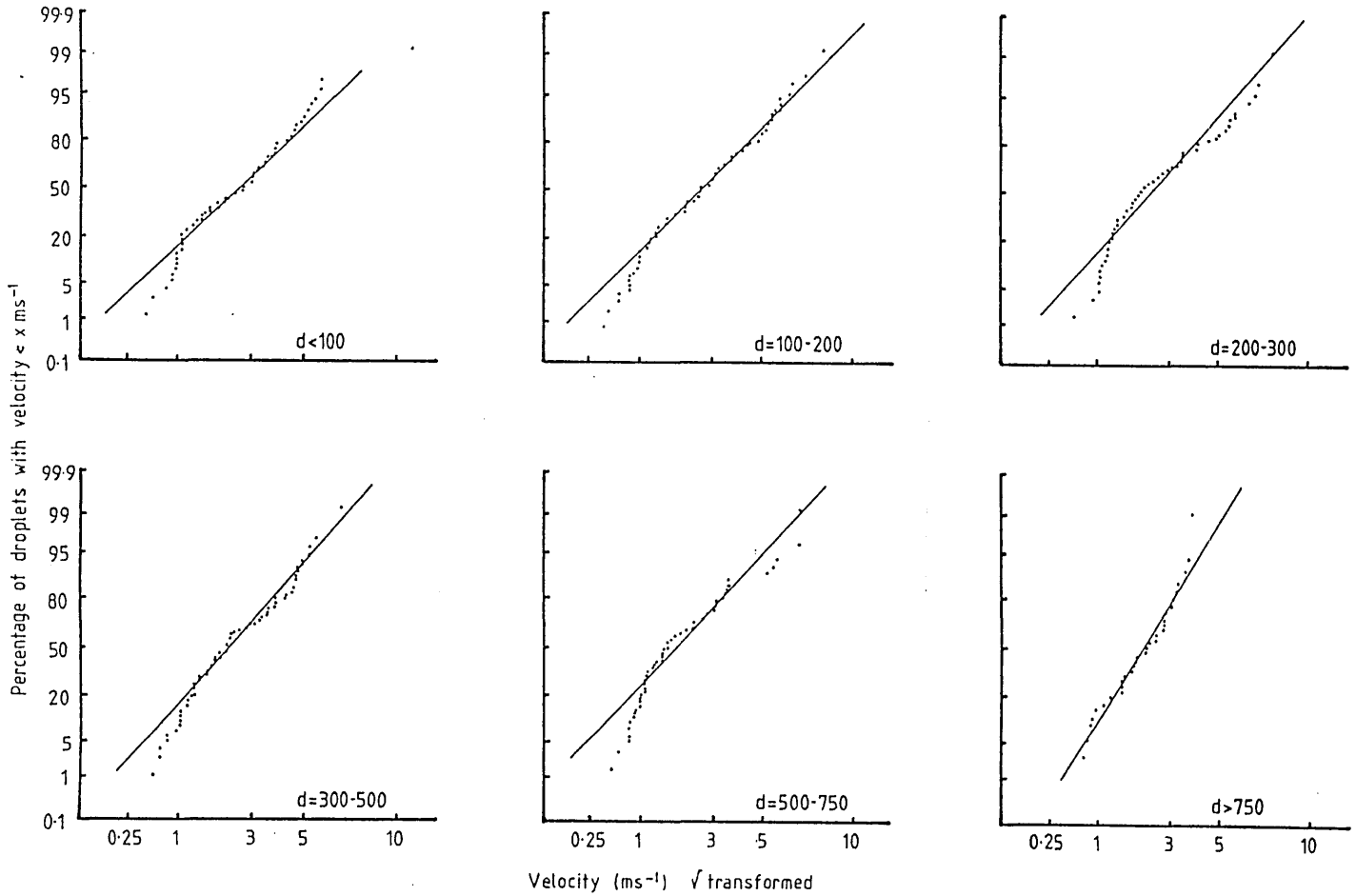


Fig 5.17. Change in velocity distribution with droplet diameter.

Bean
7.6 mg
2.8 m



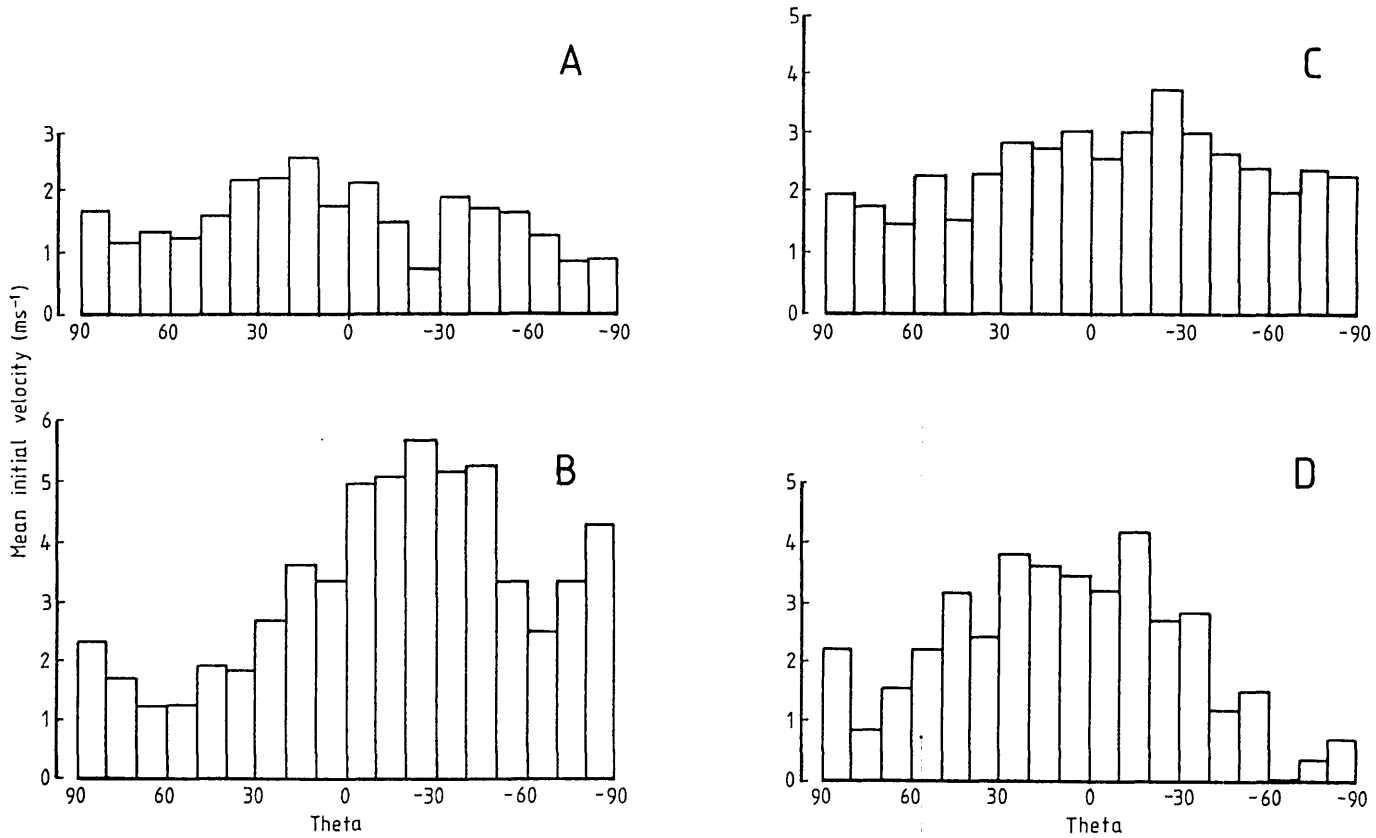


Fig 5.18. Mean initial velocity of droplets ejected at different angles.
A) Barley/34 mg/2.8 m
B) Bean/34 mg/2.8 m
C) Bean/34 mg/5.1 m
D) Bean/7.6 mg/2.8 m

although small numbers of fast moving droplets, $V_i > 4$ m s^{-1}, were also ejected vertically upwards. The proportion of droplets that were ejected within 20^o of the horizontal and had velocities greater than the median is shown in Table 5.7. The results from the different splashes on a bean leaf target show that the proportion of fast droplets ejected horizontally decreases as impact momentum increases. Faster heavier drops throw off fast moving droplets in all directions. There was a difference between bean and barley plants in the angles at which the maximum velocities were most commonly to be found. On barley plants the highest speeds were found for droplets ejected between +40 and $+5^o$, while from the splashes of similar drops on bean leaves the fastest droplets were ejected between +5 and -40^o.

Figures 5.19-5.22 and Table 5.8 show regression lines and detail the regression coefficients for the distributions of the square root of the velocity seperated into four classes by the initial angle of ejection. The values of b are plotted in Fig. 5.23 and show a 'U' shaped trend with the values of b decreasing for angles of ejection nearer to the horizontal. This indicates an increase in the velocity variance as the angle of ejection approaches the horizontal. As with the changes in velocity variance with size class this appears to be caused by an increase in the number of faster moving droplets being ejected horizontally compared with the numbers ejected vertically, either up or down.

Regression lines calculated for the log transformation do not show any regular change in the value of b, but they do not fit the data significantly better, Table 5.9.

Overall both the square root and logarithmic transformations give fairly good fits to a normal distribution. In some cases one appears to be better in some the other. For almost all of the cases where a square root transformation was carried out, the regression lines for

TABLE 5•7

Proportion of droplets with initial velocities greater than the median and ejected within 20° of the horizontal.

Expt	Median initial velocity (m/s)	Percentage of all droplets with initial velocities > median that were ejected within 20° of the horizontal.	Percentage of droplets ejected within 20° of the horizontal with initial velocities > median.
34 mg 2.8 m Barley	1.4	38.0%	63.5%
34 mg 2.8 m Bean	3.0	41.2%	68.4%
34 mg 5.1 m Bean	2.0	24.9%	61.9%
7.6 mg 2.8 m Bean	2.75	72.4%	63.1%

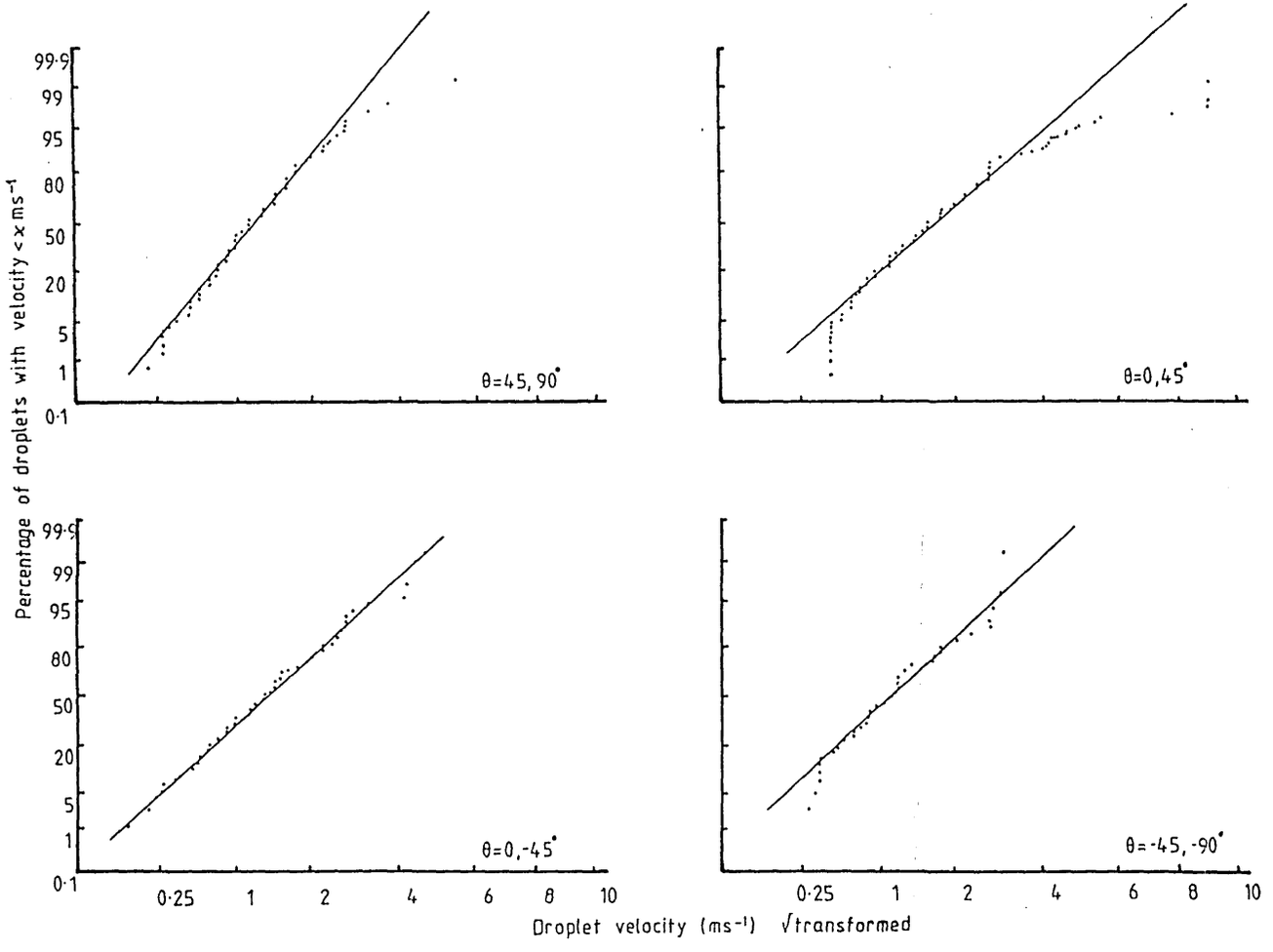


Fig 5.19. Effect of angle of ejection on droplet velocity distribution.

Barley
34 mg
2.8 m

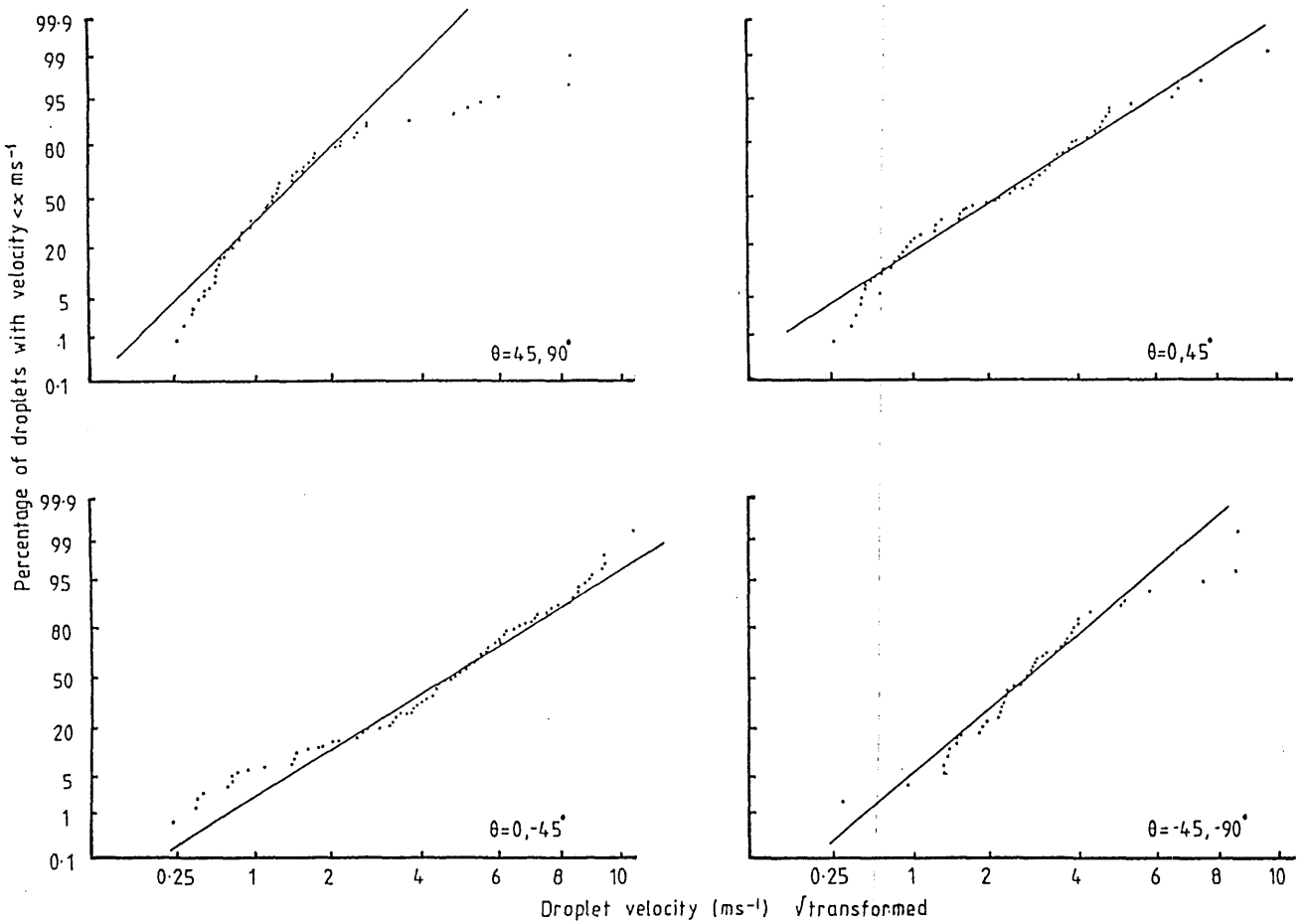


Fig 5.20. Effect of angle of ejection on droplet velocity distribution. Bean 34 mg 2.8 m

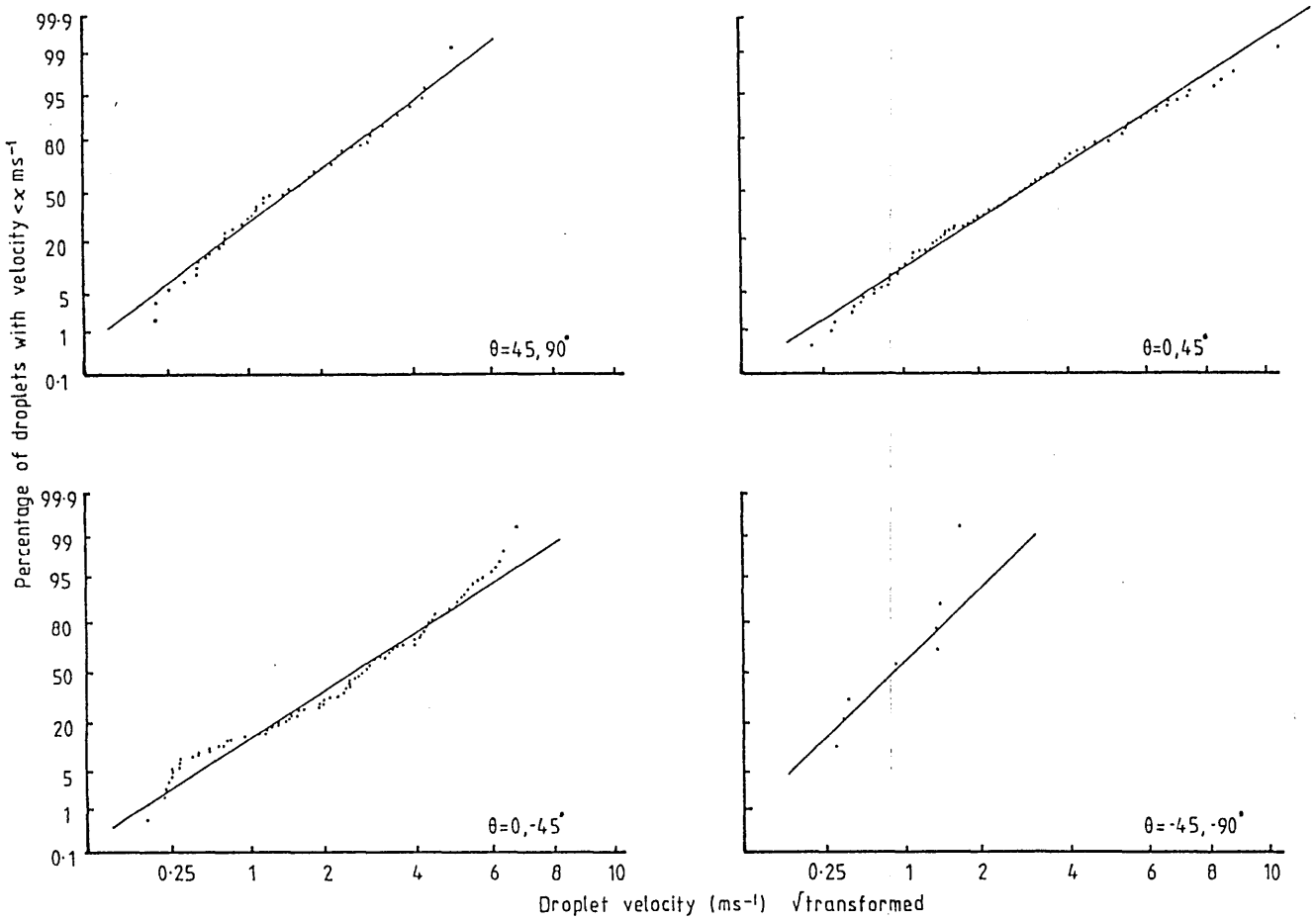


Fig 5.21. Effect of angle of ejection on droplet velocity distribution. Bean 34 mg 5.1 m

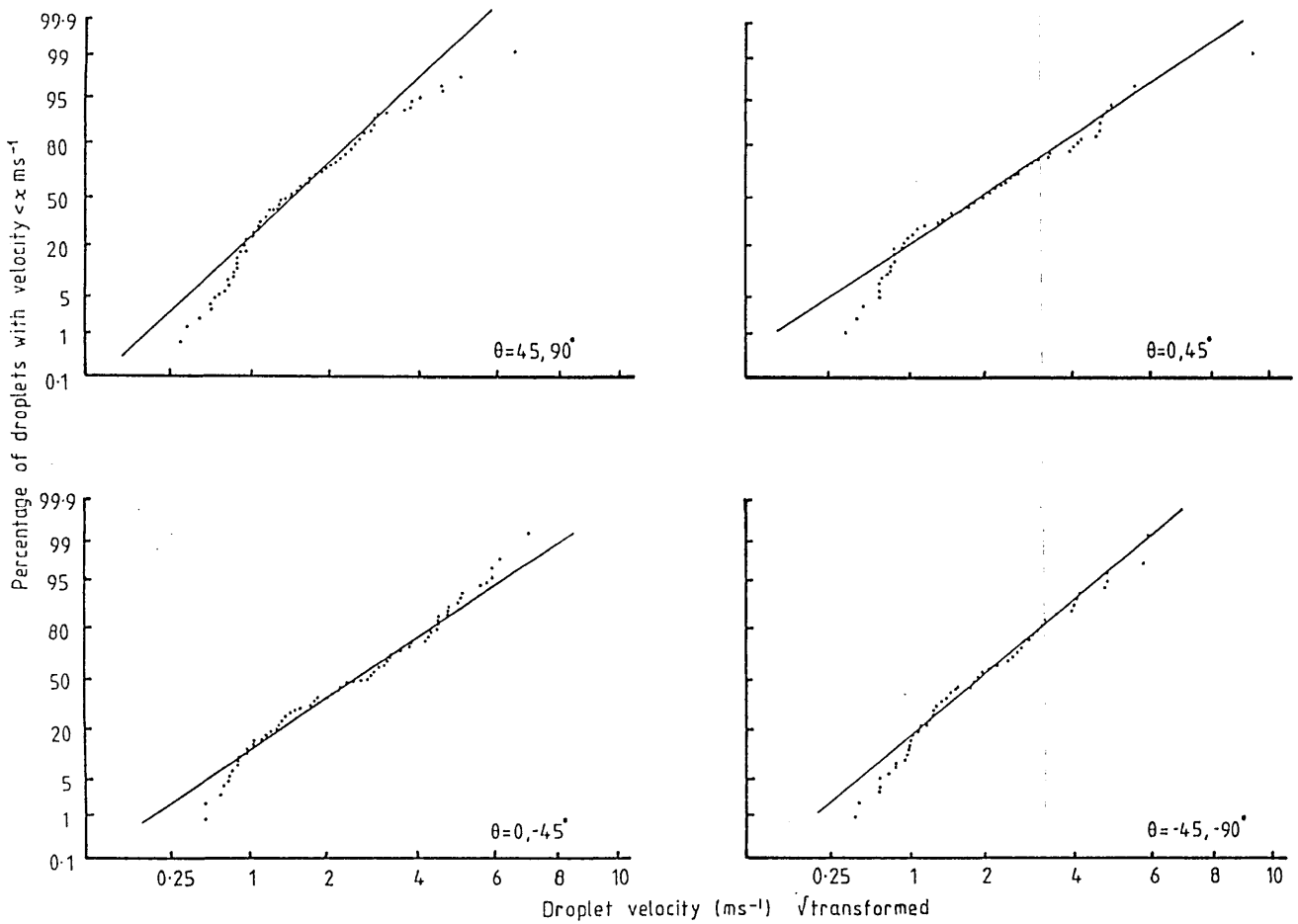


Fig 5.22. Effect of angle of ejection on droplet velocity distribution.

Bean
7.6 mg
2.8 m

TABLE 5.8

Regression coefficients for the frequency distributions of the square-root of initial droplet velocities seperated by angles of droplet ejection.

Expt		Angle of ejection (degrees)			
		Up 90-45	45-0	0-45	Down 45-90
34 mg	a	4.71	4.28	4.63	4.89
2.8 m	b	4.03	3.55	3.21	3.17
Barley	χ^2	0.49	0.73	0.80	0.28
34 mg	a	4.70	4.17	2.19	2.65
2.8 m	b	3.48	2.70	4.17	5.05
Bean	χ^2	0.97	1.26	19.07	1.03
34 mg	a	4.20	4.15	3.74	3.87
5.1 m	b	3.97	2.93	3.05	3.80
Bean	χ^2	0.53	0.68	2.16	0.39
7.6 mg	a	4.56	3.62	3.62	5.36
2.8 m	b	2.78	3.09	3.01	2.96
Bean	χ^2	0.36	1.32	65.3	60.43

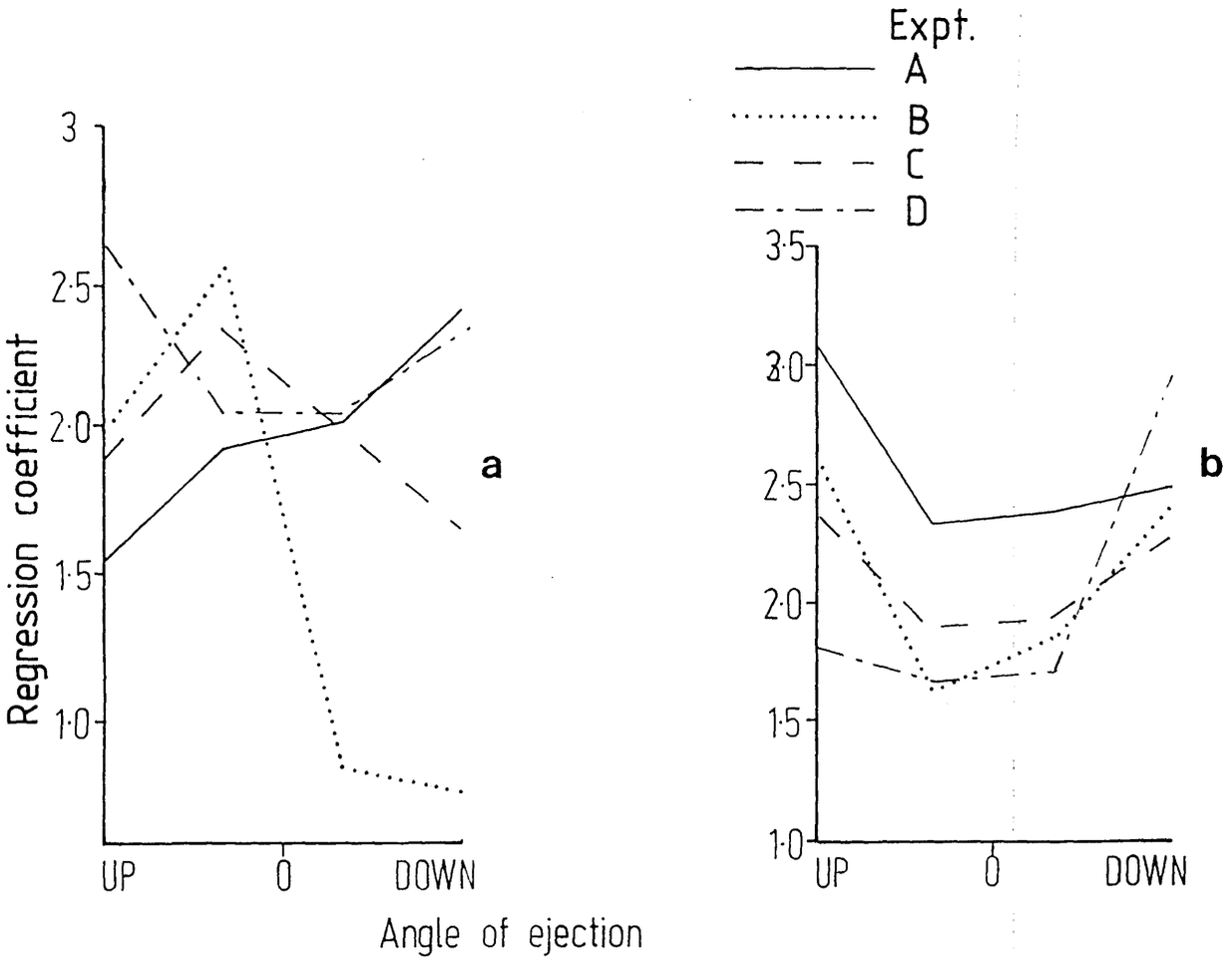


Fig 5.23. Effect of angle of ejection on the regression coefficients of the distributions of the square root of droplet velocity.

TABLE 5.9

Regression coefficients for the frequency distributions of the logarithm of initial droplet velocity seperated by angles of droplet ejection.

Expt		Angle of ejection (degrees)			
		Up 90-45	45-0	0-45	Down 45-90
34 mg	a	1.57	1.91	2.05	2.39
2.8 m	b	3.09	2.33	2.37	2.49
Barley	χ^2	0.73	1.69	0.47	0.58
34 mg	a	1.99	2.54	0.85	0.79
2.8 m	b	2.63	1.64	1.86	2.43
Bean	χ^2	5.74	0.71	1.28	1.75
34 mg	a	1.90	2.32	1.98	1.69
5.1 m	b	2.39	1.80	1.82	2.29
Bean	χ^2	1.83	0.65	0.66	0.51
7.6 mg	a	2.60	2.06	2.06	2.37
2.8 m	b	1.82	1.69	1.72	2.98
Bean	χ^2	0.37	0.22	1.34	0.29

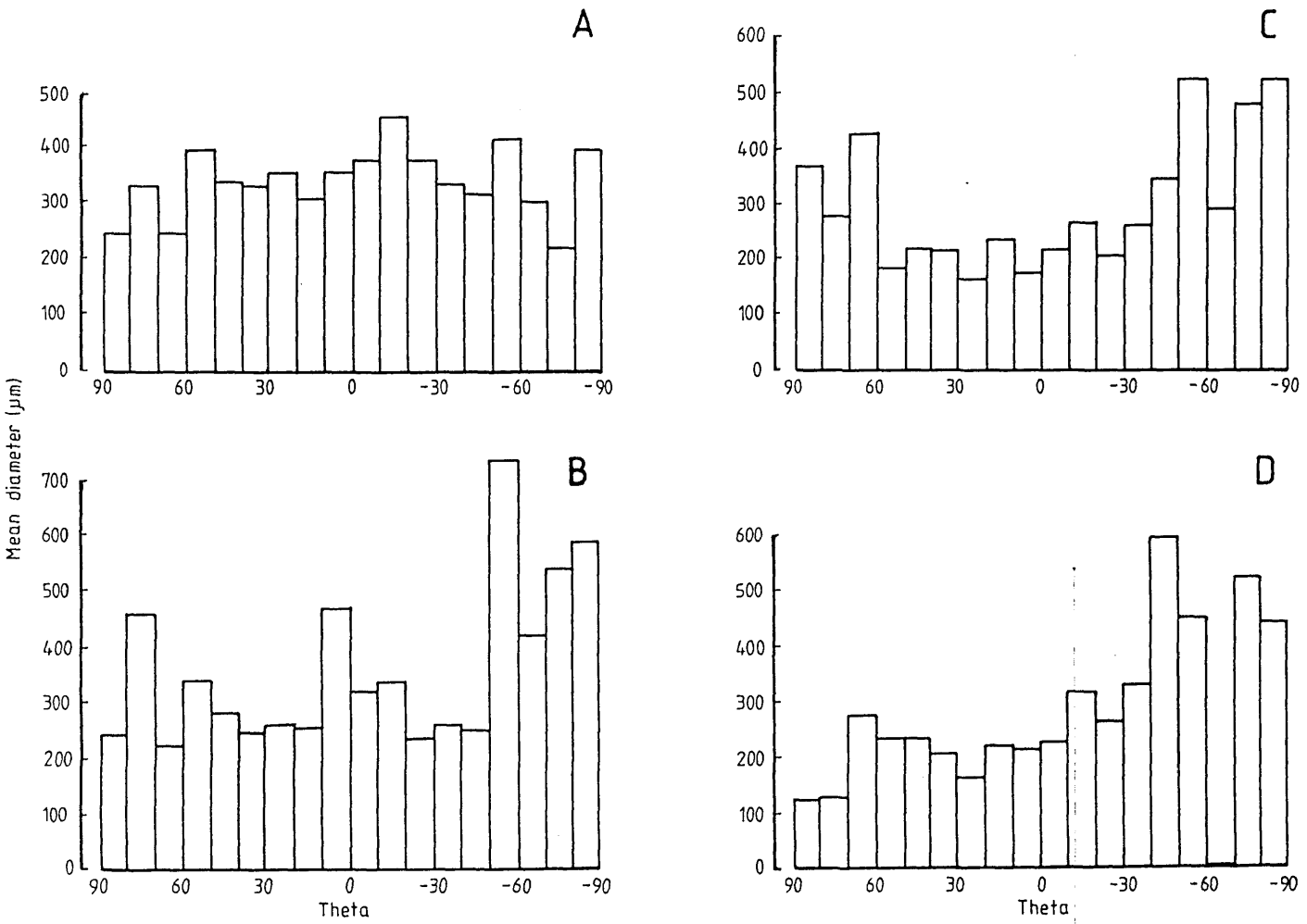


Fig 5.24. Mean diameter of droplets ejected at different angles.

A) Barley/34 mg/2.8 m
B) Bean/34 mg/2.8 m
C) Bean/34 mg/5.1 m
D) Bean/7.6 mg/2.8 m

the probability plots show a consistent pattern of changes in the value of the coefficient b, the slope of the line, with angle of ejection. These patterns were only apparent in about half of the cases for the logarithmic transformation. However in all cases where the logarithmic transformations did not show the same trend as the square root transformations there was a less good fit to a normal distribution shown by the logarithms of the velocity.

Regression lines calculated for the log probability plots tended to consistently over estimate the speed of both the fastest and slowest moving drops. The regression lines for the square root probability plots appear to more accurately match the speed of the faster droplets, but under estimate the speed of the slower ones. In some cases where the distribution of the square root of the velocity was seperated by initial angle of ejection then the speed of the faster droplets was also under estimated.

In general it is suggested that the square root transformation gives the better fit to a normal distribution and is the most useful for describing droplet velocities.

5.5.3 *Size and angle of ejection*

Figures 5.6a-d show the relationship between the angle of droplet ejection, θ, and droplet size, the mean droplet diameter is plotted for each 10^{o} arc in Fig. 5.24. Droplets produced by splashes on barley plants show little relationship between the two parameters. There was no statistically significant difference between any two ranges of θ, although larger droplets did appear to be ejected at angles closer to the horizontal. In the cases of splashes on bean leaves however there were significant differences in the sizes of droplets ejected at different angles. Droplets ejected downwards at angles within 45^{o} of the vertical were significantly larger than were

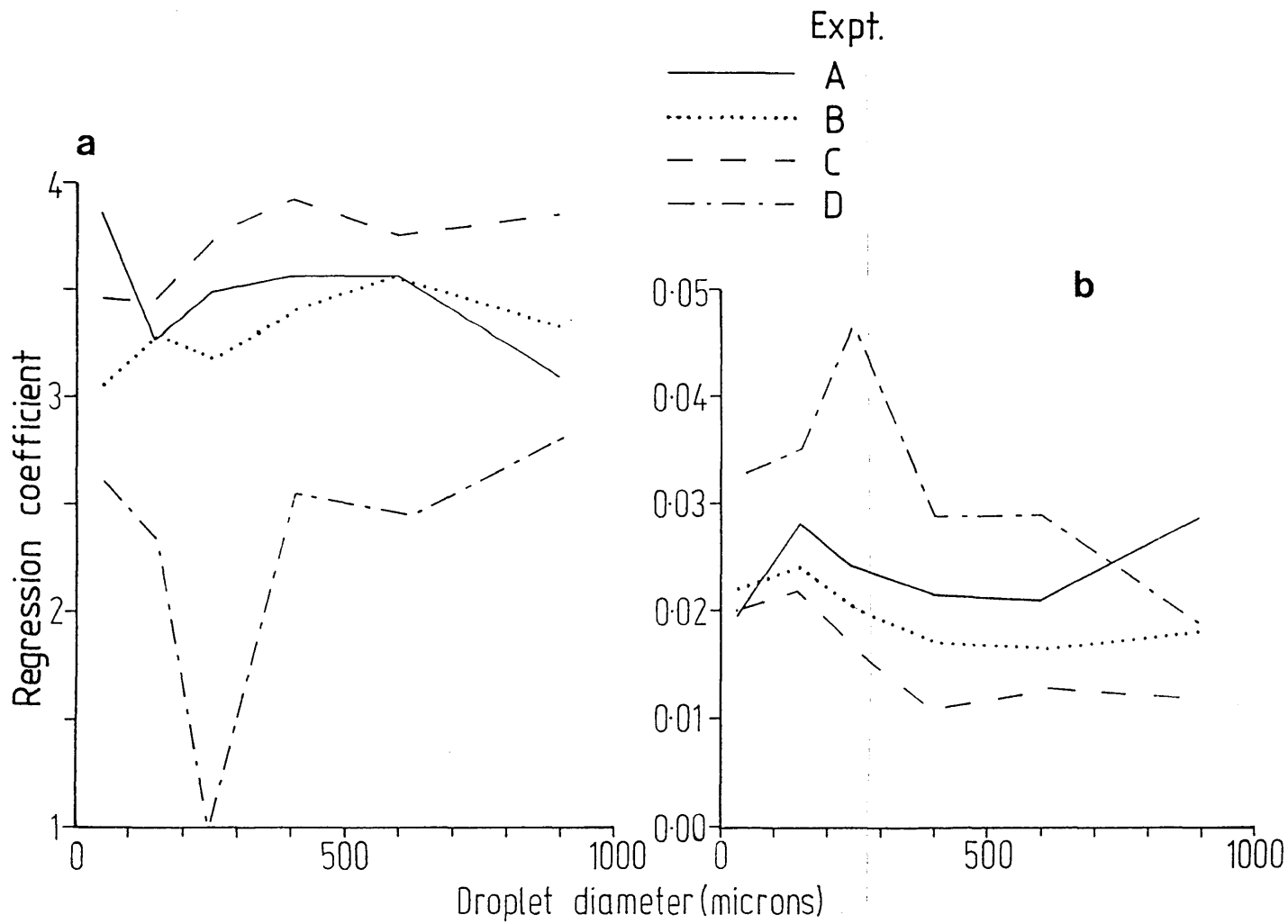


Fig 5.25. Regression coefficients of angle of ejection frequency for different droplet diameters.

TABLE 5.10

Regression coefficients for the frequency distributions of the angles of initial droplet ejection by droplet size.

Expt		Droplet diameter (μm)					
		0-100	100-200	200-300	300-500	500-750	>750
34 mg	a	3.87	3.25	3.49	3.56	3.56	3.08
2.8 m	b	0.0194	0.0279	0.0242	0.0216	0.0210	0.0289
Barley	χ^2	3.80	6.93	3.16	1.24	0.425	0.68
34 mg	a	3.05	3.28	3.19	3.42	3.54	3.35
2.8 m	b	0.0223	0.0237	0.0201	0.0170	0.0162	0.0178
Bean	χ^2	1.59	0.41	0.47	0.45	0.48	0.68
34 mg	a	3.47	3.28	3.19	3.42	3.54	3.85
5.1 m	b	0.0199	0.0216	0.0201	0.0170	0.0162	0.0178
Bean	χ^2	0.695	0.690	0.068	3.33	1.623	2.09
7.6 mg	a	2.60	2.37	1.00	2.58	2.45	3.31
2.8 m	b	0.0332	0.0355	0.0480	0.0293	0.0294	0.0194
Bean	χ^2	0.88	1.17	0.85	0.67	0.72	0.16

those ejected in other directions. This suggests that the impacting drop pushed the leaf aside and some of the liquid was deflected rather than reflected as is the case in a splash on a rigid horizontal surface. This trend was apparent even with small drops impacting on bean leaves (Fig. 5.24d), although the total number of droplets projected at angles significantly below the horizontal was relatively far fewer. Less than 4% of the droplets were ejected more than 30^{o} below the horizontal from the splash of a 7.6 mg drop compared with over 31% for one of a 34 mg drop impacting at only a very slightly greater velocity (Table 5.11a and 5.11d).

There is some indication in the case of the splash of the drops with the highest impact momentum (Fig. 5.6c) that droplets ejected directly upwards may also have been larger than those ejected horizontally, however no significant relationship was found.

The angles of ejection, θ, were separated by size class and the regression lines for cumulative frequency distributions calculated for each set of angles.

The frequency plots all show an increase in the slope of the regression line between the smallest droplets and about 200 μm. After this the slope decreases again, finally stabilising or in the case of splashes on barley plants increasing again at the largest sizes, Fig. 5.25, Table 5.10. The variation in the angle of ejection is therefore least amongst droplets with diameters between 100 and about 200 μm.

An overall description of the relationship between droplet diameter and angle of ejection is not easy to devise. On bean leaves the average size of droplets projected downwards tended to be greater than those ejected in any other direction (Figs 5.24b-d), but beyond this little can be said. Splash on barley leaves gave a somewhat different distribution of droplet sizes with angle of ejection when

	(A) Barley target 34 mg drop fallingfrom 2.8 m			(B) Bean target 34 mg drop falling 2.8m		
	Angle of ejection (degrees)	Percentage of droplets	Mean diameter (microns)	Angle of ejection (degrees)	Percentage of droplets	Mean diameter (microns)
Above horizontal	80–90	8.28	312	80–90	7.20	292
	70–80	7.41	333	70–80	5.14	462
	60–70	8.93	248	60–70	4.88	220
	50–60	5.45	391	50–60	5.40	340
	40–50	11.33	338	40–50	4.37	273
	30–40	12.85	335	30–40	6.17	243
	20–30	8.06	359	20–30	5.66	256
	10–20	7.41	312	10–20	7.20	250
	0–10	9.80	363	0–10	5.40	472
Below horizontal	0–10	3.05	380	0–10	7.71	315
	10–20	3.05	459	10–20	7.71	334
	20–30	0.87	377	20–30	6.94	232
	30–40	3.05	338	30–40	10.28	257
	40–50	1.74	320	40–50	4.63	245
	50–60	1.96	423	50–60	1.29	734
	60–70	2.83	310	60–70	3.60	539
	70–80	2.18	225	70–80	3.08	419
	80–90	1.74	401	80–90	3.34	530

TABLE 5·11

Percentage and mean size of droplets ejected at different angles

	(C) Bean target 34 mg drop falling 5.1 m.			(D) Bean target 7.6 mg drop falling 2.8 m.		
	Angle of ejection (degrees)	Percentage of droplets	Mean diameter (microns)	Angle of ejection (degrees)	Percentage of droplets	Mean diameter (microns)
Above horizontal	80–90	11.00	406	80–90	1.88	157
	70–80	8.13	280	70–80	1.07	122
	60–70	5.98	427	60–70	5.90	271
	50–60	4.78	185	50–60	4.56	228
	40–50	4.07	220	40–50	7.51	228
	30–40	5.26	211	30–40	7.51	204
	20–30	5.02	165	20–30	7.77	157
	10–20	3.59	241	10–20	13.14	215
	0–10	4.55	180	0–10	14.75	208
Below horizontal	0–10	5.26	221	0–10	18.50	220
	10–20	6.46	273	10–20	8.85	313
	20–30	5.02	208	20–30	4.83	254
	30–40	6.22	264	30–40	0.80	327
	40–50	3.59	353	40–50	0.80	588
	50–60	4.31	530	50–60	0.54	446
	60–70	4.07	397	60–70	0.00	-
	70–80	6.70	487	70–80	0.27	515
	80–90	5.98	533	80–90	1.34	435

TABLE 5.11

Percentage and mean size of droplets ejected at different angles

compared with the splash caused by identical drops on bean leaves. Larger droplets were ejected at angles closer to the horizontal rather than downwards. The difference was probably the result of the different shape of the two leaves. Barley leaves have a shallow 'V' shaped cross-section, while bean leaves are essentially flat. Drops striking a horizontal section of a barley leaf produced larger numbers of droplets with trajectories directed at right angles to the leaf axis than along the axis (see Section 6.3). The bean leaves in comparison had little structure that affected the orientation of splash droplet trajectories.

As the impact momentum of drops increases neither the overall mean nor the maximum speed of droplets increases appreciably. However larger droplets had higher velocities from impacts of greater energy and would therefore have been projected further. Also more droplets that were projected upwards had high velocities so that upward dispersal will be increased. The droplet dispersal patterns produced by the different splashes are dealt with in the next chapter.

CHAPTER 6

Dispersal of splash droplets

6.1 Horizontal distribution

An estimate of the likely distances and heights reached by spore carrying droplets produced by a splash on an infected leaf is needed in order to fully understand the importance of splash in plant disease epidemiology. This can be done either by direct measurement or by dispersal modelling. In this chapter the distances travelled by splash droplets measured in the droplet collection experiments (Chapter 4) are compared with similar patterns calculated from the sizes and initial velocities of droplets measured from the photographs (Chapter 5) using the model described in chapter 2. The model was also used to estimate the potential heights reached by the droplets produced by splashes on bean and barley leaves.

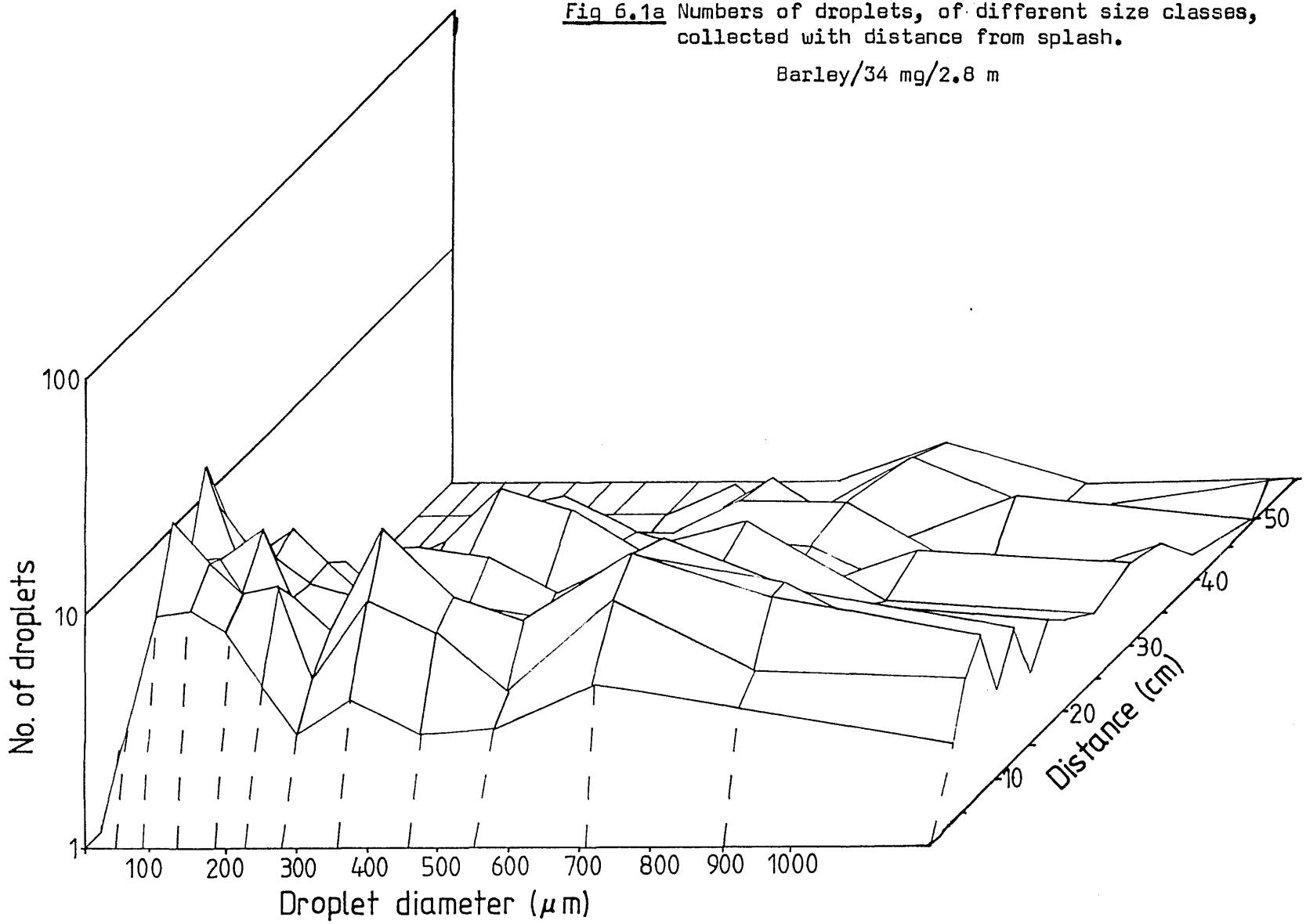
6.1.1 *Measurements*

(a) Numbers of drops per splash

Table 6.1 shows the total number of drops estimated to have been produced by one splash. Figs 6.1a-d show the log. numbers of droplets in each of several size classes collected 10 cm below the leaf, and at various distances from it, in each of the four experiments. Tables 6.2a to 6.2d show numbers of droplets collected and the total number of droplets calculated to have been produced by one splash in each size class and at each distance. The number of droplets estimated to have been produced by one splash was calculated by dividing the numbers collected by the fraction of each radius sampled.

Fig 6.1a Numbers of droplets, of different size classes, collected with distance from splash.

Barley/34 mg/2.8 m



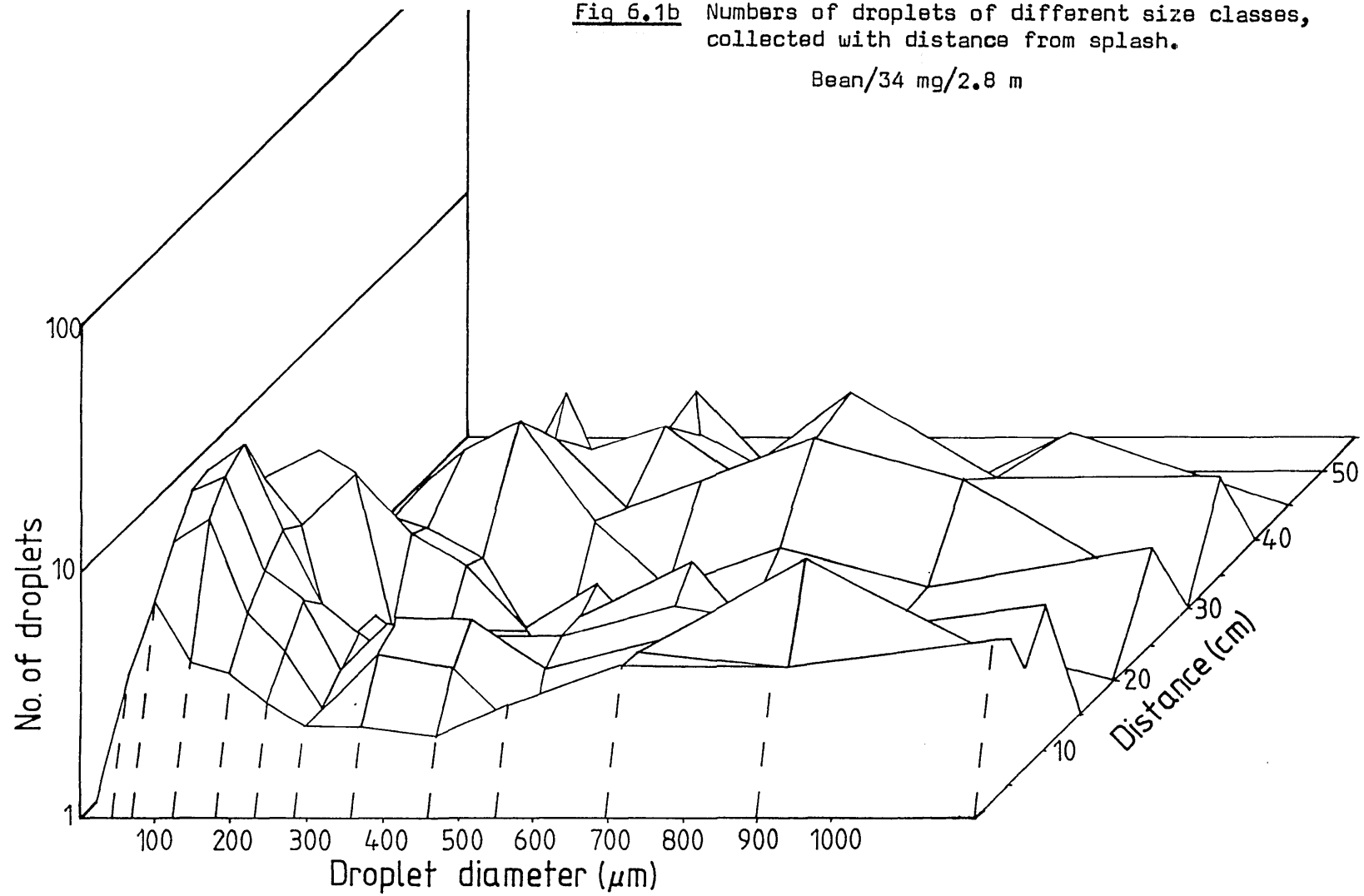


Fig 6.1b Numbers of droplets of different size classes, collected with distance from splash.

Bean/34 mg/2.8 m

Fig 6.1c Numbers of droplets, of different size classes, collected with distance from splash.

Bean/34 mg/5.1 m

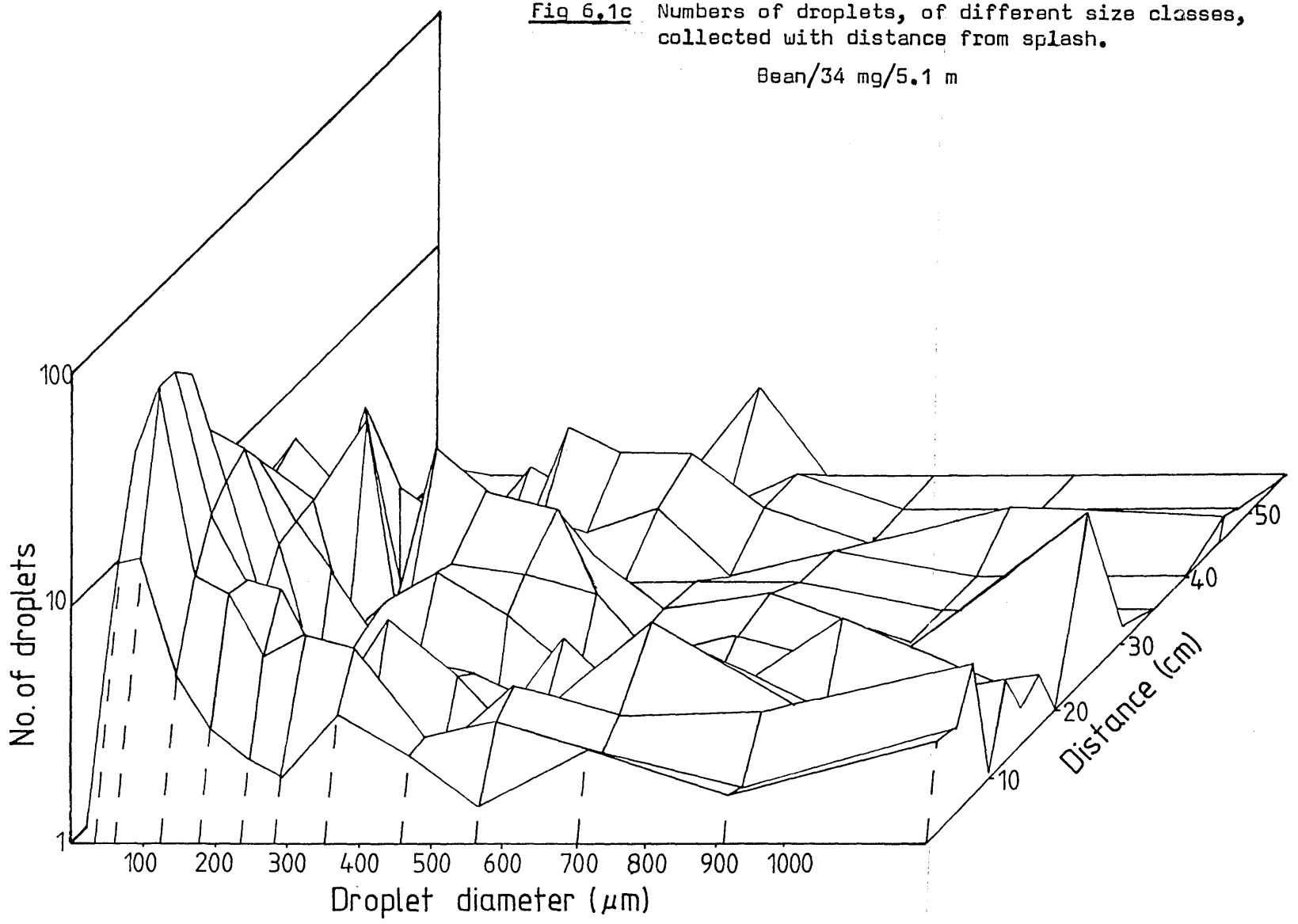


Fig 6.1d Numbers of droplets, of different size classes, collected with distance from splash.

Bean/7.6 mg/2.8 m

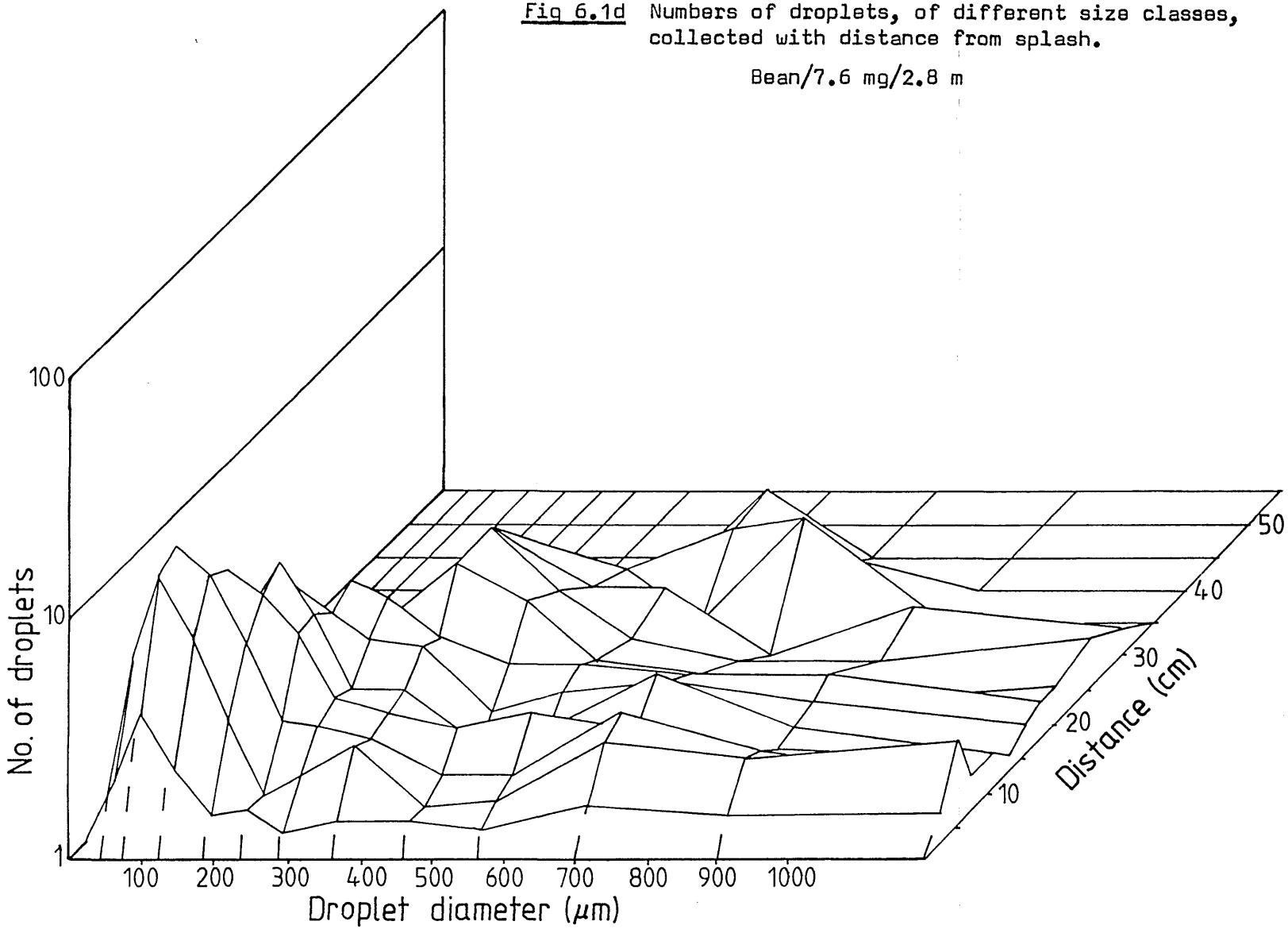


TABLE 6.1

Target	Drop size (mg)	Fall height (m)	Number of droplets/splash
Barley	34	2.8	506
Bean	34	2.8	342
Bean	34	5.1	755
Bean	7.6	2.8	181

The total number of droplets estimated to have been produced by one splash was within the values expected on the basis of those distributions described by previous investigators. More droplets are produced by larger and by faster impacting drops. Gregory *et al.* (1959) showed that a 2 mm drop falling 2.9 m onto a film of water 0.1 mm deep produced only 309 droplets, and even fewer when dropped into deeper water. A larger, 5 mm drop produced over 1000 droplets when falling into a similar film of water from the same height, though only 27 were produced when it fell onto a clean dry surface. Similar results have been obtained by other workers, (Hobbs and Kezweeny, 1967; Ghadiri-Khoorzoojhi, 1978). The splash of drops on bean leaves produced fewer splash droplets than does the splash of identical drops on barley leaves.

(b) Distances splashed

Table 6.3 shows the mean diameter of droplets collected at each of the sampling distances and Table 6.4 the mean distance travelled by droplets in each size class.

Figure 6.2 shows the changes in mean droplet diameter with distance from the splash. There is a steady, and for the main part, almost linear, increase in mean size with distance. However, there is a noticeable increase in mean droplet diameter very close to the leaf. Very small droplets were deposited close to the target, for all four experiments 90% of droplets less than 100 μm were deposited

TABLE 6.2(a)

Target = Barley
Drop size = 34 mg
Fall height = 2.8 m

Distance from splash (cm)	Droplet diameter (microns)											
	≤50	50-100	100-150	150-200	200-250	250-300	300-400	400-500	500-600	600-800	800-1000	>1000
0-2.5	2.15 17	7.24 57	7.74 61	6.09 48	3.17 25	1.52 12	2.54 20	1.52 12	1.65 13	3.17 25	2.28 18	1.27 10
2.5-5.0	3.81 10	17.14 45	11.04 29	7.62 20	8.76 23	2.67 7	7.24 19	4.95 13	2.28 6	7.24 19	3.05 8	2.67 7
5.0-7.5	7.03 15	9.37 20	9.37 20	12.65 27	6.09 13	4.22 9	13.12 28	6.09 13	4.69 10	9.84 21	6.09 13	3.75 8
7.5-10	4.59 7	21.00 32	7.22 11	7.87 12	5.91 9	5.25 8	7.22 11	4.59 7	3.94 6	7.87 12	5.91 9	1.31 2
10-12.5	0.39 1	11.42 29	6.70 17	9.06 23	6.30 16	4.33 11	7.48 19	6.70 7	4.33 11	8.27 21	4.33 11	2.76 7
12.5-15	0.13 1	2.42 18	3.09 23	4.16 31	5.37 40	3.62 27	3.09 23	2.28 17	1.75 13	4.43 33	2.28 17	1.07 8
15-17.5	0.16 1	1.59 10	1.75 11	3.97 25	3.17 20	2.86 18	3.17 20	3.17 20	3.17 20	4.13 26	2.54 16	1.90 12
17.5-20		0.73 4	0.73 4	1.83 10	3.30 18	2.56 14	3.48 19	1.83 10	1.83 10	2.75 15	1.83 10	1.46 8
20-25		0.59 2		0.89 3	2.36 8	2.95 10	5.61 19	4.43 15	2.66 9	3.84 13	1.18 4	0.89 3
25-30		0.32 1	0.32 1			2.23 7	3.19 10	1.59 5	0.64 2	0.64 2	1.59 5	1.27 4
30-35			0.32 1	0.32 1			2.24 7	1.28 4	0.96 3	0.96 3		0.96 3
35-40							0.59 2	0.59 2	1.18 4	1.18 4		0.30 1
40-45								0.33 1	1.00 3		0.67 2	0.33 1
45-50								0.37 1		0.75 2		0.37 1
55-60										0.48 1		

Top number is number of droplets calculated to be collected at each distance by one splash
Lower number is actual number of droplets collected.

TABLE 6.2(b)

Target = Bean
Drop size = 34 mg
Fall height = 2.8 m

Distance from splash (cm)	Droplet diameter (microns)											
	≤50	50-100	100-150	150-200	200-250	250-300	300-400	400-500	500-600	600-800	800-1000	≥1000
0-2.5	2.31 14	5.60 34	2.63 16	2.31 14	1.48 9	0.99 6	0.99 6	0.82 5	1.48 9	2.63 16	2.47 15	3.62 22
2.5-5.0	2.96 6	8.40 17	10.87 22	3.95 8	2.47 5	0.99 2	2.47 5	1.98 4	0.49 1	2.47 5	1.98 4	2.96 6
5.0-7.5	2.99 4	11.98 16	14.22 19	5.24 7	3.74 5	1.50 2	2.99 4	2.99 4	1.50 2	2.25 3	5.99 8	1.50 2
7.5-10	2.88 3	12.49 13	16.33 17	6.72 7	2.88 3	1.92 2	0.96 1	1.92 2	1,92 2	2.88 3	1.92 2	2.88 3
10-12.5	1.98 2	3.95 4	9.88 10	5.93 6	0.99 1	1.98 2	0.99 1		1.98 2	3.95 4		0.99 1
12.5-15		4.83 4	6.04 5	10.87 9	8.45 7	1.21 1	1.21 1	1.21 1	2.42 2			
15-17.5	0.30 1	0.30 1	0.61 2	4.25 14	3.03 10	3.64 12	2.43 8	0.61 2	0.30 1		0.30 1	
17.5-20				1.40 4	3.50 10	3.15 9	2.10 6		0.35 1	0.70 2	0.70 2	
20-25		0.73 1			3.66 5	5.12 7	7.31 10	2.19 3	0.73 1	1.46 2	0.73 1	1.46 2
25-30			1.62 2			0.81 1	4.06 5	1.62 2	2.44 3	4.06 5	2.44 3	
30-35							2.26 3	3.02 4	1.51 2	4.53 6	1.51 2	1.51 2
35-40							0.87 1	1.74 2	0.87 1	1.74 2		
40-45											0.99 1	
45-50				1.10 1			1.10 1					
50-55												

Top number is number of droplets calculated to be collected at each distance by one splash
Lower number is actual number of droplets collected.

TABLE 6.2(c)

Target = Bean
Drop size = 34 mg
Fall height = 5.1 m

Distance from splash (cm)	Droplet diameter (microns)											
	<50	50-100	100-150	150-200	200-250	250-300	300-400	400-500	500-600	600-800	800-1000	>1000
0-2.5	12.26	12.90	3.33	1.54	0.93	0.58	1.97	0.96	0.20	1.07	0.34	1.24
	110	170	34	11	7	5	11	7	4	5	3	9
2.5-5	31.98	61.77	8.82	7.30	3.45	4.57	3.83	0.98	1.36	0.69	0.22	1.15
	113	177	24	18	7	9	7	4	4	3	1	3
5-7.5	37.41	61.88	14.35	7.06	6.46	2.75	1.53	0.48	1.87	1.10	1.19	2.51
	138	193	45	20	17	12	5	3	5	5	4	6
7.5-10	39.90	50.00	16.41	4.42	3.66	1.05	3.70	1.65	0.24	0.35	0.20	
	129	132	42	13	8	3	10	5	1	1	1	
10-12.5	21.88	24.24	20.09	7.34	1.25	1.82	1,75	1,32	0,63	2.87	0.68	1.13
	57	60	51	19	3	6	4	3	2	5	1	2
12.5-15	8.75	13.23	15.12	7.71	4.40	2.11	1.64		1.84			0.35
	20	41	41	23	15	5	4		3			1
15-17.5	7.30	8.22	10.89	8.03	1.35	2.41	3.59	2.07	0.63	1.27	0.14	0.66
	13	22	33	23	3	5	6	6	3	4	1	2
17.5-20	4.91	6.78	13.32	8.60	15.95	1.05	3.25	2.89	2.18		1.47	
	11	15	18	13	15	3	5	6	3		2	
20-25	7.87	0.31	1.97	13.45	1.35	8.43	5.03	4.13	0.14	0.50		3.96
	7	3	17	37	12	9	10	5	1	3		3
25-30	1.00	0.60	0.60	3.56	2.48	1.20	1.24	1.40	0.40	0.64		0.20
	5	3	3	13	10	6	5	7	2	2		1
30-35		1.61		2.23	1.27	1.60	1.28	0.31	0.32	0.31		
		5		7	4	5	4	1	1	1		
35-40	0.27	1.64		0.41	0.27	0.55	0.55	0.95		0.27		
	1	6		1	1	2	2	3		1		
40-45		0.29			0.29	2.10	1.40	1.40	0.41		0.41	0.29
		1			1	6	4	4	1		1	1
45-50		0.41		0.42	0.26		0.26		0.41			
		1		2	1		1		1			
50-55					0.27	0.27		1.42				
					1	1		3				

Top number is number of droplets calculated to be collected at each distance by one splash
Lower number is actual number of droplets collected.

TABLE 6.2(d)

Target = Bean
Drop size = 7.6 mg
Fall height = 2.8 m

Distance from splash (cm)	Droplet diameter (microns)											
	<50	50-100	100-150	150-200	200-250	250-300	300-400	400-500	500-600	600-800	800-1000	>1000
0-2.5	0.81 30	2.45 91	0.94 35	0.27 10	0.35 13	0.08 3	0.22 8	0.22 8	0.11 4	0.40 15	0.27 10	0.30 11
2.5-5	3.72 46	10.50 130	4.77 59	1.70 21	0.32 4	0.57 7	1.13 14	0.16 2	0.24 3	1.21 15	0.89 11	1.21 15
5-7.5	1.96 17	12.12 105	8.54 74	3.92 34	1.27 11	1.15 10	0.92 8	0.35 3	0.35 3	1.50 13	0.69 6	0.35 3
7.5-10	1.13 5	5.66 35	7.76 48	5.82 36	3.56 22	1.45 9	1.13 7	0.81 5	1.13 7	0.81 5	0.48 3	0.32 2
10-12.5	0.18 1	1.09 6	3.09 17	6.91 38	3.64 20	1.27 7	1.27 7	0.36 2	0.55 3	1.64 9	0.55 3	0.18 1
12.5-15	0.18 1	0.71 4	0.53 3	4.27 24	3.02 17	2.13 12	1.96 11	0.53 3	0.89 5	1.07 6	0.71 4	0.36 2
15-17.5				1.54 7	3.74 17	3.08 14	1.76 8	1.10 5	1.10 5	0.88 4	0.88 4	0.44 2
17.5-20					2.12 10	2.12 10	3.81 18	2.33 11	0.85 4	0.63 3	0.21 1	0.42 2
20-25			0.33 1	0.33 1	0.33 1	1.63 5	3.92 12	1.63 5	0.65 2	0.33 1	0.33 1	0.65 2
25-30							1.91 6	0.96 3	0.96 3		0.64 2	0.32 1
30-35							1.09 3	0.73 2		1.82 5		
35-40								0.42 1	0.84 2	0.42 1		
40-45									0.89 2			
45-50												
50-55												

Top number is number of droplets calculated to be collected at each distance by one splash
Lower number is actual number of droplets collected.

Mean diameter of droplets collected at each distance (μm).

TABLE 6.3

Distance from target (cm)	Barley 34 mg 2.8 m	Bean 34 mg 2.8 m	Bean 34 mg 5.1 m	Bean 7.6 mg 2.8 m
0 - 2.5	302	448	181	248
2.5 - 5	308	312	121	218
5 - 7.5	369	301	137	184
7.5 - 10	316	274	97	214
10 - 12.5	377	274	155	271
12.5 - 15	389	208	150	328
15 - 17.5	457	260	198	386
17.5 - 20	467	332	210	404
20 - 25	467	421	338	433
25 - 30	542	525	279	539
30 - 35	554	663	249	545
35 - 40	607	533	250	562
40 - 45	741	900	432	550
45 - 50	786	263	267	-
50 - 55	700	-	394	-

TABLE 6.4

Mean distance (cm) travelled by droplets of different sizes

Size (um)	Barley 34 mg 2.8 m	Bean 34 mg 2.8 m	Bean 34 mg 5.1 m	Bean 7.6 mg 2.8 m
0-50	60	63	87	52
51-100	70	74	80	58
101-150	73	84	114	73
151-200	87	113	153	101
201-250	99	127	154	126
251-300	126	153	181	143
301-400	123	195	162	177
401-500	134	181	219	193
501-600	143	164	154	205
601-800	121	175	128	152
801-1000	113	135	140	126
>1000	138	96	137	122

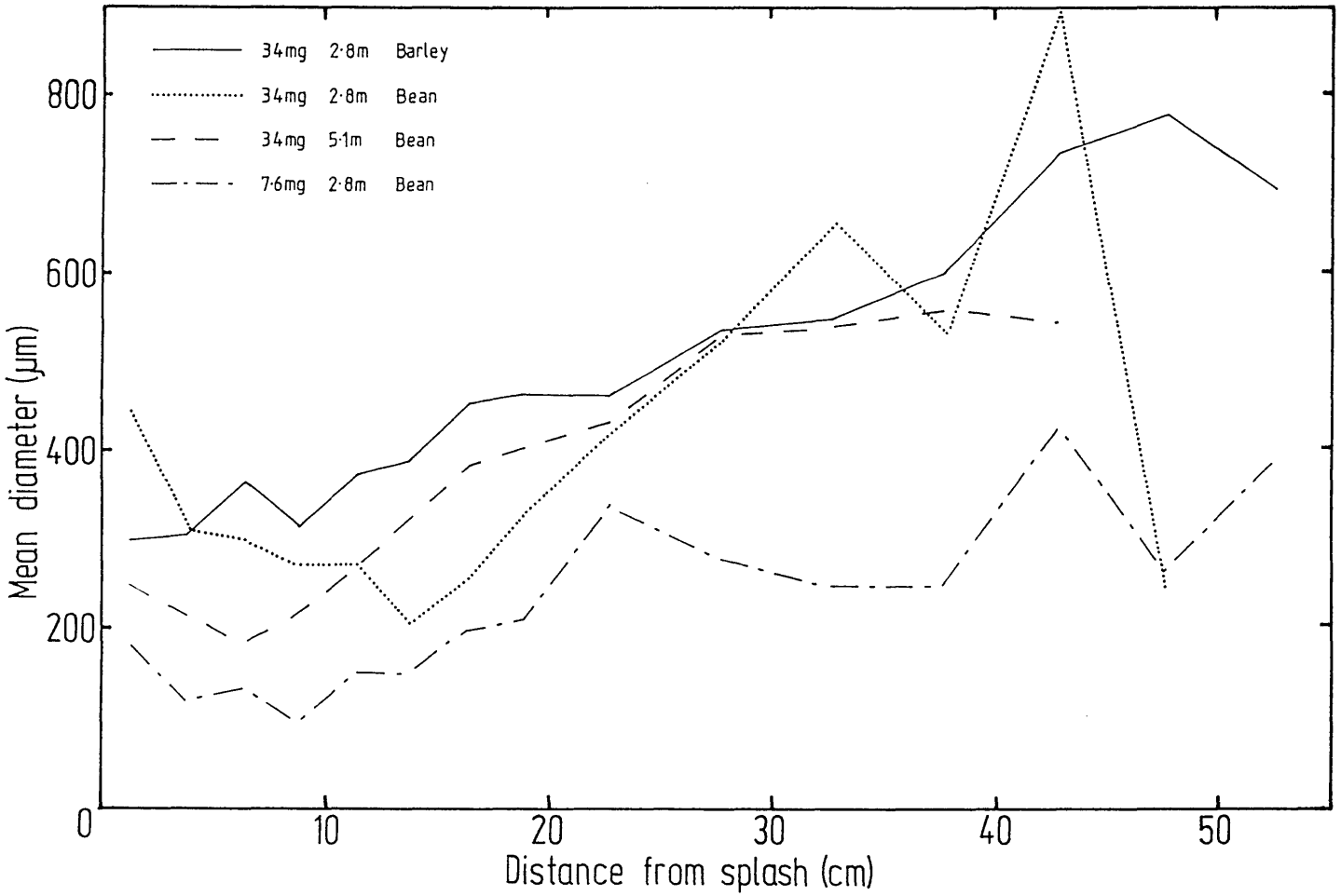


Fig 6.2 Variation in mean droplet size with distance from splash.

within 100 mm of the splash. Similarly the majority of very large droplets, those over 1000 µm, were also deposited within the first 100 mm. In the case of the small droplets this is because they lose their initial velocity very quickly, in the case of the larger droplets it was because their velocities were relatively low to start with.

For droplets with diameters less than about 500 µm those produced by the splash of larger and faster drops tended to travel further. This trend was less clear for droplets larger than 500 µm, this was possibly because of the small sample size, relatively small numbers of droplets >500 µm having been collected. Droplets from splashes on barley leaves travelled a shorter distance than did those from bean leaves. This agrees with the photographic results which show that the initial velocity of droplets from splash on barley leaves was less than those from bean leaves, with the likely result that droplets will travel less distance. This is discussed in more detail in Chapter 5.

6.1.2 *Calculated horizontal distances*

The distances that droplets travelled away from the leaf before falling onto a surface 100 mm below the point of impact were calculated from the measurements made from the photographs of droplet diameters and initial velocities. This gave a droplet dispersal pattern equivalent to that observed in the collection experiments, thus allowing the two sets of data to be compared both with each other and with previous splash dispersion studies.

The estimated and observed distribution of droplet numbers with distance is compared in Figs 6.3a-d, the estimated and observed distributions of splash volume in Figs 6.4a-d. In all four cases the observed dispersal pattern shows a smaller proportion of droplets



Fig 6.3(a)

Difference in the percentage number of droplets collected and the calculated number of droplets deposited with distance from splash.

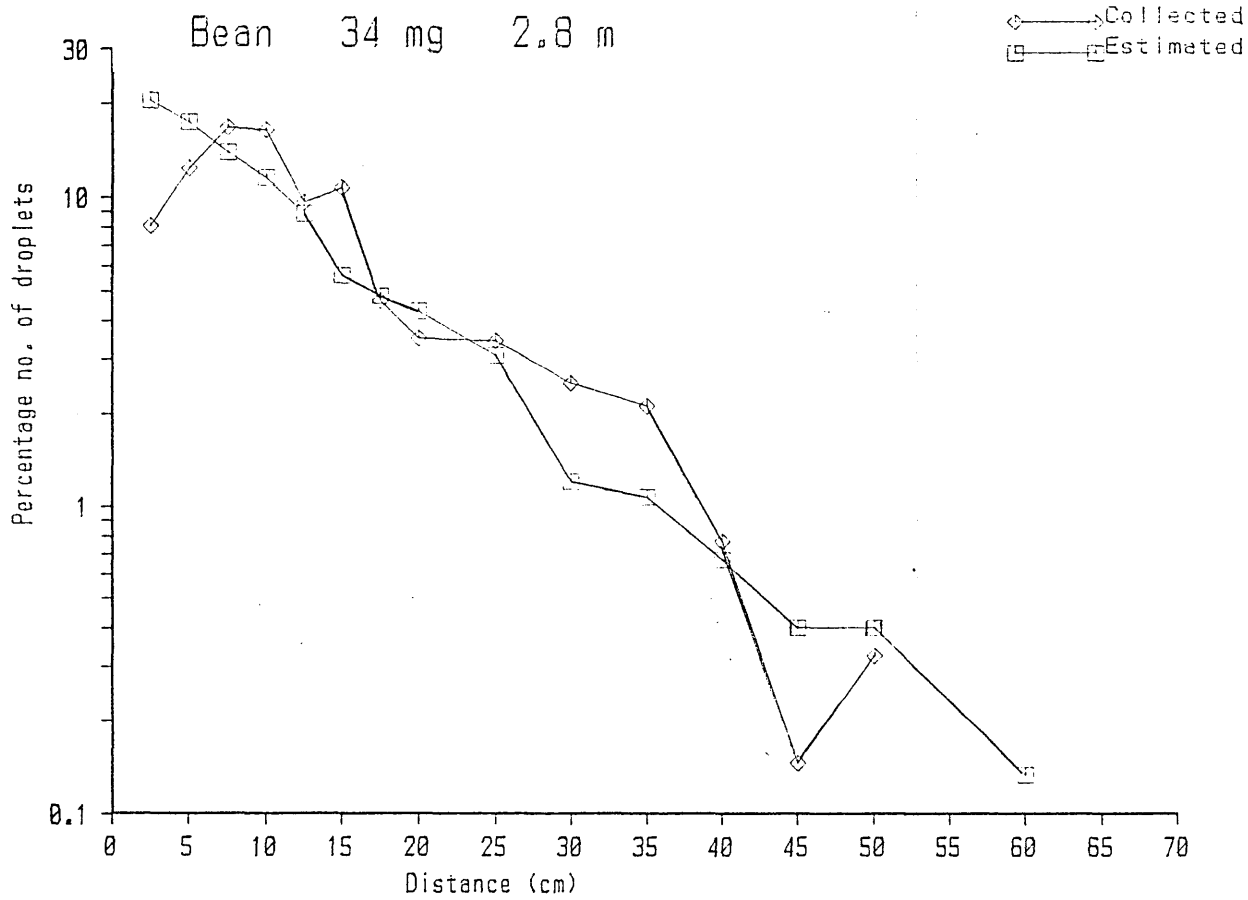


Fig 6.3(b)

Difference in the percentage number of droplets collected and the calculated number of droplets deposited with distance from splash.

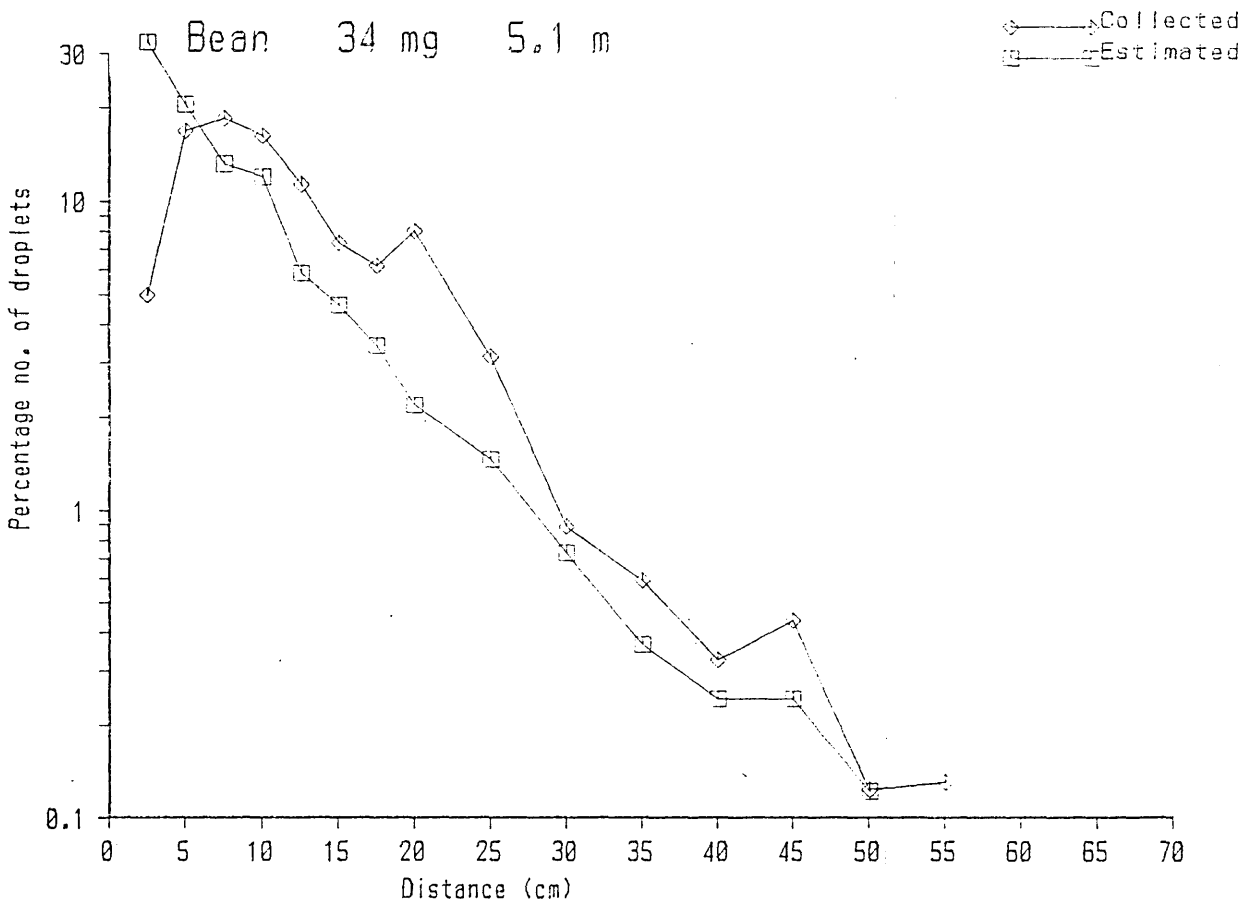


Fig 6.3(c)

Difference in the percentage number of droplets collected and the calculated number of droplets deposited with distance from splash.

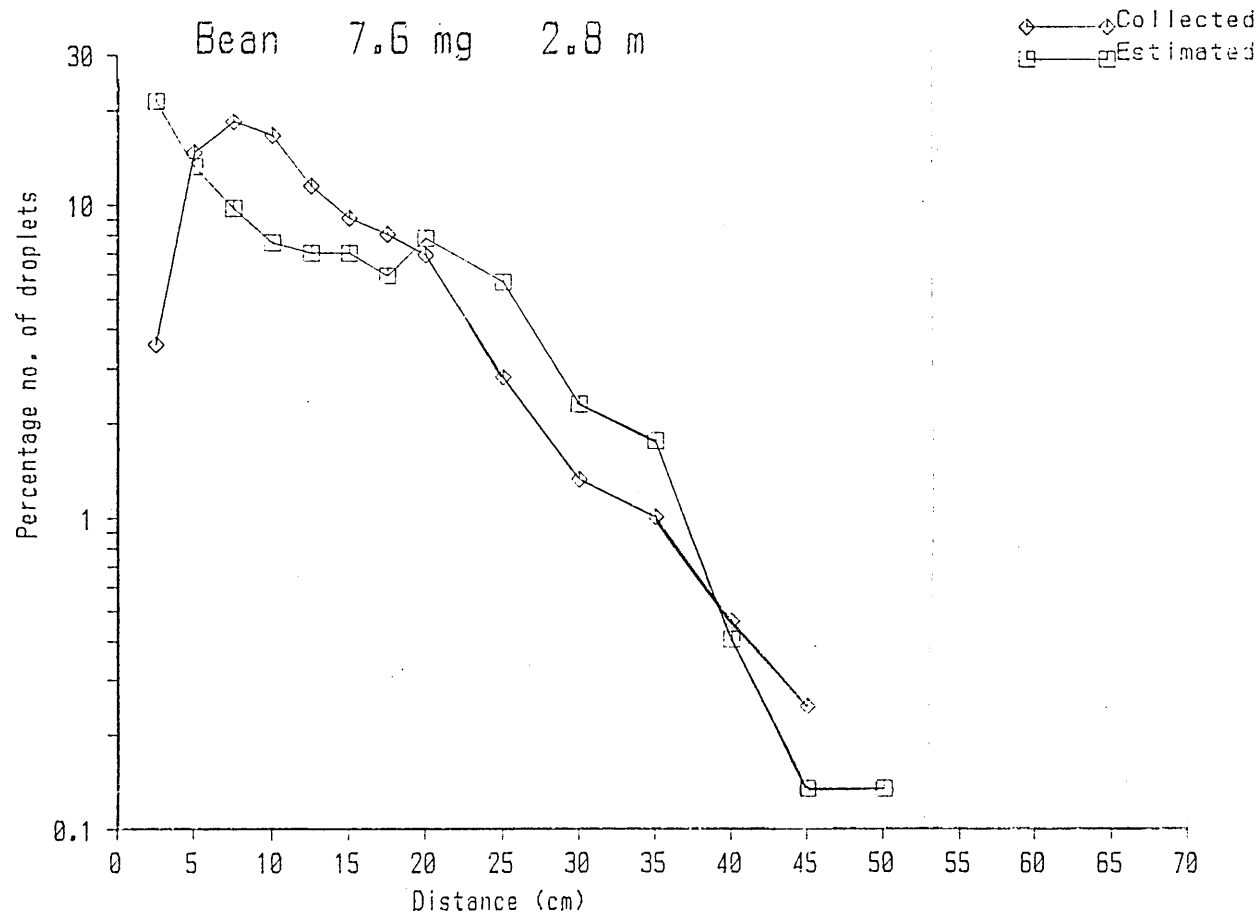


Fig 6.3(d)

Difference in the percentage number of droplets collected and the calculated number of droplets deposited with distance from the splash.

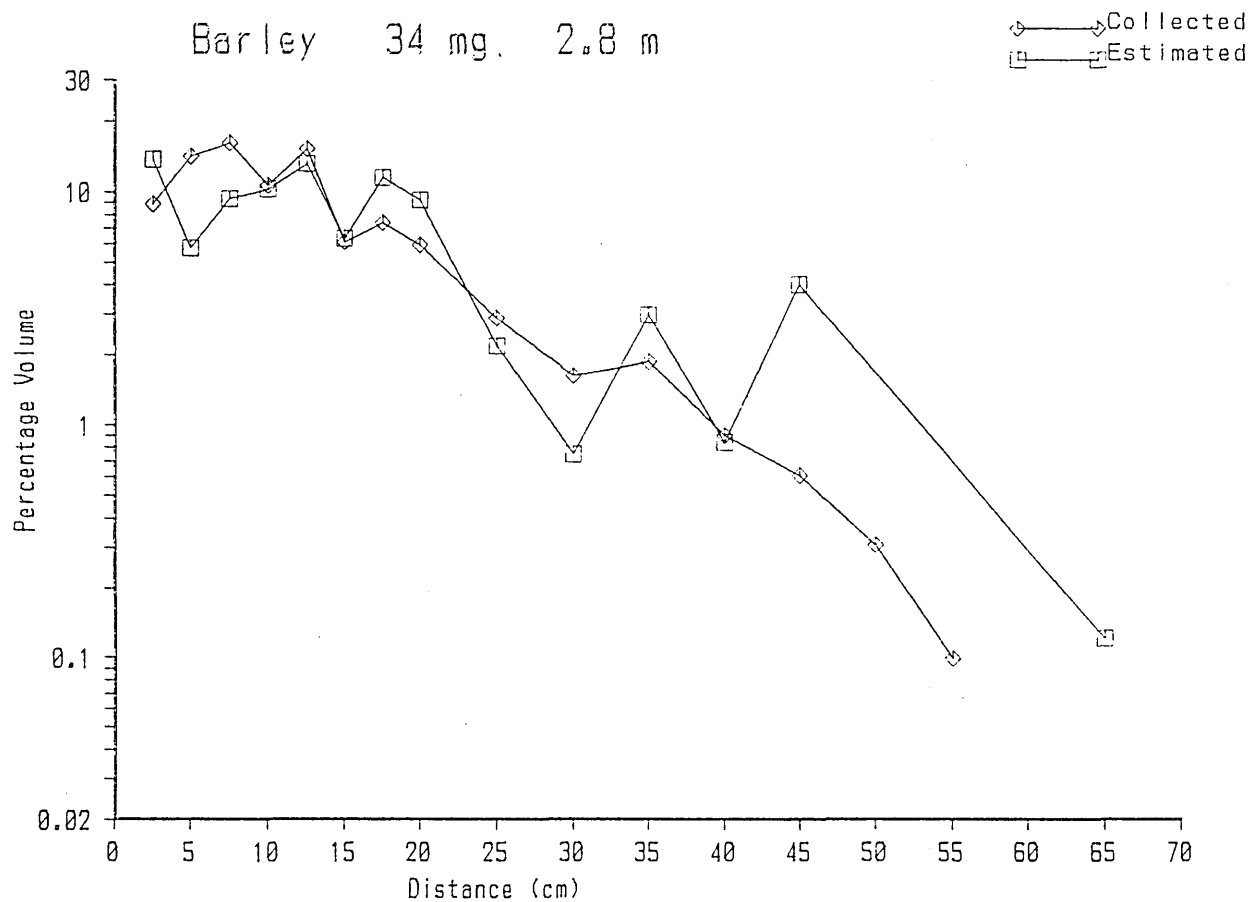


Fig 6.4(a)

Difference between the volume of splash droplets collected and the volume calculated to have been deposited with distance from splash.

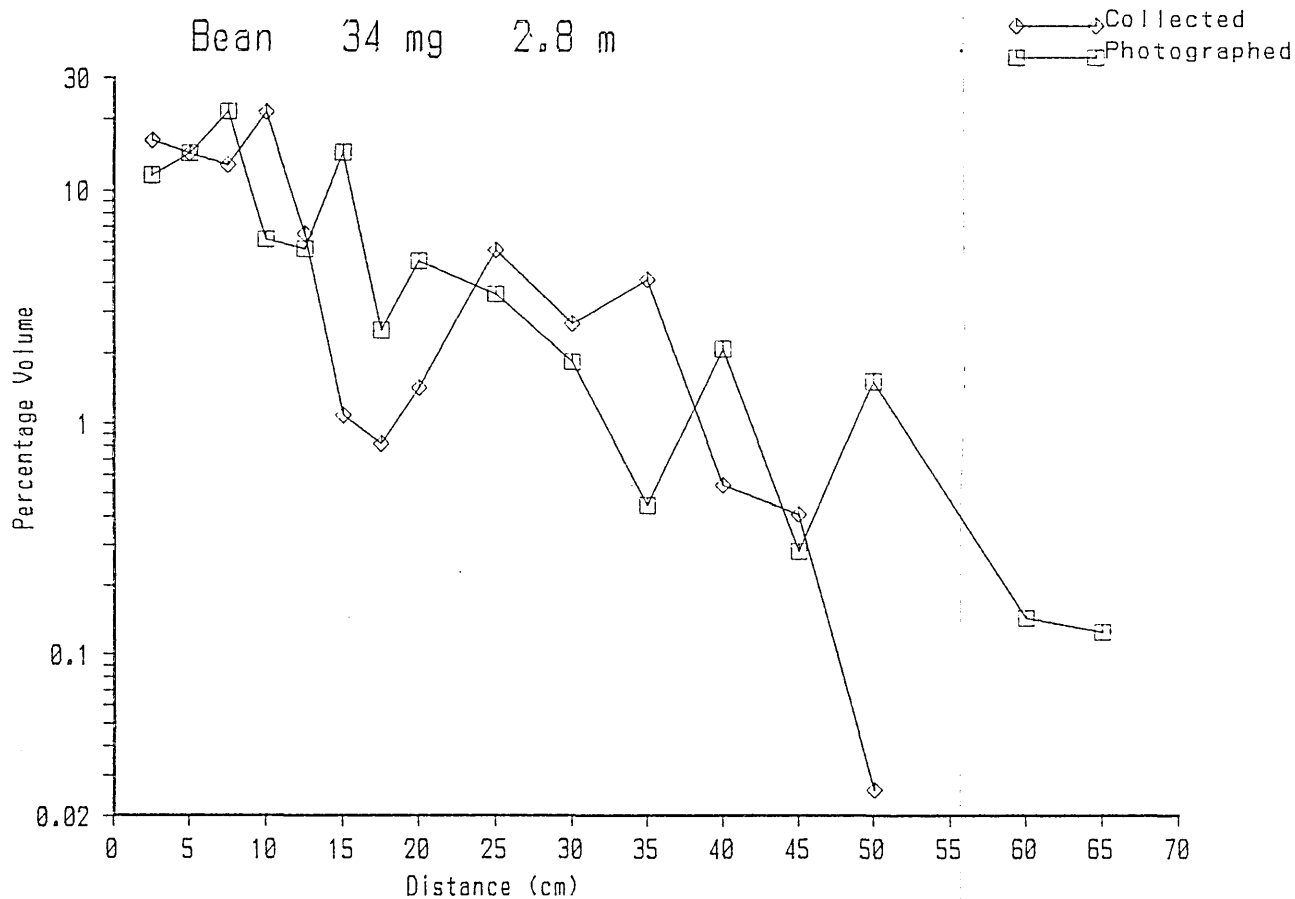


Fig 6.4(b)

Difference between the volume of droplets collected and the volume calculated to be deposited with distance from splash.



Fig 6.4(c)

Difference between the volume of splash droplets collected and the volume calculated to have been deposited with distance from splash.

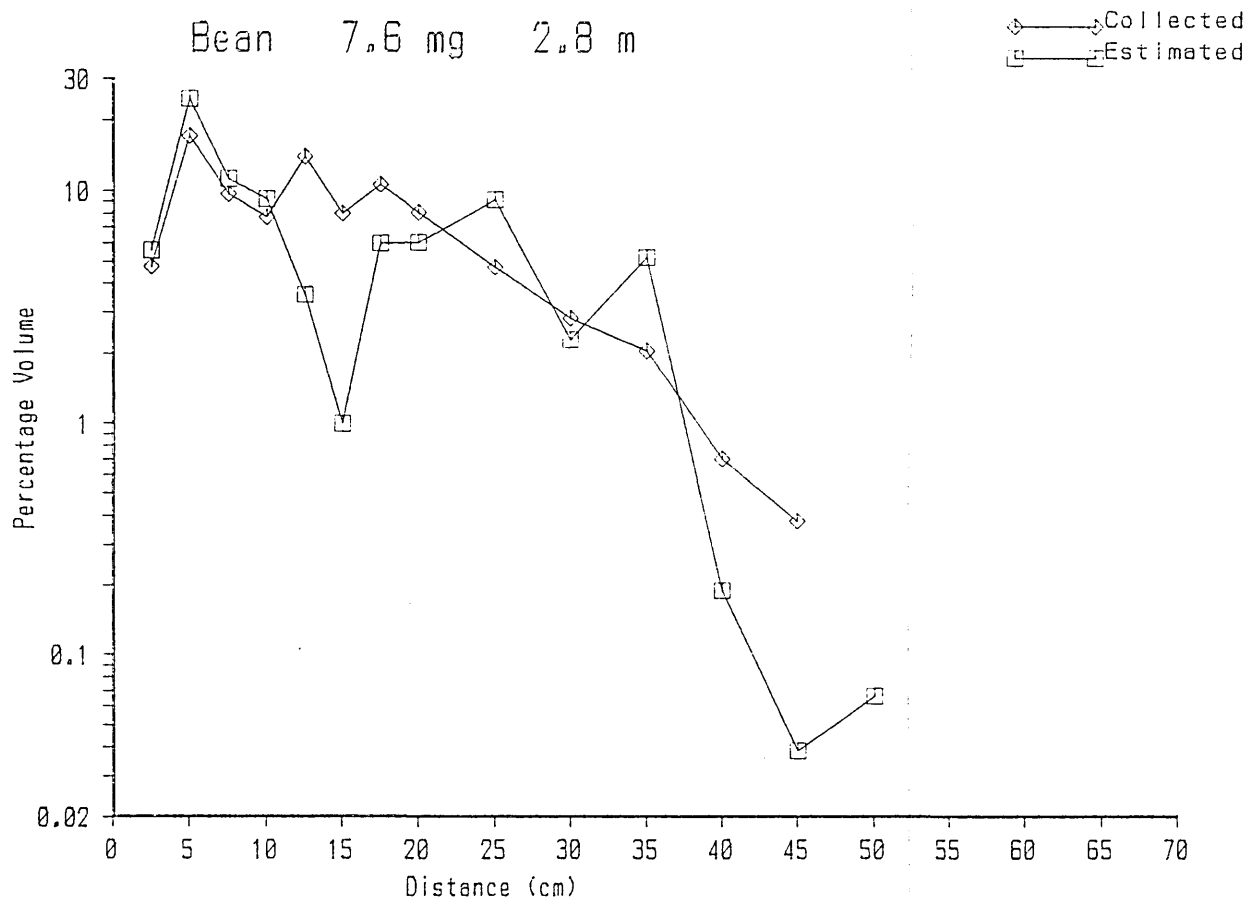


Fig 6.4(d)

Difference between the volume of splash droplets collected and the volume calculated to have been deposited with distance from splash.

close to the splash than does the dispersal pattern calculated on the basis of observed initial droplet velocities. However this is not neccessarily an important difference. The distributions of volume do not show the same trend and indicate that the difference between the two distributions of droplet number are the result of a smaller proportion of small droplets being detected on the collecting surfaces close to the source. Plotting the mean distances travelled by droplets in different size classes, both observed (Fig. 6.5) and estimated (Fig. 6.6) confirms this. The average distance travelled by droplets with diameters of less than 200 μm appears to be considerably greater in the collection experiments.

The samples taken closest to the splash are those most subject to error. As discussed in Section 4.2 the sampling film may become flooded because of too many droplets falling onto it. This would have the effect of reducing the apparent number of droplets present as some craters would be covered by others, the smaller a crater the more likely it is to have been totally obscured. Also the extrapolation of photographed trajectories did not take into account two other factors that may affect the estimated dispersal pattern. First, there is the possibility that the target leaf may have shielded the nearest section of sampling surface and that, therefore, those droplets which only travelled a very short distance may have been re-deposited onto the leaf rather than on to the sampling film. Second, the calculated trajectories used to determine the estimated distribution were assumed to start from the centre of the splash whereas in reality they started from the top of the splash corona, this was often 10 to 20 mm away from the point of impact, in both the horizontal and vertical planes. This may have resulted in a slight under estimate of the distances travelled by the droplets. Initially the majority of water from an impacting drop flows outwards only

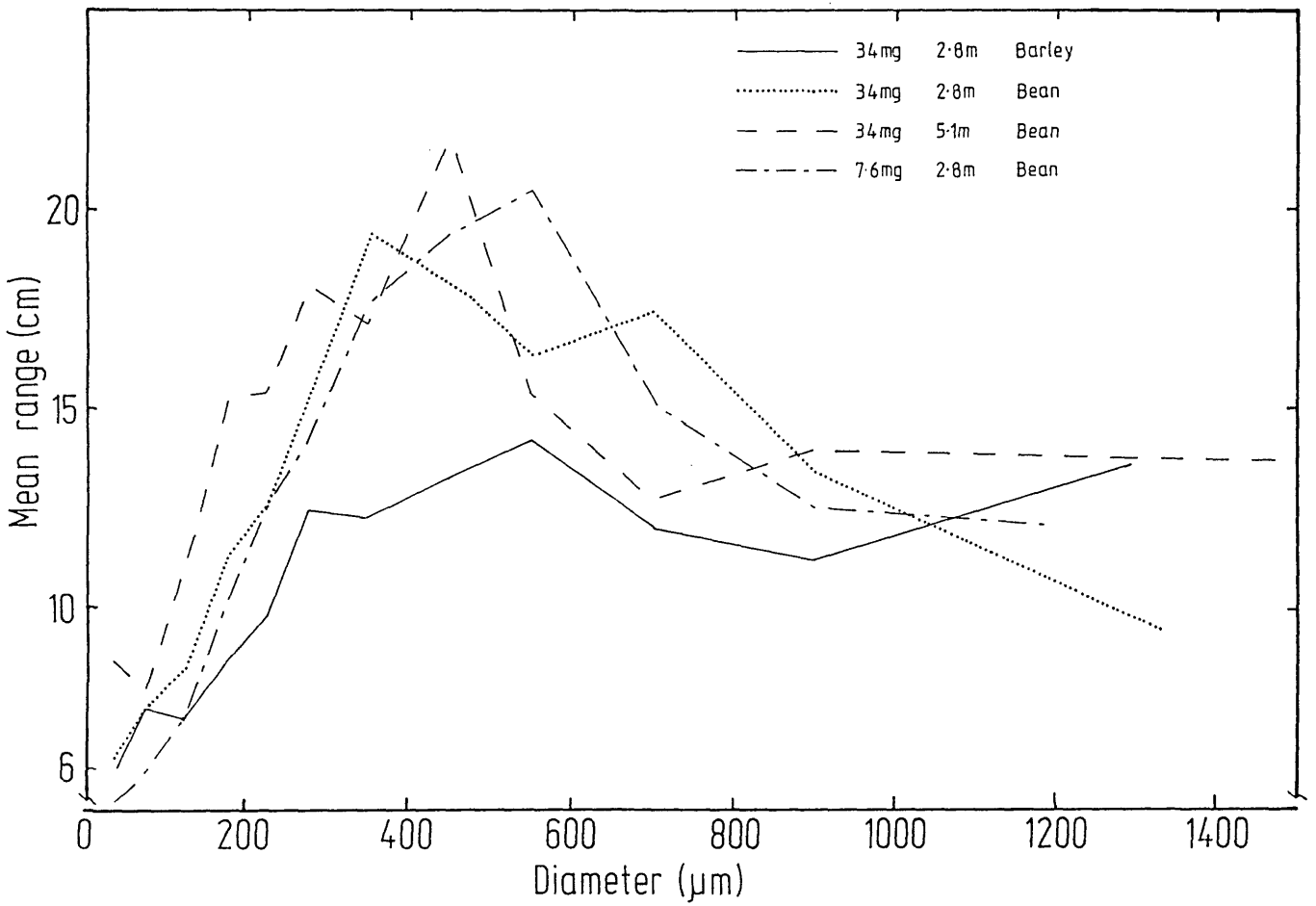


Fig 6.5 Mean observed range of different sized droplets.

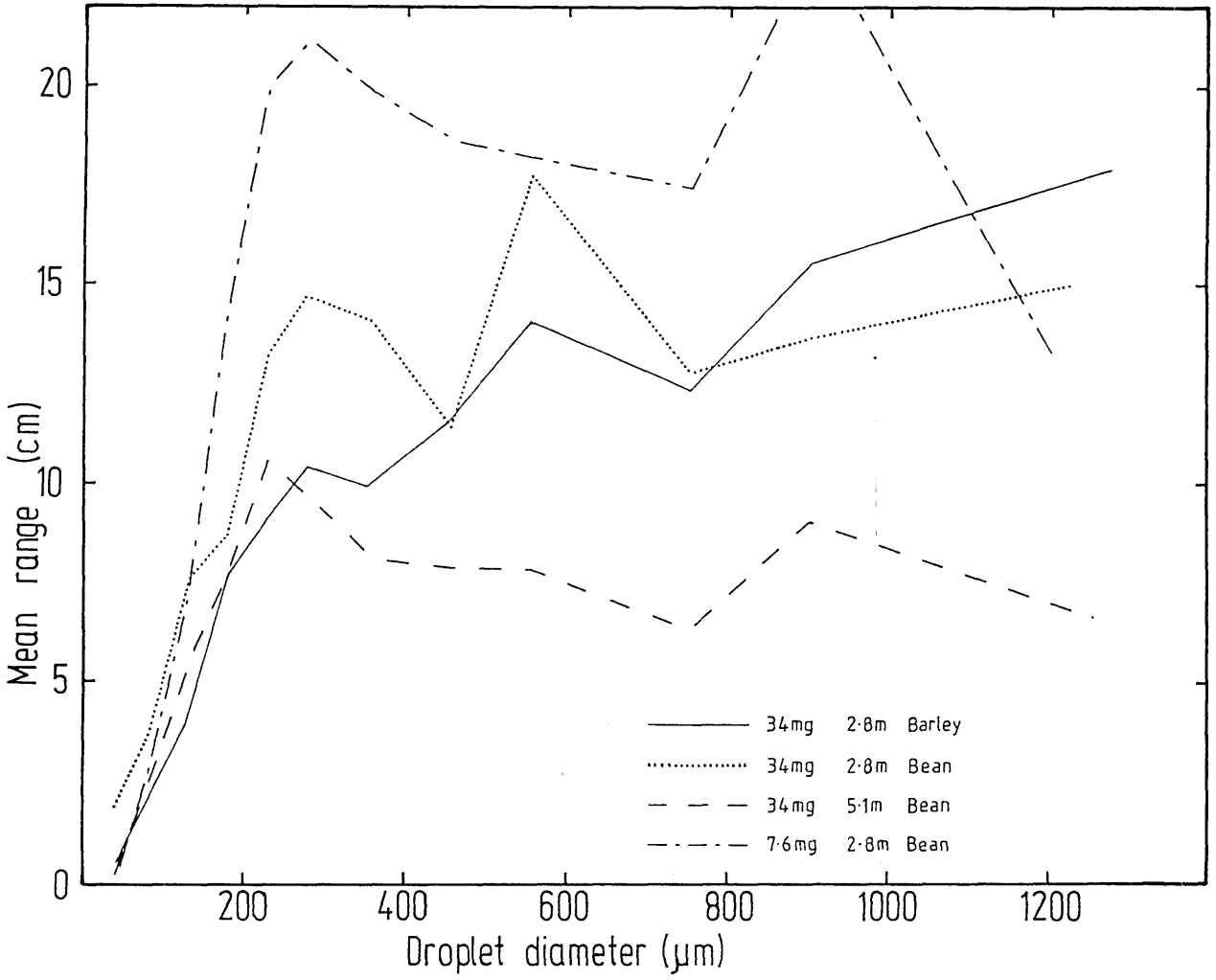


Fig 6.6 Mean calculated range of different sized droplets.

being deflected upwards after travelling several millimetres. Thus a small increase in range may be obtained over a droplet following a simple trajectory from the point of impact.

At distances greater than 2.5 cm from the splash the calculated and observed dispersal patterns compare well although, as with the distributions of droplet size for the case of 34 mg droplets falling 5.1 m onto a bean leaf there was greater difference between the observed and calculated dispersal patterns than for the other three cases. The general patterns are also similar to those expected for splash dispersal showing an exponential decay of splash products with distance and with a half distance of about 10 cm (Fitt *et al.*, 1987).

Larger droplets travelled further in still air than smaller ones; droplets with diameters between 200 and 500 µm travelled furthest. Figure 6.6 shows that the droplets with the greatest ranges have diameters between 200 and 500 µm. Most spore carrying droplets are also in this range (Fatemi and Fitt, 1983).

The general similarities between the observed and calculated horizontal distributions of splash droplets show that the measurements of droplet size and velocity taken from the photographs were representative of the population as a whole. The calculations based on photographic measurements may have underestimated the range of small droplets. The enhanced projection of small droplets is only important over the first few centimetres from the target and will have very little impact on the overall distribution of volume from a splash, thus it will probably have little effect on disease dispersal. However, it will result in the enhanced penetration by small droplets through the boundary layer surrounding the leaf and therefore in the likelihood of their being carried away from the plant into turbulent flow within the canopy. Once in more turbulent air these small droplets have the potential to remain airborne and

consequently be carried long distances. The importance of these small airborne droplets is discussed elsewhere (see Section 1.2.3).

There is broad agreement between the two sets of data, what differences there are tend to be a reflection of predictable, if not quantifiable, errors caused by the methods used to determine the dispersal patterns. The dispersal patterns are similar to those that have been found in previous investigations of splashes on various surfaces.

6.2 Vertical droplet range

The maximum height reached by droplets is simpler to model than the horizontal range as only the vertical component of velocity needs to be considered. Figure 6.7a-d shows the relationship between droplet diameter and the vertical component of velocity for the four cases investigated (droplets with initial velocities below the horizontal are not shown). The contour lines represent the maximum height reached by droplets of a given size and velocity. Most droplets do not attain heights of greater than 10 cm.

Bean leaves project droplets to greater heights than do barley leaves. This is because although droplets produced by splashes on barley leaves are more likely to be ejected above the horizontal splashes on bean leaves produce droplets with higher speeds, so that the mean vertical speed is greater. Walklate, Macdonald, McCartney and Fitt (in preparation) examined the data from these experiments together with that from previous work and found an exponential relationship between impact momentum and maximum splash height. Large drops do eject droplets to greater heights than do smaller ones (Figs 6.7b and c) however as the momentum is increased beyond a certain point the relationship appears to break down with the maximum height reached by droplets appearing to decrease slightly. The

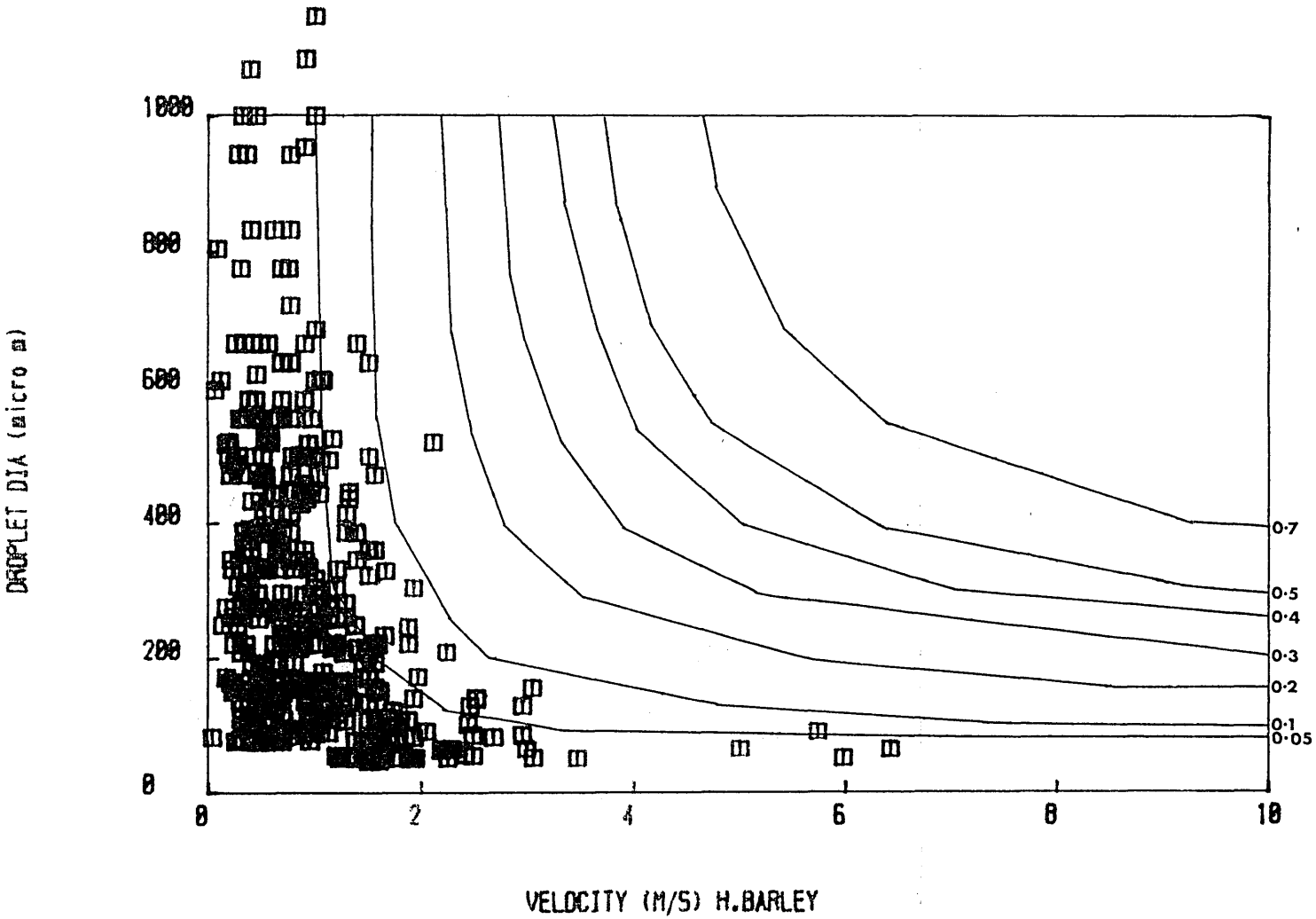


Figure 6·7a
Relationship between droplet diameter and the vertical component of velocity. Contour lines show heights reached (m).
34 mg drop, falling 2.8 m onto a barley leaf.

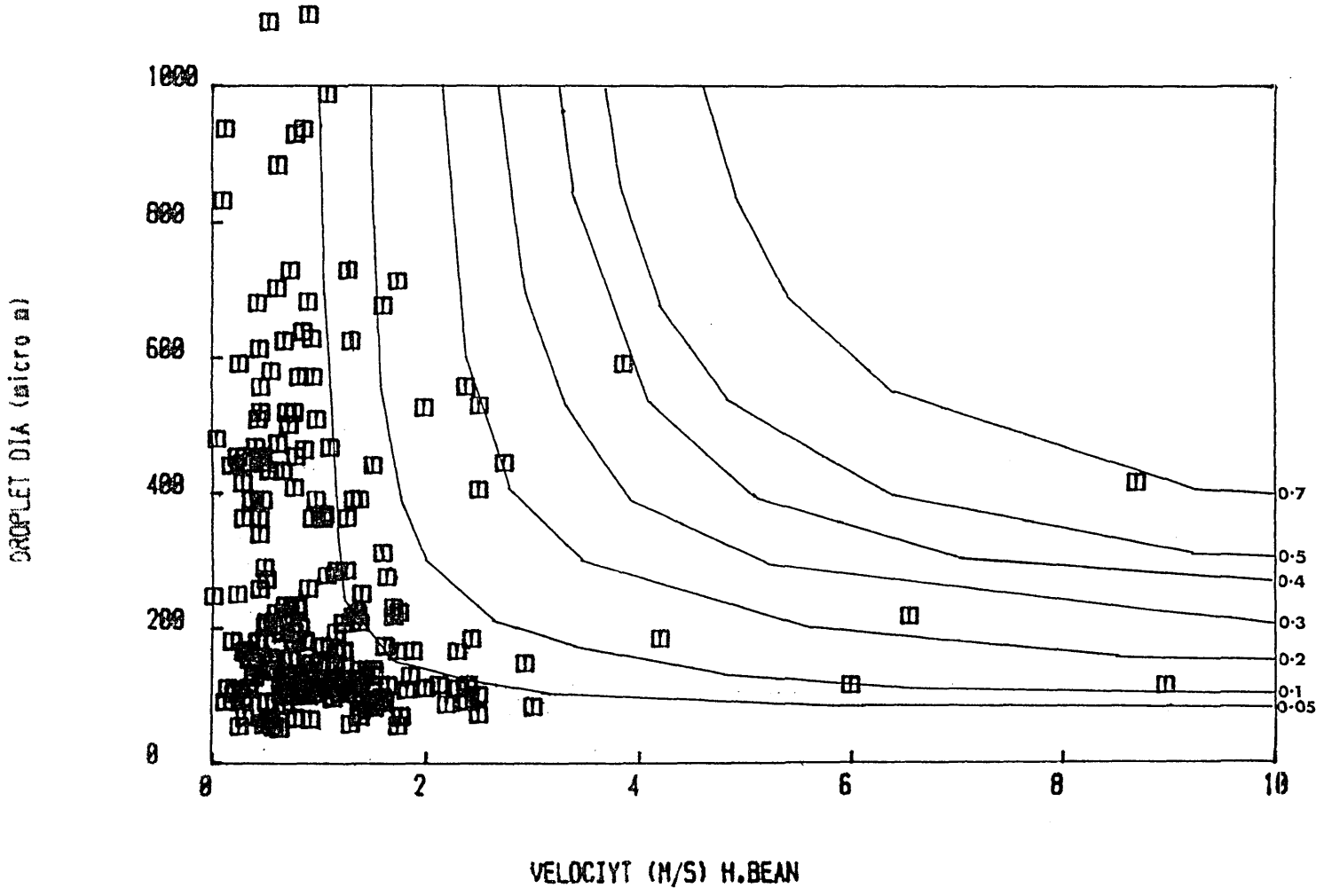


Figure 6.7b
Relationship between droplet diameter and the vertical component of velocity. Contour lines show heights reached (m).
34 mg drop, falling 2.8 m onto a bean leaf.

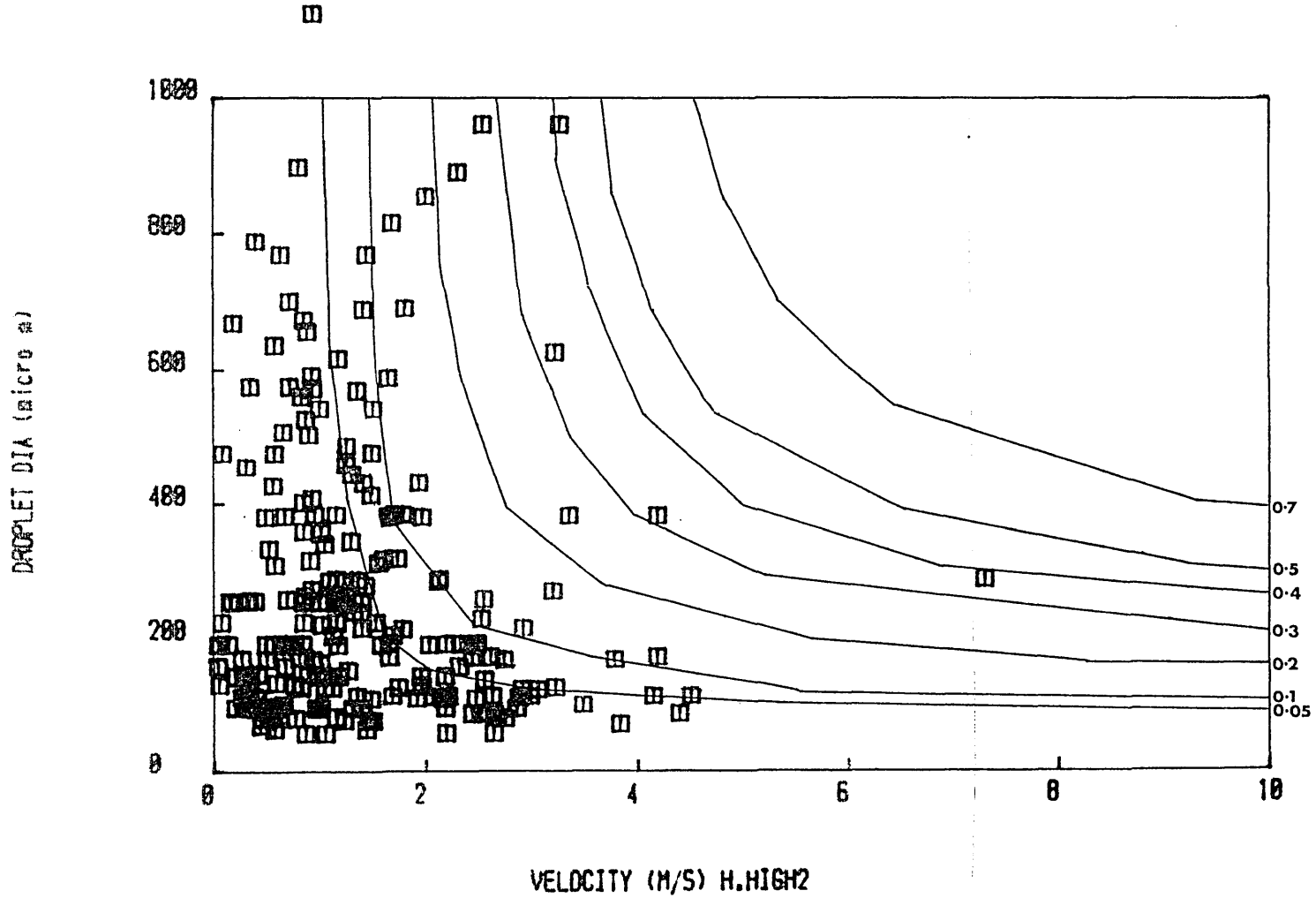


Figure 6.7c
Relationship between droplet diameter and the vertical component of velocity. Contour lines show maximum height reached (m). 34 mg drop, falling 5.1 m onto a bean leaf.

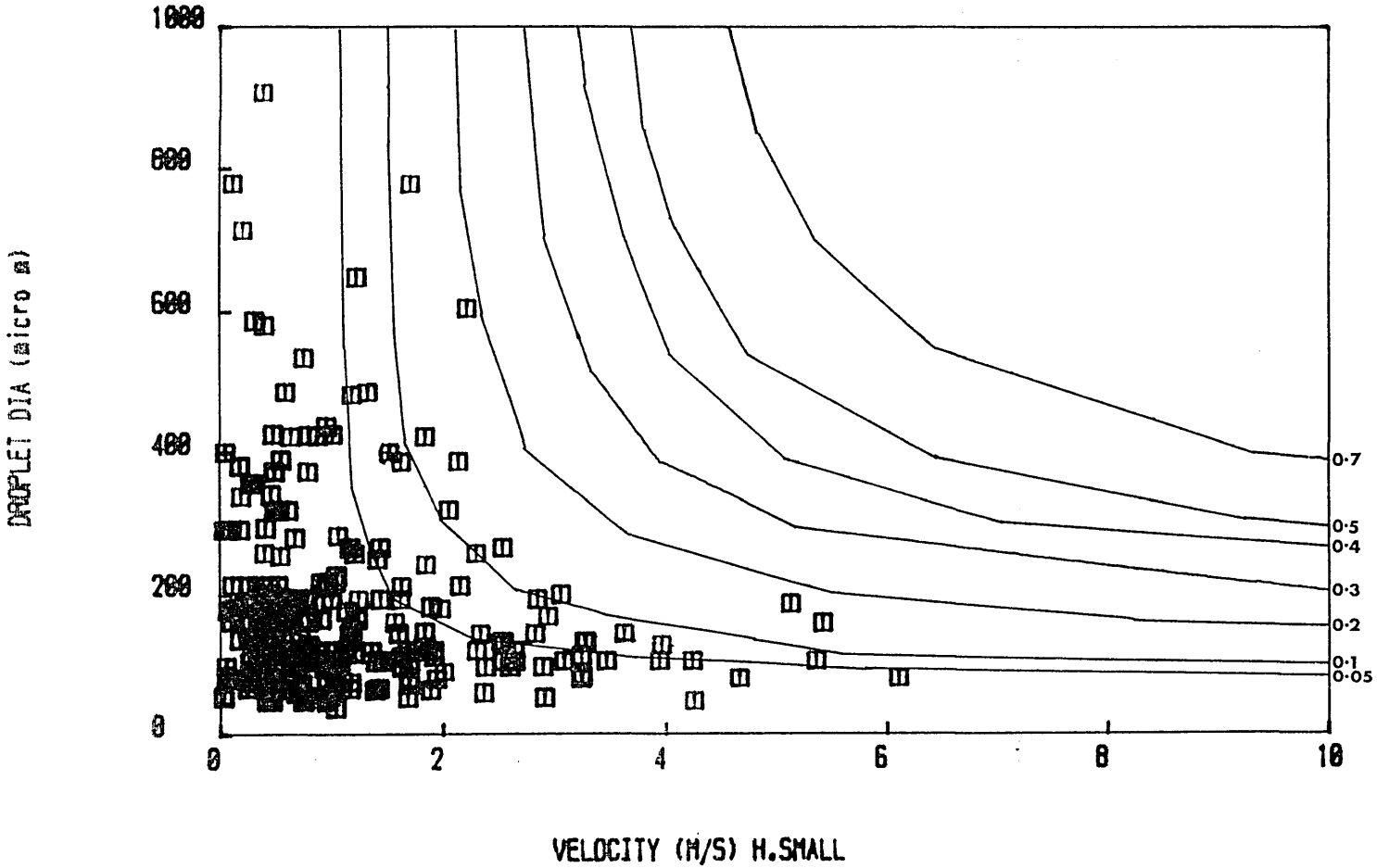


Figure 6.7d
Relationship between droplet diameter and the vertical component of velocity. Contour lines show heights reached (m).
7.6 mg drop, falling 2.8 m onto a bean leaf.

explanation for this phenomena was discussed in Section 5.5.1; as the momentum of the impacting drop increases the flexible leaf surface tends to be pushed out of the way, this has the effect of deflecting the splash products sideways thus decreasing upward dispersal.

Upward dispersal is important because it relates to the spread of disease up the canopy and the potential for long range dispersal when disease propagules are carried out of the canopy. The dispersal of droplets vertically will also have an effect on horizontal ranges. As wind speed rises with increasing height, droplets that are splashed higher will tend to travel further. Unfortunately the sample size for those droplets that had initially fast upward trajectories and were therefore likely to reach the greatest heights was small. Since these droplets are potentially of the greatest interest in disease dispersal studies further experiments of this type may do well to concentrate on these.

It would also be interesting to further study the impact forces that leaves can withstand before giving way. This is clearly an area where leaf splash differs from splash on other surfaces. Al-Durrah and Bradford (1982) showed that the ability of a particulate surface to deform had an effect on splashing which suggests that the flexibility of a target may also. For splash on soil there is a direct relationship between impact momentum and maximum splash height, however, for splashes on leaves there appears to be a maximum impact momentum above which the maximum vertical range of splash droplets will decay. The magnitude of this momentum will vary depending on leaf rigidity which as well as varying between species and varieties may change with the age and condition of plants, and possibly also with the spacing of plants if leaves rest upon one another giving support as is the case in developed cereal canopies.

6.3 Radial distribution

Bean leaves have little structure that is likely to cause droplets to be preferentially ejected in any given direction when splash occurs on a horizontal leaf. However bean leaves rarely lie perfectly horizontally, tending to slope downwards away from the plant. Ghadiri-Khorzoojhi (1978) showed that when splashing occurs on a slope most of the droplets are ejected in the downslope direction, the proportion increasing with the angle of slope. The majority of droplets from splashes on bean leaves would therefore be expected to be directed away from the plant.

Barley leaves differ from bean leaves in having a 'V' shaped cross section. This may result in the splash products favouring a given lateral orientation. To investigate this a small number of photographs were taken looking down onto splashes occuring on horizontal sections of barley leaves, Plate 7 shows an example of one of these photographs. The angle of ejection relative to the leaf axis was recorded for each droplet, the size and velocity of droplets was not measured.

The mean and standard deviation in the number of droplets ejected over each 10^{o} arc is presented in Table 6.5, and in diagramatic form in Fig. 6.8. There is a clear tendency for greater numbers of droplets to be ejected perpendicular to the long axis of the leaf. It is likely also that the shape of the leaf will cause most of these droplets to have significantly upward trajectories. However, this situation is only found when drops impact on sections of the leaf that lie within a few degrees of the horizontal. Observation showed that even slight deviations from the horizontal cause droplets to be preferentially ejected along the axis of the leaf. On a free standing barley plant only short sections of the leaf will lie horizontally. Most splashes will therefore occur on sloping sections



PLATE 7 Vertical view of splash on a barley leaf.
34 mg drop falling 2.8 m.

TABLE 6.5

Numbers of droplets ejected at different angles to the axis of a barley leaf by the splash of a 34 mg drop falling 2.8 m onto a horizontal section of leaf.

Angle to leaf axis	Mean number of droplets/photo	SD
0–10	3.28	2.95
10–20	4.08	4.08
20–30	4.52	3.92
30–40	4.78	4.46
40–50	5.78	5.20
50–60	6.32	5.89
60–70	7.28	7.49
70–80	6.50	6.96
80–90	9.23	9.31

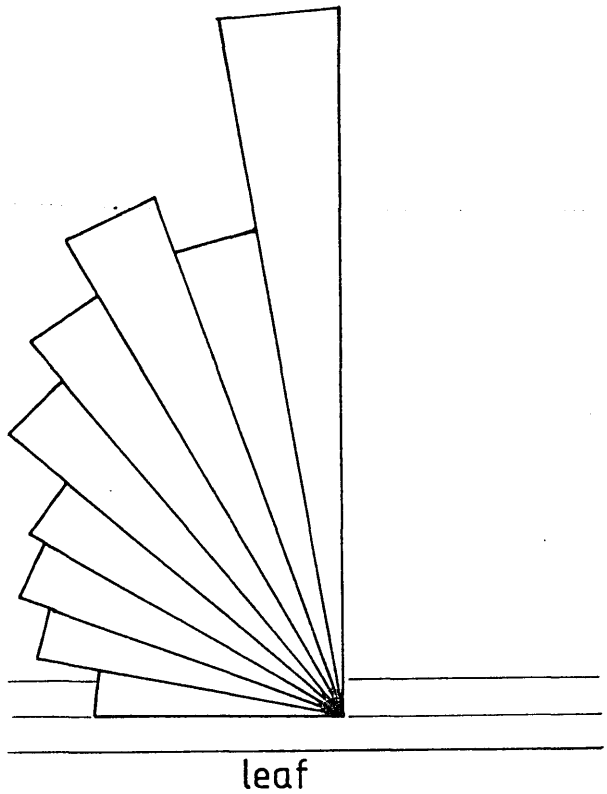


Fig 6.8
Numbers of droplets ejected at different angles from splash on a horizontal barley leaf. Numbers of droplets is indicated by length of the triangles.

of the leaf and most droplets will be ejected along the leaf axis. In a developed crop canopy where plants are close together the situation may be different. Leaves interefere with one another and may support each other so that a far higher proportion of splashes may occur on roughly horizontal leaves.

Assuming that leaves are oriented randomly, which may not be the case (Royale, pers. comm.) any favoured orientation of splash droplets in the horizontal plane will have little if any affect on disease dispersal. However such effects should be borne in mind when sampling splash from isolated plants as the positioning of samplers may affect the results obtained.

CHAPTER 7

7.1 Applications

Using the model described in Chapter 2, and the information on the initial velocities and sizes of splash droplets (Chapter 5) it is possible to calculate the trajectories of individual spore carrying droplets. Equations 8 and 10 can be used to estimate the range and height likely to be reached by splash droplets in still air. The motion of droplets is calculated relative to the air surrounding the droplet. Provided that the movement of the air can itself be modelled there should be little problem in applying the equations to problems in moving air.

7.2 Horizontal ranges

Figures 7.1 and 7.2 show the ranges and Figs 7.3 and 7.4 the heights reached by droplets of two different sizes (200 and 1000 μm) plotted against the initial angle of ejection, θ for different initial velocities, V_0. The greater effect of air resistance on the trajectory of the smaller droplet is clearly shown. The 200 μm droplets travel a much shorter distance and reach a lower height than 1000 μm droplets given the same initial velocity. If air resistance were negligible then the droplet trajectories would be independent of mass and the maximum range would be the same for all sizes and be reached when $\theta = 45^o$. The maximum height reached would be equal to $\frac{1}{2} V_0^2/g$. These distances are only approached when initial speeds are low and the droplet is large. Because of the drag of the air the maximum horizontal range is reached when $\theta<45^o$. This angle becomes smaller with decreasing droplet size as the air resistance becomes a more significant factor affecting the trajectory with smaller droplets.

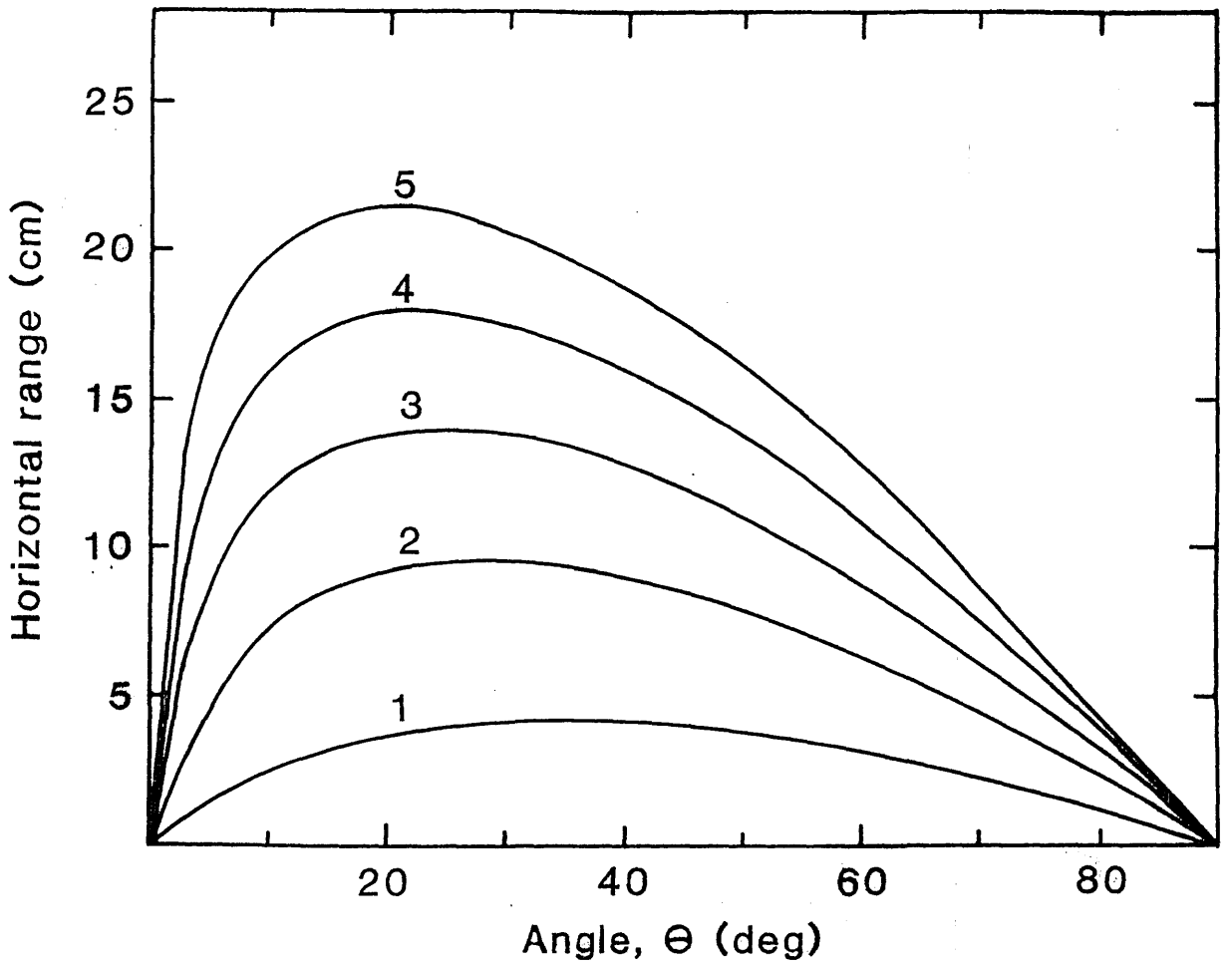


Fig 7.1 Calculated horizontal range of a 200 μm droplet ejected with different initial velocities and angles to the horizontal. The initial velocities in ms^{-1} are shown above each curve.

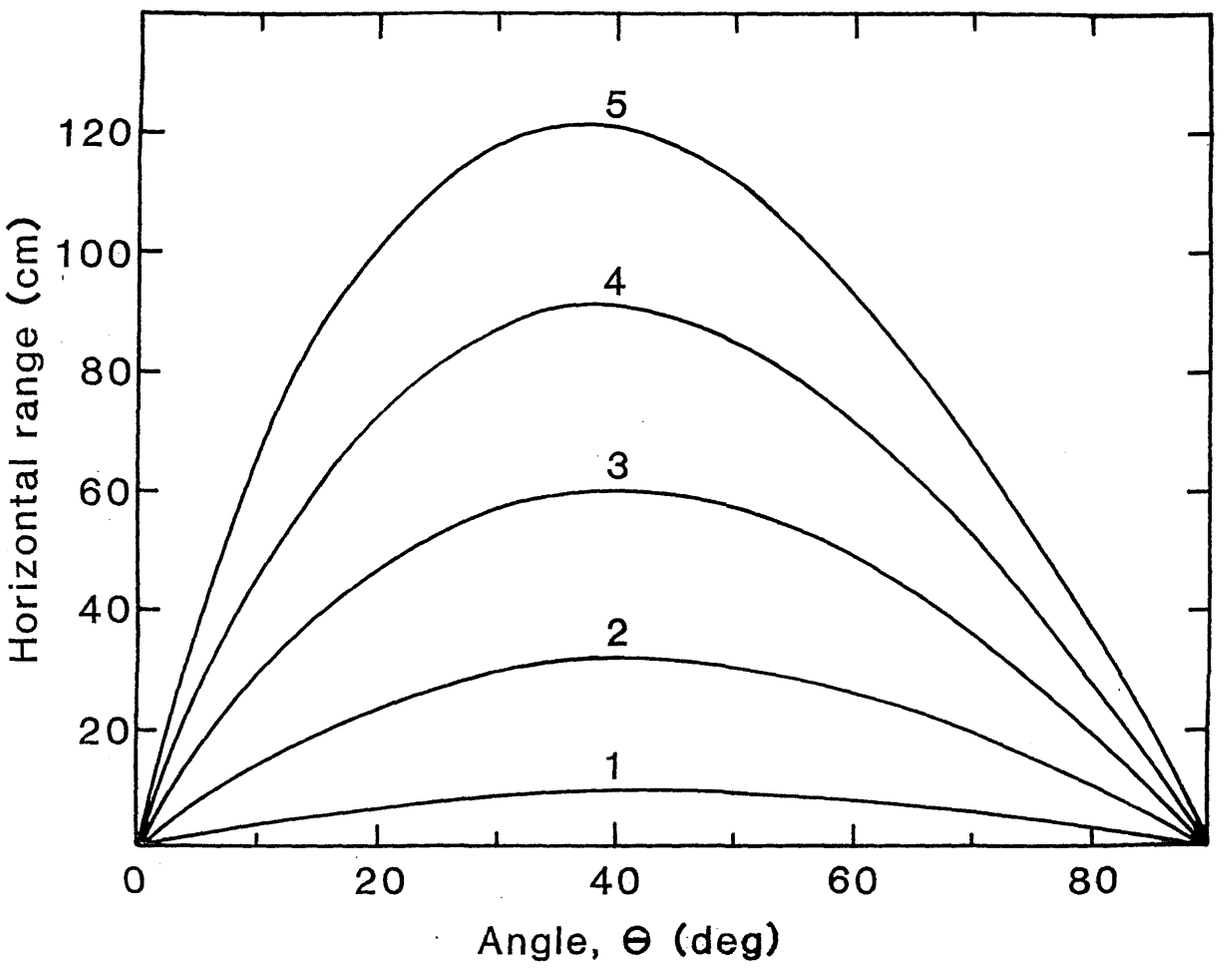


Fig 7.2 Calculated horizontal range of a 1000 μm droplet ejected with different initial velocities and angles to the horizontal. The initial velocities in ms^{-1} are shown above each curve.

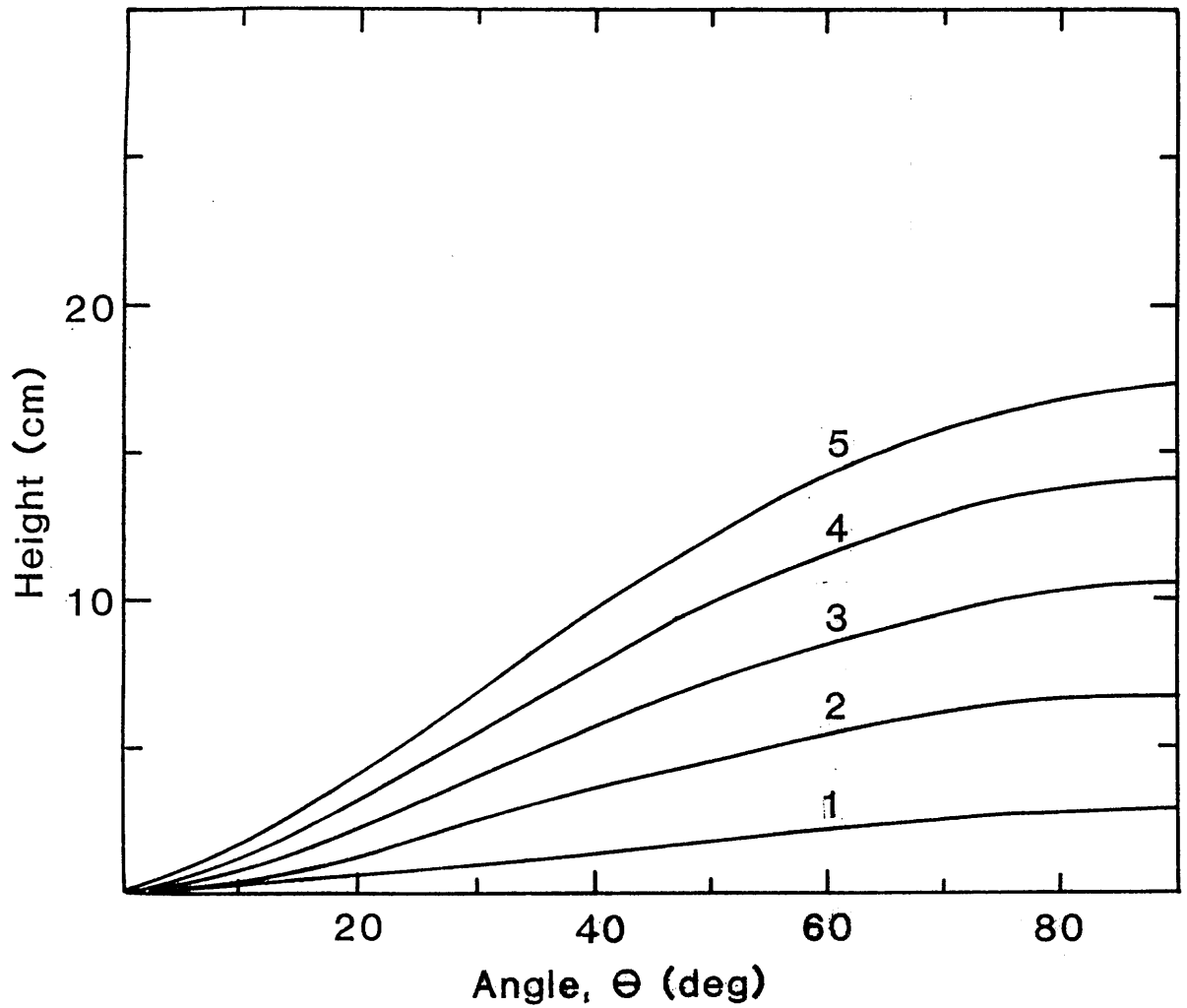


Fig 7.3 Calculated maximum height reached by a 200 μm droplet ejected with different initial velocities and angles to the horizontal. The initial velocities in ms^{-1} are shown above each curve.

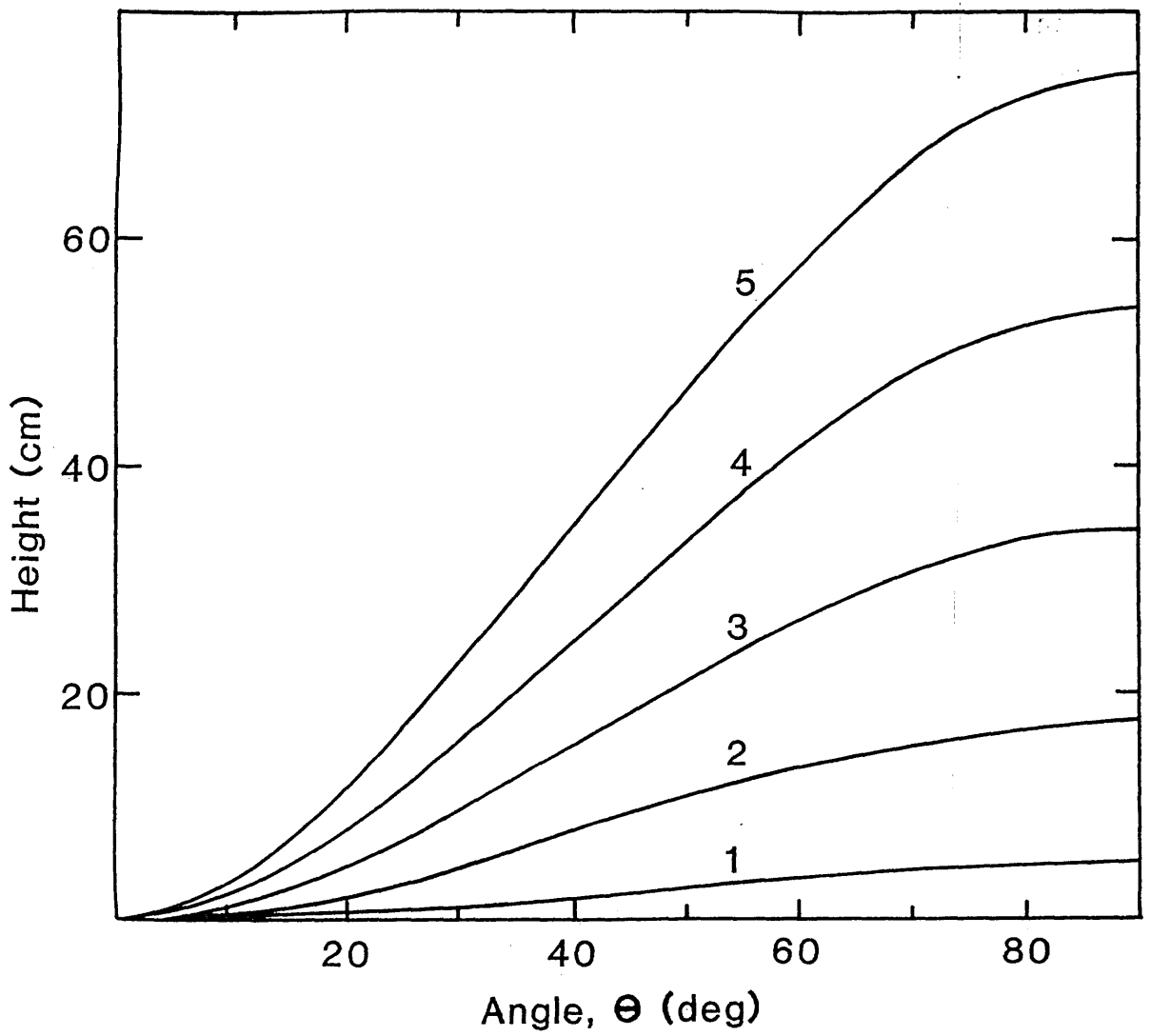


Fig 7.4 Calculated maximum height reached by a 1000 μm droplet ejected with different velocities and angles to the horizontal. The initial velocities in ms^{-1} are shown above each curve.

Table 7.1 shows the stopping distance (i.e. the distance that a droplet will travel before its horizontal component of velocity has decayed to zero) for a range of droplets projected horizontally with a variety of initial velocities. Also shown are the distances the droplets would fall before reaching 90% of the stopping distance. Large droplets have the potential to travel substantial distances even with moderate initial velocities. For example, a droplet with a diameter of 1000 μm ejected horizontally with a speed of 1 m s^{-1} will reach a distance of over half a metre. However, in doing so the droplet will have fallen over 2 m. Thus, for horizontally projected droplets only those released near the top of the canopy are likely to travel more than few tens of centimetres.

7.3 Effect of splash height on droplet dispersal

Tables 7.2-7.5 show the mean distances travelled by droplets in different size classes in all four of the cases investigated before settling on a surface 10 cm below the splash. The trajectories of the droplets observed in photographs of the splash of a 34 mg drop falling 2.8 m onto a bean leaf were again calculated using the model but with the droplets falling a metre below the release point before impacting onto the target. Table 7.6 shows the mean distance travelled by different drop sizes after this additional fall. Figure 7.5 illustrates the difference between the two dispersal patterns graphically. These show clearly the effect of the short stopping distance of small droplets. For droplets with diameters of less than about 200 μm there is virtually no difference in the average horizontal distance travelled between those droplets falling 0.1 m and those falling 1 m. The mean distances travelled by larger droplets is several times greater when the splash occurs 1 m above the ground, than when it is at 0.1 m. For droplets of all sizes

TABLE 7•1

Stopping distances of droplets projected horizontally at different velocities. The numbers in parenthesis are the distances the droplets would fall in reaching 90% of stopping distance.

Initial speed ($m\ s^{-1}$)	Stopping distance (cm)								
	Droplet diameter (μm)								
	200	300	400	500	600	800	1000	1500	2000
1	7.1 (7.2)	12.5 (22)	18.4 (40)	24.1 (64)	30.2 (102	41.6 (206)	52.8 (367)	77.2 (534)	96.7 (844)
2	12.3 (6.9)	22.0 (18)	33.1 (40)	43.5 (60)	55.2 (101)	77.3 (181)	99.3 (323)	147.5 (529)	186.5 (780)
3	16.6 (5.9)	30.1 (17)	45.4 (39)	60.0 (56)	76.8 (98)	108.4 (172)	140.4 (303)	210.8 (518)	268.0 (758)
4	20.5 (5.6)	37.1 (16)	56.1 (37)	74.5 (54)	95.7 (93)	136.0 (162)	177.2 (283)	267.3 (571)	342.0 (752)
5	23.9 (5.)	43.4 (15)	65.7 (35)	87.5 (51)	112.7 (89)	160.1 (152)	210.3 (266)	318.3 (500)	409.4 (749)

TABLE 7•2

Calculated mean horizontal range of droplets produced by the splash of a 34 mg drop falling 2.8 m onto a barley leaf.

Droplet diameter (μm)	Range (mm)	Number of droplets
<50	5	5
50–100	20	70
100–150	40	54
150–200	77	46
200–250	91	39
250–300	105	32
300–400	100	69
400–500	116	51
500–600	141	32
600–800	124	33
800–1000	156	17
>1000	180	11

TABLE 7•3

Calculated mean horizontal range of droplets produced by the splash of a 34 mg drop falling 2.8 m onto a bean leaf.

Droplet diameter (μm)	Range (mm)	Number of droplets
<50	19	1
50–100	34	63
100–150	75	79
150–200	87	30
200–250	132	33
250–300	147	25
300–400	141	27
400–500	114	43
500–600	178	36
600–800	129	29
800–1000	137	14
>1000	151	9

TABLE 7•4

Calculated mean horizontal range of droplets produced by the splash of a 34 mg drop falling 5.1 m onto a bean leaf

Droplet diameter (μm)	Range (mm)	Number of droplets
<50	2	1
50–100	24	69
100–150	54	64
150–200	77	51
200–250	106	28
250–300	97	41
300–400	82	54
400–500	79	23
500–600	79	27
600–800	64	37
800–1000	91	14
>1000	67	9

TABLE 7•5

Calculated mean horizontal range of droplets produced by the splash of a 7.6 mg drop falling 2.8 m onto a bean leaf.

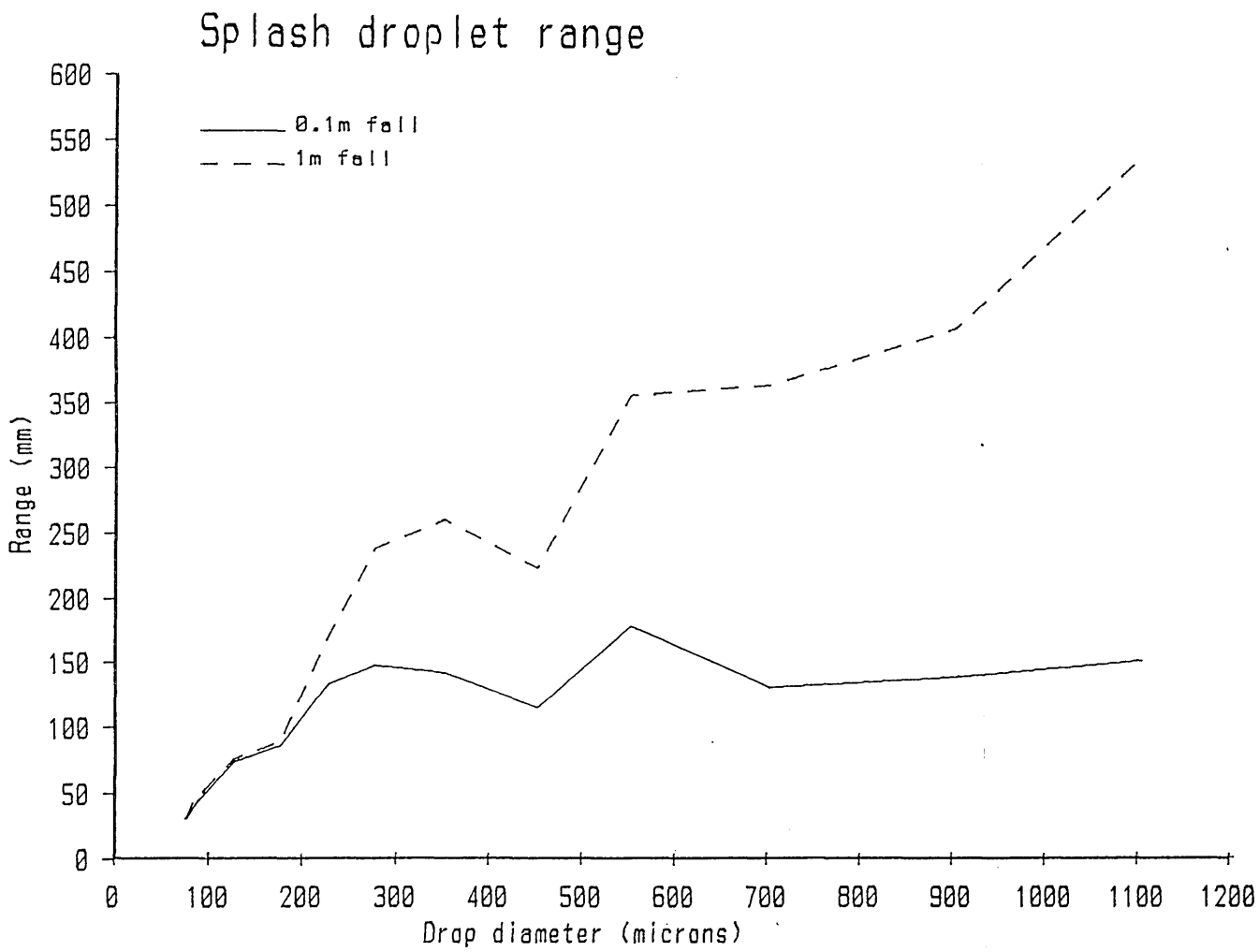
Droplet diameter (μm)	Range (mm)	Number of droplets
<50	4	15
50–100	25	76
100–150	71	83
150–200	144	63
200–250	200	25
250–300	212	21
300–400	199	30
400–500	187	28
500–600	183	9
600–800	175	16
800–1000	238	1
>1000	133	6

TABLE 7.6

Range of droplets produced by the splash of 34 mg drop falling 2.8 m onto a bean leaf in still air when impacts occur at heights of 10 cm and 1 m.

Height	10 cm	1 m		
Droplet diameter	range (cm)	range (cm)	Δr	$r_{1m}/r_{0.1m}$
< 75	30	30	0	1
75-100	43	43	0	1
101-150	73	75	2	1.03
151-200	85	88	3	1.04
201-250	132	169	37	1.28
251-300	147	238	91	1.62
301-400	141	260	119	1.84
401-500	114	223	109	1.96
501-600	178	355	177	1.99
601-800	130	363	233	2.79
800-1000	138	407	269	2.95
>1000	151	538	387	3.56

Fig 7.5


Splash droplet range
0.1m fall
1m fall
Range (mm)
600
550
500
450
400
350
300
250
200
150
100
50
0
0
100
200
300
400
500
600
700
800
900
1000
1100
1200
Drop diameter (microns)

there will be a threshold height above which, in still air, the initial height of the splash has no effect on the maximum horizontal range of the droplet. However, for the largest droplets this will be several metres, far higher than most crop canopies.

7.4 Effect of wind

Table 7.7 shows the effect of wind on the distance travelled by splash droplets. Droplets were assumed to be released into a stream of moving air at a height of 1 m and with the same observed initial velocities as in the previous section. Above a height of one meter the windspeed was described by the equation $z^2 \times 2.0 + 0.37$ m s^{-1} while below one meter height it was described by the equa tion LOG(z x 10 + 1), where z is the height above the ground. These values are similar to those described by Legg and Raupach (1982) for the wind velocity within a typical 1 m high crop canopy.

In moving air droplets of all sizes have greater horizontal range but as would be expected this effect is enhanced for the smaller droplets. For droplets released at this height the effect of the wind on the trajectories of small droplets is so strong that the trend for larger droplets to travel greater distances is now reversed. Where the largest droplets have about twice the range that they did in still air the smallest ones travel 10-20 times further.

7.5 Turbulence

The above calculations are applicable only to dispersal in still air or in laminar flows, where there is no turbulence. Such conditions exist only rarely, if ever, either in, or above, a crop in the field. In very light winds when the air currents within a canopy are likely to be slight, droplet trajectories will be little affected by air movements and in conditions such as these the assumptions made

TABLE 7.7

Mean range of droplets produced by the splash of a 34 mg drop released 2.8 m above a bean leaf. Impact occurs 1m above ground in a laminar airstream.

Droplet diameter (μm)	n	Mean Range (m)	Variance
<75	40	16.2	24.06
75-100	25	10.13	2.10
101-150	76	6.13	1.39
151-200	29	3.73	0.15
201-250	33	2.75	0.15
251-300	24	2.45	4.35
301-400	27	1.64	0.07
501-600	36	1.18	0.24
601-800	29	0.93	0.15
801-1000	14	0.80	0.12
>1000	9	0.92	0.56

above may be acceptable. However, under most conditions the air flow within a crop canopy is highly turbulent due to the penetration of large scale eddies into the canopy (Shaw *et al.*, 1979; Shaw and McCartney, 1985) and the formation of eddies behind crop structures. A possible exception will be very young crops that present little profile to the wind.

The likely influence of turbulence on the trajectories of droplets was investigated using the same model modified to generate a simulated turbulent air-stream. This was done by the addition of the Markov chain model described by Legg (1983) and Wilson *et al.* (1983) to generate instantaneous wind speeds in a Lagrangian time frame. vertical Wind speed, W was calculated by the equation.

$$W_{n+1} = \alpha W_n + \beta \sigma_{w_{n+1}} r_{n+1} + \gamma \overline{W}_{LR} \qquad - 15 -$$

$\alpha=\exp(-\Delta t/T_L)$ where Δt is the timestep and T_L is the Lagrangian time scale, $\beta=(1-\alpha^2)^{1/2}$, σ_w is the root-mean-square Eulerian vertical velocity, r a Gaussian random number with a mean of zero and variance 1, $\gamma=1-\alpha$ and

$$W_{LR}=T_L \left(\frac{d\sigma_w^2}{dz} \right). \qquad - 16 -$$

The trajectories of a number of droplets moving in a turbulent airstream were calculated using the values for mean windspeed, velocity variance and Lagrangian time scale similar to those suggested by Legg and Raupach (1982), as being typical of those found within and just above a crop canopy. The mean horizontal windspeed profiles were the same as those used in section 7.4; above the crop (1.0 m in height) σ_w = 1.25 x U^* (= 0.3), Lagrangian time scale = 0.32 x $(z-D)/\sigma_w$ where D=0.75 x crop height; within the crop σ_w = (1.25 x (z/1.0) + 0.125) x U^* and the Lagrangian time scale = 0.32 x

(1.0-D)/(U* x 1.25).

Again the initial velocities of droplets produced by the splash of a 34 mg drop falling 2.8 m onto a bean leaf were used as the initial conditions for the model. To average out the effects of random turbulence on individual trajectories several replicate trajectories were calculated for each droplet size and velocity. Because some small droplets could potentially remain air-borne indefinitely trajectories were only calculated up to a distance of 15 m downwind from the source.

The mean ranges of droplets in different size classes is shown in Table 7.8. These results are compared to those described above for droplets released into a laminar airstream (but with a maximum range of 15 m) in Fig. 7.6. The solid line shows the mean range of different sized droplets released into a smooth flow of air, the dashed lines the mean range of droplets in a turbulent airflow. The mean ranges were calculated only on the basis of those droplets that had been deposited. Some droplets with diameters of less than 150 μm were still airborne after 15 m (short dashed lines). Above that size all droplets had been deposited with 15 m of the target. Above a diameter of about 120 μm the addition of turbulence to the equation appears to have little effect on the pattern of deposition, below that size the majority of droplets appear to be deposited sooner. Of course, it is in this size range where droplets may remain airborne. While these airborne droplets account for only a small proportion of the total number they have potentially huge ranges, and would have a disproportionate effect on the overall mean were their total ranges to be included.

In general turbulence, if of an order large enough to significantly affect the trajectory of a particle, will cause the majority of particles to be deposited sooner than they would be in a

TABLE 7.8

Mean range of droplets produced by the splash of a 34 mg drop released 2.8 m above a bean leaf. Impact occurs 1 m above the ground in a turbulent airstream. Mean windspeed is the same as for table 7.7.

Droplet diameter (μm)	number deposited (m)	Mean range	Variance	% airborne at 15 m
<75	29	7.71	12.11	36
76-100	55	7.25	9.61	27
101-150	208	5.61	5.97	9
151-200	84	3.51	0.74	
201-250	99	2.67	0.45	
251-300	72	1.95	0.25	
301-400	81	1.58	0.10	
401-500	129	1.31	0.53	
501-600	108	1.16	0.33	
601-800	87	0.98	0.17	
801-1000	42	0.85	0.11	
>1000	27	0.80	0.42	

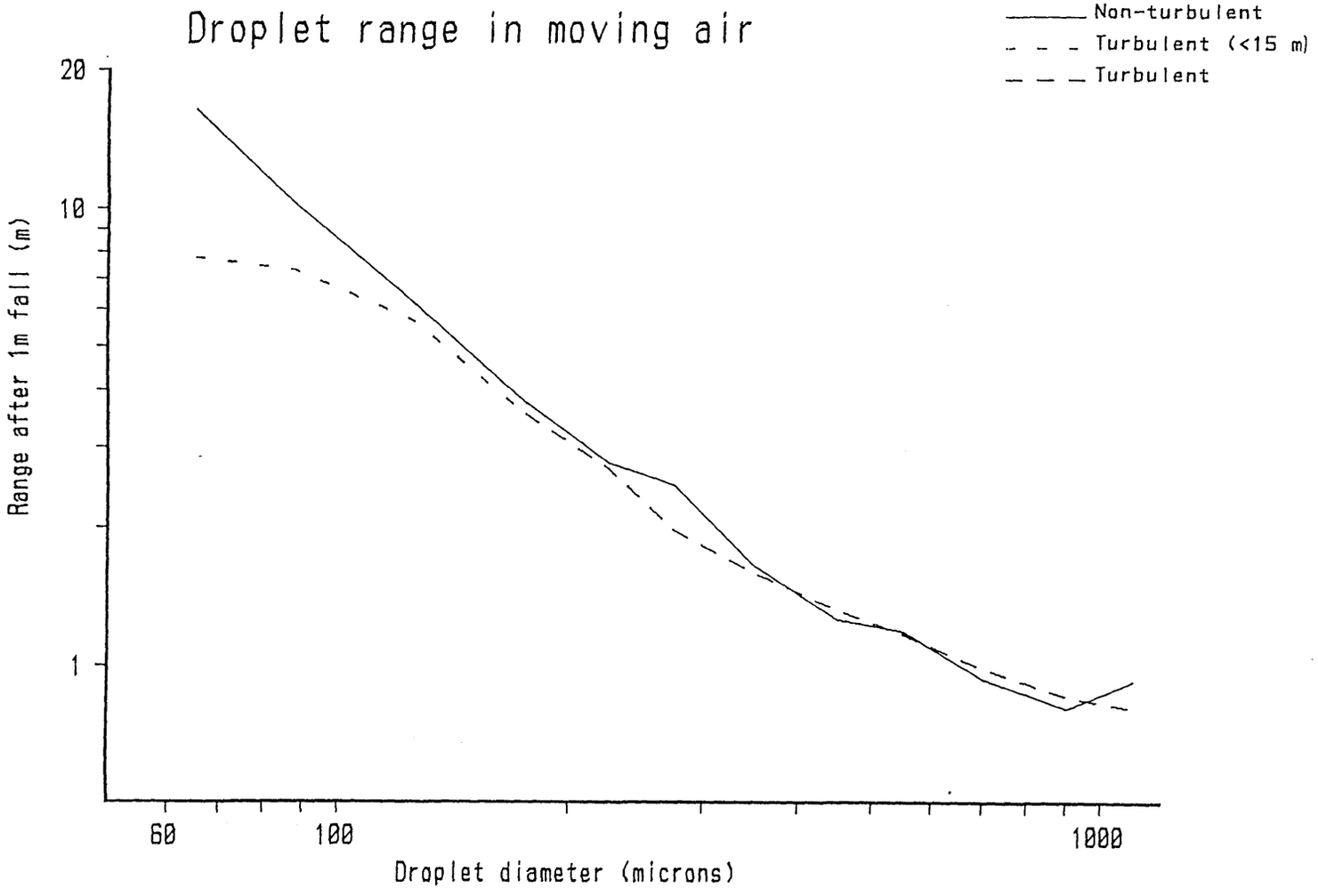


Fig 7.6

Mean ranges of different sized droplets in moving air. Dashed lines show the effect of turbulence, the shorter dashes indicate the region in which some droplets became airborne and were not deposited.

laminar airstream. This is because the larger the size of the vertical eddies and greater is the chance that a particle carried by them will be brought into contact with the ground. Equally though, those few particles that escape contact with the ground are likely to be carried to far greater heights and distances.

7.6 Spore dispersal

Predicting the trajectories of splash droplets is not all that must be done in order to predict the spread of splash dispersed diseases, or even the distribution of disease propagules. To predict the dispersal of propagules rather than just droplets it is neccesary to also model the spore carrying properties of droplets, ie the probability of a droplet of a given size carrying spores and the number of spores that those droplets will carry.

Several investigations of the spore carrying properties of droplets have been carried out. Table 7.9 details the relationships between droplet size and the number of spores for several cases for splashes from suspensions of spores in water. There is no suitable data available for the number of spores contained in droplets splashed off living plants. Not all droplets will carry spores, and the relationships between droplet size and the proportion of droplets carrying spores has never been properly investigated. From the raw data presented by Lysandrou (1980) for the eyespot fungus of cereals, *Pseudocercosporella herpotrichoices*, the percentage of different sized droplets carrying spores was determined to be described by the relationship; $P=(3.76\sqrt{D})-29$; where D is droplet diameter in microns and P, the percentage of droplets carrying spores, has a maximum value of about 95%.

Assuming the number of spores per droplet to be given by the equation $\sqrt{n} = D \times 0.003 + 0.5$, for droplets splashed from a spore

TABLE 7.9

Relationships between droplet size and number of spores carried.

Disease	Droplet diameter	Target	Relationship
P. herpotrichoides(1)	4 mm	120,000 spores/ml	$n=(d \times 0.03 + 0.5)^2$
P. herpotrichoides(1)	5 mm	320,000 spores/ml	$n=(d \times 0.0067 + 0.09)^2$
P. herpotrichoides(2)	5 mm	320,000 spores/ml	$n=(d \times 0.0138 - 1.02)^2$
P. brassicae(2)	5 mm	120,000 spores/ml	$n=(d \times 0.0167 - 1.47)^2$

(1) Fitt and Lysandrou (1984)
(2) Fatemi and Fitt (1983)

All droplets fell 13 m onto a spore suspension 0.5 mm deep, concentration of spores as given.

P' = *Pyrenopeziza*

suspension, and the proportion of droplets carrying spores as given by the equation above. The numbers of spores deposited on the ground at distances of up to 15 m is shown in Fig. 7.7, for both smooth and turbulent airflows. The proportions of spores deposited at different distances in each case are shown in Table 7.10.

The results suggest that turbulence would have very little effect on the gradients of spore deposition. This is because the smallest droplets, which are those that will be most affected by turbulence, carry very small numbers of spores. The simulated windspeed of 2 m s^{-1} and the levels of turbulence were only moderate and obviously in stronger winds a somewhat greater difference might have been expected. The simulation does, however, show the importance of turbulence in the long range dispersal of spores. In both turbulent and non-turbulent flows a very small proportion, <1%, of spores were still airborne after 15 m. In turbulent airflow, however, the number is more than 10 times that in a laminar air stream, 0.13% of spores still being airborne compared with 0.0004%. Since the heights attainable by airborne droplets is greater in turbulent air, Section 7.5, the chances of being carried out of the canopy, and therefore the potential for further transport, will also be greater.

7.7 Deposition

So far only the distribution of splash droplets on the ground has been discussed. Droplets moving through a crop canopy may impact on plant elements before reaching the ground. Indeed since it is the spores carried by these droplets that cause new lesions it is these droplets that are of most interest, although spores deposited onto the ground may be transported in subsequent secondary splashes or remain in the soil to act as a reservoir for future infections.

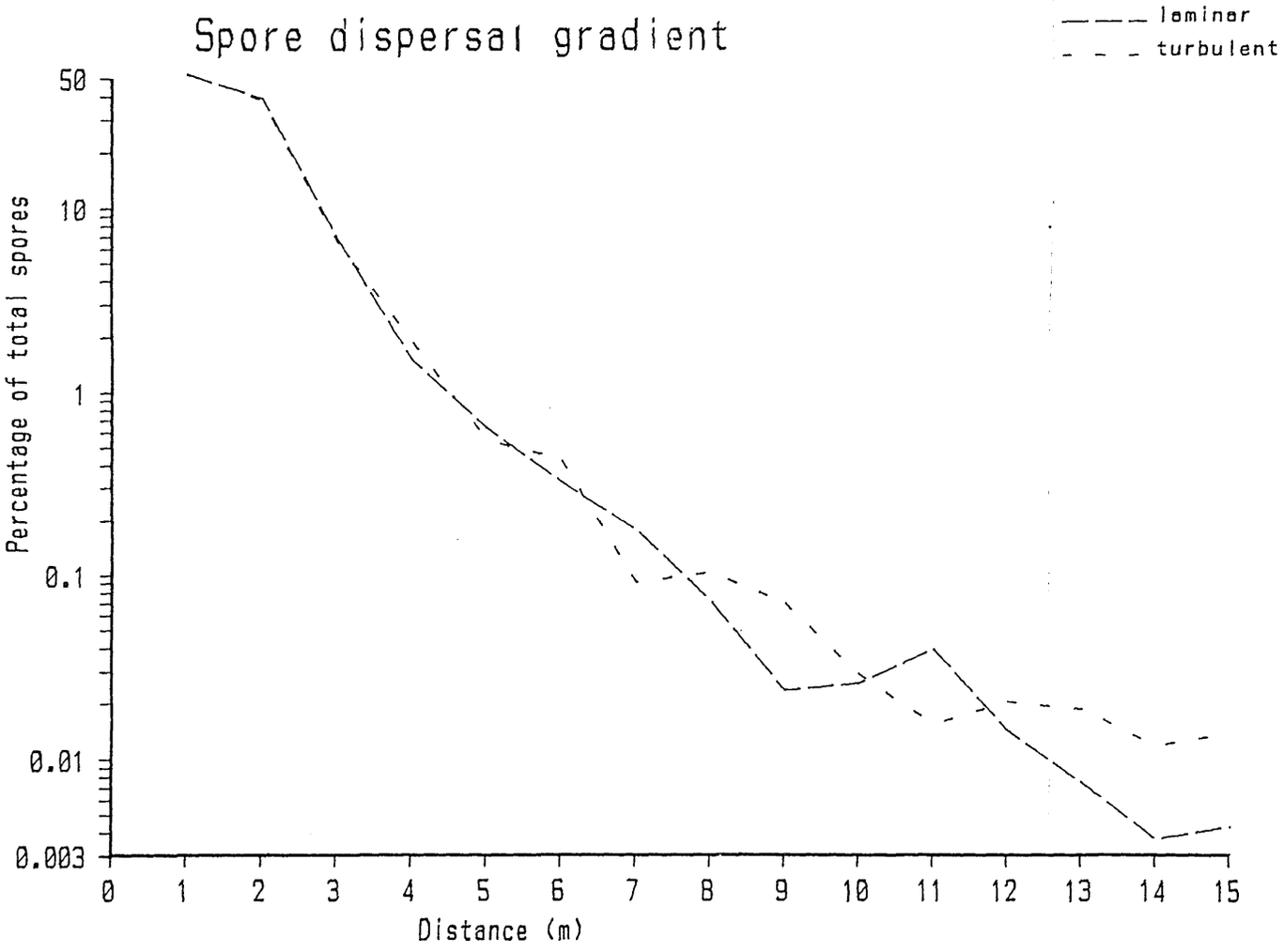


Fig 7.7

Calculated spore dispersal gradient from the splash of a 34 mg drop falling 2.8 m onto a bean leaf. Long dashes show gradient in laminar flow, short dashes in turbulent conditions.

TABLE 7.10

Percentage of spores deposited at different distances assuming the number of spores in each splash droplet is given by the equation:
$n=(d \times 0.003 + 0.5)^2$
and the percentage of droplets of a given size carrying spores by the equation:
percentage spore carrying = $3.7572 \times d^{0.5} - 29$.

Distance (m)	Percentage of spores.
1	52.44
2	37.67
3	6.56
4	1.86
5	0.54
6	0.42
7	0.09
8	0.10
9	0.07
10	0.03
11	0.02
12	0.02
13	0.02
14	0.01
15	0.01
Still airborne	0.13

However, the droplets that are most likely to carry spores, large droplets created from the splash of big, fast moving, raindrops, appear to have predominantly downward directed trajectories, this suggests that the movement of spores may be predominantly downward. Seem, pers. comm., has found striking cone shaped regions of infection of apple scab extending down from the tops of apple trees. Infection was seen to start at the top of the tree, presumably as a result of spores being carried into an orchard from outside, and then to spread in an expanding cone down through the tree. In several splash dispersed diseases of cereals (*Septoria nodorum, Septoria tritici* and *Rhynchosporium secalis*) lesions are found predominantly near the base of the plant. This may simply be because conditions are more favourable for the development of the fungus near the base of the plant but it may also be an indication of a lack of upward spore movement. When lesions do occur near the top of the crop it can frequently be shown that the infection was initiated when the plants were young before stem extension (e.g. *Septoria* in wheat, Royale *et al.*, 1986), the lesions can thus be carried up by the growth of the plant.

In field crops the result of such downward transport will be to deposit the majority of spores on to the ground. From here they may well be carried back up into the crop, but are unlikely to reach a great height, at least in one stage. Walklate *et al.* (in preperation) relates the maximum height reached by splash droplets to the product of impacting drop diameter and velocity (DV), and suggests that only raindrops with a value of DV greater than a certain threshold are likely to produce splash droplets capable of reaching heights of any significance. For splash droplets to reach a height of 30 cm a free falling raindrop of at least 2.7 mm diameter was shown to be required, while the absolute maximum height likely to

be reached by rain-splash droplets was around 70 cm. The experiments described here show some evidence that, due to the deflection of leaves, the maximum height reached by droplets splashed from leaves may well be less than this. Overall this perhaps indicates an important role for spores splashed from the soil. Gregory *et al.* (1984) in describing the disease cycle of cocoa black pod (*Phytophthora megakarya*) suggested that ballistic rain splash from the soil was responsible for the high incidence of the disease within the first 70 cm above the ground. It could well prove extremely valuable to investigate the importance of secondary splash from soil as a stage in the dispersal of splash borne pathogens.

The height at which a splash occurs will obviously affect the pattern of droplet dispersal. Splashes near the top of the canopy will be more affected by the wind, and the changes in canopy structure with height will affect the probability of splashing and the deposition of splash droplets. Walklate (1987) used the crop area density profile index of a mature wheat crop, described by Denmead (1976) to estimate the distribution of rain drop penetration, and therefore splashing, within a crop under different wind conditions. In general most impacts take place around half way up the canopy or on the ground. A similar approach using the crop area profile might be used to determine the distribution of splash droplet depositions within the canopy.

The probability that spore carrying droplets will collide with raindrops and be washed out of the air to be deposited sooner than would otherwise be expected also needs to be investigated. For most droplets a good approximation to this can be obtained by calculating the chance of collision on the basis of the density of raindrops in the air. However, the real chance of collision will be less than this as the airflow around a drop will reduce the collision

efficiency. This becomes particularly important when collisions between large raindrops and small splash droplets is considered. This problem was tackled in a theoretical way by Chow (1979), though only for the limited case where one drop is substantially larger than the other and both are travelling at terminal velocity.

Even if spores carried in splash droplets are deposited onto plant elements, it is possible that further impacts of raindrops or drips from higher up in the canopy will once again wash the spores off the leaf. Also, the accumulation of water on a leaf during rain will eventually lead to run off and spores may be carried down in drips from leaves. Spores may have adhesive properties that prevent this from happening, Webster and Davey (1984) describe the attachment of the spores of aquatic fungi to surfaces in flowing water, however little work has been done on the adhesive properties of the spores of splash dispersed diseases.

Overall this suggests that infection caused by the upward movement of spores is a fairly rare event. Gregory *et al.* (1984) through some rough calculations estimated that 1000 mm of rain produced only two disease initiators per cocoa tree. In terms of rain drops this translates as one initiator for every 1×10^9 drops, or 10^{12} splash droplets. This is not to say that there is no purpose in the modelling of individual droplet trajectories. Disease obviously is spread by rain splash and modelling the processes involved can aid us in determining where and how far disease is likely to travel from a source of infection under a given set of conditions. The sudden appearence of *Septoria* lesions at some height above the ground after heavy rain (Royale *et al.*, 1986) suggests that even if upward transport is a relatively rare event it can be important in some diseases.

However to effectively use such information further work needs to be done on the movement of spores during natural rain, the adhesive properties of spores, the relationship between spore numbers and drop size and the importance of spores splashed from the soil in disease cycles. This last point may be particularly worthy of investigation given the evidence pointing to a substantial downward movement of droplets and spores.

CHAPTER 8

CONCLUSIONS

8.1 Modelling Droplet Trajectories

A model for calculating splash droplet trajectories was investigated. Experiments proved it to be accurate to within at least 15% when used to calculate the trajectories of droplets with sizes and velocities that have previously been shown to be typical of those produced by water splash. It was only possible to compare observed and calculated trajectories in still air. It proved impossible to measure droplet trajectories in moving air because of the difficulties of isometrically sampling droplets from an airstream in such a way that they could be sized. A suggested alternative approach that would get round the problem of sizing droplets would be to use solid particles. Glass spheres of various sizes can be obtained from several sources. These have a similar density to water and could be released into a moving airstream, either smooth or turbulent, and the distance that they travel measured. The size distribution of the spheres can be determined before-hand which would therefore make it easier to design appropriate sampling surfaces.

Atmospheric pressure and temperature would appear to have little effect on droplet trajectories and can safely be ignored. However, temperature and humidity may have a significant effect on droplet evaporation. This should be taken into account when looking at the movement of small water droplets.

8.2 Experimental Techniques

Water splash on leaves of beans and barley plants was investigated using two different techniques. Overall the two techniques gave similar results for the size distributions and

dispersal patterns of droplets. Both techniques appear to underestimate the number of droplets with diameters less than about 50 μm. In the case of splash caused by the drops with the highest investigated impact momentum, significant differences between the two sets of results were observed. This was probably because the falling drop impacted with sufficient force to effect a substantial movement of the leaf, which results in most of the splash droplets having similar downward trajectories. A limitation of both techniques for splash investigation is that when many droplets follow similar trajectories they become difficult to separate. When droplets impact on a surface they tend to coalesce or obscure one another. Similarily, it is difficult to distinguish sequences of images of the same droplet when many trajectories are overlaid in multiple image photographs. To a large extent these problems can be overcome when droplets are collected, either by exposing a collector to a limited number of splashes or by moving it further away from the splash.

With certain limitations, the technique of taking multiple image still photographs that was developed has therefore proved useful for measuring the initial velocities of splash droplets. It has also proved possible to measure droplet sizes in this way but the laborious nature of the technique suggests that other methods would better serve the purpose.

8.3 Splash on leaves

In comparison with other surfaces, splashes on leaves show several significant differences. Splashes are less regular with only partial coronas, and there is a much greater variation in the form of splashes. However, there appears to be less variation in the speeds of droplets. Although smaller droplets are still ejected with higher

speeds than larger ones the mean and maximum speeds of smaller droplets appear to be less than for splashes on other surfaces.

The distribution of droplet sizes from splashes on leaves follows a log-normal pattern, this was also observed by Levin and Hobbs (1971) for splashes on solid surfaces. The distribution of droplet velocities, which does not appear to have been investigated before, appears to be square root-normal.

Splashes on bean leaves bear some similarities to splashes on sloping surfaces, with the effective angle of the target surface increasing with the momentum of the impacting drop. The fastest droplets from splashes on bean leaves are ejected at angles close to, and usually slightly below, the horizontal. Also on beans, the largest droplets tended to be ejected below the horizontal. Splashes from barley leaves differs from that on bean leaves in several ways. The droplet collection experiments suggest that droplets from barley leaves are on average larger than those from splashes from impacts of similar momentum on beans. There was less variance in the speeds of droplets and a greater proportion of droplets were ejected at angles above the horizontal.

The size and speed of the impacting drop affected both the size and the speed of the splash droplets. The greater the momentum of the impacting drop the faster were the splash droplets. The greatest changes in speed were observed with the smaller droplets. The size of splash droplets did not show any regular change with impact momentum. 34 mg drops produced bigger droplets than did 7.6 mg drops falling the same distance. However, a 34 mg drop falling 2.8 m produced larger droplets than one falling 5.1 m, equivalent to an increase in the impact momentum of about 22%.

As noted above, as the impact momentum increased the proportion of droplets ejected below the horizontal also increased. However,

this was not a simple relationship as the numbers of droplets with steeply upward trajectories also increased.

The difference in impact velocity between a 34 mg droplet falling 2.8 m and one falling 5.1 m was only 1.45 m s^{-1}. Attempts were made to use a 13 m fall to obtain an even greater impact velocity using the Rothamsted rain tower. However, turbulent updrafts made the accurate targetting of drops impossible and the lower height had to be accepted.

8.4 Significance of results

The results show that the majority of the water ejected as droplets from a splash travels only a very short distance, and further, that most of it will be deposited below the level of the splash. This suggests that the movement of pathogenic material from leaves will be predominantly downwards. This suggests that secondary splash from soil may play a major role in the dispersal of splash bo rne diseases. This needs to be further investigated.

Most raindrops will be considerably smaller than those investigated. However, the larger the impacting drop the further will droplets travel. The greatest potential for rain splash dispersal will therefore be when the greatest number of large droplets are produced, i.e. in convective rain showers. Whether the largest raindrops will produce the greatest vertical dispersal length scales is not clear. There appears to be a point above which the momentum of the impacting drop is so great that a leaf may be forced aside and so diminish vertical dispersal. The point at which this happens will vary with the rigidity of the leaves. This itself will vary not only between crops but also within a given crop, depending on variety, age and physiological condition. Such factors would be extremely difficult to quantify, and whether any rainfall conditions

would produce significant numbers of droplets with these very high momentums is doubtful.

The effect of turbulence on the dispersal of splash borne pathogens is doubtful. If anything, high levels of turbulence will decrease the distance over which most spores are dispersed, as the increased vertical movements of spores and droplets will bring them in contact with the canopy sooner. However, as turbulence levels increase, the numbers of droplets and spores that become airborne will increase, and the distances that they travel will also increase. Turbulence may also assist in the penetration of the canopy by droplets by causing plants to move about, and therefore opening up the canopy. The effect this would have on dispersal is not really quantifiable. As with dry dispersed spores strong gusts that penetrate the canopy may be more likely to blow water containing spores of the leaves, again assisting dispersal.

Turbulence is very difficult to model, and to build a model that would accurately simulate splash dispersal, in a crop canopy, in turbulent rainfall conditions, would be a formidable undertaking. However, to accurately sample splash dispersed spores, is itself very difficult. To measure turbulence, in a crop, in the rain, is virtually impossible at present. Even a simple model could, therefore, be extremely useful.

If spore sampling is to be attempted, it would appear that there are two areas that need to be concentrated on. Most local dispersal would appear to be caused by large droplets, and may be largely restricted to the base of a canopy. Not only do large droplets appear to travel predominantly downwards, but most lesions occur low down the canopy, and it is in this area where droplets may travel furthest, the base of a canopy often being relatively open. Sampling for spores, in relatively large droplets, near the base of the

canopy, may, therefore, give a good indication of local dispersal scales. Collecting droplets in petri dishes, or on slides, shielded from the rain, is the simplest method of sampling. Soil particles can make spores difficult to detect however. This problem may possibly be solved either by staining spores or by culturing from the sample.

Long distance dispersal will be caused by airborne spores, either in very small droplets, or on their own after the surrounding droplet has evaporated. Sampling for these spores may be carried out using suction samplers or rotorods, although care must be taken to shield the sampler from the rain in such a way as to minimally interfere with the local airflow.

REFERENCES

ALLEN, C.M. (1978). *The Physics of splashing of large water drops on solid and wetted surfaces.* Ph.D. Thesis, University of Manchester.

AL-DURRAH, M.M. and BRADFORD, J.M. (1982). The mechanism of raindrop splash on soil surfaces. *Soil Sci. Soc. Am. J.*, 46. 1086-1090.

BEST, A.C. (1950). The size distribution of raindrops. *Quart. J. R. meteorol. Soc.*, 76, 16-36.

BLANCHARD, D.C. and WOODCOCK, A.H. (1957). Bubble formation in the sea and its meteorological significance. *Tellus*, 9, 145-158.

BRENNAN, R.M., FITT, B.D.L., TAYLOR, G.S. and COLHOUN, J. (1985a). Dispersal of *Septoria nodorum* pycnidiospores by simulated raindrops in still air. *Phytopath. Z.*, 112 281-290.

BRENNAN, R.M., FITT, B.D.L., TAYLOR, G.S. and COLHOUN, J. (1985b). Dispersal of *Septoria nodorum* pycnodiospores by simulated rain and wind. *Phytopath. Z.*, 112, 291-297.

CHAMBERLAIN, A.C. (1967). Transport of *Lycopodium* spores and other small particles to rough surfaces. *Proc. Roy. Soc. Lond.*, A 296, 45-70.

CHAMBERLAIN, A.C. and CHADWICK, R.C. (1972). Deposition of spores and other particles on vegetation ans soil. *Ann. appl. Biol.*, 71, 141-158.

CHELLA, G., TOGNOTTI, L. and ZANELLI, S. (1986). A high speed photographic system and its application to spray diagnostics. *Atomisation and Spray Technology*, 2, 1-30.

CHOW, C. (1979). *An Introduction to Computational Fluid Mechanics.* John Wiley and Sons.

DENMEAD, O.T. (1976). Temperate cereals. In; Monteith, J.L. (Ed.), *Vegetation and the Atmosphere.* Vol. 2, 125-137.

DOWDING, P. (1969). The dispersal and survival of spores of fungi causing bluestain in pine. *Trans. Br. mycol. Soc.*, 52, 125-137.

EDMONDS, R.L. (1979). *Aerobiology: The Ecological Systems Approach.* Academic Press.

ELLIOT, J.G. and WILSON, B.J. (Eds.) (1983). *The influence of weather on the efficiency and safety of pesticide application: The drift of herbicides.* BCPC. occasional publication No. 3.

ENGEL, O.G. (1955). Water drop collisions with solid surfaces. *J. Res. nat. Bur. Stand.*, 54, 281-298.

FATEMI, F. and FITT, B.D.L. (1983). Dispersal of *Pseudocercosporella herpotrichoides* and *Pyrenopeziza Brassicae* spores in splash droplets. *Plant Pathology*, 32, 401-404.

FAULWETTER, R.C. (1917a). Dissemination of the angular leafspot of cotton. *J. agric. Res.*, 8, 457-475.

FAULWETTER, R.C. (1917b). Wind blown rain, a factor in disease dissemination. *J. agric. Res.*, 10, 639-648.

FERREIRA, A.G., LAROCK, B.E. and SINGER, M.J. (1985). Computer simulation of water drop impact in a 9.6-mm deep pool. *Soil Sci. Soc. Am. J.*, 49, 1502-1507.

FERREIRA, A.G. and SINGER, M.J. (1985). Energy dissipation for water drop impact into shallow pools. *Soil Sci. Soc. Am. J.*, 49, 1537-1542.

FINNEY, D.J. (1971). *Probit Analysis.* Cambridge University Press.

FITT, B.D.L. and BAINBRIDGE, A. (1983). Dispersal of *Pseudocercosporella herpotrichoides* spores from infected wheat straw. *Phytopath. Z.*, 106, 214-225.

FITT, B.D.L., GREGORY, P.H., TODD, A.D., MCCARTNEY, H.A. and MACDONALD, O.C., (1987). Spore dispersal and plant disease gradients; a comparison between two empirical models. *J. Phytopath.*, 118, 227-242.

FITT, B.D.L. and LYSANDROU, M. (1984). Studies on mechanisms of splash dispersal of spores using *Pseudocercosporella herpotrichoides* spores. *Phytopath. Z.*, 111 323-331.

FITT, B.D.L, LYSANDROU, M. and TURNER, R.H. (1982). Measurement of spore-carrying splash droplets using photographic film and an image-analysing computer. *Plant Pathology*, 31, 19-24.

FITT, B.D.L. and MCCARTNEY, H.A. (1986). Spore dispersal in splash droplets. In: P.G. Ayres and L. Boddy, (eds.) *Water, Fungi and Plants*, Cambridge University Press, pp 87-104.

FITT, B.D.L. and NIJMAN, D.J. (1983). Quantitative studies on dispersal of *Pseudocercosporella herpotrichoides* spores from infected wheat straw by simulated rain. *Neth. J. Pl. Path.*, 89, 198-202.

FITT, B.D.L, WALKLATE, P.J, MCCARTNEY, H.A, BAINBRIDGE, A, CREIGHTON, N.F, HIRST, J.M, LACEY, M.E, and LEGG, B.J. A rain tower and wind tunnel for studying the dispersal of plant pathogens by rain and wind. *Ann. appl. Biol*, 109, 661-671.

FUCHS, N.A. (1964). *The Mechanics of Aerosols*. 3rd edition, Pergamon Press.

GHADIRI, H. and PAYNE, D. (1979). *Raindrop impact and soil splash.* In Lal, R and Greenland, D.J. (eds). Soil Physical properties and crop production in the tropics. Wiley.

GHADIRI-KHORZOOJHI, H. (1978). *Raindrop Impact, Soil Splash and Cratering*. Ph.D. Thesis, University of Reading.

GOERING, C.E., BODE L.E. and GEBHARDT, M.R. (1972). Mathematical modelling of spray droplet deceleration and evaporation. *Trans. Am. Soc. Agric. Eng.*, 15, 220-225.

GREGORY, P.H. (1952). Fungus spores. *Trans. Brit. mycol. Soc.*, 35, 1-18.

GREGORY, P.H., (1973). *The Microbiology of the Atmosphere*. 2nd. ed. Leonard Hill: London.

GREGORY, P.H., GRIFFIN, M.J., MADDISON, A.C. and WARD, M.R. (1984). Cocoa black pod: a reinterpretation. *Cocoa growers bulletin*, 35, 5-22.

GREGORY, P.H., GUTHRIE, E.J. and BUNCE, M.E. (1959). Experiments on splash dispersal of fungus spores. *J. gen. Microbiol.*, 20, 328-354.

GUTHRIE, E.J. (1957). *A Study of the Rain-Splash Dispersal of Fungi*. Ph.D. Thesis, University of London.

HARLOW, F.H. and SHANNON, J.P. (1967). The splash of a liquid drop. *J. appl. Physics*, 38, 3855-3866.

HARLOW, F.H. and WELCH, J.E. (1965). Numerical calculation of time-dependent viscous incompressible flow of fluid with free surface. *Phys. fluids*, 8, 2182-2189.

HIGGINS, S. and FITT, B.D.L. (1984). Production and pathogenicity to wheat of *Psedocercosporella herpotrichoides* conidia. *Phytopath. Z.*, 111, 222-231.

HIRST, J.M. (1959). Spore liberation and dispersal. In: Holton, C.S., Fisher, G.W., Fulton, R.W., Hart, H. and McCallan, S.E.A., (Eds.) *Plant Pathology Problems and Progress,* 529-538. University of Wisconsin Press.

HIRST, J.M. and STEDMAN, O.J. (1963). Dry liberation of fungus spores by rain drops. *J. gen. Microbiol.*, 33, 335-344.

HOBBS, P.V. and KEZWEENY, A.J. (1967). Splashing of a water drop. *Science*, 155, 1112-1114.

HIRST, J.M. (1959). Spore liberation and disperal. In: C.S. Holton, G.W. Fisher, R.W. Fulton, H. Hart, and S.E.A. McCallan, (eds.) *Plant Pathology problems and progress*, pp 529-538. University of Wisconsin Press.

INGOLD, C.T., (1971). *Fungal Spores: Their Liberation and Dispersal.* Clarendon Press, Oxford.

JARVIS, W.R. (1962). The dispersal of spores of *Botrytis cinerea* Fr. in a raspberry plantation. *Trans. Brit. mycol. Soc.*, 45, 549-559.

KOENIG, L.R. and SPYERS-DURAN, P.A. (1961). Simple methods of determining water drop sizes by means of photographic emulsions. *Rev. Scient. Instr.*, 32, 909-913.

LECLAIR, B.P., HAMIELEC, A.E., PRUPPACHER, H.R. and HALL, W.D. (1972). A theoretical and experimental study of the internal circulation in water drops falling at terminal velocity in air. *J. Atmos. Sci.*, 29, 728-740.

LEGG, B.J. (1983). Turbulent dispersion from an elevated line source: Markov chain simulations of concentration and flux profiles. *Quart. J. R. Met. Soc.*, 109, 645-660.

LEGG, B.J. and RAUPACH, M.R. (1982). Markov-chain simulation of particle dispersion in inhomogeneous flows: The mean drift velocity induced by a gradient in Eulerian velocity variance. *Boundary-Layer Meteorology.*, 24, 3-13.

LEVIN, Z. and HOBBS, P.V. (1971). Splashing of water drops on solid and wetted surfaces: Hydrodynamics and charge seperation. *Phil. Trans. R. Soc.*, A269, 555-585.

LOO, S.L. (1967). *Fluid Dynamics of Multiphase Systems.* Blaidsall Publishing Co. Waltham, Massachusetts.

LYSANDROU, M. (1980). Mechanisms of dispersal of *Pseudocercosporella herpotrichoides* by splash. M.Sc. Thesis, University of Reading.

MACDONALD, O.C. and MCCARTNEY, H.A. (1987). Calculation of splash droplet trajectories. *Agric. For. Meteorol.*, 39, 95-110.

MARSHALL, J.S. and PALMER, W.M. (1948). The distribution of raindrops with size. *J. Meteorology*, 5, 165-166.

MASON, B.J., JAYARATNE, O.W. and WOODS, J.D. (1963). An improved vibrating capillary device for producing uniform water droplets of 15 to 500 um radius. *J. Sci. Instrum.*, 40, 247-249.

MATTHEWS, G.A. (1982). *Pesticide Application Methods.* Longman, London.

MAY, K.R. and CLIFFORD, R. (1967). The impaction of aerosol particles on cylinders, spheres, ribbons and discs. *Ann. occup. Hyg.*, 10, 83-95.

MUTCHLER, C.K. (1971). Splash droplet production by water drop impact. *Water Res. Research*, 7, 1024-1030.

PERRIER, E.R., ROBERTSON, J.M., MILLINGTON, R.J. and PETERS, D.B. (1972). Spatial and temporal variation of wind above and within a soybean canopy. *Agric. Meteorol.*, 10, 421-442.

PRUPPACHER, H.R. and BEARD, K.V. (1970). A wind tunnel investigation of the internal circulation and shape of water drops falling at terminal velocity in air. *Quart. J. R. Met. Soc.*, 96, 247-256.

RAMALINGAM, A. and RATI, E. (1979). Role of water in the dispersal of nonwettable spores. *Ind. J. Bot.*, 2. 8-11.

RAPILLY, F. and JOVIET, E. (1976). Construction d'un modele (EPISET) permettent la simulation d'une epidemic de *Septoria nodorum* Berk. sur ble. *Revue de Statistique Applique,* 24, 31-60.

ROYALE, D.J., SHAW, M.W. and COOK, R.J. (1986). Patterns of development of *Septoria nodorum* and *S. tritici* in some winter wheat crops in Western Europe, 1981-83. *Plant Pathology* 35, 466-476.

RUCKDESCHEL, F.R. (1981). *Basic Scientific Subroutines vol II.* McGraw Hill.

SHAW, R. and MCCARTNEY, H.A. (1985). Gust penetration into plant canopies. *Atmosph. Environ.*, 19, 827-830.

SHAW, R.H., WARD, D.P. and AYLOR, D.E. (1979). Frequency of occurence of fast gusts of wind inside a corn canopy. *J. appl. Met.*, 18, 161-171.

SPILLMAN, J.J. (1984). Spray impaction, retention and adhesion: An introduction to basic characteristics. *Pestic. Sci.*, 15, 97-106.

SREERAMULU, T. and RAMALINGAM, A. (1964). Some short period changes in the atmospheric spore content associated with changes in the weather and other conditions. *Proc. Indian Acad. Sci.*, 59 B, 154-172.

STEDMAN, O.J. (1979). Patterns of unobstructed splash dispersal. *Ann. appl. Biol.*, 91, 271-285.

STEDMAN, O.J. (1980a). Splash droplet and spore dispersal studies in field beans (*Vicia faba* L). *Agric. Meteorol.*, 21, 111-127.

STEDMAN, O.J. (1980b). Splash dispersal studies in wheat using a fluorescent tracer. *Agric. Meteorol.*, 21, 195-203.

STEPANOV, K.M. (1935). Dissemination of infective diseases of plants by air currents. *Bull. Pl. Prot. Leningr. Ser. 2, Phytopathology*, 8, 1-68.

THOROLD, C.A. (1955). Observations of black-pod disease (*Phytophthora palmivora*) of cacao in Nigeria. *Trans. Brit. mycol. Soc.*, 38(4), 435-452.

TIMMONS, D.R., MUTCHLER, C.K. and SHERSTAD, E.M. (1971). The use of flourescein to measure the composition of waterdrop splash. *Water Resources Research.*, 7, 1020-1023.

ULBRICH, C.W. (1983). Natural variations in the Analytical form of the raindrop size distribution. *J. Climate Appl. Meteor.*, 22. 1764-1775.

WALKER, J.C. and PATEL, P.N. (1964). Splash dispersal and wind as factors in epidemiology of halo blight of bean. *Phytopathology*, 54, 140-141.

WALKLATE, P.J., MCCARTNEY, H.A. and FITT, B.D.L. (198-). Vertical dispersal of plant pathogens by splashing; experimental study of the relationship between raindrop size and the maximum splash height. Submitted to *Plant Pathology*.

WEBSTER, J. and DAVEY, R.A. (1984). Sigmoid shape in aquatic fungi. *Trans. Br. mycol. Soc.*, 83(1), 43-52.

WEDDING, J.B., KIM, Y.J. and DENNISON, R.S. (1986). Mass transfer from water droplets under simulated free fall conditions. *Atmospheric Environment*, 20, 1039-1045.

WILLIAMSON, R.E. and THREADGILL, E.D. (1974). A simulation for the dynamics of evaporating spray droplets in agricultural spraying. *Trans. Am. Soc. Agric. Eng.*, 17, 254-261.

WILSON, J.D., LEGG, B.J. and THOMSON, D.J. (1983). Calculation of particle trajectories in the presence of a gradient in turbulent-velocity variance. *Boundary-Layer Meteorology*, 27, 163-169.

WOLF, W.R. (1961). Study of the vibrating reed in the production of small droplets and solid particles of uniform size. *Rev. Sci. Instruments*, 32, 1124-1129.

WORTHINGTON, A.M. (1877a). On the forms assumed by drops of liquid falling vertically on a horizontal plate. *Proc. Roy. Soc.*, 25, 261-271.

WORTHINGTON, A.M. (1877b). A second paper on the forms assumed by drops of liquid falling vertically on a horizontal plate. *Proc. Roy. Soc.*, 25, 498-503.

WORTHINGTON, A.M. (1882). On impact with a liquid surface. *Proc. Roy. Soc.*, 34, 217-230.

WORTHINGTON, A.M. and COLE, R.S. (1897). Impact with a liquid surface, studied by the aid of instantaneous photography. *Phil. Trans. R. Soc.*, A189 137-148.

YALIN, M.S. (1977). *Mechanics of sediment transport. 2nd ed.* Pergamon.

Appendix 1
Details of delay circuit

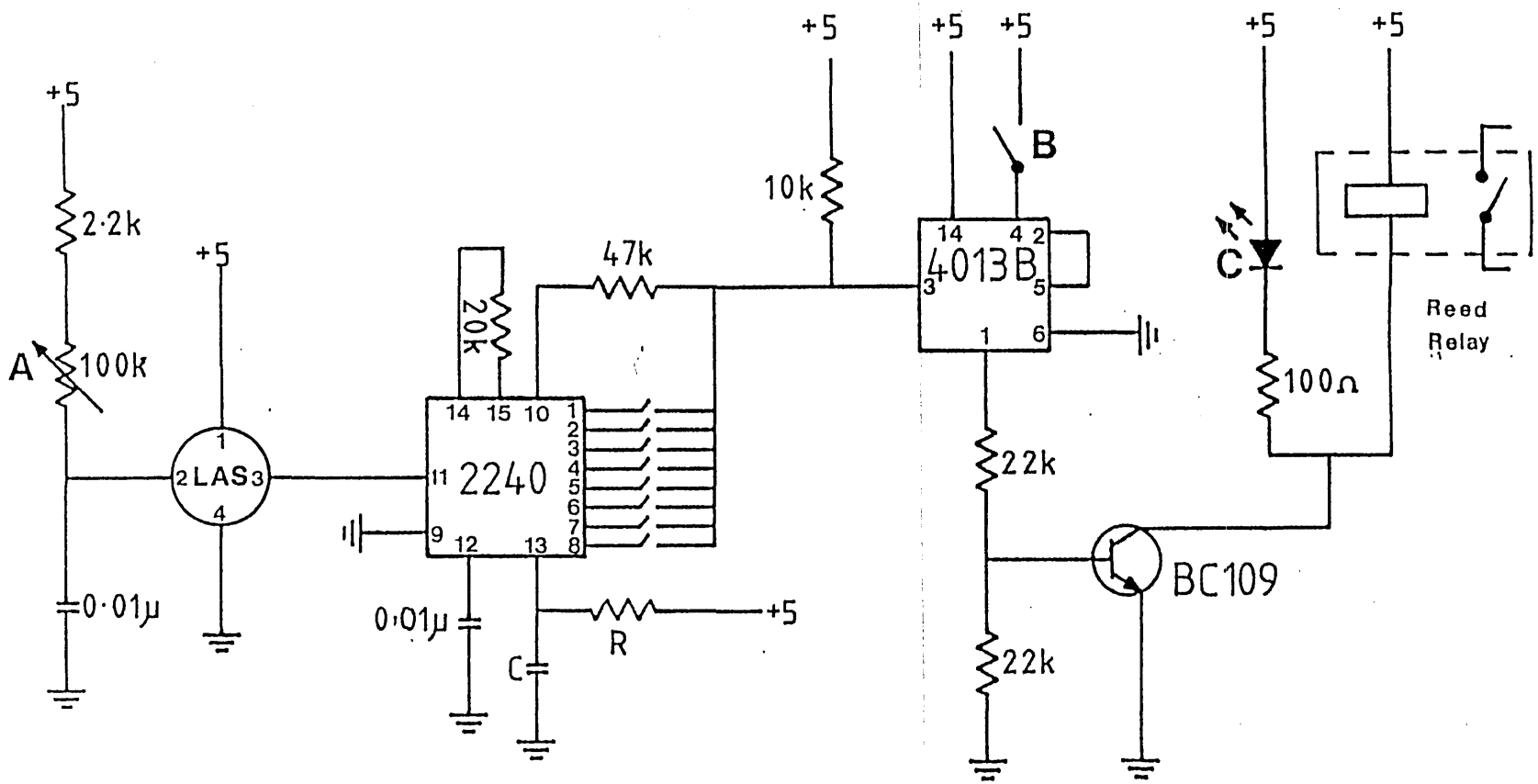
A light sensitive switch (**LAS**) (Radio spares part no. 305-434), when exposed to a light of sufficient intensity, allows a current to flow to pin 10 of an integrated circuit timer (**2240**). The sensitivity of the switch can be adjusted using the variable 100kΩ resistor (**A**).

The time delay, **t**, generated by the timer is equal to **nRC**, where **R** (ohm) and **C** (farad) are the resistance and capacitance of the RC network connected to pin 13, and **n** is a number, between 1 and 255, selected in binary by closing the switches on pins 1 to 8.

The output signal from pin 10 of the timer, triggers the flip-flop (**4013B**) to switch the state of pin 1. In the ground state no current can flow through the transistor (**BC109**), and consequently the light emitting diode (**C**) is unlit and the reed relay is switched open. When the output from the flip-flop is high, the transistor is switched, allowing a current to flow, thus lighting the LED and closing the relay. Closing the relay triggers the attached device (either camera or flash gun).

Switch (**B**) is used to reset the flip-flop to the ground state, the LED indicating whether the relay is open or closed.

Three identical circuits, as illustrated but with different set time delays, were used to produce the flash sequence. The circuit used to trigger the camera was slightly modified. Because the drop in light intensity at the LAS caused by a falling drop was so slight, the setting of the sensitivity of the switch was critical. To make the adjustment simpler and prevent the camera from being triggered while doing so, a switch was placed between pin 3 of the light activated switch and pin 11 of the timer. An additional transistor and LED were also added, to indicate the state of the LAS.


+5
2·2k
A
100k
0·01µ
+5
LAS3
20k
47k
2240
0·01µ
C
R
+5
10k
+5
+5
B
4013B
+5
+5
C
Reed
Relay
100Ω
22k
22k
BC109

Appendix 2

Trajectory program listing

The Fortran 4 program for calculating droplet trajectories is listed on the following pages. The listing includes the routines for calculating turbulence. The program was implemented on Rothamsted's HP1000 minicomputer, and also, in a different form on a BBC micro.

Some routines are not included in the listing, these perform the following functions.

AXLL	Axis plotting routine
CODE	Writes hollerith string specified by next statement into array
GAUSS	Generates a pseudo-random number between -1 and 1 with a gaussian distribution
GCLER	Clears graphics screen
GDUMP	Dumps graphics screen to printer
PLTL	Plots values in arrays specified by first two parameters as lines on screen
RMPAR(<var>)	Places an integer value corresponding to the current terminal into <var>

List of Principle variables.

A	$1+\rho/2$
ALFAW,ALFAU	α_w, α_u
B	$(1-\rho)g$
BETAW,BEATU	β_w, β_u
C	$3\rho/4d$
CDMC	Drag coefficient of sphere, Cd
CH	Crop height, m
D	Droplet diameter, *d*, m
D (in MC4)	Zero plane height, m

D1U etc	Increments $\Delta_1 U_i$, etc
DIV etc	Increments $\Delta_1 V_i$, etc
DIX etc	Increments $\Delta_1 x_i$, etc
DIY etc	Increments $\Delta_1 y_i$, etc
DSWZ2	$d\sigma_w^2/dz$
DT	Size of time steps, s
DTONTL	DT/TLZ
G	Gravitational acceleration, g, m s^{-2}
GAMAW,GAMAU	γ_w, γ_u
H	Size of increment in T, s
I	Step counter
IP	Value returned by RMPAR
IREP	Step counter
IXL,IYL	Arrays holding x and y axis labels
IY	Branch determination variable
LOOP	Step counter
LU	Terminal device number
NU	Kinematic viscosity of air, υ, $m^2 s^{-1}$
PI	π
RE	Reynolds number
RHO	Density of water, ρ
RHOBAR	Density ratio, ρ, or ρ_f/ρ_p
RHOF	Density of air, ρ_f, kg m^{-3}
SEED	Value used to initialise gaussian random number generator
SU,SW	Horizontal and vertical components of root, mean square Eulerian velocity, σ_u, σ_w
T	Time, s
T0	Initial time, s
TIC	Axis tic spacing, cm
THETA0	Initial angle of droplet ejection, deg
TLX,TLZ	Horizontal and vertical Lagrangian time scale, T_L
U	Horizontal component of droplet velocity, u, m s^{-1}
USTAR	Wind friction velocity, U_*
UF	Horizontal component of air velocity, u_f, m s^{-1}

UF	Horizontal component of air velocity, u_f, m s^{-1}
V	Vertical component of droplet velocity, u, m s^{-1}
VF	Vertical component of air velocity, v_f, m s^{-1}
W	$Log_{10}Re$
W0	Initial speed of droplet, w_0, m s^{-1}
WF	Speed of air relative to sphere, w_r, m s^{-1}
WRAND	Gaussian random number, r
X,Y	Horizontal, x, and vertical, y position of droplet, m
X0,Y0	Initial horizontal, x_0, and vertical, y_0, position of droplet, m
XMIN,YMIN	Limits of axis to be plotted on screen, cm
XMAX,YMAX	
XP,YP	Arrays holding last 10 calculated horizontal, XP, and vertical, YP, positions of droplet, to be plotted on screen
Z	Droplet height, m, (in MC4)

```
0001 FTN4,L
0002       PROGRAM FLIT4
0003
0004 C     Program to calculate and plot the trajectory of
0005 C     a droplet in a turbulent airstream.
0006       DIMENSION IP(5),XP(10),YP(10),IXL(10),IYL(10)
0007       EXTERNAL FYMC,FXMC
0008       COMMON A,B,C,D,NU,PI
0009       REAL NU
0010       CALL RMPAR(IP)
0011       LU=IP(1)
0012       WRITE(LU,100)
0013       READ(LU,*)LP
0014 100   FORMAT('**TYPE PRINTER LU NUMBER**'/
0015       WRITE(LU,110)
0016 110   FORMAT('Enter  seed for random  number  generator  (0-1)',
0017       READ(LU,*)SEED
0018       CALL GAUSS(SEED)
0019 C     Assign input data
0020       DATA RHO,RHOF,G /2950.0,1.22,9.8/
0021       DATA T0,X0 / 2*0.0 /
0022 200   CONTINUE
0023
0024       WRITE(LU,120)
0025 120   FORMAT(/'Input min and max height [cm]'/)
0026       READ(LU,*)YMIN,YMAX
0027       WRITE(LU,130)
0028 130   FORMAT('Input tic spacings'/)
0029       READ(LU,*)TIC
0030       XMAX=(YMAX-YMIN)*1.38*2
0031       CALL CODE
0032       WRITE(IXL,140)
0033       CALL CODE
0034       WRITE(IYL,140)
0035 140   FORMAT('cm')
0036 210   CONINUE
0037       CALL AXLL(0.,XMAX,YMIN,YMAX,100,20,500,310,TIC,TIC,
0038      +IXL,IYL,3,3)
0039       YMIN=YMIN/100
0040       XMAX=XMAX/100
0041       YMAX=YMAX/100
0042       IL=3
0043       WRITE(LU,150)
0044 150   FORMAT ('Enter droplet diameter (microns) 0 to quit')
0045       READ(LU,*)D
0046       DT=0.002
0047       IF (D.EQ.0.) GOTO230
0048       IF(D.LE.100.)DT=0.0002
0049       D=D*1.0E-6
0050
0051       WRITE(LU,155)
0052 155   ('Enter height of droplet release [cm]',/)
0053       READ(LU,*)Y0
0054       WRITE(LU,160)
0055 160   FORMAT('Enter droplet speed and angle to x-axis'/)
```

```
0056        READ(LU,*)WO,THETAO
0057        RHOBAR=RHOF/RHO
0058        NU=1.49E-5
0059        PI=3.14159
0060        A=1.+RHOBAR/2
0061        B=(1. -RHOBAR)*G
0062        C=3.*RHOBAR/(4.*D)
0063
0064        DO 340 IREP=1,20
0065
0066        WRITE(LP,20)D,WO,THETAO
0067        T=TO
0068        X=XO
0069        Y=YO/100
0070        VF=0.01
0071        UFA=VF
0072        U=WO * COS(THETAO*PI/180.)
0073        V=WO * SIN(THETAO*PI/180)
0074        WOLD=WO
0075 1      CONTINUE
0076        I=0
0077 2      WRITE(LP,30) T,X,Y,U,V
0078        CALL PLTL(XP,YP,0.,XMAX,YMIN,YMAX,100,20,500,310,IL,10)
0079        IF((X.GT.XMAX).OR. (Y.GT.YMAX)) GOTO 6
0080 C      ************************************************
0081 C      Forth order Runge Kutta method used to integrate
0082 C      the equations of motion.
0083 3      IF (Y.GT.0.0)CALL MC4(X,Y,UFA,VF,DT)
0084        CALL KUTTB(X,Y,U,V,T,FXMC,FYMC,VF,UFA,DT)
0085        IF (Y.LE.YMIN)GOTO 4
0086        I=I+1
0087        XP(I)=X
0088        YP(I)=Y
0089        IF(I.EQ.10) GOTO1
0090        GOTO 3
0091 4      WRITE(LP,30)T,X,Y,U,V
0092        DO 5 LOOP=I,10
0093        XP(LOOP)=XP(LOOP-1)
0094        YP(LOOP)=YMIN
0095 5      CONTINUE
0096        CALL(PLTL(XP,YP,0.,XMAX,YMIN,YMAX,100,20,500,310,IL,10)
0097 6      CONTINUE
0098 340    CONTINUE
0099 230    WRITE(LU,60)
0100        READ(LU,50)IY
0101        IF(IY .NE. 2HYE) GOTO240
0102        CALL GDUMP
0103 240    WRITE(LU,70)
0104        READ(LU,*)IY
0105        IF(IY.EQ.0)STOP
0106        IF(IY.EQ.2.OR.IY.EQ.3)CALL GCLER
0107        IF(IY.EQ.1.OR.IY.EQ.2)GOTO 260
0108        IF(IY.EQ.3)GOTO200
0109        GOTO240
```

```
0110 260  CONTINUE



0111       YMIN=YMIN*100
0112       YMAX=YMAX*100
0113       XMAX=XMAX*100
0114       GOTO 210
0115
0116
0117 20    FORMAT(//1X, 'DIAMETER=',E13.4,'      INITIAL SPEED ='
0118      +,F6.3,19H M/SEC,      THETA0 =,F3.0 , 8H DEGREES /
0119      +4X,1HT, 12X,1HX, 12X1HY,15X,'U',12X,'V',/ 2X,5H(SEC)
0120      +9X,3H(M), 10X,3H(M), 11X,'(M/SEC)',6X,'(M/SEC)' )
0121 30    FORMAT(F7.2, 2X, 1P2E13.4, 3X, 1P2E13.4 )
0122 50    FORMAT(10A2)
0123 60    FORMAT(/'Do you wish to dump graphics YE\NO'/,)
0124 70    FORMAT(/'>0< to stop',/,'>1< to continue',
0125      +/,'>2< to clear graphics and continue',
0126      +/,'>3< to draw new axis and continue'/)
0127
0128       END
```

```
C*************************************************************************
      SUBROUTINE MC4 (X,Z,UFA,WF,DT)
C     Markov chain routine
      CH=1.0
      USTAR=0.24
      D=0.75*CH
      IF(Z.LE.CH)GOTO 1
      SW=1.25*USTAR
      SU=SW
      TLZ=0.32*(Z-D)/SW
      TLX=TLZ
      GOTO 2
1     SW=(1.25*(Z-CH)+0.125)*USTAR
      SU=SW
      TLZ=0.32*(CH-D)/(USTAR*1.25)
      TLX=TLZ
2     CONTINUE
      DSWZ2=0.09+1.0E-20*Z
      DTONTL=DT/TLZ
      ALFAW=EXP(-DTONTL)
      ALFAU=EXP((-DTONTL)*TLZ/TLX)
      BETAW=SQRT(1-ALFAW**2)
      BETAU=SQRT(1-ALFAU**2
      GAMAW=1-ALFAW
      GAMAU=1-ALFAU
      WRAND=SW*GAUSS(0.0)
      WF=ALFAW*WF+BETAW*WRAND+GAMAW*DSWZ2*TLZ
      WRAND=SU*GAUSS(0.0)
      UFA=UFA*ALFAU+BETAU*WRAND+GAMAU*DSWZ2*TLX
      RETURN
      END
C*************************************************************************
      FUNCTION FYMC(X,Y,U,V,T,VF,UFA)
      COMMON A,B,C,D,NU,PI
      IF(Y.GE.1.01)UF=Y*Y*2.0+0.37
      IF(Y.LT.1.01.AND.Y.GT.0)UF=ALOG(Y*10+1)
      UF=UF+UFA
      WR=SQRT((UF-U**2+(VF-V)**2)
      FYMC=(-B+C*CDMC(WR)*(VF-V)*WR)/A
      RETURN
      END
C*************************************************************************
      FUNCTION FXMC(X,Y,U,V,T,VF,UFA)
      COMMON A,B,C,D,NU,PI
      IF(Y.GE.1.01)UF=Y*Y*2.0+0.37
      IF(Y.LT.1.01.AND.Y.GT.0)UF=ALOG(Y*10+1)
      UF=UF+UFA
      WR=SQRT((UF-U**2+(VF-V)**2)
      FXMC=     C*CDMC(WR)*(UF-U)*WR /A
      RETURN
      END
```

```
C*****************************************************************
      SUBROUTINE KUTTB(X,Y,U,V,T,F1,F2,VF,UFA,H)
C     Fourth order two dimensional Runge-Kutta formulae
      COMMON A,B,C,D,NU,PI
      D1X = H*U
      D1Y = H*V
      D1U = H*F1(X,Y,U,V,T,VF,UFA)
      D1V = H*F2(X,Y,U,V,T,VF,UFA)
C
      D2X = H*(U+D1U/2.)
      D2Y = H*(V+D1V/2.)
      D2U = H*F1(X+D1X/2.,Y+D1Y/2.,U+D1U/2.,V+D1V/2.,T+H/2,VF,UFA)
      D2V = H*F2(X+D1X/2.,Y+D1Y/2.,U+D1U/2.,V+D1V/2.,T+H/2,VF,UFA)
C
      D3X = H*(U+D2U/2.)
      D3Y = H*(V+D2V/2.)
      D3U = H*F1(X+D2X/2.,Y+D2Y/2.,U+D2U/2.,V+D2U/2.,T+H/2,VF,UFA)
      D3V = H*F2(X+D2X/2.,Y+D2Y/2.,U+D2U/2.,V+D2V/2.,T+H/2,VF,UFA)
C
      D4X = H*(U+D3U)
      D4Y = H*(V+D3V)
      D4U = H*F1(X+D3X,Y+D3Y,U+D3U,V+D3U,T+H,VF,UFA)
      D4V = H*F2(X+D3X,Y+D3Y,U+D3U,V+D3U,T+H,VF,UFA)
C
      T=T+H
      X=X+(D1X+2.*D2X+2.*D3X+D4X)/6
      Y=Y+(D1Y+2.*D2Y+2.*D3Y+D4Y)/6
      U=U+(D1U+2.*D2U+2.*D3U+D4U)/6
      V=V+(D1V+2.*D2V+2.*D3V+D4V)/6
      RETURN
      END
C*****************************************************************
      FUNCTION CDMC(V)
      COMMON A,B,C,D,NU,PI
      REAL NU
      RE = ABS(V)*D/NU
      IF( RE.EQ.0. )CDMC=0
      IF( RE.LT.0.01 .AND. RE.GT.0. )CDMC=3./16.+24./RE
      IF (RE.LT.0.01) GOTO 11
      W = ALOGT(RE)
      TEMP=1.+0.1315*RE**(0.82-0.05*W)
      IF( RE.GT.0.01 .AND. RE.LE.20. )CDMC =24./RE* TEMP
      IF(RE.GT.20..AND.RE.LE.260.)CDMC=24.RE*(1.+0.1935*RE**0.6305)
      TEMP=1.6435-1.242*W+0.1558*W*W
      IF(RE.GT.260..AND.RE.LE.1500.)CDMC=EXP(2.303*TEMP)
      TEMP=-2.4571+2.5558*W-0.9295*W*W+0.1049*W**3
      IF(RE.GT.1.5E+3.AND.RE.LE.1.2E+4)CDMC=EXP(2.303*TEMP)
11    RETURN
      END
C*****************************************************************
```

Publications

Macdonald, O.C. and McCartney, H.A., (1987). Calculation of splash droplet trajectories. *Agricultural and Forest Meteorology*, **39**, 95-110.

Macdonald, O.C. and McCartney, H.A., (1989). An investigation of the splashing of water drops on leaves. *Annals of Applied Biology*, **113**, 627-638.

Ann. appl. Biol. (1988), **113**, 627–638
Printed in Great Britain

A photographic technique for investigating the splashing of water drops on leaves

BY O. C. MACDONALD* AND H. A. MCCARTNEY

Plant Pathology Department,
AFRC Institute of Arable Crops Research,
Rothamsted Experimental Station, Harpenden, Herts. AL5 2JQ

(*Accepted 15 July 1988*)

SUMMARY

The formation of splash from water drops falling onto bean leaves was investigated by multiple exposure flash photography. A relatively simple technique was developed which recorded up to four images at 2 ms intervals, of a splash on one photograph. The images were recorded on colour reversal film, and the flash sequence was colour coded to aid the interpretion of the superimposed images. Analysis of the photographs allowed measurement of the initial speed and angle of ejection of different sized splash droplets. Droplets were ejected at speeds of up to about 10 m s^{-1} although most speeds were less than about 3 m s^{-1}, and small droplets tended to travel faster than large ones. Droplets were ejected at all angles but the majority were ejected almost horizontally; there was little correlation between droplet size and angle of ejection. Deposition patterns estimated from calculated droplet trajectories compared well with measured ones.

INTRODUCTION

In this paper we describe a technique for measuring the initial velocities and sizes of droplets ejected by splash from leaves. Disease propagules can be transported by rain splashing on infected plant material (Gregory, 1973) or on soil containing spores (Gregory, Griffin, Maddison & Ward, 1984). Most studies of the role of splash in disease dispersal have concentrated either on the entrainment of propagules into water drops or on the description of spore deposition gradients or disease gradients resulting from dispersal (Brennan, Fitt, Taylor & Colhoun, 1985; Fitt & Lysandrou, 1984; Gregory, Guthrie & Bunce, 1959; Stedman, 1980; Walker & Patel, 1964). However, Shaw (1987) describes a simple 'splashmeter' apparatus to estimate the potential for vertical transport of splash droplets in crops by measuring the distance travelled by splash droplets from an annular trough containing dye.

If the parameters of velocity and speed can be quantified, trajectory models, such as that described by Macdonald & McCartney (1987), can be applied to the dispersal of splash-borne pathogens. Splashing has only been studied in detail for drop impacts on solid and particulate surfaces or with water films lying on such surfaces (Engel, 1955; Ghadiri & Payne, 1979; Gregory *et al.*, 1959; Hobbs & Kezweeny, 1967). There is little information about splash on leaf surfaces or considering splash in relation to disease dispersal.

Previous investigations have used high speed cinematography to analyse the splash process on various surfaces (Ghadiri & Payne, 1979; Ferriera & Singer, 1985). The equipment and materials required for such a study are expensive. Reynolds, Madden, Reichard & Ellis (1987) described a technique using high-speed multi-image photography to investigate splash. In

* Present address: MAFF, Harpenden Laboratory, Hatching Green, Harpenden, Herts. AL5 2BD

© 1988 Association of Applied Biologists

this paper we describe a similar, though simpler technique and illustrate its use by describing experiments examining splash on bean leaves.

METHODS

The objective was to measure the speed, size and angle of ejection of splash droplets from photographs of splash. The diameter of a droplet can be measured directly from photographs, provided the exposure time is sufficiently short to freeze any motion. The velocity and direction of motion can be computed by recording the droplet's position at two different times. All three objectives can be achieved by multiple exposure photography. Because the splash process is completed in only a few milliseconds it is impractical to use a conventional mechanical shutter to achieve a multiple exposure image. We therefore chose a method where the splash process was illuminated by successive short duration flashes while the camera shutter remained open.

Apparatus for photographing splash

Fig. 1 illustrates the apparatus used to take multiple image photographs of drops of water falling onto a leaf. When a drop was detected above the leaf, a signal opened the shutter of a

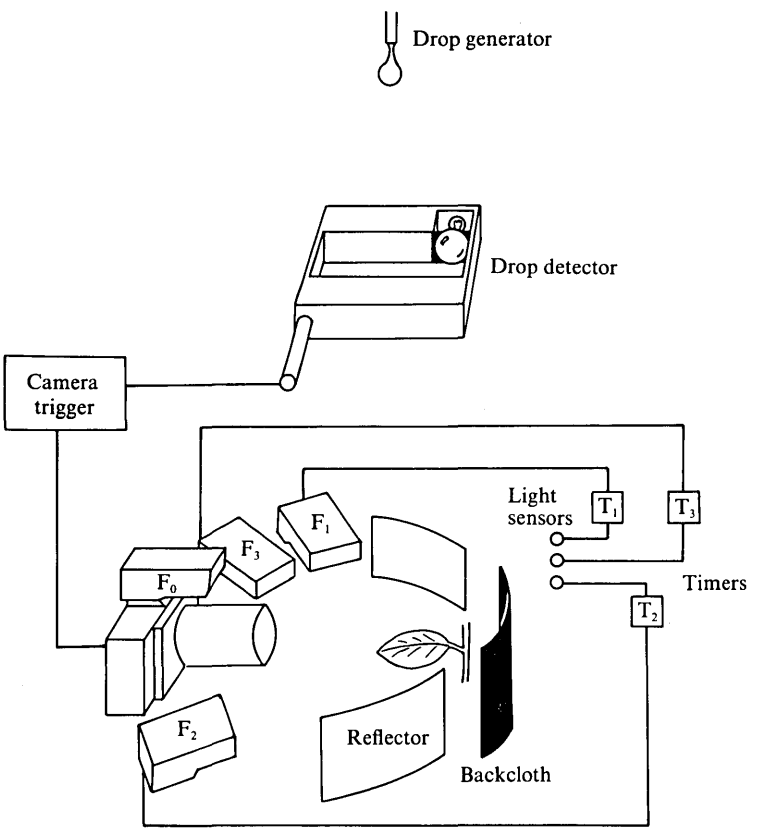


Fig. 1. Schematic diagram of the layout for taking multiple image photographs. Droplets fall through the drop detector triggering a light activated switch and activating the camera trigger. Flash gun F_0 is fired by the camera when the shutter opens. Light sensors detect this flash, starting timers T_1–T_3 which after pre-set delays trigger flash guns F_1–F_3.

camera and triggered up to four flash lamps in a predetermined sequence while the shutter remained open.

The drop detector comprised a collimated light beam from a 6 V torch bulb directed at a shallow angle between two parallel mirrors about 5 × 2·5 cm placed 5 cm apart (Fig. 2). Reflecting the light beam between the two mirrors increased the area over which a drop could be detected. The light was gathered at the opposite end of the mirrors by a light-sensitive switch (Radio Spares part no. 305 – 434) mounted in a long tube to shield it from ambient light. A drop passing between the mirrors reduced the light intensity entering the tube and activated the light-sensitive switch. The signal from the switch, after an adjustable time delay (Fig. 3), closed a relay operating the camera shutter. The height of the droplet detector above

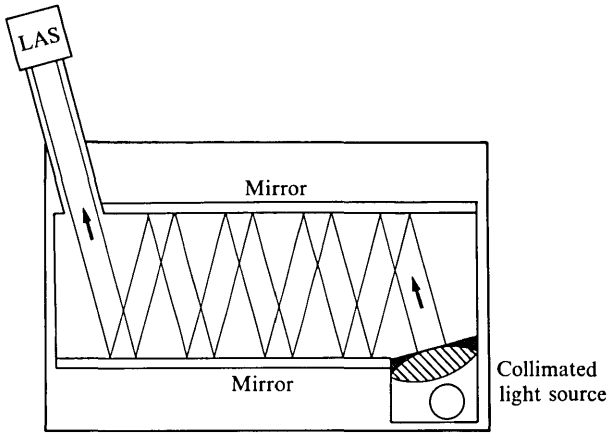


Fig. 2. Schematic diagram of drop detector. Drops moving through the plane of the paper are detected when they cause a reduction in light intensity at the light activated switch (LAS).

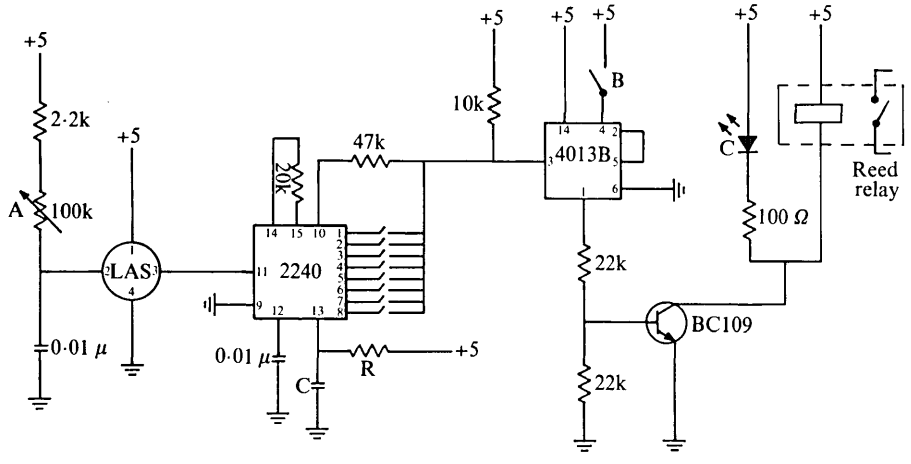


Fig. 3. Circuit diagram of delay circuit used to trigger camera and flash guns. The 100KΩ variable resistor (A) controls the sensitivity of the light activated switch (LAS). The time delay is determined by t = nRC, where R (ohm) and C (farad) are the resistance and capacitance of the RC network connected to pin 13 of the integrated circuit timer (2240) and the value of n (between 1 and 255) is set by closing the switches on pins 1 to 8. The output from the timer triggers the flip-flop (4013B) which determines whether the relay is activated or not. The switch (B) can be used to reset the flip-flop. The state of the relay is indicated by the LED (C).

the target leaf and the length of the time delay were adjusted so that the splash and the photography coincided. The time delay was usually set to zero as there was an inherent delay of about 100 ms between closure of the relay contact and the opening of the camera shutter.

Two methods of synchronising the drop impact and flash sequence were used. In one method the leaf was replaced by a microphone connected to a dual trace oscilloscope. The signal from the drop striking the microphone was compared with the simultaneously recorded signal from a light sensor responding to the flash lamps and the height of the drop detector or the time delay adjusted accordingly. In the other method a video camera (Hitachi HV730K), was substituted for the film camera and the splash recorded using a video tape recorder (JVC BR6400-TR). The recorded image was used to synchronise the splash and photography. The film camera was returned after the droplet detector had been correctly adjusted. The use of the video camera had two advantages; the leaf did not have to be moved, and some idea of the appearance of the splash in the photographs was obtained before the pictures were actually taken. The resolution of the recorded video image was insufficient to allow accurate measurement of droplet size or velocity and so could not be used in the experiments.

The photographs were taken using an Olympus OM-2 or OM-2n 35 mm single lens reflex camera. A flash lamp (Olympus T32) mounted on the camera was fired automatically when the shutter opened. The light from this flash was detected by three light-sensitive switches each of which operated another flash lamp after a preset adjustable delay (Fig. 1). The time delay circuits were similar to that used for the droplet detector (Fig. 3). The secondary flash lamps were placed to give oblique lighting across the field of view. Water drops illuminated by a single bright source produced strong localised internal reflections leaving much of the drop invisible. This can lead to the size of the drop being underestimated. To give more even illumination, reflectors were placed around the target, outside the field of view. A small amount of sodium fluorescein (about 1 g/litre) added to the water rendered the droplets slightly opaque. This amount of fluorescein has no significant effect on surface tension and is therefore unlikely to have any effect on the splash process (Timmons, Mutcheler & Sherstad, 1971). The bright field illumination used by Reynolds *et al.* (1987), in which light sources shine directly into the lens, can give better quality photographs and make droplets more easily visible. However, this form of illumination is costly and is particularly difficult to arrange if the film is to retain enough reactivity to record subsequent superimposed images.

Separation of the multiple-images was aided by placing coloured filters over the flash lamps and using colour reversal film (Ilford, Ilfochrome, rated at ASA 100 or Agfa, Agfa-Chrome rated at ASA 200). The time delay between the flashes, typically 2 ms, was measured with an accuracy of about 0·05 ms using a light sensor and oscilloscope. For most of the photographs the duration of each flash was about 0·025 ms. However to aid the measurements of fast-moving droplets one or more of the flash lamps could be set to produced a flash of about 0·5 ms duration. The droplet then left a streak rather than a frozen image and the velocity of the droplet was determined by measuring the length of the streak. However, as the distance over which measurements were taken was small and the exact ends of the streak were difficult to define, the accuracy of this method of determining droplet velocities, typically around $\pm$ 0·4 m s^{-1}, was not as good as that (about $\pm$ 0·1 m s^{-1}) obtained when measuring the distance between images.

Several lens and extension tube combinations were used to give fields of view between about 70 × 50 mm and 140 × 100 mm on 35 mm film. The resolution of the film allowed measurements of distance to be made with an accuracy of better than 50 μm.

Analysis of the photographs

The developed photographs were projected onto a screen and the size and position of individual droplets relative to the centre of splash was recorded. To ensure that droplet

trajectories were parallel to the focal plane of the camera only the images of droplets which remain in sharp focus during the exposure were measured. The uncertainty in speed due to droplets moving through the focal plane depended on droplet speed, but was generally small. For fast moving droplets this uncertainty was less than 1% while the speed of slow moving droplets would have been underestimated by at most 10%. The speed and direction of a droplet was then calculated from its position at different times. When a flash of long duration was used the image streak aided in identifying the series of images corresponding to individual droplets.

Droplets are not produced at the point of impact but at the edge of the corona over a period of several ms. Measurements of droplet velocity were therefore made at distances of up to 100 mm from the splash. All droplets would have lost a proportion of their initial speed and may also have changed their direction due to the effects of gravity. In some cases, particularly for smaller droplets, this change was quite large in relation to their initial velocity. As a convenient reference point the effective velocity of droplets at the point of impact was calculated using the model described by Macdonald & McCartney (1987). Initial velocities were estimated either by running the model in reverse or by comparing the trajectories observed with a table of trajectories calculated by the model.

Photographic experiments

Drops of water were allowed to fall from a height of 2·8 m onto the lower leaves of greenhouse-grown broad bean plants (*Vicia faba* cv. Minden). Whole plants about 30 cm tall were used for the experiments. The target leaves were attached to the plant and were not artificially supported in any way. Only near horizontal leaves were chosen as targets. When upper leaves shielded the target leaf they were removed.

The drops were produced by pumping water from a syringe pump at a steady rate through a hypodermic needle. The size of drops was determined by collecting a known number in a Petri dish and weighing them. The average weight of each drop was found to be 34 mg. Measuring drop diameter from photographs may have been misleading as large drops are not spherical but tend to be flattened at the leading edge, and oscillate as they fall (Pruppacher & Beard, 1970). Drops of 34 mg have an equivalent spherical diameter of about 4 mm. Although 4 mm drops are larger than most rain drops, experimental measurements (Fitt *et al.*, 1988) and theoretical analysis (P. J. Walklate, unpublished data) suggest that only large rain drops are important in dispersing plant pathogens. The steady stream of droplets produced meant that splashes occurred on wet leaves; no attempt was made to remove water that settled on the leaves.

Droplet collection experiments

In a parallel series of experiments carried out under identical conditions to the photographic investigations, splash droplets were collected and sized.

Droplets were collected on photographic film that had been fixed to remove the silver halide. Droplets landing on the film dissolved the gelatine layer and left a crater the diameter of which is directly proportional to the size of the droplet (Fitt, Lysandrou & Turner, 1982). The film was placed at distances up to 1 m from the target. To allow for droplets being ejected at angles close to or even below the horizontal, the sampling surfaces were placed 100 mm below the target. At each distance from the splash, the number and sizes of all droplets in a known area were measured and the number of droplets in each of 12 size classes deposited on concentric annuli around the splash calculated.

RESULTS AND DISCUSSION

Splash droplet diameters

The initial velocities of almost 400 splash droplets were determined from the photographs. Droplets ranged in size from less than 50 μm to over 1500 μm in diameter. Droplets that produced a projected image, on enlargement, less than 1 mm across were recorded as having diameters of that size. This corresponded to an actual diameter of about 50 μm. Droplets were ejected at all angles to the horizontal and with speeds of up to 11·5 m s^{-1}.

In the collection experiments droplets were detected at distances of up to 0·55 m from the target. The smallest droplets that could be detected on the collecting film were between 30 and 40 μm, the largest that were measured were nearly 2 mm in diameter. It was estimated that about 350 droplets larger than 50 μm were produced by each splash. The method of collection may have resulted in an underestimation of the number of droplets deposited close to the target because the large numbers deposited near the target tended to swamp it.

For both experiments droplet diameters were distributed log-normally with geometric means of 235 μm from the photographs and 228 μm for collected droplets. Geometric standard deviations were 0·35 and 0·38 respectively (Fig. 4). A similar distribution was previously described by Levin & Hobbs (1971) for splashes on solid surfaces. Between 100 and 1000 μm diameter, the distributions, as determined by the two methods, were indistinguishable suggesting that there was little bias in determining these size droplets from the photographs. The differences between the two distributions over the whole size range can be accounted for by the lower sensitivity of the photographic technique in the lower size range and to the small sample size measured in the photographs for the higher size range.

Droplet velocities

The distribution of droplet speeds was also approximately log-normal (Fig. 5) (geometric mean = 2·5 m s^{-1}, geometric standard deviation = 0·51). The maximum speed found was slower than has been observed from splashes on other surfaces such as liquid films and soil.

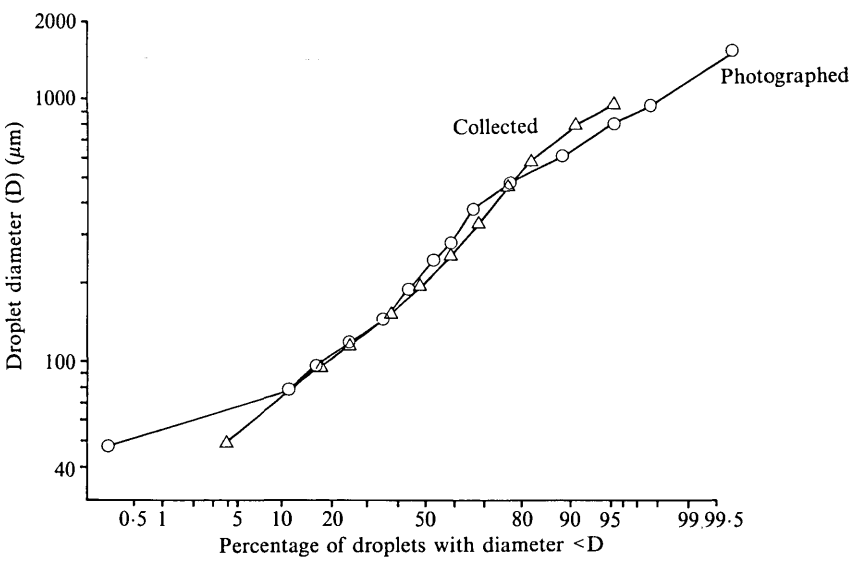


Fig. 4. Log-probability of droplet diameter distribution for both photographic (○ – ○) and collection (△ – △) experiments.

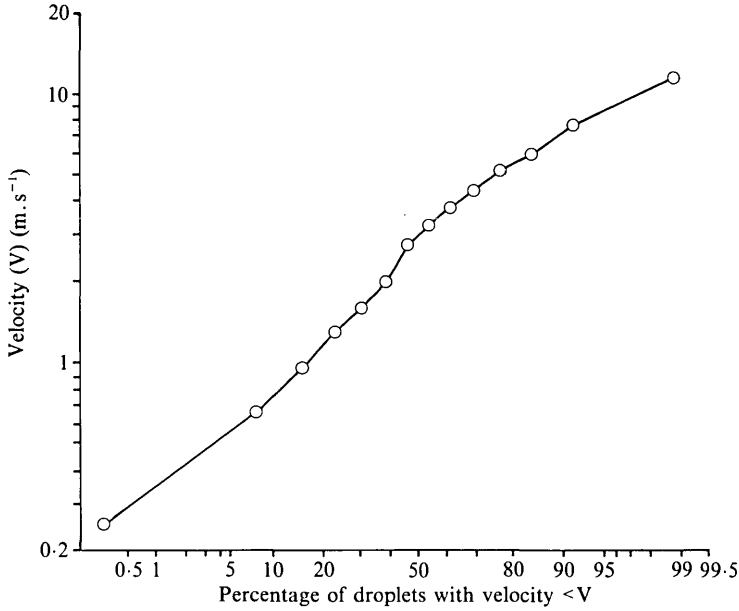


Fig. 5. Log probability plot of splash droplet velocity distribution.

For example, Ghadiri & Payne (1981) observed splashes of 22 mg drops falling 6·5 m onto saturated soil paste, the kinetic energy of those drops at impact was about 1·37 mJ which is similar to that for 34 mg droplets falling 2·8 m onto bean leaves (1·44 mJ). In their experiments, splash droplets with speeds of up to 20 m s^{-1} were observed while the maximum speed of droplets found in these experiments was only about 10 m s^{-1}.

The relationship between droplet speed and diameter is shown in Fig. 6. Smaller droplets had higher mean and maximum velocities than larger ones; the maximum speed of small

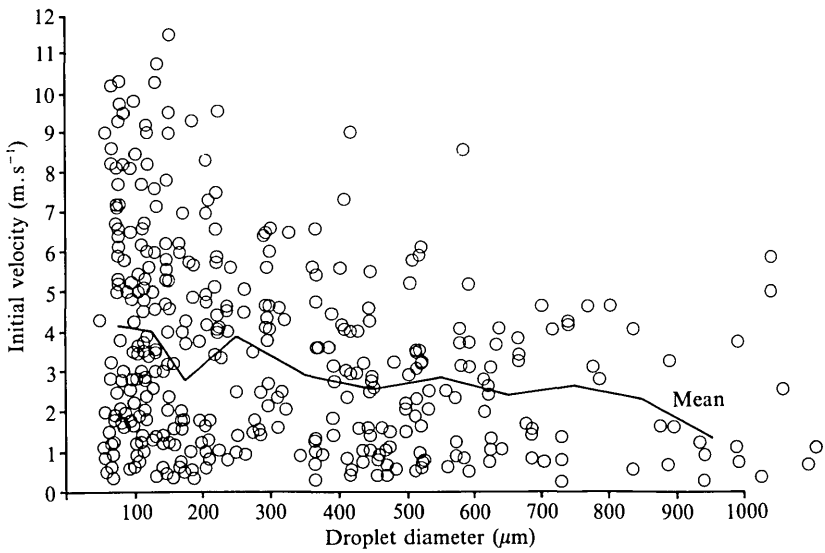


Fig. 6. Plot showing relationship between droplet diameter and droplet speed. ○ individual measurements, —— mean value.

droplets (< 100 μm) was about 2·5 times that for large droplets (> 800 μm). Ghadiri-Khorzoojhi (1978) found a similar trend for splashes on various particulate substrates, though the difference between the mean velocities of large and small droplets was greater in his experiments. For example, the mean speed of droplets between 200 and 400 μm produced by the splash of a 22·5 mg droplet falling 6·5 m onto soil paste was 5·24 m s^{-1} compared with only 3·70 m s^{-1} in our experiments; however the mean speed of droplets between 800 and 1000 μm was only 0·46 m s^{-1} from splashes on soil compared with 1·1 m s^{-1} for the leaf splash.

Fig. 7 shows the relationship between droplet speed and angle of ejection. There is a clear trend for faster moving droplets to be ejected at angles close to the horizontal, 41% of droplets with initial velocities greater than the median (3 m s^{-1}) were ejected at angles within 20° of the horizontal. Fig. 8 shows the same relationship for different droplet size classes and indicates that there is little dependency of the angle of ejection on droplet size. The only noticeable exceptions are for droplets with trajectories close to the vertical. The few droplets with high initial speeds, > 5 m s^{-1}, and vertically upward trajectories are all less than 500 μm in diameter while most droplets with steeply downward trajectories within 20° of the vertical, are larger than 300 μm. Studies of splash from liquid films or soil surfaces show that droplets splashed from such surfaces are ejected at steeper angles than those observed here. For example, for thin water films droplets are usually splashed at angles of between 40 and 60° to the horizontal (Mutchler, 1967) while from fine soils the angle of ejection is normally between 20 and 60° (Ghadiri-Khorzoojhi, 1978).

The initial speeds of droplets and the angles of their ejection appear to be different for splashes from bean leaves when compared to splashes from thin liquid films or soil (Ghadiri-Khorzooghi, 1978). These differences may be largely explained by considering the partitioning of the energy of the impacting raindrop during the splash process. Some of the momentum of the impacting drop would have been transferred to the leaf causing it to be deflected. We observed leaf movement of up to 20 mm during the splash process. Thus less energy would have been transferred to splash droplets resulting in lower initial velocities. The differences in angle of ejection were also partly a result of the change in leaf angle away from

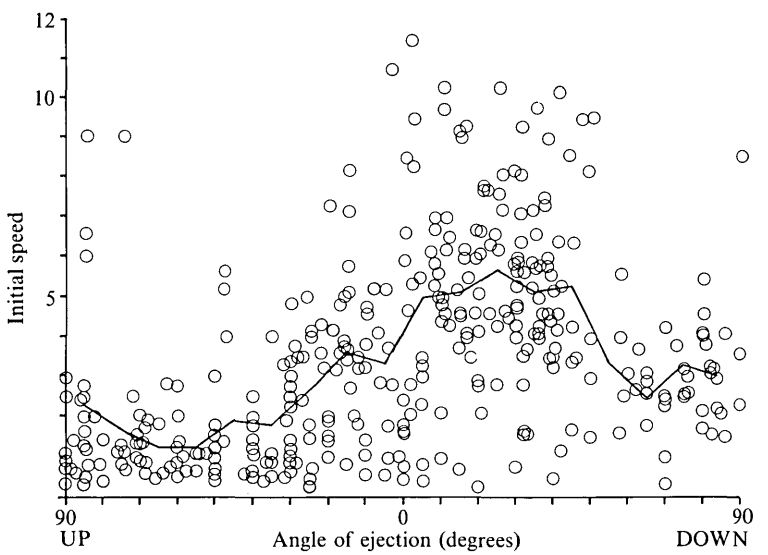


Fig. 7. Plot showing relationships between initial droplet speed and angle of ejection from splash. ○ individual measurements, —— mean value.

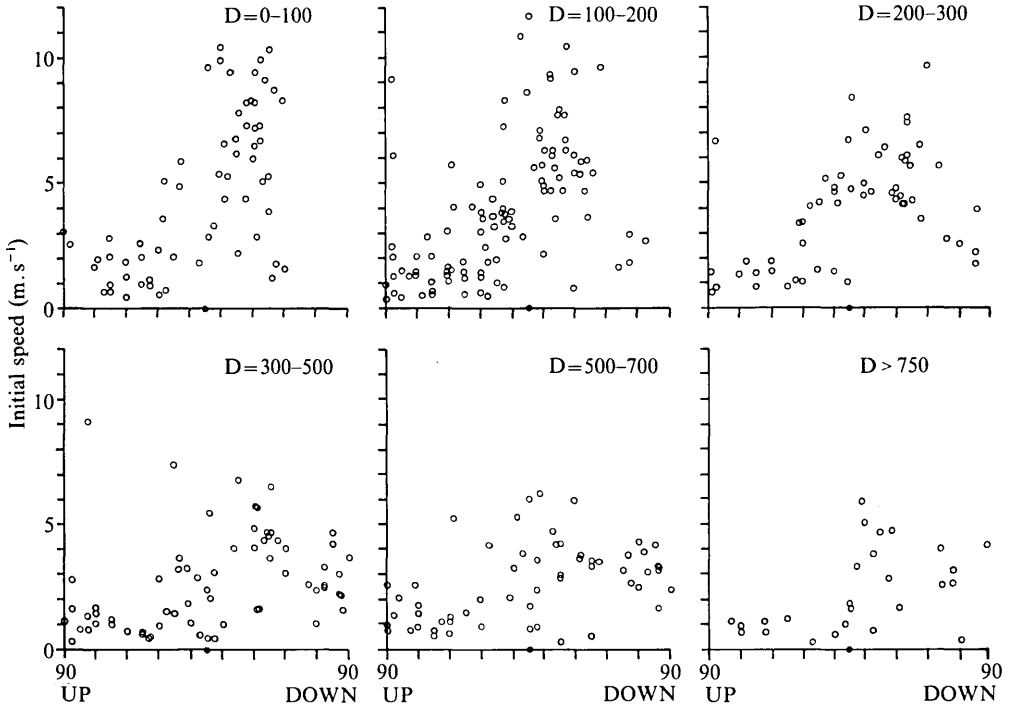


Fig. 8. Relationship between initial droplet speed and angle of ejection for different droplet size classes (D).

the horizontal due to leaf deflection although the leaf surface at the point of impact was often not horizontal which would also contribute to lowering ejection angles.

Horizontal dispersal

The number of droplets collected decreased exponentially with distance away from the splash. The exponential decay constant was about 0·087 cm^{-1}, corresponding to a half distance of about 8 cm. Droplet dispersal gradients of this type with similar length scales are typical of those produced by rain splash (Fitt & McCartney, 1986).

Measured values of initial velocities were used to calculate the trajectories of different sized droplets. From the calculations the relative number of droplets deposited 100 mm below the leaf at various distances was estimated. The deposition pattern derived from these estimates is compared with that found in the droplet collection experiments in Fig. 9. The two patterns compare well for distances greater than 7 cm from the point of impact suggesting that the photographic measurements are unbiased and form a representative sample of the population. The difference between estimated and collected deposition for distances less than 7 cm, is probably an experimental artefact. The number of droplets deposited very close to the target were difficult to measure accurately for two reasons: first, some droplets that travelled only a very short distance were re-deposited on the leaves, which were several centimetres across; second, the target tended to become swamped with the large numbers of droplets deposited close to the splash.

Vertical distribution

Knowledge of the maximum height reached by droplets is important in the prediction of the potential for vertical disease spread and for the dispersal of pathogen propagules out of a crop

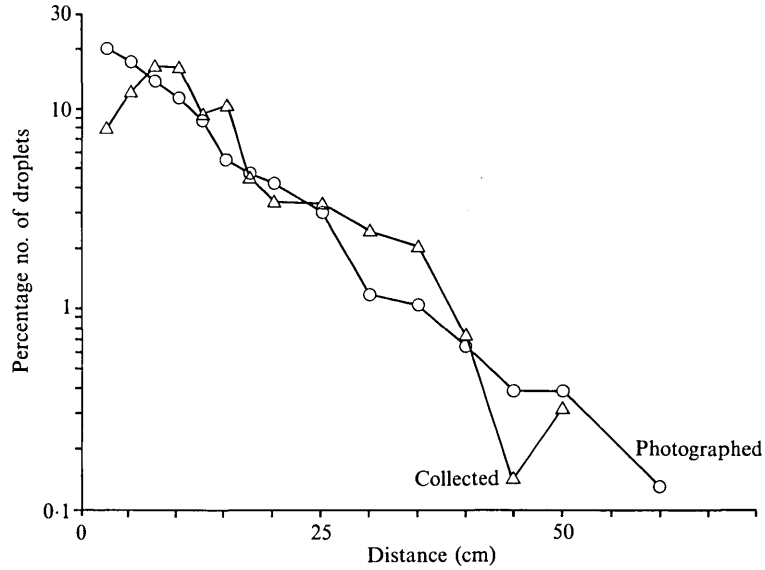


Fig. 9. Plot showing the percentage number of droplets collected △ − △, and calculated number of droplets deposited ○ − ○ with distance from the splash.

canopy. The maximum height reached by spash droplets was calculated from measurements of droplet diameter and initial velocity. The calculated maximum heights are shown plotted against droplet diameter in Fig. 10. There is little relationship between diameter and height except that the greatest heights were reached by droplets between 200 and 600 μm. Droplets of this size are probably the most important in dispersing fungal spores (Fitt & McCartney, 1986). In these experiments the maximum height reached was about 70 cm, but the vast majority of droplets (> 90%) did not travel more than 5 cm above the target.

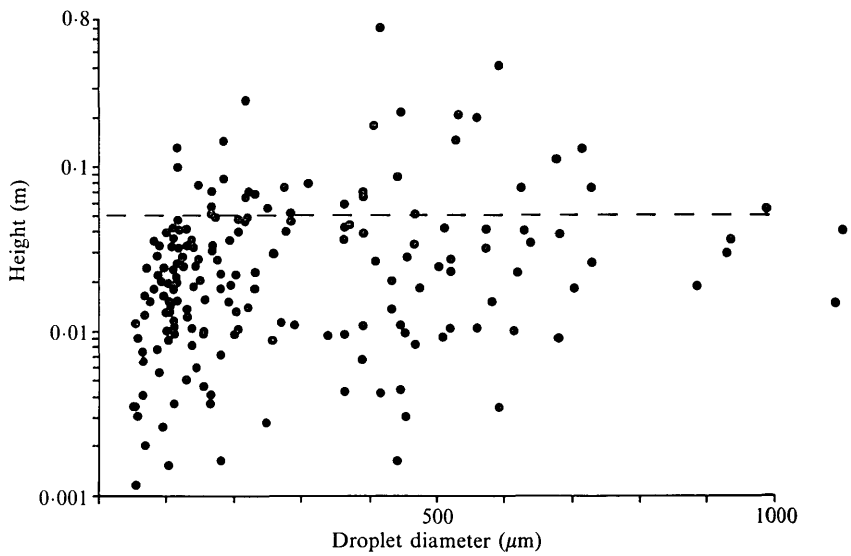


Fig. 10. Plot showing relationship between droplet diameter and the maximum height reached by droplets. The broken line indicates a height of 5 cm above the leaf.

GENERAL CONCLUSIONS

The apparatus and techniques described have proved suitable for measuring the initial velocities of splash droplets. The apparatus has the advantages of being cheap, portable and easy to use. Taking measurements from the resulting photographs proved rather tedious but it may be possible, at least partly, to automate the data extraction process using computerised image analysis techniques.

Droplets are ejected with velocities of up to about 12 m s^{-1} at all angles to the leaf, though the largest proportion were ejected horizontally. The maximum horizontal range at the height of the splash was about 55 cm and the maximum vertical range about 70 cm. However 90% of droplets were deposited within 15 cm of the target and did not reach heights greater than 5 cm above the leaf. Nevertheless, small droplets ($< 100\ \mu m$) may be dispersed significantly further by turbulent dispersal than indicated by these calculations. This is especially true if splashing occurs near the top of the canopy. The significance for disease spread of these droplets is not known.

The results described here, and those from subsequent experiments to be reported elsewhere, show that leaf splash is significantly different from splash on other surfaces. This suggests that care must be exercised when interpreting splash dispersal from liquid films or rigid surfaces in relation to dispersal from leaves. A detailed understanding of the splash process on leaves will allow an accurate prediction of the spatial and temporal dispersal of splash-borne pathogens, and the identification of rainfall events most likely to cause dispersal by splash. Thus an ability to identify when and how far splash-borne pathogens travel will lead to improvements in modelling and forecasting epidemics.

ACKNOWLEDGEMENTS

The authors would like to thank Dr P. J. Walklate for helpful discussions while preparing this paper.

REFERENCES

BRENNAN, R. M., FITT, B. D. L., TAYLOR, G. S. & COLHOUN, J. (1985). Dispersal of *Septoria nodorum* pycnidiospores by simulated rain and wind. *Phytopathologische Zeitschrift* **112**, 291–297.

ENGEL, O. J. (1955). Waterdrop collisions with solid surfaces. *Journal of Research of the National Bureau of Standards* **54**, 5, 281–298.

FERREIRA, A. G. & SINGER, M. J. (1985). Energy dissipation for water drop impact into a shallow pool. *Soil Science Society of America Journal* **49**, 1537–1541.

FITT, B. D. L. & LYSANDROU, M. (1984). Studies on mechanisms of splash dispersal of spores using *Pseudocereosporella herpotrichoides* spores. *Phytopathologische Zeitschrift* **111**, 323–331.

FITT, B. D. L., LYSANDROU, M. & TURNER, R. H. (1982). Measurement of spore-carrying splash droplets using photographic film and an image analysing computer. *Plant Pathology* **31**, 19–24.

FITT, B. D. L. & McCARTNEY, H. A. (1986). Spore dispersal in splash droplets. In *Water, Fungi and Plants*, pp. 87–104. Eds P. G. Ayres and L. Boddy. Cambridge: Cambridge University Press.

FITT, B. D. L., McCARTNEY, H. A., CREIGHTON, N. F., LACEY, M. E. & WALKLATE, P. J. (1988). Dispersal of *Rhynchosporium secalis* conidia from infected barley leaves and straw by simulated rain. *Annals of Applied Biology* **112**, 49–59.

GHADIRI-KHORZOOJHI, H. (1978). Raindrop impact, soil splash and cratering. Ph.D. Thesis, University of Reading.

GHADIRI, H. & PAYNE, D. (1979). Raindrop impact and soil splash. In *Soil physical properties*, pp. 95–104. Eds R. Lal and D. J. Greenland. Chichester: John Wiley.

GHADIRI, H. & PAYNE, D. (1981). Raindrop impact stress. *Journal of Soil Science* **32**, 41–49.

GREGORY, P. H. (1973). *The microbiology of the atmosphere*, 2nd edition. Aylesbury: Leonard Hill.

GREGORY, P. H., GRIFFIN, M. J., MADDISON, A. C. & WARD, M. R. (1984). Cocoa Black Pod: A reinterpretation. *Cocoa Growers Bulletin* No. 35.

GREGORY, P. H., GUTHRIE, E. J. & BUNCE, M. E. (1959). Experiments on splash dispersal of fungus spores. *Journal of General Microbiology* **20**. 328–354.

HOBBS, P. V. & KEZWEENY, A. J. (1967). Splashing of a water drop. *Science* **155**, 1112–1114.

LEVIN, Z. & HOBBS, P. V. (1971). Splashing of water drops on solid and wetted surfaces: hydrodynamics and charge separation. *Philosophical Transactions of the Royal Society* **A269**, 555–585.

MACDONALD, O. C. & McCARTNEY, H. A. (1987). Calculation of splash droplet trajectories. *Agricultural and Forest Meteorology* **39**, 95–110.

MUTCHELER, C. K. (1967). Parameters for describing rain splash. *Journal of Soil and Water Conservation* **22**, 91–94.

PRUPPACHER, H. R. & BEARD, K. V. (1970). A wind tunnel investigation of the internal circulation and shape of water drops falling at terminal velocity in air. *Quarterly Journal of the Royal Meteorological Society* **96**, 247–256.

REYNOLDS, K. M., MADDEN, L. V., REICHARD, D. L. & ELLIS, M. A. (1987). Method for study of raindrop impact on plant surfaces with application for predicting inoculum dispersal by rain. *Phytopathology* **77**, 226–232.

SHAW, M. W. (1987). Assessment of upward movement of rainsplash using a fluorescent tracer method and its application to the epidemiology of cereal pathogens. *Plant Pathology* **33**, 201–213.

STEDMAN, O. J. (1980). Splash droplet and spore dispersal studies in field beans (*Vicia faba* L.). *Agricultural Meteorology* **21**, 195–203.

TIMMONS, D. R., MUTCHELER, C. K. & SHERSTAD, E. M. (1971). The use of fluorescein to measure the composition of water drop splash. *Water Research* **7**, 1020–1023.

WALKER, J. C. & PATEL, P. N. (1964). Splash dispersal and wind as factors in the epidemiology of Halo blight of bean. *Phytopathology* **54**, 140–141.

(*Received 29 January 1988*)

Agricultural and Forest Meteorology, 39 (1987) 95–110
Elsevier Science Publishers B.V., Amsterdam — Printed in The Netherlands

CALCULATION OF SPLASH DROPLET TRAJECTORIES

O.C. MACDONALD and H.A. McCARTNEY
Rothamsted Experimental Station, Harpenden, Herts. AL5 2JQ (Gt. Britain)
(Received November 26, 1985; revision accepted July 15, 1986)

ABSTRACT

Macdonald, O.C. and McCartney, 1987. Calculation of splash droplet trajectories. Agric. For. Meteorol., 39: 95–110.

A model to predict the trajectories of water droplets in still air is presented and its application to the study of splash dispersed plant pathogens is briefly discussed. Comparison of predicted and observed sedimentation velocities showed there is very close agreement for droplets within the range of sizes typically produced by a splash. The initial velocities, size and distance travelled by droplets produced by a spinning disc atomiser and a vibrating needle were measured using a combination of photographic and collection techniques. Using the measured values for droplet size and initial velocity as the starting parameters for the model, the observed and predicted ranges of droplets were compared and good agreement between the two was found.

INTRODUCTION

After wind, splash is probably the most important mechanism for dispersing fungal and bacterial plant pathogens (Fitt and McCartney, 1986), particularly those that affect foliage and soft fruit. Despite its importance we still know very little about the physical mechanisms involved in the dispersal of pathogen propagules by splash. One important component process in dispersal is the flight of individual, spore-carrying, droplets.

Dispersal of foliar pathogen propagules, such as fungal spores, can be divided into three phases, the removal of spores from the site of infection, their movement through the air and finally their deposition onto a new site. Spores of splash-dispersed fungi are generally tightly held in a mat of mucilage that effectively prevents their removal from the leaf by wind or by leaf movement. When the mat is wetted however, as happens during rain or a heavy dew-fall, it swells and the spores are free to move into the surrounding film of liquid. Dispersal can then occur when either the liquid containing the spores drips off the original surface, possibly breaking up and further scattering spores on impact, or when a large rain drop or a drip from another leaf lands in the spore suspension causing a splash and thus dispersing spores in droplets.

Laboratory (Gregory et al., 1959; Brennan et al., 1984b) and field (Fitt and Bainbridge, 1983) studies indicate that most spores are generally carried in large droplets, ($> 200\,\mu m$). For example, the number of spores of *Pseudocercos-*

0168-1923/87/$03.50 © 1987 Elsevier Science Publishers B.V.

porella herpotrichoides and *Pyrenopeziza brassicae* carried by droplets were dependent upon the surface area of the droplet (Fatemi and Fitt, 1983); about 90% of *Pseudocercosporella herpotrichoides* spores were dispersed in droplets greater than 400 μm (Fitt and Lysandrou, 1984). Such droplets are quickly deposited because of their relatively large settling velocity and are likely to travel only short distances, even in moving air (Stedman, 1980a; Brennan et al., 1984a). Observations that disease incidence caused by typically splash-dispersed pathogens declines quickly within a short distance away from a source of infection (Fitt and McCartney, 1986) also indicate that spore dispersal in splash is generally over short distances. Smaller droplets may be entrained in air currents and carried much further, possibly to start new disease foci. Small numbers of airborne spores were collected above wheat straw naturally infected with *P. herpotrichoides*, spread on fallow ground (Fitt and Bainbridge, 1983). However the epidemiological significance of this is uncertain as the number of spores required to cause a lesion is unknown.

The trajectories of splash droplets of a given size and therefore the distance they travel, depend upon their initial velocities and on local wind speed and turbulence. Within crop canopies, turbulent intensity levels can be large (Perrier et al., 1972), but instantaneous wind speeds are generally small; for example, wind speed at mid canopy in a mature barley stand was less than 0.3 m s^{-1} for 90% of the time (Shaw and McCartney, 1985). Thus, within canopies, the flight of most large droplets (> 200 μm) which carry the majority of spores is likely to be little affected by local air flow. A few may be deflected by those gusts that do manage to penetrate the canopy but for the first stage of modelling these will be ignored. However, this may not be the case for splash dispersal from seedling crops or from stubble where wind speeds are much greater than within developed canopies (McCartney and Bainbridge, 1984; Stedman, 1980b). When the effects of turbulence on droplet dispersal can be ignored, the trajectories of individual droplets may be calculated by allowing only for viscous drag on the droplet and the force of gravity. The heights and distance to which splash droplets are likely to travel may be predicted from knowledge of the initial velocities imparted to the droplets during splash formation.

As a first step towards modelling splash dispersal we present below comparisons between measured droplet trajectories in still air and trajectories calculated using a model presented by Chow (1979).

THE MODEL

A droplet moving through the air is acted upon by several forces:

(1) A force due to gravity, $\hat{\mathbf{F}}_g = m.\hat{\mathbf{g}}$, where m is the mass of the particle and $\hat{\mathbf{g}}$ is the acceleration due to gravity (9.8 m s^{-1}) and is directed downwards (n.b., $\hat{}$ symbol represents a vector quantity).

(2) A force on the droplet caused by the viscosity of the surrounding medium acting in the opposite direction to the particle's motion,

$$\hat{\mathbf{F}}_D = -\tfrac{1}{2}\varrho_f \hat{\mathbf{v}}_r . v_r \frac{\pi}{4} d^2 C_d$$

d is the particle diameter, $\hat{\mathbf{v}}_r$ is the particle velocity and v_r the particle speed relative to the surrounding fluid, and ϱ_f is the density of the fluid. This drag force is the resultant of two components, friction drag due to a gradient of velocities at the droplet's surface, and form drag caused by a reduction in pressure at the rear of the droplet in comparison with that at the front. The sum of these two drag terms is generally expressed using the dimensionless drag coefficient C_d, which is a function of the shape of the particle and the particle/fluid Reynolds number $Re = v_r d/V$, where V is the Kinematic viscosity of the surrounding medium ($1.49 \times 10^{-5}\,m^2 s^{-1}$ in air at 1 atm, 20°C).

(3) An Archimedean buoyant force equal to the weight of fluid displaced by the particle, $\hat{\mathbf{F}}_A = -m_f.\hat{\mathbf{g}}$ where m_f is the mass of fluid displaced. In the case of a droplet in the air this force is very small but is included in the model nonetheless.

(4) The force of an accelerating body, $\hat{\mathbf{F}}_a$, acting against the direction of motion. This is the energy needed to induce a field of flow within the surrounding fluid and is given by:

$$\hat{\mathbf{F}}_a = -\tfrac{1}{2}.m_f d\hat{\mathbf{v}}_r/dt$$

If we include all the forces acting on a droplet the equation of motion in vector form can be written as:

$$m\frac{d\hat{\mathbf{v}}}{dt} = \hat{\mathbf{F}}_g + \hat{\mathbf{F}}_A + \hat{\mathbf{F}}_D + \hat{\mathbf{F}}_a \qquad (1)$$

$d\hat{\mathbf{v}}/dt$ is the particle acceleration. Rearranging and resolving into the horizontal (x) and vertical (y) components of particle acceleration, eq. 1 becomes (Chow, 1979):

$$\frac{d^2x}{dt^2} = \frac{\gamma}{\alpha} w_r(u_f - u)\, C_d \qquad (2a)$$

and

$$\frac{d^2y}{dt^2} = \frac{1}{\alpha}[\gamma w_r(v_f - v)\, C_d - \beta] \qquad (2b)$$

where u, u_f and v, v_f are the horizontal and vertical components of velocity of the particle and fluid respectively, w_r is the speed of the particle relative to the fluid ($=[(u_f - u)^2 + (v_f - v)^2]^{1/2}$) and α, β and γ are constants: $\alpha = 1 + \frac{1}{2}\varrho$, $\beta = (1 - \varrho)g$ and $\gamma = 3\varrho/4d$ where ϱ is the ratio of the density of surrounding fluid to the density of the particle. For a water droplet moving through air at 20°C $\varrho = 0.00122$, $\alpha = 1.00061$, $\beta = 0.1019$ and $\gamma = 0.000915/d$.

Equations 2a and b can be solved if the initial velocity of the droplet, the fluid velocity at all points in space and the drag coefficient are known. For solid spheres the relationship between Re and C_d has been extensively investigated (Clift et al., 1978) and several empirical functions are available. For water droplets at large Reynolds numbers (> 600), the situation is potentially complicated by two factors. First, the flow of air around the surface of a droplet can

induce a flow of liquid within the droplet resulting in a reduction in the skin friction component of the drag. Second, the pressure on the droplet can deform it so that calculating the drag coefficient on the basis of a sphere is no longer appropriate. However, *Re* for splash droplets is unlikely to be large enough for these phenomena to be important. The equations for calculating C_d presented by Clift et al. (1978, p. 112) were chosen as they give a better coverage of the region of low Reynolds number than do those suggested by Chow (1979).

Equations 2a and b were solved numerically using 4th order Runge–Kutta integration as described by Chow (1979). Trajectories of droplets in the size range 50 to 2000 μm were estimated for a range of initial velocities.

METHODS

To assess the usefulness of the above model in predicting the trajectories of splash droplets, initial velocities of water droplets and the distances travelled were measured for comparison with calculated distances.

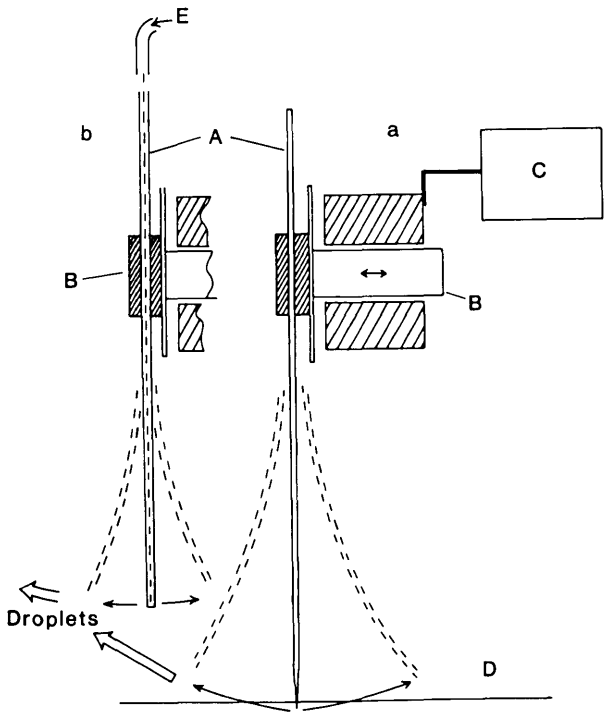


Fig. 1. Schematic diagram of the vibrating needle droplet generators. (a) Solid needle generator. (b) Hollow needle generator. A, needle; B, loudspeaker core; C, signal generator and amplifier; D, water surface; E, water feed from a syringe pump. Arrows indicate the direction of droplet movement.

Droplet production and velocity measurement

Droplets were photographed in flight to determine their initial velocities. Two methods of droplet production were used in order to cover a range of droplet velocities and sizes similar to those expected from a splash.

In the first method, droplets were generated by means of a vibrating solid or hollow needle. The needle was attached to the core of a loudspeaker leaving the tip free to traverse an arc of 5 mm or more when the needle was gently flexed with a finger (Fig. 1). The needle was then vibrated by connecting the speaker to a waveform generator. The solid needle was placed above a container of water in such a way that the vibrating end picked liquid up from the surface (Fig. 1a). When the needle was vibrated at its resonance frequency the motion generated was violent enough that similar sized water droplets were thrown from the end. Alternatively, water was pumped through a hollow needle at a constant rate and droplets were thrown from the vibrating end (Fig. 1b). In both

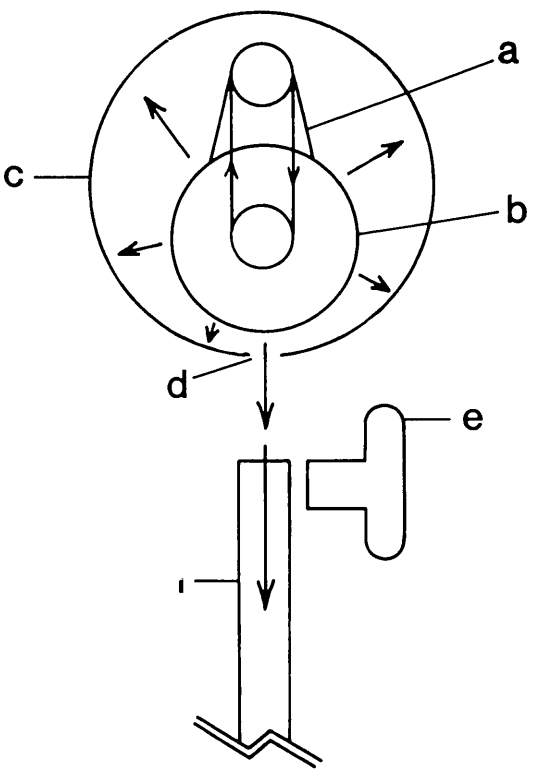


Fig. 2. Schematic diagram (plan) of droplet production using a spinning disc. a, spinning disc droplet generator; b, disc; c, enclosure containing droplet generator; d, vertical slot to allow droplets to escape; e, camera; f, fixed photographic film for droplet collection. Arrows indicate droplet movement.

cases, provided conditions were kept constant, a stream of mono-sized droplets with the same velocities was produced. This method produced droplets in the range from 200 to 1000 μm, with velocities between 0.5 and 1.5 m s^{-1}. During operation the size and velocity of the droplets was remarkably constant and the standard deviation of both variables was typically only 2–3% of the mean value.

The droplet streams were photographed using electronic flash to freeze their motion. From these photographs it was then possible to determine the path taken and distance travelled by the droplets. The speed of the droplets, v, was calculated from the vibration frequency of the needle, f, and the measured distance, D, between consecutive droplets in the stream thus: $v = D.f$. It was verified that one droplet was produced for each oscillation of the needle by observing the needle using a stroboscopic lamp. In a number of cases when the flow rate of liquid was very low, it was found that droplets were produced at half the frequency of the vibration of the needle, in such cases the calculation of v was adjusted accordingly.

In the second method, droplets were produced using a Micromax (Micron Sprayers Limited) spinning disc droplet generator. This sprayer produced a spectrum of droplets with diameters in the range 100 μm to 700 μm and with initial velocities of several metres per second, much faster than those attainable with the vibrating needles. The sprayer was mounted inside an enclosure with a thin slot cut in one side to allow only a narrow stream of droplets to escape (Fig. 2). A constant flow rate of liquid to the sprayer was maintained to ensure a constant size spectrum of droplets.

A camera was positioned close to the slot to photograph the droplets, and electronic flash was used to freeze the motion. The droplets were photographed by using two flashes with a known time interval between them and the speed of the droplets was found by measuring the distance between the two images. The minimum duration of flash was about 4×10^{-4} s: this was not quite sufficient to freeze the motion of objects moving faster than about 5 m s^{-1} and the image appeared as a streak. In such cases the measurements were made from the beginning of each streak. Additionally the streaks were used to show in which direction the droplet was travelling. The droplet size was also estimated from the recorded images.

Droplet sizing and range measurement

In the vibrating needle experiments, the distances droplets travelled were measured from photographs of droplet trajectories. In the spinning disc experiments, the distances were measured by collecting droplets on fixed photographic film placed at different distances from the droplet source. This method of collection also allowed the droplets to be sized, as they dissolved the gelatine layer leaving a crater proportional to their size (Fitt et al., 1982).

RESULTS

Chow (1979) showed that the one dimensional from of eq. 1 could be used to predict sedimentation velocity accurately for droplets of up to 3500 μ diameter. Since the present model differs only in the values chosen for C_d it would be expected to give similar results. Sedimentation velocities were calculated for a range of droplet sizes and the results are compared with values reported by several workers in Fig. 3. The figure shows excellent agreement between calculated and reported values for droplets with dimensions up to about 1500 μm. The sedimentation velocities for larger droplets are overestimated because deformation causes increased drag; this was not allowed for in the calculations. The small discontinuities in the slope of the curve occur because the equations for calculating C_d change for different size ranges; however the differences between adjacent equations are less than 1%. Possible sources of

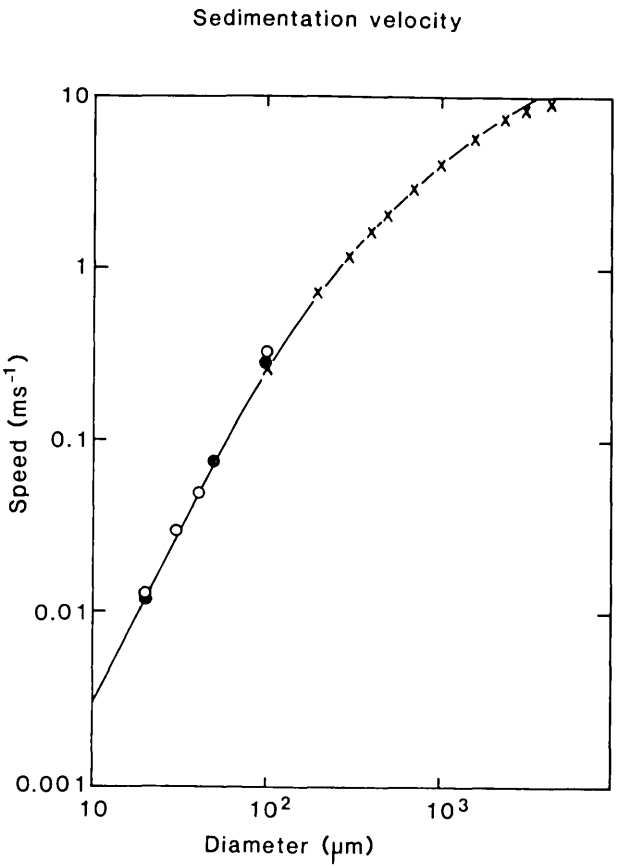


Fig. 3. Comparison of calculated droplet sedimentation velocity with reported measured values. — Model calculations. ●, Matthews (1982); ○, Edmonds (1979); x, Fuchs (1964).

measurement error are variations in air and water density and in air viscosity, due to changes in temperature and pressure and the presence of impurities. Sensitivity analysis of the likely errors, using the model, showed them to be negligible ($< 2\%$).

Trajectories were calculated from the initial velocities (speed and direction) and diameters of droplets measured; the measured ranges compared well with those predicted by the model. Figure 4 shows predicted and measured distances for the vibrating needle experiments. Uncertainties due to the limits in accuracy with which droplet size and velocity could be measured are indicated by error bars. The predicted results are generally within 10% of the measured distances of droplet travel. The points plotted in the figure represent droplets in the size range 200–1000 μm with initial speeds in the range 0.6–2.0 m s^{-1}. The plotted points fall close to a 1:1 relationship and the best fit line is not statistically different from it. There is a slight tendency for the model to underestimate the distance travelled by droplets. This may be an experimental artifact caused by the entrainment of air in the droplet stream. Because each droplet was moving in the wake of the previous one, its drag may have been slightly reduced and so it travelled further than would be expected,

Comparison of the results of the spinning disc experiments with calculated trajectories is less straightforward than for the vibrating needle. Although droplet sizes and distances travelled were measured, trajectories of individual

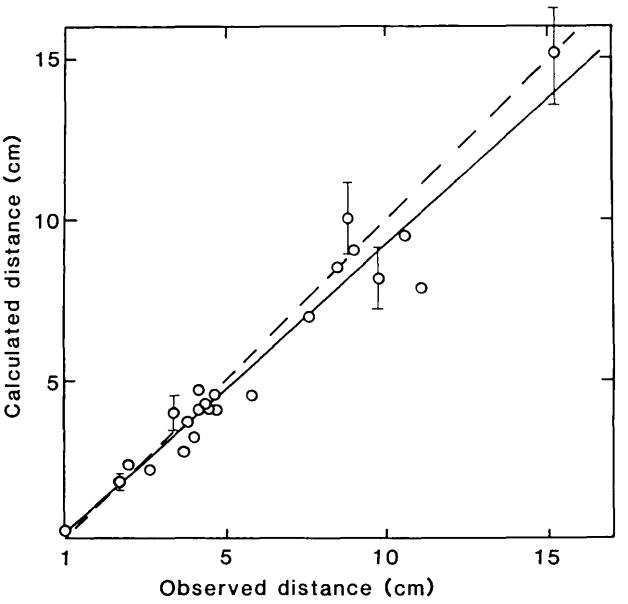


Fig. 4. Observed and calculated distance travelled of drops in the vibrating needle experiments. Sample error bars show typical levels of uncertainty in calculated ranges. —— Regression line (calculated vs. observed); ---- 1:1 line.

droplets could not be identified because of the greater distances travelled by the droplets. Therefore a representative sample of droplets was chosen from the photographs and their theoretical trajectories and distances travelled determined from the measurements of initial velocity and droplet size. The relationship between droplet size and distance travelled was measured from the traces left on the fixed photographic film. Figures 5a–c show comparisons, from three separate experiments, of the mean diameter of droplets collected at various distances from the camera and the travelled distances calculated from measured velocities of individual drops. Error bars for collected droplets show the standard deviation in diameter and the distance range over which the sample was collected. Sample error bars for the calculated ranges give an indication of the effect of uncertainties in measuring the diameter and velocity of droplets from photographs. The resolution and magnification of the film only allowed measurements of diameter to be made with an accuracy of about 40 μm and those for velocity to be made with an accuracy of about 0.1 m s^{-1}. The predicted and measured relationships between droplet size and distance travelled are similar in each of the three experiments. For any droplet size the predicted distance is usually within 15% of the measured value, which is within the limits of accuracy due to uncertainties in size and velocity estimates. As the relationship between distance travelled and droplet diameter was approximately linear, regressions lines were fitted to both the predicted and measured relationships. There was no significant difference between regression lines for predicted and measured relationships in two of the three experiments. In the experiment (Fig. 5b) where a significant difference between prediction and measurement was found, the differences in mean distance travelled for a given size were rarely greater than 25% the majority were less than 15%. The predicted values tended to be larger than the measured distances especially for larger droplets.

Both types of experiments have shown that this model is capable of predicting the trajectory of a water drop in still air with an accuracy better than 15%. The experimental tests included droplets with Reynolds numbers in the range 100 to > 1000. The model should be applicable up to Reynolds numbers of about 1500; beyond this point the value of C_d of a water drop begins to differ significantly from that for a solid sphere (Clift et al., 1978) due to deformation of the drop, and to internal circulation within the drop. A *Re* of 1500 corresponds to a 3500 μm droplet moving at about 6 m s^{-1}, or a 100 μm droplet moving at 225 m s^{-1}. Typically, during splash, droplets range in size from < 100 μm to 2500 μm with a maximum initial velocity of about 20 m s^{-1} and 1 m s^{-1} respectively (Ghadiri-Khorzoojhi, 1978). These results show that the model accurately describes the range of travel of the majority of droplets typically produced in rain splash and therefore it appears to be adequate for predicting their dispersal. It must be noted however that the model does not consider the effects of turbulence which may significantly affect the dispersal of small droplets.

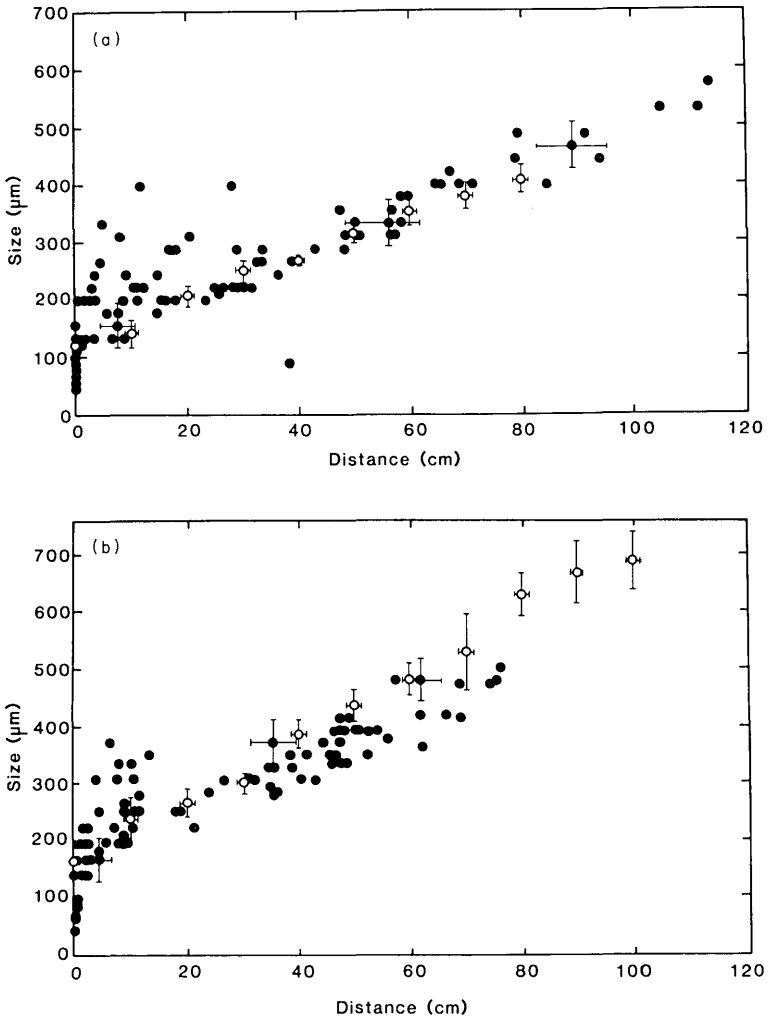


Fig. 5. (Legend is on the facing page.)

APPLICATIONS AND DISCUSSION

Equations 2a and b can be used to estimate the range and height likely to be reached by splash droplets in still or moving air (low turbulence) if the initial speeds and directions of the droplets are known. For example, Figs. 6 and 7 show the ranges and heights of 200 and 1000 μm droplets plotted against the initial angle of flight, θ (measured from the horizontal) for different initial velocities, v_0. They clearly show the greater effect of air resistance on the trajectory of the smaller drop; 200 μm droplets travel a much shorter distance and reach a lower height than 1000 μm droplets given the same starting con-

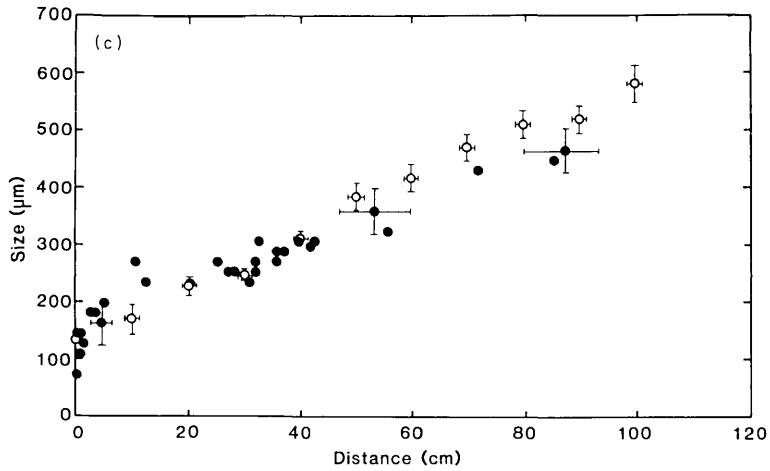


Fig. 5. Relationship between droplet size and distance travelled by droplets in the spinning disc experiments. ○, Observed; error bars represent mean and standard deviation of droplets collected at each distance. ●, Distances calculated from measured velocities of individual drops. Points with error bars represent typical uncertainties due to errors in size and velocity measurements. a,b,c refer to three separate experiments.

ditions. If air resistance was negligible then the droplet trajectories would be independent of mass and the maximum range reached by a droplet would be when $\theta = 45°$, and maximum height ($=\frac{1}{2}v_0^2/g$) when $\theta = 90°$. The figures clearly show that these distances are only approached when the initial speeds are low and the droplet is large. For fast-moving small particles the maximum horizontal range is reached when the droplet is launched close to the horizontal.

The formation of splash on solid and liquid surfaces has been studied by high-speed flash photography (Worthington and Cole, 1897) and high-speed cinematography (Mutchelar, 1967; Ghadiri-Khorzoojhi, 1978). During the initial stages of impact between a water drop and a solid surface or a thin water film, a crater or 'corona' is formed as liquid from the film and droplet moves rapidly outwards. As the corona expands the walls thin and droplets are thrown upwards and outwards from the point of impact. Small droplets are ejected with greater velocities than large ones.

Ghadiri and Payne (1979) studied in detail the splashing of artificial rain drops, on various soil and artificial surfaces, using high-speed cinematography and were able to estimate the initial velocities of different sized splash droplets. When 6 mm diameter drops were splashed onto fine sand, the average velocity of 100 μm droplets was about 13 m s^{-1} while 1000 μm droplets were ejected with speeds of only about 1 m s^{-1}.

The angle of ejection of droplets from splashes on horizontal surfaces tends to increase with the depth of liquid on the surface and to get steeper as the splash process develops (Mutchlar, 1967; Ghadiri, 1978). For thin liquid films

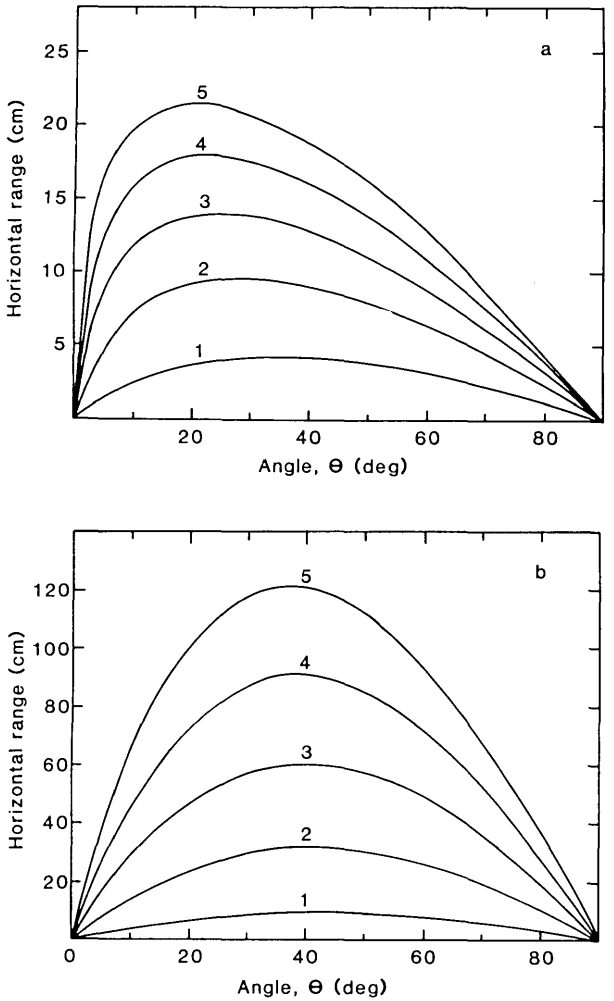


Fig. 6. Calculated horizontal range of droplets released with different initial velocities and angles to the horizontal. The initial velocities in $m\,s^{-1}$ are shown above each curve. (a) 200 μm droplets (b) 1000 μm droplets.

(< 1 mm) the splash angle, θ, is usually between 40 and 60° (Mutchlar, 1967) while from fine soil it is 20°–60° (Ghadiri-Khorzoojhi, 1978).

The distances and heights that splash droplets will travel can be calculated from the initial velocities of splash droplets, determined from observations of splash processes using eqs. 2a and b. Figure 8 shows average distances (and standard deviations) of droplets splashed by a 126 mg droplet (diameter about 6.5 mm) impacting onto fine sand plotted against droplet diameter from experimental measurements by Ghadiri-Khorzoojhi (1978). Also shown on the figure are the horizontal ranges of droplets calculated using Ghadiri-Khorzoojhi's

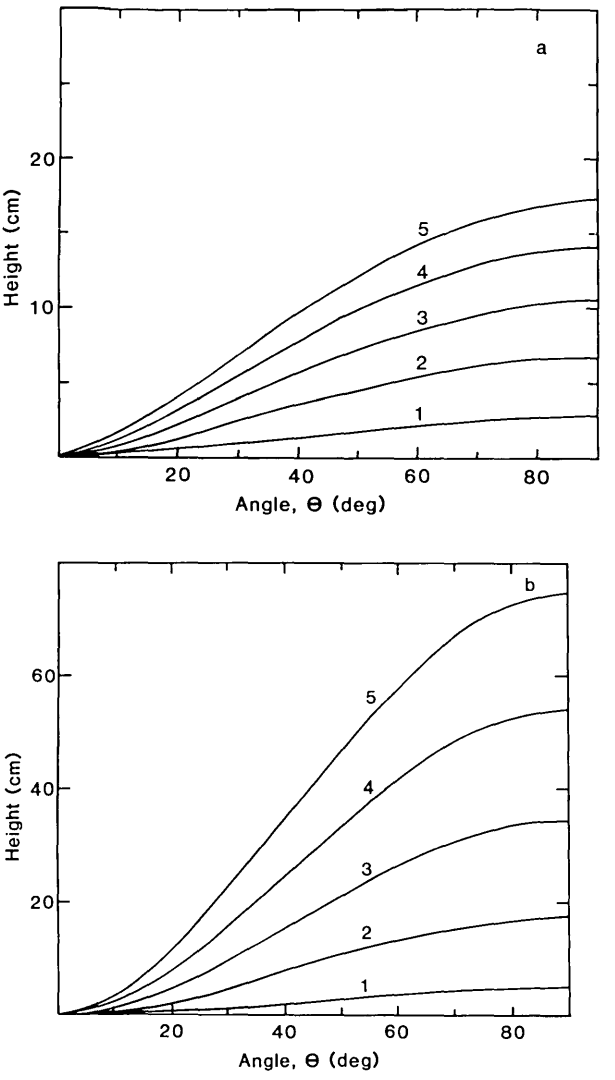


Fig. 7. Calculated maximum height reached by droplets released with different initial velocities and angles to the horizontal. The initial velocities in $m\,s^{-1}$ are shown above each curve. (a) 200 μm droplets (b) 1000 μm droplets.

estimates of average ejection speed of different sized droplets and assuming initial angles of 20° and 60°. The calculated values generally fall within the measured range for droplets with diameters between about 200 and 1000 μm, but tend to underestimate the range for smaller droplets and overestimate it for larger droplets. For very large droplets, those greater than 1000 μm, the model

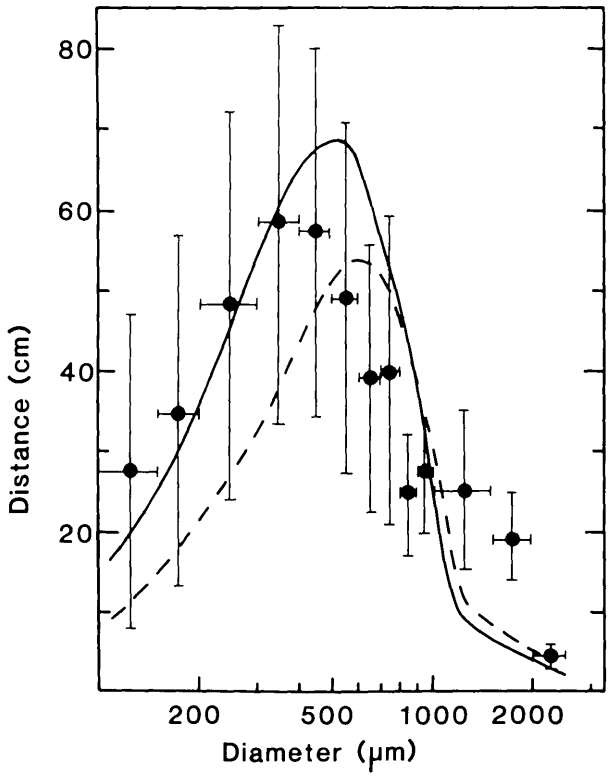


Fig. 8. Distances travelled by different size droplets after 6.5 mm drop impacted on fine sand, from Ghadiri-Khorzoojhi (1978). Error bars represent standard deviations in distance. The curves are ranges calculated from mean initial velocities for each droplet size class given by Ghadiri-Khorzoojhi. ——, $\theta = 20°$; – – –, $\theta = 60°$.

again appears to underestimate the range. The mean initial velocities, especially for the large droplets, were estimated from only a few droplet trajectories and no indication of the range of velocities was given. The measurements were made in still air, but small droplets will be affected by even the most gentle of air currents and may even be carried in the wake of other, larger, droplets, thus apparently increasing their range. Thus the discrepancies between observations and calculations may not be particularly significant. The figure indicates that calculated trajectories could prove useful in estimating likely dispersion of droplets, greater than about 200 μm, from rain splash.

The formation of splash on leaves has been little studied, although some work has been carried out comparing the volumes of liquid splashed from leaves and from artificial surfaces (Stedman, 1979). It is usually assumed that the splash sequence is qualitatively similar to that for solid surfaces or liquid

TABLE I

Stopping distance of droplets projected horizontally at different velocities. The numbers in parentheses are the distances the droplets would fall in reaching 90% of stopping distance

Initial speed ($m\,s^{-1}$)	Stopping distance (cm) Droplet diameter μm								
	200	300	400	500	600	800	1000	1500	2000
1	7.1	12.5	18.4	24.2	30.2	41.6	52.8	77.2	96.7
	(7.2)	(22)	(40)	(64)	(102)	(206)	(367)	(534)	(844)
2	12.3	22.0	33.1	43.5	55.2	77.3	99.3	147.5	186.5
	(6.9)	(18)	(40)	(60)	(101)	(181)	(323)	(529)	(780)
3	16.6	30.1	45.4	60.0	76.8	108.4	140.4	210.8	268.0
	(5.9)	(17)	(39)	(56)	(98)	(172)	(303)	(518)	(758)
4	20.5	37.1	56.1	74.5	95.7	136.0	177.2	267.3	342.0
	(5.6)	(16)	(37)	(54)	(93)	(162)	(283)	(571)	(752)
5	23.9	43.4	65.7	87.5	112.7	160.1	210.3	318.3	409.4
	(5.1)	(15)	(35)	(51)	(89)	(152)	(266)	(500)	(749)

films. However, preliminary photographic investigation of splash formation on barley leaves has suggested that many splash droplets are ejected nearly horizontally ($\theta = 0°$) (Macdonald and McCartney, in preparation). Such droplets, when ejected from a surface sufficiently raised above the ground, have the potential to travel greater horizontal distances than those projected at an angle. Table I shows the stopping distance (i.e. the distance by which u has decayed to zero) for droplets, projected horizontally, of a range of sizes and for a number of initial speeds. Also shown are the distances the droplets would fall before reaching 90% of the stopping distance. Large droplets ($> 800\,\mu m$) have the potential to travel substantial distances even with moderate initial velocities ($\sim 1\,m\,s^{-1}$). However to reach such distances they would have to be released several metres above the ground. Thus for horizontally projected droplets only those released near the top of a plant canopy are likely to travel more than a few tens of centimetres.

CONCLUSIONS

Many important plant pathogen propagules are predominantly dispersed in rain splash droplets. The mechanism of droplet formation and the subsequent dispersal of the droplets are predominantly physical processes and are common to a range of plant pathogens. Thus an ability to predict the dispersal of rain splash droplets will aid the understanding of the epidemiology of many important diseases.

A first step in modelling dispersal in splash droplets is to calculate the flight of larger droplets ($> 200\,\mu m$) which tend to carry more spores than smaller droplets. The results of the experiments reported above suggest that, when

there is little turbulence, droplet trajectories can be satisfactorily predicted from Newtonian dynamics (eqs. 2a and b) using drag coefficients given by Clift et al. (1978). However, to apply this type of model to specific diseases further work is needed on the formation of splash on infected leaves combined with information on the sizes of droplets which carry spores. There is also a need to extend the model to cover situations where turbulence has a significant effect on drop trajectories.

REFERENCES

Brennan, R.M. Fitt, B.D.L., Taylor, G.S. and Colhoun, J., 1984a. Dispersal of *Septoria nodorum* pycnidiospores by simulated raindrops in still air. Phytopathol. Z., 112: 281–290.

Brennan, R.M., Fitt, B.D.L., Taylor, G.S. and Colhoun, J., 1984b. Dispersal of *Septoria nodorum* pycnidiospores by simulated rain and wind. Phytopathol. Z., 112: 291–297.

Chow, C., 1979. An Introduction to Computational Fluid Mechanics. J. Wiley.

Clift, R., Grace, J.R. and Weber, M.E., 1978. Bubbles, Drops and Particles. Academic Press, New York.

Edmonds, R.L., 1979. Aerobiology: The Ecological Systems Approach. Academic Press, New York.

Fatemi, F. and Fitt, B.D.L., 1983. Dispersal of *Pseudocercosporella herpotrichoides* and *Pyrenopeziza brassicae* spores in splash droplets. Plant Pathol., 32: 401–404.

Fitt, B.D.L. and Bainbridge, A., 1983. Dispersal of *Pseudocercosporella herpotrichoides* from infected wheat straw. Phytopathol. Z., 106: 214–225.

Fitt, B.D.L. and Lysandrou, M., 1984. Studies on mechanisms of splash dispersal of spores using *Pseudocercosporella herpotrichoides* spores. Phytopathol. Z., 111: 323–331.

Fitt, B.D.L. and McCartney, H.A., 1986. Spore dispersal in splash droplets. In: P.G. Ayres and L. Boddy (Eds.) Water, Fungi and Plants, Cambridge University Press, Cambridge (U.K.), pp. 87–104.

Fitt, B.D.L., Lysandrou, M. and Turner, R.H., 1982. Measurement of spore carrying splash droplets using photographic film and an image-analysing computer. Plant Pathol., 31: 19–24.

Fuchs, N.A., 1964. The Mechanics of Aerosols. Pergamon Press, Oxford.

Ghadiri-Khorzoojhi, H., 1978. Raindrop Impact, Soil Splash and Cratering. Ph.D. Thesis, University of Reading.

Ghadiri, H. and Payne, D., 1979. Raindrop impact and soil splash. In: R. Lal and D.J. Greenland (Eds.), Soil Physical Properties and Crop Production in the Tropics, J. Wiley, Chichester, pp. 95–104.

Gregory, P.H., Guthrie, E.J. and Bunce, M.E., 1959. Experiments on splash dispersal of fungus spores. J. Gen. Microbiol., 20: 328–354.

McCartney, H.A. and Bainbridge, A., 1984. Deposition gradients near to a point source in a barley crop. Phytopathol. Z., 109: 219–236.

Matthews, G.A., 1982. Pesticide Application Methods. Longman, London.

Mutchler, C.K., 1967. Parameters for describing raindrop splash. J. Soil Water Conser., 22, 91–94.

Perrier, E.R., Robertson, J.M., Millington, R.J. and Peters, D.B., 1972. Spatial and temporal variation of wind above and within a soybean canopy. Agric. Meteorol., 10, 421–442.

Shaw, R.H. and McCartney, H.A., 1985. Gust penetration into plant canopies. Atmosph. Environ., 19, 827–830.

Stedman, O.J., 1979. Patterns of unobstructed splash dispersal. Ann. appl. Biol., 91, 271–285.

Stedman, O.J., 1980a. Splash droplet and spore dispersal studies in field beans. Agric. Meteorol., 21, 111–127.

Stedman, O.J., 1980b. Splash dispersal studies on wheat using a fluorescent tracer. Agric. Meteorol., 21, 195–203.

Worthington, A.M. and Cole, R.S., 1897. Impact with a liquid surface, studies by the aid of instantaneous photography. Phil. Trans. R. Soc. London, Ser. A, 189, 137–148.